

# Flow in Porous Media

Jens Feder

November 8, 2011



# Preface

These lecture notes are based on a series of seminars I held at the Institute of Physics at the University of Oslo. The background for these lectures is the work over many years that Torstein Jøssang and I have spent in building a laboratory to study the connection between microscopic and macroscopic physics. We decided to use laser light scattering techniques to study such phenomena as structural phase transitions, hydrodynamic instabilities, aggregation of proteins and other phenomena where dynamics on the microscopic level becomes organized to macroscopic behavior. Related efforts consist of crystal growth, thermal expansion measurements, studies of interface waves, and protein adsorption. In order to bridge the gap between the sub-micron range of light scattering with length scales from 0.1 to 100  $\mu\text{m}$ , we had also developed a Nanopar analyzer that by studying electric properties of single capillary pores permits the study of aggregates in a regime where normally light scattering is the only method.

After a stay for a week in January 1983 at Statoil, and several visits later we have become aware of the fact that properties of porous media represent a very challenging and rapidly developing branch of solid state physics, where again the connection between the micro-scale of the pore level and the percolative phase transition like behavior on the macroscopic scale is of central interest. K. S. Årland at Statoil was particularly helpful and easy for us to communicate with. The general result of these interactions so far is a new optimism in our part of the physics community — clearly we now have an industry in Norway that actually needs physics, not only people who can compute, measure and write reports.

The aim of these seminars was to present the language, concepts and problems of porous media. This should give our graduate students a basis for work on porous media related problems, and prepare the audience for guests we invite.

It has been very interesting to prepare these seminars. What is written

here represents a part of what I have discussed in the period January 31 to March 21 1984. In fact the last sections of the chapter on the Geometry of Random Media, and a chapter on the hydrodynamic flow past a single cylinder or sphere exist only in my unreadable hand-writing, simply because I have not found the time to type them into my friendly Wordstar. In addition A. Skjeltorp held a seminar on random and regular arrangements of "magnetic holes" in ferro-fluids. A few figures from his work will be entered later. A seminar on the mechanical instabilities in partially wetted sand under gas flow was held by R. Risnes from Statoil.

Since I have made the effort to type these notes and Liv Feder, has converted my sketches into drawings, I hope that our students and colleagues will make constructive comments as to how to conduct the seminars, how to make the lecture notes more useful, and help in defining the direction of this part of our activity.

Oslo April 10 1984

Jens Feder

---

After the first semester of seminars the lecture notes have been expanded and form the basis of the course on porous media most of our master students take.

We have had the generous support of VISTA a research cooperation between Statoil and the Norwegian Academy of Science and Letters. We have had many students and visitors since 84 and have learned much. Some of what we have learned is written up in my book *Fractals* (Plenum, New York, 1988), where also some material on flow in porous media can be found. Torstein Jøssang and I have had a wonderful collaboration all these years and I thank him for his support and friendship. Together we have had an activity called the *Cooperative Phenomena Program* where our guest professors Amnon Aharony, Ivar Giaever and Paul Meakin have played a key role, both in formulating the program and through their contributions to our research.

The present version of the lecture notes represent much of the material used in the course FYS347 *Flow in Porous Media*. What is lacking here is a description of the class-room experiments I usually perform. The section on capillary action together with the appendix on thermodynamics, were

written for the 1995 course. Previously these sections were based on lecture notes taken by Marit Døvle during Professor Jens Lothe's lectures on this subject. I would like to include sections on nucleation theory here, since many phenomena relating to the nucleation of bubbles in porous media are important in practice. It is not generally appreciated that these phenomena are quite easily understood in terms of nucleation theory.

Most of our students work with flow in porous media or properties of random systems. They are therefore familiar with the invasion percolation, fractal viscous fingering, dispersion in porous media, concepts central for flow in porous media but not included in these notes. On the other hand, our students tend to come without any background in hydrodynamics, which is included in these notes. In the future I hope to expand these lecture notes to discuss many of the phenomena we have studied: Single and multi-phase flow in network-models. Real-space renormalization of the permeability and relative permeabilities in correlated random media. Invasion percolation and the effect of gravity. Fractal viscous fingering. Onsager coupling of flows in multiphase flow. Dispersion both longitudinal and transverse, and the effect of stagnation points on mixing. Convection in porous media is also of interest. We have also studied fracturing, and the flow in fractures. Secondary migration and the flow migration of ganglia under the combined effect of gravity and flow in porous media. Much of what has been learned is now well enough understood that the ideas can be included in a course. However, the size of the course needs to be increased — or an additional course planned, since many of the master students do not have a sufficient background in fractals and in percolation theory to allow easy access to the experimental work on invasion percolation and cross-over effects.

Oslo December 13 1995

Jens Feder



# Contents

<b>1</b>	<b>Introduction</b>	<b>1</b>
<b>2</b>	<b>Mixing During Single Phase Flow</b>	<b>3</b>
2.1	An Experiment on Geometric Dispersion . . . . .	6
<b>3</b>	<b>Porous Media and Packing of Spheres</b>	<b>10</b>
3.1	Two-Dimensional Packing of Spheres . . . . .	12
3.1.1	Aksel Thue's Proof . . . . .	13
3.2	Frustration in Two-Dimensional Packings . . . . .	14
3.3	Random Packings in Two Dimensions . . . . .	16
3.3.1	Euler-Poincaré Theorem . . . . .	17
3.4	Three-dimensional Packing of Spheres . . . . .	21
3.5	Poisson Porous Media . . . . .	30
3.5.1	Poisson Probabilities . . . . .	30
3.5.2	Porosity of Overlapping (hyper) Spheres . . . . .	34
3.5.3	Porosity of Overlapping Triangles . . . . .	34
3.5.4	Void-Void Correlation Function . . . . .	35
<b>4</b>	<b>Laminar Flow in Channels and Tubes</b>	<b>38</b>
4.1	Laminar Flow in a Channel . . . . .	39
4.2	Lubrication . . . . .	42
4.2.1	Reynolds' Description of Lubrication . . . . .	42
4.2.2	Lubrication — an Analysis . . . . .	46
4.3	Laminar Flow in a Pipe . . . . .	49

---

<b>5 The Hydrodynamic Equations</b>	<b>53</b>
5.1 The Continuity Equation . . . . .	53
5.2 Conservation of Momentum . . . . .	54
5.2.1 The Substantive Derivative . . . . .	56
5.2.2 The Rate of Strain Tensor . . . . .	58
5.3 The Stress Tensor . . . . .	59
5.4 The Navier-Stokes Equation . . . . .	62
5.5 Boundary Conditions . . . . .	63
5.6 The Reynolds Number and Scaling . . . . .	64
5.7 Stokes Flow past a Sphere . . . . .	69
<b>6 Darcy's Law</b>	<b>74</b>
6.1 Differential Form of Darcy's Equation . . . . .	77
<b>7 Models for Flow in Porous Media</b>	<b>80</b>
7.1 The Capillary Model . . . . .	80
7.1.1 $k$ expressed in terms of macroscopic quantities . . . . .	81
7.2 Kozeny Expression for $k$ . . . . .	84
7.2.1 Flow at finite Reynolds Numbers in Porous Media . . . . .	86
7.2.2 Reynolds Number Dependence of the Permeability . . . . .	89
<b>8 Conduction through Porous Media</b>	<b>92</b>
8.1 A Single Sphere . . . . .	92
8.1.1 Homogeneous Electric Fields . . . . .	93
8.1.2 Electric Dipole Fields . . . . .	94
8.1.3 A Sphere in a Homogeneous Field . . . . .	95
8.1.4 Many Spheres . . . . .	97
<b>9 Hydrodynamic Flow in Periodic Media</b>	<b>102</b>
9.1 The Fundamental Solution . . . . .	106
9.1.1 Periodic Functions and Lattice Fourier Sums . . . . .	106
9.1.2 The Stokes Equation in Reciprocal Space . . . . .	108
9.2 Lattice of Small Spheres . . . . .	111
9.3 The General Case . . . . .	112

<b>10 Capillary Action</b>	<b>115</b>
10.1 Mechanical Theory of Capillary Action . . . . .	116
10.2 Curved Surfaces . . . . .	119
10.3 Surface Tension Thermodynamics . . . . .	120
10.3.1 Reversible Work, and Surface Tension . . . . .	121
10.3.2 Thermodynamic Surface Quantities . . . . .	123
10.4 The Young-Laplace Law . . . . .	123
10.4.1 The Vapor Pressure of a Drop . . . . .	124
10.5 Nucleation . . . . .	126
10.6 Nucleation Kinetics . . . . .	129
10.7 Young's Law . . . . .	133
10.7.1 Angle of Contact Thermodynamics . . . . .	135
10.8 Capillary Rise . . . . .	137
<b>11 Viscous Fingering in the Hele-Shaw Cell</b>	<b>138</b>
11.1 Linear Stability Analysis . . . . .	141
11.2 Observations of Viscous Fingers . . . . .	144
11.3 The Nonlinear Regime . . . . .	148
11.4 Experiments on Viscous Finger Dynamics . . . . .	153
<b>12 Multiphase Flow</b>	<b>156</b>
12.1 Buckley-Leverett Displacement . . . . .	160
12.2 Two-Phase Flow in a Capillary . . . . .	163
<b>A Thermodynamics</b>	<b>171</b>
A.1 Entropy . . . . .	171
A.2 Information . . . . .	172
A.2.1 The Gibbs Distribution . . . . .	173
A.3 Temperature . . . . .	175
A.3.1 Temperature in the Gibbs Distribution . . . . .	176
A.4 Pressure . . . . .	176
A.5 Work and Heat . . . . .	178
A.6 Maximum Work . . . . .	179
A.6.1 Carnot Process . . . . .	180

A.7 Work in an External medium . . . . .	182
A.8 The Number of Particles Dependence . . . . .	186
A.9 The Landau Potential $\Omega$ . . . . .	187
A.10 Thermodynamics of Solutions . . . . .	189
A.10.1 Dilute solutions . . . . .	190
A.10.2 Osmotic pressure . . . . .	192
A.11 General Forces . . . . .	193
A.12 The Maxwell's Distribution . . . . .	195

# Chapter 1

## Introduction

The flow of fluids in porous media is of great technological importance. Clearly the flow of oil, gas and water in reservoirs has a very significant economical aspect. With a background in science it is surprising to learn that only 20 to 30 % of the oil in a reservoir is usually recovered. It should be possible to do better than that!

The information about flows in porous media is spread over many fields of science and technology. For instance, in biochemistry and microbiology the separation of macromolecules on packed columns of ‘chromatographic’ materials is a standard technique. The separation of pieces of DNA by electrophoresis in gel layers is a common analytical and preparative method in biotechnology. The understanding of how these methods work in scientific terms is, however, rather limited.

In this series of seminars we will try to learn about various physical aspects of flows in porous media. The properties of porous media clearly is a part of condensed matter physics. Indeed, much of the current effort in solid state physics and in statistical physics concentrates on the properties of disordered systems, fluctuations, *phase-transitions* and *percolation*. Associated problems include the precipitation and clustering phenomena that may occur both in bulk fluids and in fluids in porous media. Other areas of relevant active scientific inquiry includes polymer and colloidal chemistry and physics, interfacial phenomena, and the adsorption of molecules on interfaces and solids.

At the present stage it is not clear where the emphasis of these seminars will be. In fact I intend to invite outside speakers to discuss relevant subjects. I will also try to respond to any wishes or contributions from the

audience I hope it will be possible to illustrate many of the central ideas by demonstration experiments, or by visits to our laboratory.

As a guiding principle I will try to make the connection between the microscopic and the macroscopic aspects of porous media. In addition I will try to understand what aspects of our work may be of practical interest — this clearly must be based on intuition rather than knowledge at present.

We will start by a demonstration of the longitudinal dispersion of flow at low Reynolds numbers. This simple and beautiful experiment will give us the opportunity to discuss a number of basic concepts in hydrodynamics. Later we will discuss this problem more fully — and find that many subtle and advanced concepts of the flow and diffusion of fluids are need to fully understand what is easily observed.

I hope this will give sufficient motivation for us to go through the elements of hydrodynamics so that we get a few of the important ideas and mathematical tools needed.

We will study the flow of fluids through capillaries, also with droplets or other phases present.

The phenomenological *Darcy equations* for flows through porous media will be discussed next, and capillary models of porous media allow some insight into the nature of the permeability  $k$ .

A rather detailed discussion of flow through regular arrays of spheres will allow a precise expression for the permeability, and its dependence on the porosity.

Capillary pressure, wetting, and interfacial tension are important for the multiphase flow in porous media. Also because of the large specific surface area of porous media the surface adsorption of molecules is of great interest and will be discussed in some detail.

Later we will discuss the percolation problem. In particular we will discuss the statistical, structural and transport properties of percolating systems. This will include a discussion of critical behavior and the scaling properties of various physical quantities. In this connection we will also discuss the fractal behavior of regular and random objects.

The simultaneous flow of several fluids in porous media will be discussed in detail, and we will demonstrate both immiscible and miscible flow.

## Chapter 2

# Mixing During Single Phase Flow

Dispersion in porous media is an important process in industry, pollution control, and chromatography. Here we discuss longitudinal mixing of fluid flow in a porous medium. The discussion is introductory and allows me to illustrate several concepts relevant to flow in porous media by simple demonstration experiments.

Consider a column packed with a fine powder, with a typical particle diameter  $d$ , and saturated with a fluid flowing at a constant average velocity,  $U$ , as indicated in figure 2.1. In the one-dimensional version of the problem a thin layer of marker molecules is found as a sheet across the sample at  $x = 0$  for  $t = 0$ .

At time  $t$  the average position of the marker molecules will be at  $x = Ut$ . This is the one-dimensional *plug flow*. However, the tracer molecules will be smeared around the average position.

In a fluid at rest ( $U = 0$ ) tracers can only spread by molecular diffusion. The spread after time  $t$  will be of order  $\Delta x$ , given by the Einstein relation:<sup>1</sup>

$$\langle \Delta x^2 \rangle = 2D_m t , \quad (2.1)$$

where  $D_m$  is the molecular diffusion coefficient of the marker molecules.

When the fluid moves, additional mixing (dispersion) occurs because of velocity gradients that arise in even the simplest flow geometries. Taylor (1953) studied the dispersion of tracers in a capillary tube (radius  $a$ ) at low flow velocities.<sup>2</sup> He found that the tracers dispersed relative to the plane

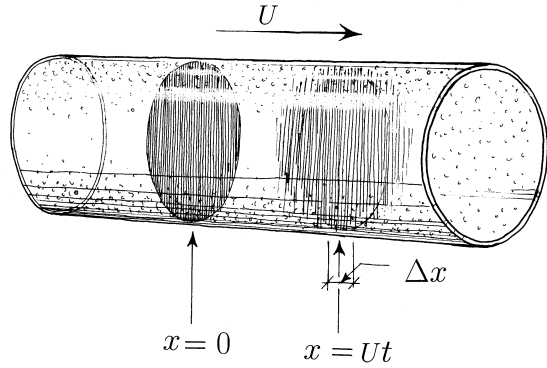


Figure 2.1: Dispersion of tracers convected by flow through a porous medium. The flow is one-dimensional since the average velocity,  $U$ , is constant over the cross section. A sheet of tracers starts at  $x = 0$ . After a time  $t$  the average position of the tracers is  $x = Ut$  with a characteristic spread of  $\Delta x$ .

that moves with the average flow velocity  $U$  ‘*exactly as though it were being diffused by a process which obeys the same law as molecular diffusion*’ but with a diffusion coefficient  $D_{\parallel}$  given by

$$D_{\parallel} = \frac{a^2 U^2}{48 D_m} \quad (2.2)$$

In a porous medium there is an additional mixing or *dispersion* due to the stagnation points that separate flow lines and bring the random nature of the medium into play. Again the spread of a tracer obeys the law of diffusion but with a (longitudinal) dispersion coefficient  $D_{\parallel}$ , replacing the ordinary molecular diffusion coefficient. Experimentally one may determine  $D_{\parallel}$  by observing the mean square spread of the tracer (around the average position of the front) as a function of time using the expression

$$\langle \Delta x^2 \rangle = 2D_{\parallel}t. \quad (2.3)$$

The longitudinal coefficient of dispersion has the same dimension as the diffusion coefficient

$$[D_{\parallel}] = \text{m}^2/\text{s}. \quad (2.4)$$

What physical quantities determine  $D_{\parallel}$ ? Clearly the flow velocity  $U$ , with dimension  $[U] = \text{m}/\text{s}$ , and the powder packing particle size  $d$ , with

dimension  $[d] = \text{m}$ , must enter since without flow and without particles only diffusion gives rise to mixing. To characterize the competition between molecular diffusion and convective dispersion one defines the *Peclet number*

$$\text{Pe} = \frac{Ud}{D_m} . \quad (2.5)$$

This dimensionless number may be viewed as the ratio of two time scales. The time it takes to diffuse a typical pore size,  $d$ , is  $t_{\text{diff}} \simeq d^2/D_m$ , whereas the convection time for tracers is estimated by  $t_{\text{flow}} = d/U$ . With these expressions we find that Pe may be expressed as  $\text{Pe} = t_{\text{diff}}/t_{\text{flow}} = (Ud)/D_m$ .

At very low flow velocities,  $\text{Pe} \ll 1$ , dispersion is controlled by molecular diffusion and we expect the form

$$D_{\parallel} = \gamma D_m , \quad \text{for } \text{Pe} \ll 1 . \quad (2.6)$$

Here the dispersion coefficient is equal to the diffusion coefficient reduced by a factor  $\gamma$  since diffusion confined to the pore space is less efficient than unconstrained diffusion. The coefficient  $\gamma$  depends on the pore structure. For packings of beads or sands<sup>3</sup>  $\gamma \simeq 0.7$ .

At high velocities dispersion should no longer depend on molecular diffusion, but rather on the (average) flow velocity  $U$ , and the geometric mixing length, which is of the same order of magnitude as the typical pore size  $d$ . Since  $Ud$  has the same dimension as  $D_{\parallel}$  we expect that

$$D_{\parallel} \sim Ud = D_m \text{Pe} , \quad \text{for } \text{Pe} \gg 1 . \quad (2.7)$$

These limiting forms may be obtained from the *empirical* expression<sup>3,4</sup>

$$D_{\parallel} = D_m \left( \gamma + \lambda_{\parallel} \frac{\text{Pe}}{1 + C_{\parallel}/\text{Pe}} \right) , \quad (2.8)$$

Experimental results on fluid flow in sand packs<sup>3</sup> give  $\lambda_{\parallel} \simeq 2.5$  and  $C_{\parallel} \simeq 8.8$ .

If, in the one-dimensional flow geometry shown in figure 2.1, the tracer starts in a small volume instead of a sheet across the sample one finds that the tracer also disperses in a direction perpendicular to the flow direction. This dispersion is characterized by a transverse dispersion coefficient  $D_{\perp}$ . For very low flow velocities transverse dispersion is also controlled by diffusion so that  $D_{\perp} = D_{\parallel} = \gamma D_m$  for  $U \rightarrow 0$ . However, in the regime of convective dispersion, that is, for  $\text{Pe} \gg 1$  one finds that  $D_{\perp} \ll D_{\parallel}$ . Again an empirical relation<sup>4</sup> connects low and high Peclet number regimes:

$$D_{\perp} = D_m \left( \gamma + \lambda_{\perp} \frac{\text{Pe}}{1 + C_{\perp}/\text{Pe}} \right) , \quad (2.9)$$

where empirical values are  $\lambda_{\perp} \simeq 0.08$  and  $C_{\perp} \simeq 78$ . For large Peclet numbers ( $\text{Pe} \gg 78$ ) equations (2.8) and (2.9) lead to the asymptotic expression  $D_{\perp} \simeq D_{\parallel}/31$ . This relatively simple picture gets modified in the presence of stagnation effects, whereby the fluid can get trapped in porous grains where the flow velocity is zero. Porous rocks are not all that homogeneous and further dispersion is caused by variations in permeability and porosity.

## 2.1 An Experiment on Geometric Dispersion

The effects of diffusion and mixing due to flow through a random structure are easily demonstrated. A channel  $1 \times 5 \times 30$  cm, was filled with glycerol that was pumped through the channel by a peristaltic pump. The channel was blocked by a random array of cylinders as seen in figure 2.2.

The fluid was glycerol with a viscosity  $\mu = 900$  cp =  $0.9$  Ns/m<sup>2</sup>. In front of the random array of cylinders that traverse the 1 cm gap between the Perspex windows, we injected a line of colored glycerol. We used Nigrosin as a dye, which was also used by Hiby (1962) in a similar experiment.<sup>5</sup> For the success of the experiment it is essential that the dye solution has the same density as the fluid in the chamber, and that there are no temperature gradients in the system. In the sequence of photographs (2.2) we see that an initially straight streak of dye became deformed and snaked through the array of cylinders as the clear glycerol was pumped from the left to the right in figure 2.2. The dye string got stuck at the stagnation point of each cylinder, where it became thinner and thinner as the flow proceeded. When the flow direction was reversed, the dye string, marking the flow, retraced its steps — and finally the original straight dye streak was recovered! If however, the flow proceeded longer before it was reversed, we observed that the ‘time reversed’ flow did not reproduce the original dye streak exactly. We observed a spread at positions that corresponded to the stagnation points of the random array (see figure 2.3b). The physical basis of this effect is simple. Since the fluid cannot flow past the stagnation points in the array, fluid elements containing dye virtually stop at these points, get stretched and must thin down, eventually to molecular dimensions. A detailed discussion of this phenomenon can be found in a paper<sup>6</sup> by Oxaal et al. (1994).

As an example of the qualitative arguments needed in the discussion of complex phenomena, such as flow in porous media, let us get some feeling for the parameters involved by a discussion of the simplified problem in figure 2.3a. Here a single cylinder was placed in the duct. In figure 2.3a the white line marks the position of the initial dye streak, that is at  $t = 0$ .

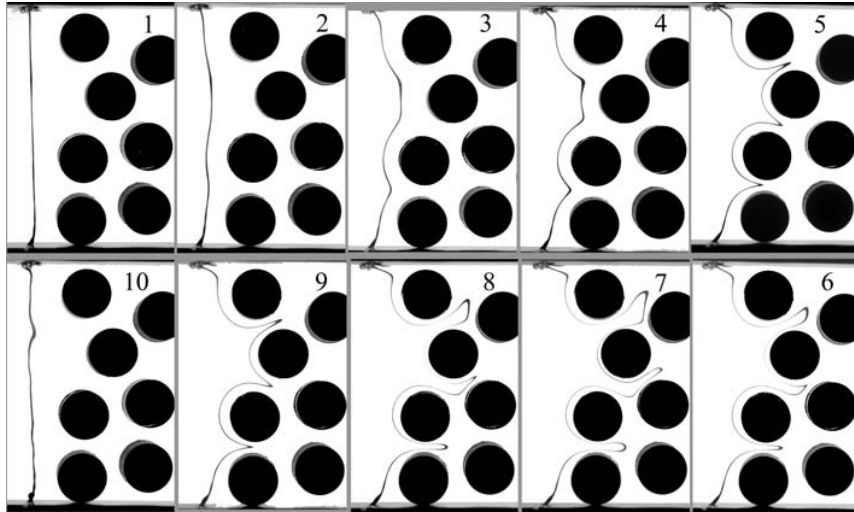


Figure 2.2: The reversible flow through a random array of cylinders. The flow of a glycerol solution was from left to right in parts 1–7. At part 7 the flow was reversed. The line of dye (nigrosine) tracer molecules were convected with the flow and could not pass the stagnation points defined by the cylinders that traverse the channel. As the flow was reversed (part 7) the flow and tracer molecules retraced their paths and finally (in part 10) the initial straight line of dye was recovered. The dye line ‘echo’ was not completely straight in its original place. This error was due to imperfections in the experiment such as temperature gradients, and the fact that the original dye streak was not in the symmetry plane of the channel.

After a time  $t$ , the dye streak was deformed as seen in figure 2.3a. The two lobes of the dye streak reached a distance  $x = ut$ , where  $u$  is the maximum velocity in the channel. Let  $a$  be the initial dye streak radius. The dye in a segment of length equal to the cylinder diameter,  $d$ , must be distributed over a string of length  $L \simeq 2ut$ , therefore it is thinned down to an average radius  $b$  given by the relation

$$\pi b^2 L = \pi a^2 d . \quad (2.10)$$

In the time  $t = L/2u$ , the molecular diffusion gave rise to a mean square spread in  $b$  of  $\Delta b^2 = 2D_m t = D_m L/u$ . At the return of the dye streak to its original position, the returned streak will now have a spread  $\Delta a$ , due to molecular diffusion, which dominated when the streak was thinned down

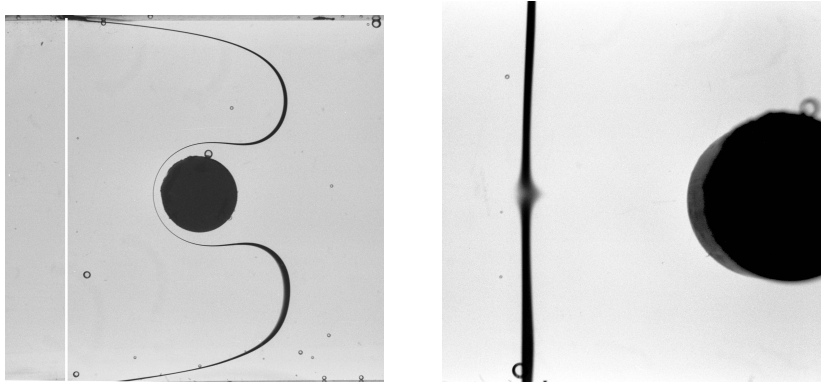


Figure 2.3: The deformation of a dye streak around an obstacle. Glycerol flows from left to right in a channel where the flow is blocked by a single cylinder traversing the channel. (a) The nigrosine colored glycerol dye streak started at the white line. The streak became very thin at the stagnation point since it was stretched there. When the flow was reversed and the dye streak returned to its original position a broadening of the original line at a position that corresponded to the stagnation point was observed. The broadening is due to diffusion.

at the stagnation point. In the reversed flow, instead of thinning down the streak in the stagnation region gets pushed back together and thickened to its original thickness, but with an increased spread. The relative spreads  $\Delta a/a$  and  $\Delta b/b$  must be equal, therefore we find using equation (2.10) that

$$(\Delta a/a)^2 = \frac{D_m L}{b^2 u} = (L/a)^2 / \text{Pe} , \quad (2.11)$$

where again  $\text{Pe}$  is the Peclet number. At high  $\text{Pe}$ , the relative spread is small because diffusion is negligible compared with convection. The critical value of the Peclet number is obtained by setting  $\Delta a/a = 1$ , with the result

$$\text{Pe}^* = (L/a)^2 . \quad (2.12)$$

The condition that the stagnation point dispersion is negligible, and therefore the flow appears to be reversible, is given by the condition  $\text{Pe} > \text{Pe}^*$ , which can always be achieved by increasing the velocity. However, as we will discuss later, to obtain the simple reversible creeping flow as observed in our experiments we must also satisfy the condition of low Reynolds num-

ber flow

$$\text{Re} = \rho u d / \mu \ll 1 \quad (2.13)$$

where the density is  $\rho$ , and  $\mu$  is the fluid viscosity. Combining these two conditions we find that

$$D_m (L/a)^2 \ll u d \ll \mu / \rho \quad (2.14)$$

As is seen from this condition, the experiment is always possible for small displacements  $L$ . But in order to have a reasonable value of  $L$ , without too much smearing by diffusion, a high viscosity fluid is preferred. The relation between the viscosity and the molecular diffusion is given approximately by the Einstein-Stokes relation<sup>1</sup>

$$D_m = \frac{kT}{6\pi\mu R_m}, \quad (2.15)$$

where  $R_m$  is the molecular radius,  $k$  is Boltzmann's constant and  $T$  is the absolute temperature of the fluid. With this expression for  $D_m$  we rewrite the combined condition (2.14) of reversible flow as

$$\left(\frac{L}{a}\right)^2 \ll \frac{6\pi\mu^2 R_m}{\rho k T}. \quad (2.16)$$

Therefore a high viscosity is necessary and a large molecular radius is favorable for reversible flow.

## Chapter 3

# Porous Media and Packing of Spheres

In the discussion of porous media we immediately get involved with the question as to how to describe the geometry of the medium. Any soil or sand consists of mineral grains of various sizes that are packed together. For a complete geometric description one would need the shape, position and orientation of all the grains. For the fluid flow problem in porous media we are mostly interested in the void space between particles. The individual particles may be loose (unconsolidated) or cemented together in geological or laboratory processes that form the porous medium.

The simplest geometrical measure of a porous medium is the *porosity*  $\phi$

$$\phi = \frac{\text{Volume of pore space}}{\text{Total sample volume}}. \quad (3.1)$$

In oil production porosities in the range .05 to .4 are of practical interest. The measurement of the porosity of samples of reservoir rocks is, of course, of prime interest since the recoverable hydrocarbons are found in the pore space.

The porosity  $\phi$  is the most important geometric characterization of a porous medium. As will be discussed later porous media are also characterized by their specific surface  $S$  and by their formation factor  $F$ , *capillary pressure curves*, permeability, relative permeability, dispersion and other physical properties.

Before we go into the intricacies of real porous media we discuss some of the geometric questions that arise for the much simpler problem of packing

spheres together. This discussion will reveal that this problem has many surprising features easily overlooked by a naive investigation. We shall therefore start with the packing of spheres in two dimensions before we consider the three-dimensional packing of spheres. Sloane (1984) gives an interesting discussion<sup>7</sup> of the packing of spheres, its relation to information theory and to group theory. What is the arrangement of spheres that maximizes density? This is called the *Kepler problem* (see reference [] for a popular discussion) since it was discussed by Kepler (1611). The problem is nontrivial in three dimensions (the packing of spheres) and it remains one of the major unsolved problems in mathematics.<sup>1</sup>

Sand that is deposited with water, or shaken in a box, will form a random dense packing, that is, a packing that will dilate (increase its volume) if deformed. Dilatancy fascinated Osborne Reynolds:<sup>10</sup>

A well-marked phenomenon receives its explanation at once from the existence of dilatancy of sand. When the falling tide leaves the sand firm, as the foot falls on it, the sand whitens and appears momentarily to dry round the foot. When this happens the sand is full of water, the surface of which is kept up to that of the sand by capillary actions; the pressure of the foot causing dilatation of the sand more water is required, which has to be obtained either by pressing the level of the surface against the capillary attractions, or by drawing water through the interstices of the surrounding sand. This latter requires time to accomplish, so that for the moment the capillary forces are overcome; the surface of the water is lowered below that of the sand, leaving the latter white or drier until a sufficient supply has been obtained from below, when the surface rises and wets the sand again. On raising the foot it is generally seen that the sand under the foot and around becomes momentarily wet; this is because, on the distorting forces being removed, the sand again contracts, and the excess of water finds momentary relief at the surface.

Lord Kelvin was so impressed by this explanation that he wrote:<sup>11</sup>

Of all the two hundred thousand million men, women, and children who, from the beginning of the world, have ever walked on wet sand, how many, prior to the British Association Meeting at Aberdeen in 1885, if asked, “Is the sand compressed under your foot?” would have answered otherwise than “Yes!”?

---

<sup>1</sup>It is an important part of Hilbert’s 18th problem.<sup>9</sup>

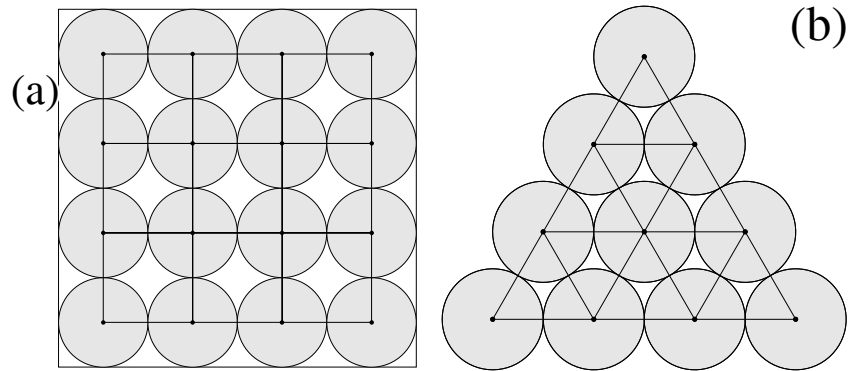


Figure 3.1: Simple Lattice packings of disks on a surface. (a) The quadratic (square) lattice with coverage  $c = \pi/4 \approx 0.7853\dots$  (b) The close-packed triangular lattice with coverage  $c = \pi/(2\sqrt{3}) = 0.9068\dots$

### 3.1 Two-Dimensional Packing of Spheres

It is quite easy to construct two-dimensional packings of spheres or discs on a plane surface. A simple question to ask is: What is the maximum packing density of spheres that may be obtained? Any solid state physicist will have no problem at all in deciding that a simple hexagonal, or triangular, arrangement as illustrated figure 3.1b, will indeed give the highest number of spheres on a given area.

We see that each disk is a part of 6 triangles, and that each triangle contains 3 such pieces. Therefore there is  $1/2$  disk per triangle. Since the area of the triangle is  $\sqrt{3}a^2$ , we find that the coverage is

$$c = \frac{\pi r^2}{2\sqrt{3}r^2} = 0.9068\dots , \quad (3.2)$$

whereas the porosity of the close-packed two-dimensional structure is

$$\phi = 1 - c = 0.0931\dots . \quad (3.3)$$

Thus in the close-packed structure only about 9.3% of the surface is not covered. The simple quadratic lattice covering shown in figure 3.1a has one disk per unit cell. Therefore the coverage is only

$$c = \frac{\pi r^2}{(2r)^2} = 0.7853\dots . \quad (3.4)$$

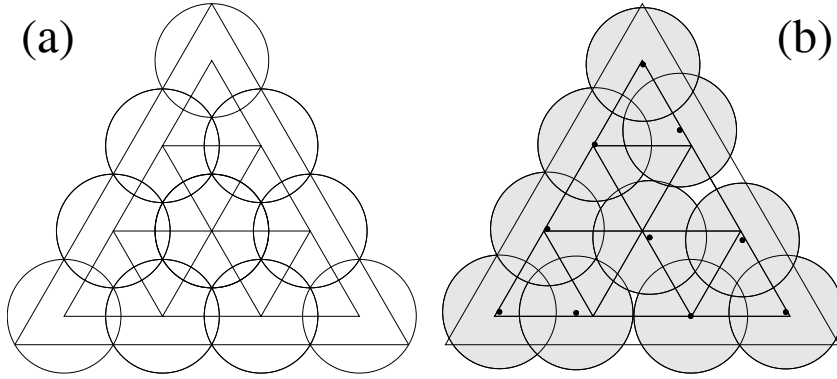


Figure 3.2: Triangular lattice (triangle side  $k$ ) with circles of radius  $r = k/\sqrt{3}$ , and lines at a distance  $\frac{k}{6}\sqrt{3}$  from the outside contour. (a) – the circles have centers at the triangle corners (illustration after Thue 1892). (b) – the circle centers are not placed on the corners of the triangles, but they are all within the triangles. This configuration has points separated by less than  $k$ , consistent with Thue's theorem. The area covered by the circles, inside the outer triangular contour, is less than the outer contour's area.

### 3.1.1 Aksel Thue's Proof

Now one might ask whether there is any other arrangement of disks on a surface that has a lower porosity. The answer is no. Axel Thue (1892) proved that no packing has a higher density than the triangular lattice.<sup>12</sup> In my translation from Norwegian his proof reads:

From an extensive investigation on a certain class of maximal- and minimal-problems the following theorem is reported:

*Is on a planar area, consisting of congruent equal-sided triangles with coinciding corners and sides, placed as many points, as there are corners, then there exists at least one pair of points, having a distance not exceeding the triangle side  $k$ .*

Constructing circles, having a radius  $\frac{k}{3}\sqrt{3}$ , around each point as a center, then can — if our theorem is incorrect — three circles not have any common area. Drawing straight lines parallel with the contour's edges at a distance  $\frac{k}{6}\sqrt{3}$  from the same could no two circles have any area in common outside the new contour, provided, what we may suppose, this does not have external angles of  $60^\circ$ .

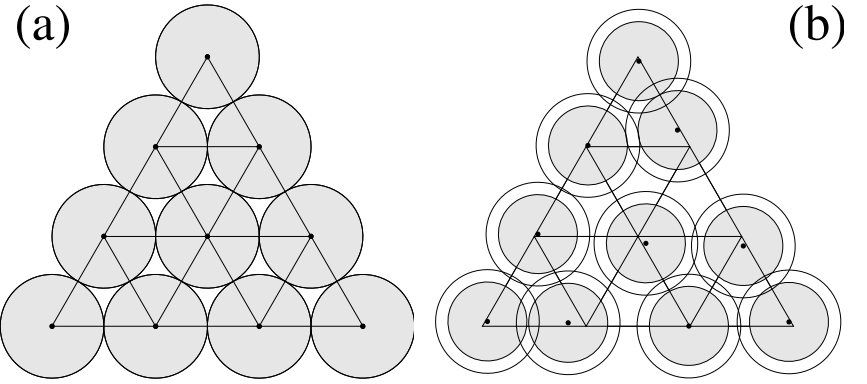


Figure 3.3: (a) – disks placed on a triangular lattice with lattice constant  $k$ . The discs have diameters equal to the lattice constant. (b) – the disks placed at random displacements from the corners of the triangles, but all within the triangular contour. In order to avoid overlap the disk diameter has to be decreased from the original diameter (circle) to the new smaller shaded disks.

Are our points at the corners of the triangles, then the outer contour's area equals the sum of the area of the circles, minus their common area, minus the circle segments that fall outside the contour.

Were the points placed in an arbitrary different position,<sup>2</sup> so that all distances became greater than  $k$ , then the above named expression would increase, which is impossible.

It follows that discs of equal radius,  $r$ , placed on a surface will all have the separation  $k = 2r$  if they are arranged on a triangular lattice of lattice constant  $k$  (see figure 3.3a). According to Thue's theorem any other arrangement of the discs will have at least one pair of discs that overlap. Thus the disc diameter must be decreased in order to avoid the overlap, as illustrated in figure 3.3b, and the porosity becomes higher.

## 3.2 Frustration in Two-Dimensional Packings

In two dimensions Thue's theorem does not appear to be very surprising from the physical point of view. Let us, however, pursue the matter a little

<sup>2</sup>as illustrated in figure 3.2b.

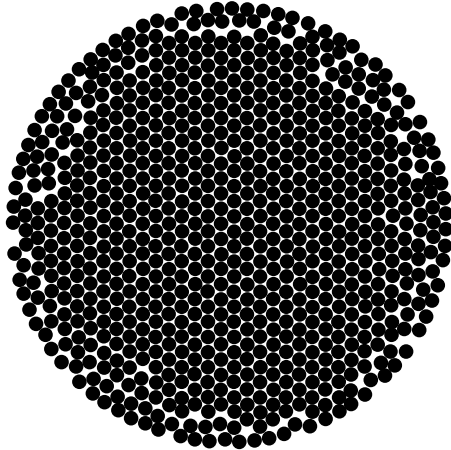


Figure 3.4: Steel balls (4.7 mm in diameter) in a circular dish.

further as this gives us the possibility to introduce some of the concepts needed to discuss the three-dimensional packing problem.

Consider the picture of a collection of ball-bearing steel balls in a circular dish, see figure 3.4. Two important features become apparent when such arrangements of spheres are studied:

1. If we start with some random configuration it seems that we can cover the surface homogeneously. However, as the density increases we observe that the spheres tend to arrange in a nice hexagonal way with only a few defects.
2. We observe that no matter how we arrange the spheres we cannot have a regular hexagonal pattern all the way to the circular border. The boundary condition is incompatible with the crystalline arrangement of the spheres. This leads to conflicting constraints on the optimum sphere configuration and we have a *frustrated* system.

There are other sources of frustration. As discussed by Nelson,<sup>13</sup> the addition of spheres of a different diameter results in a structure that cannot crystallize — it becomes a real problem to determine the optimum packing density in this case. Clearly, unless this system phase-separates, it must be disordered. In figure 3.5 an arrangements of spheres with ‘impurities’ are shown. The frustration in the packing is apparent, and the optimum packing may not be unique. Nelson also discusses the packing of discs on

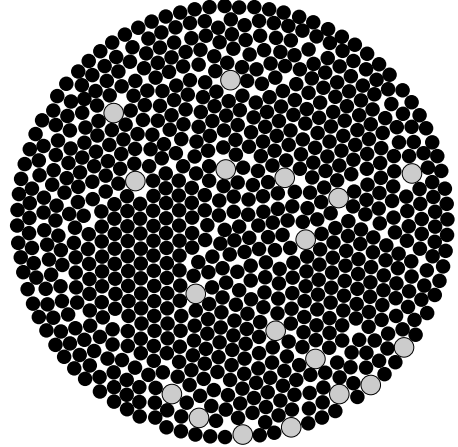


Figure 3.5: The frustrated close packing of 2 size spheres. The small spheres are 4.7 mm in diameter, and there are 18 spheres (gray) 6.35 mm in diameter.

curved surfaces. In this case the curvature of space introduces frustration in the packing of discs.

### 3.3 Random Packings in Two Dimensions

In figure 3.6 we show a configuration of disks obtained by placing them at random, without overlap, onto a surface. At first there is no problem placing disks. However, as the surface begins to fill, the next disk to be placed will in general overlap one or more disks already in place, and therefore a new attempt has to be made. More and more attempts are required before a space for the disk is found. This process is called *random sequential adsorption* (RSA). This process ends in the *jammed state*, in which all open spaces are too small for a disk. Such a jammed configuration is shown in the left hand part of figure 3.6. The coverage in the jammed state is<sup>14,15,16</sup>  $c_2(\text{RSA}) = 0.547$ . Note that this is a random process that has complete memory of its past. RSA has found many applications and has several surprising features. Also illustrated in the right hand part of figure 3.6 is the result of a process in which the position of each disk is adjusted so that it maximizes the distance to its neighbors. When this process is iterated many times a random close packing (RCP) of disks is in two dimensions is

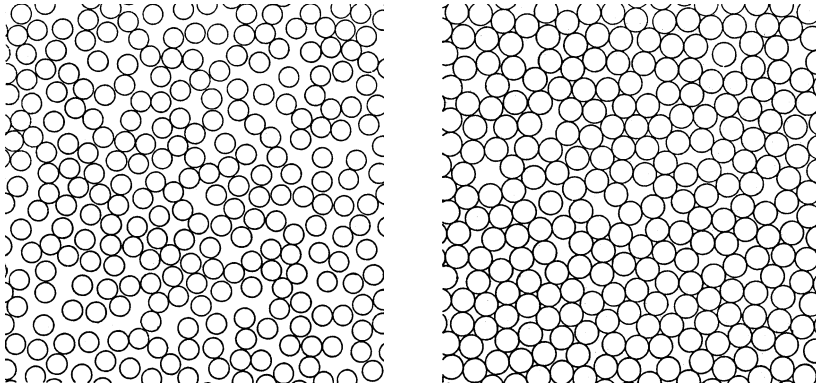


Figure 3.6: A random sequential packing of discs (left). The packing at the right is obtained by making small local adjustments to the packing. This is a procedure that leads to a maximal random sequential packing of disks, which is an approximation for the random close packing of disks (RCP). See references [1].

Figure 3.6: A random sequential packing of discs (left). The packing at the right is obtained by making small local adjustments

obtained. We found<sup>17</sup>  $c_2(\text{RCP}) = 0.772$ .

In figure 3.7 we show a portion of the random sequential packing together with the so called *Voronoi polyhedra*. All the points within a Voronoi polyhedron are closer to the center of the disk it contains than to any other disk center. Clearly the edges of these polyhedra bisect the distance between neighboring discs, and are orthogonal to this distance vector. Most of the discs are contained in polygons with six sides. However, other polygons also exist as seen in the part (b) of figure 3.7.

Polygons with  $p = 4, 5, 6, 7$ , and  $8$  sides occur quite frequently<sup>16</sup> (with frequencies of 1.115 %, 24.428 %, 50.413 %, 21.598 %, 2.396 %, respectively). Triangular  $p = 3$ , polygons are possible but rare, and in principle arbitrarily large  $p$  are obtainable in special configurations.

### 3.3.1 Euler-Poincaré Theorem

There are strong topological constraints on the number of edges. Let  $F_p$  be the number of polygons with  $p$  edges. Then the average number of edges

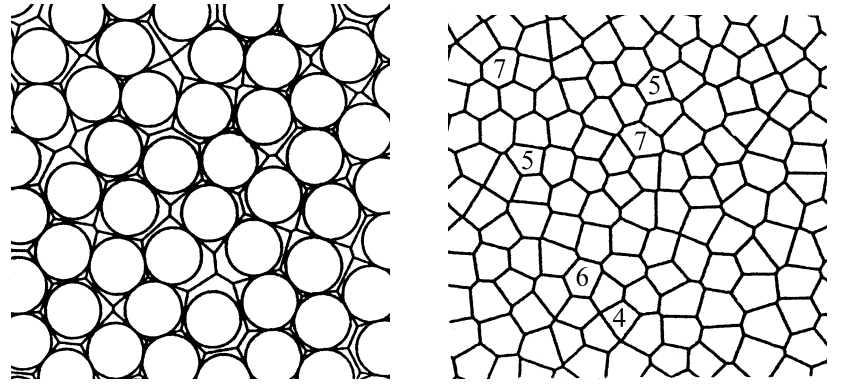


Figure 3.7: The Voronoi polyhedra of a random packing of disks. Left part: Each disc is surrounded by a polyhedron that contains all points that are closer to the center of that disk than to any other disk. Right part: On the average the Voronoi polyhedra have 6 edges. However, polyhedra with 4–10 edges are found for very large RSA configurations.

per particle is

$$\langle p \rangle = \frac{\sum_{p=3}^{\infty} p F_p}{\sum_{p=3}^{\infty} F_p}. \quad (3.5)$$

It can be shown that  $\langle p \rangle = 6$ , independent of the state of order in a two-dimensional system.

Let us consider the elements of such a discussion. In the following table we have listed the number of vertices  $V$ , the number of edges  $E$ , and the number of surfaces  $F$  for various polyhedra.

Playing with configuration of cells you will always find the *Euler-Poincare theorem*<sup>18</sup>

$$V - E + F - N = 1, \quad (3.6)$$

is satisfied (see figure 3.8 for a proof). Here  $N$  is the number of cells in the three-dimensional case, and  $N = 0$  for the two-dimensional case discussed here. See for instance reference []. Here we have used the definitions shown in table 3.2. Here  $d$  is the spatial dimension of the object defined. Clearly for the two-dimensional arrangements listed in the table 3.1 there are no cells so  $N = 0$ . Note that the theorem holds also for three dimensions: a cube will have  $V = 8$ ,  $E = 12$ ,  $F = 6$ ,  $N = 1$ , so the theorem is satisfied.

For a regular quadratic lattice the average number of edges per particle  $\langle p \rangle$ , is not 6 but 4. However, it is easy to see that a vertex where 4 edges

Configuration	V	E	F	$(V - E + F)$
	4	4	1	1
	6	7	2	1
	3	3	1	1
	5	6	2	1
	5	5	1	1
n	n	1	1	1
6	7	2	1	1

Table 3.1: Examples of geometrical relations for polyhedra.

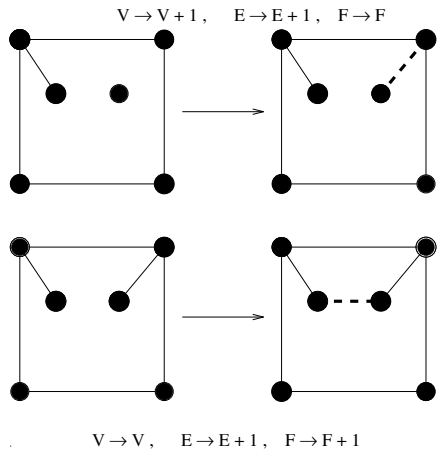


Figure 3.8: Two processes used in the generation of an arbitrary two-dimensional network: (Top) Adding an unconnected vertex increases the number of vertices and the number of edges by one but leaves the number of faces unchanged. (Bottom) Joining two vertices that already are connected by an edge increases the number of edges and the number of faces by one but leaves the number of vertices unchanged. In both cases the sum  $V - E + F$  is unchanged. But we must start the construction of a network with  $V = 1$   $E = F = 0$  — therefore we have  $V - E + F = 1$  for any network.

$V$	=	number of vertices	$d = 0$
$E$	=	number of edges	$d = 1$
$F$	=	number of faces	$d = 2$
$N$	=	number of cells	$d = 3$

Table 3.2: Definitions for polyhedra

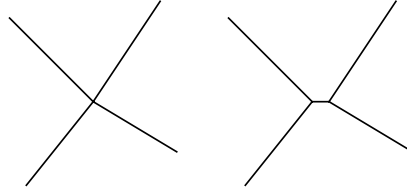


Figure 3.9: Unstable and stable vertices. A vertex of four edges (left) in a Voronoi network is unstable with respect to infinitesimal displacements of the centers defining the network. An unstable vertex splits into two vertices that each connect three edges (right).

meet is unstable and splits into 2 vertices with 3 edges each as indicated in the figure 3.9, by an infinitesimal shift of the discs defining the Voronoi polyhedra. In any random array the situation where 4 edges meet at a vertex is extremely rare. Since each edge ends at two vertices it follows that

$$3V = 2E , \quad (3.7)$$

for almost all 2-dimensional configurations of disks.

Since each edge is shared by 2 neighboring polygons, and since there are  $pF_p$  edges belonging to polygons with  $p$  sides we have

$$E = \frac{1}{2} \sum_p pF_p . \quad (3.8)$$

Using equations (3.7) and (3.8) in (3.6), we find

$$V - E + F = \frac{1}{3} \sum_p pF_p - \frac{1}{2} \sum_p pF_p + \sum_p F_p = 1 , \quad (3.9)$$

which for systems with a large number of cells:

$$F = \sum_p F_p \rightarrow \infty ,$$

allows us to ignore the 1 on the right hand side of equation (3.9) and we find that

$$\sum_p p F_p = 6 \sum_p F_p.$$

Therefore the average number of edges per polyhedron is given by equation (3.5) is  $\langle p \rangle = 6$ .

Since we have precisely 6 edges per polygon on the average, we must find that polygons with  $p = 5$ , are compensated for by polygons with  $p = 7$ . Polygons with  $p = 4$  are rare and they are compensated by polygons with  $p = 8$ , or two polygons with  $p = 7$  each. In fig. 3-8, we have marked a few polygons with  $p = 5$  and 7. The statistical properties of such ‘defects’ — also called *disclinations*, have been of much interest recently. For a discussion see reference [] .

## 3.4 Three-dimensional Packing of Spheres

The packing of spheres in has a long history. Kepler<sup>19, 20</sup> discussed in 1611 the packing of spheres in his essay ‘*De Nive Sexangula*’, that is, *On the Six-Cornered Snowflake*. Kepler’s discussion of packings is interesting: If equal pellets are loose in the same horizontal plane and you drive them together so tightly that the touch each other, they come together either in a three-cornered or in a four-cornered pattern.... With a five-sided pattern uniformity cannot be maintained. A six-sided pattern breaks up into three-sided. Thus there are only two patterns as described.

Now if you proceed to pack solid bodies as tightly as possible, and set the files that are first arranged on the level on top of others, layer on layer, the pellets will be either squared (A in diagram), or in triangles (B in diagram). If squared, either each single pellet of the upper range will rest on a single pellet of the lower, or, on the other hand, each single pellet of the upper range will settle between every four of the lower. In the former mode any pellet is touched by four neighbors in the same plane, and one above and one below, and so on throughout, each touched by six others. The arrangement will be cubic, and the pellets when subjected to pressure will become cubes. But this will not be the tightest pack.

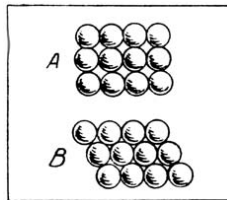


Figure 3.10: Illustration from Kepler

In the second mode not only is every pellet touched by its four neighbors in the same plane, but also by four in the plane above and by four below, and so throughout one will be touched by twelve, and under pressure spherical pellets will become rhomboid. This arrangement will be more comparable to the octahedron and pyramid. The packing will be the tightest possible, so that in no other arrangement could more pellets be stuffed into the same container.

Here Kepler discussed *periodic* packings of spheres and noted that the *simple cubic lattice* (SC) is less dense than what is called the *face-centered cubic lattice* (FCC). The filling factors for these packings are:

$$c = (1 - \phi) = \pi/6 = 0.5235\dots; \text{SC}$$

$$c = (1 - \phi) = \pi/3\sqrt{2} = 0.7404\dots; \text{FCC}$$

Kepler continues referring to (B in the diagram):

Again, if the files built up on the level have been triangular, then in solid packing either each pellet of the upper range rests upon one of the lower, when the packing again is loose; or each one of the upper range will settle between every three of the lower. In the first mode any pellet is touched by six neighbors in the same plane, by one above and by one below its level, and thus throughout by eight others. This pattern will be comparable to the prism, and, when pressure is applied, columns of six four-cornered sides and two six-cornered bases will be formed instead of the pellets. In the second mode the same result will occur as before in the second mode of the four-sided arrangement, thus: (Kepler here refers to figure 3.11) let B be a group of three balls; set one, A, on its apex; let there be also another group, C, of six balls; another D, of ten; and another, E, of fifteen. Regularly superimpose the narrower on the wider to produce the shape of a pyramid. Now, although in this construction each one in an upper layer is seated between three in the lower, yet if you turn the figure around so that not the apex but the whole side of the pyramid is uppermost, you will find, whenever you peel off one ball from the top, four lying below it in a square pattern. Again as before, one ball is touched by twelve others, to wit, by six neighbors in the same plane, and by three above and three below. Thus the closest pack in three dimensions the triangular pattern cannot exist without the square, and vice versa.

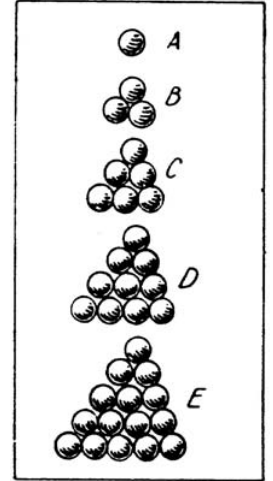


Figure 3.11: Illustration from Kepler

Kepler concluded that the packing on a triangular base leads to the

same close-packing based on the square lattice, that is, the face-centered cubic lattice. Kepler discussed many other geometrical features of packings, but concluded that he could not explain why snowflakes are six cornered. In fact ice crystallizes in many forms, depending on pressure and temperature. Ice forms hydrogen-bonded crystals, that are not close-packed. However, the common form of ice has a hexagonal base. The macroscopic form of snow crystals depends on humidity and temperature in the atmosphere, and many varieties have been found. (See the discussion by Mason in reference [1]).

Kepler explained clearly regular lattices, the foundation of crystallography. However, he did not discuss other close packings, notably the hexagonal close packed lattice, and packings with stacking faults, that have the same density. Mason (in reference [1], pp. 47–56) states that Thomas Harriot (1599), an Englishman, really preceded Kepler, and was the first to postulate closest packing was achieved when one ball was surrounded by twelve others. Harriot also understood the difference between the hexagonal and cubic close-packings.

The close-packing of spheres are well known models of solids. Among the 100 or so elements in the Periodic Table, approximately 55 form solids that maximize the packing of the atoms in that the number of spheres representing atoms are arranged in such a way that the volume fraction of the spheres is the largest of any possible arrangement of spheres.

Both the *face centered cubic* (FCC) and the *hexagonal close-packed* (HCP) lattices have the maximum density with a volume fraction  $c$  that is larger than the *simple cubic* (SC) lattice. The densities and the porosities are given by

$$c = (1 - \phi) = \pi/3\sqrt{2} = 0.7404\dots ; \text{FCC} \quad (3.10)$$

The close packed structures may be generated by the procedure described in figure 3.12. However, there is a family of structures that may be generated by choosing arbitrary sequences such as ...ABACBCBACBCAB... that all have the same porosity. The FCC structure has been attributed<sup>8,21</sup> to Kepler (1611). The mathematician Wu-Yi Hsiang, has a paper that proves that the close packed lattices represent the maximal packing density.<sup>8,22</sup> However, the proof is controversial. Thomas C. Hales has criticized Hsiang's work<sup>23,24</sup> and has recently published a proof of his own on the internet.<sup>25</sup>

Four spheres in mutual contact define a tetrahedron. The volume fraction of the spheres inside the tetrahedron is  $c_u = \sqrt{2}(3 \arccos(1/3) - \pi) = 0.77964\dots$ . This value represents an upper limit to the packing fraction, since space cannot be filled by tetrahedra.<sup>7,8,26</sup>

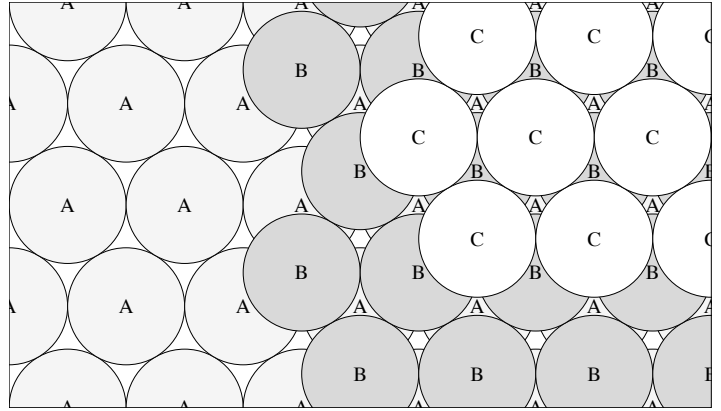


Figure 3.12: Close-packing of spheres is obtained when a triangular layer of spheres (A) is overlaid by a next triangular layer (B) positioned with centers at the symmetry centers between the spheres in the previous layer. The next layer may now be positioned directly over (A) or in the position (C) as indicated in the figure. The sequence ...ABCABCABC... corresponds to the face-centered cubic close-packing. The sequence ...ABABAB... is the hexagonal-close-packed structure.

### Random Close-Packing of Spheres

The *random close-packing* (RCP) has a long history. Many experiments by Bernal<sup>27, 28, 29</sup> and also by Scott and Kilgour<sup>30</sup> conclude that

$$c = (1 - \phi) = 0.6366 \pm 0.0005 . \quad (3.11)$$

Thus the porosity is  $\phi = 0.3634$ . Random close-packings as models for liquid structure motivated Bernal<sup>28, 29, 31</sup> to study random packings of balls in detail. Bernal and Mason<sup>27</sup> packed several thousand  $\frac{1}{4}$  inch steel balls into a balloon. The balls were squeezed and shaken to obtain a random close-packed structure. Paint was filled into the balloon and drained. When the paint was dry the balloon was removed. Where the balls touched, or nearly touched paint was left. They took about 500 balls from the center and counted the number of close-or near contacts (see figure 3.13).

The average number of contacts were 7.9 for RCP and 7.1 for RLP. A sphere must make contact with at least 3 others to be stable (in a gravi-



Figure 3.13: Portion of random close-packed ball assembly showing marks of further contacts (after Bernal and Mason [1]).

Figure 3.13: Portion of random close-packed ball assembly showing marks of further contacts (after Bernal and Mason [1]).

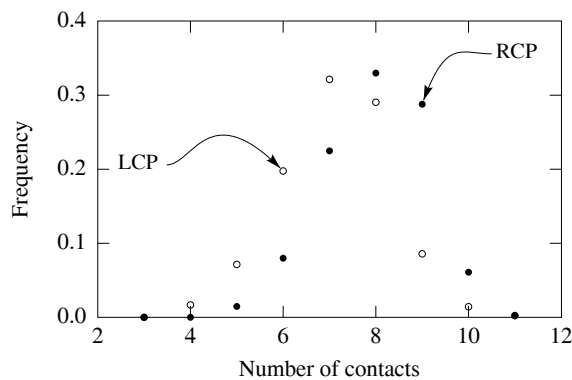


Figure 3.14: Frequency of spheres having a given number of contacts to other spheres in random sphere packings. ●—random close-packings; ○—random loose packings (Bernal and Mason [1]).

Figure 3.14: Frequency of spheres having a given number of contacts to other spheres in random sphere packings. ●—random cl

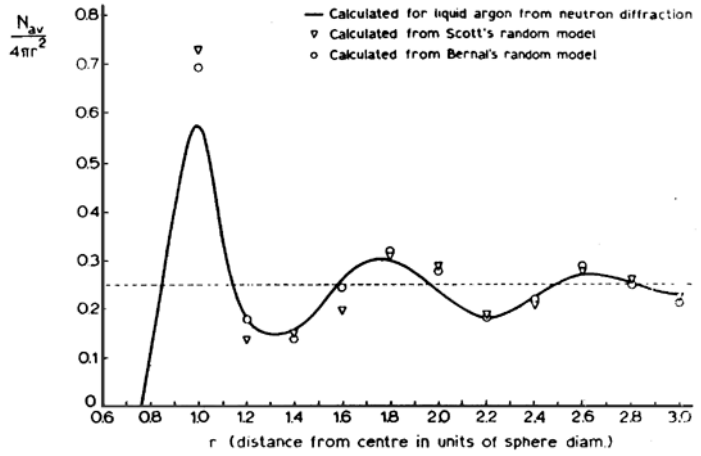


Figure 3.15: The radial distribution of random close-packings of equal spheres. ( $N_{av}$  is the average number of spheres in intervals of 0.2 of sphere diameter) (Bernal [1]).

Figure 3.15: The radial distribution of random close-packings of equal spheres. ( $N_{av}$

tational field). A sphere can make contact with at most 12 other spheres<sup>3</sup> of the same size, which is the number of neighbors in the HCP and FCC packings.

The shape of the Voronoi-Dirichlet polyhedra surrounding spheres in a random packing has also been studied extensively. The shape of the polyhedron must fluctuate throughout the medium. Coxeter<sup>32</sup> argues that the number of faces is on the average  $F = (23 - \sqrt{313})/3 = 13.56$ . It follows then from Euler's theorem (with  $N = 1$ ):  $V - E + F = 2$  and  $3V = 2E$ , that the average number of vertices or sides of a face,  $p$ , is given by  $p = 2E/F = 6(F - 2)/F \approx 5.115$ . Experimentally measured values are<sup>33</sup>  $p = 5.158 \pm 0.003$  and  $F = 14.251 \pm 0.015$ . Bernal<sup>29</sup> points out that two spheres within  $\sqrt{2}$  diameters are geometric neighbors defining a face of the Voronoi polyhedron. Experimentally he finds that the number of spheres within a radius of  $\sqrt{2}$  diameters is 13.4.

A simple way to characterize random packings of spheres and fluids is by the radial distribution function  $G(r) = n(r)dr/4\pi r^2$ , where  $n(r)dr$  is the number of spheres that have a distance,  $r$ , from a sphere at the

<sup>3</sup>As maintained by Isaac Newton in his famous dispute with the Scottish astronomer David Gregory.<sup>7</sup>

origin, in the range  $[r, r + dr]$ . The radial distribution function may be interpreted as the conditional probability that with a sphere at the origin one finds another sphere in a shell of width  $dr$  at a distance  $r$ . For liquids  $G(r)$  has been measured by X-ray and neutron-scattering experiments, and Bernal measured  $G(r)$  for a random packing of steel balls by measuring the location of a very large number of spheres in a random packing. His results are shown in figure 3.15. The RCP model captures much of the structure in the correlation function of argon.

### Random Loose Packing of Spheres

If spheres are just poured into a container the density will be somewhat less (see the review [] of granular media by Jaeger & Nagle (1992)). Scott<sup>35</sup> noted different ways of packing  $1/8$ -balls into containers that “there is a range of random packings lying between two well defined limits. The limits are called here ‘dense random packing’ and ‘loose random packing’.” Scott measured the packing density of spheres in cylinders with dimpled walls as a function of filling height  $h$ . The packing density was extrapolated to  $1/h = 0$ , and the resulting values plotted as shown in figure 3.16. For loose packings the balls fill the vessel essentially by rolling down a slope of random-packed balls. The dense packing are the obtained by gentle shaking and tapping. ‘In both types of packings the balls are always rigid in the sense that uniform pressure over the top will not alter the packing.’

As the distance between the particles is increased there are less ‘paths’ that can transmit force. These paths<sup>36</sup> and the distribution of forces can be observed experimentally, see figure 3.17. The force distribution was measured in a separate experiment where 3.5 mm glass spheres in container 90 mm in diameter and 75 mm high were pressed down with a 310 N force on the top. A layer of carbon paper on the container bottom left marks that were used to measure the vertical component of the force,  $f$ , between individual spheres and the bottom. The measured probability density,  $P(f)$ , for this force had a simple exponential distribution:

$$P(f) = C \exp^{-f/f_0},$$

with  $C = 736$  and  $f_0 = 0.98$  N. Thus most of the load is carried by only a few spheres. The large fluctuations in force make granular packs highly inhomogeneous as illustrated in the force paths shown in figure 3.17.

The loosest random packing that is still mechanically stable under a give force  $F$  is called the *random loose packing* (RLP). In sand-piles the

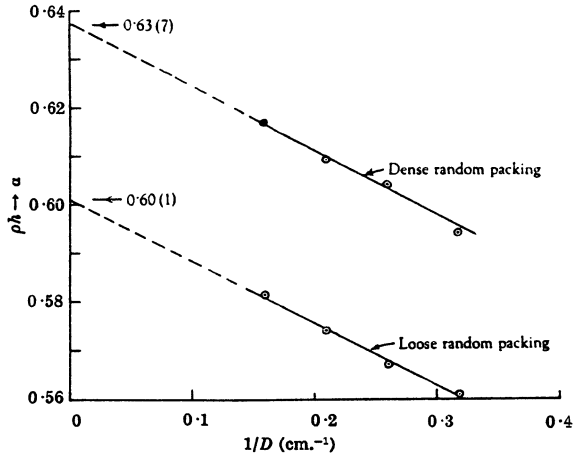


Figure 3.16: The packing density in cylinder of ‘infinite’ length obtained from extrapolation, plotted against reciprocal of the cylinder diameter  $D$ .

force  $F$  is due only to the weight of the particles and thus to the acceleration of gravity  $g$ . Experiments<sup>37</sup> by Onoda and Lininger (1990) show that in the limit  $g \rightarrow 0$  one finds  $c_{\text{RLP}} = 0.555 \pm 0.005$ . A random packing that has a density larger than the RLP density must *expand* when the packing is deformed. In recent computer simulations<sup>38</sup> packing densities of spheres in the range 0.5447 and 0.6053 were found for various algorithms for generating the packings. Thus the lowest density was below the RLP limit.

Packings of sand or particles has many interesting features and many practical applications. Recently much interest has centered on *granular materials*<sup>34</sup> or the ‘granular state.’ Granular materials are peculiar in that they behave as solids when at rest, but more or less like fluids when they move. The top surface of a granular material is stable as long as the slope is less than the *angle of repose*  $\theta_r$ . When the slope is increased beyond some maximum angle, which is characteristic of the material, a relatively thin surface layer flows almost like a liquid leaving the rest of the heap at rest. The flow consist of avalanches that move particles down the slope. The avalanche dynamics may have scaling properties and provide examples of *Self-Organized Critical behavior* (SOC), see Reference [ ]. A remarkable feature of granular media is that the pressure at the bottom of a container filled with a granular material is independent of the height  $h$  to which the container is filled. In an hour glass there is an approximately linear relation

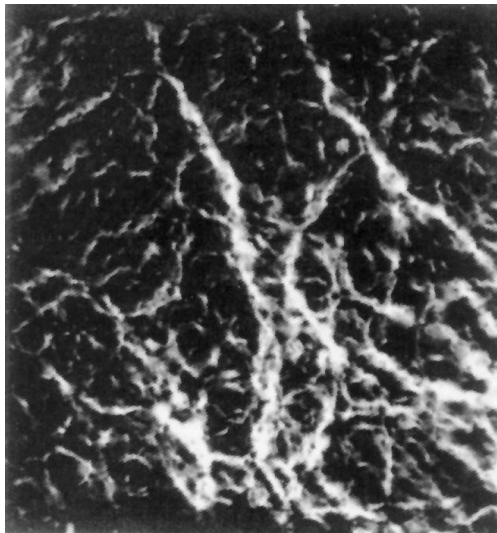


Figure 3.17: Forces between 3 mm Pyrex spheres visualized by birefringence. The spheres are in a container filled with a water-glycerol mixture that has the same refractive index as Pyrex. The system is placed between crossed circular polarizers, therefore no light is transmitted unless the spheres become birefringent due to stress. The bright regions therefore show the force paths that carry the load placed on a piston on top of the bead pack. The box had sides  $70 \times 70$  mm and was 40 mm thick. (from Liu et al. [1]).

Figure 3.17: Forces between 3 mm Pyrex spheres visualized by birefringence. The spheres are in a container filled with a water-

between the filling height and the time it takes to empty the top container. If the two bulbs of an hour glass are not evacuated, then air must flow from the bottom container to the top container as the sand flows down. The resulting two phase flow through the small orifice is unstable and the sand flows periodically,<sup>40</sup> in effect, the hour glass ticks.

For powders consisting of particles of different size one finds that the big particles move to the top by shaking.<sup>41</sup>

The packing of sand, silt and clay is only the first step in the formation of sedimentary rocks. Sedimentation takes place in water, which has to be expelled in order for the compaction of particles to proceed. Further process involving the dissolution, and regrowth of various minerals contribute to geological compaction. Biological material that sediments together with

Table 3.3: Common packings of spheres in two and three dimensions.

Two dimensions	Symbol	c	$\phi$
Square lattice		$\pi/4 \simeq 0.7853$	0.2147
Triangular lattice		$\pi/(2\sqrt{3}) \simeq 0.9068$	0.0931
Random Sequential Adsorption		0.547	0.453
Random close packed		0.772	0.228
Three dimensions	Symbol	c	$\phi$
Simple cubic lattice	SC	$\pi/6 \simeq 0.5235$	0.4765
Body centered cubic lattice	BCC	$\pi\sqrt{3}/8 \simeq 0.6802$	0.3198
Face-centered cubic lattice	FCC	$\pi/(3\sqrt{2}) \simeq 0.7404$	0.2596
Hexagonal close packed lattice	HCP	$\pi/(3\sqrt{2}) \simeq 0.7404$	0.2596
Random close packed	RCP	0.6366	0.3634
Random loose packed	RLP	0.555	0.445
Upper limit (tetrahedron)		$\sqrt{2}(3 \arccos(1/3) - \pi) \simeq 0.7796$	0.2204

sand, silt, and clays, may be buried deeply enough for the temperature and pressure to increase sufficiently to form *source rocks* in which the biological material may be transformed into oil and gas. Oil in source rocks may seep out by *primary migration*, which is a poorly understood process. The oil then moves in water filled sands to the trap, if it exists, or to the surface by the process of *secondary migration*, a process that is relatively well understood, which we will discuss in a later chapter.

## 3.5 Poisson Porous Media

### 3.5.1 Poisson Probabilities

A simple way to generate a (mathematical) model porous medium is to place spheres of radius  $r$  at *random* positions in space. This process of placing points, that is the centers of spheres, with uniform probability in space, is a useful model for many processes.

Consider a volume  $V$  where  $N$  points are placed randomly and independently. The density of points representing centers of hyper-spheres

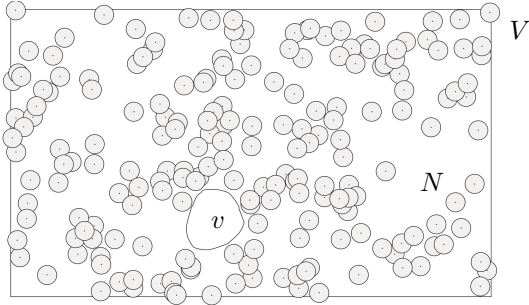


Figure 3.18: The Poisson process of placing at random  $N$  points in a volume  $V$  so that none are found in the volume  $v$ . In this illustration there are  $N = 200$  discs placed in a ‘volume’  $V = 477.5$  in units of the disc area, and  $n = N/V = 0.4189$  in units of inverse disc area. Thus the porosity is  $\phi = \exp(-n\pi r^2) = \exp(-0.4189) = 0.658$ .

is

$$n = \frac{N}{V} . \quad (3.12)$$

The probability that a sphere center lands in a volume  $v$  is  $v/V$ . Therefore the probability for *not* placing a sphere in a given volume  $v$  is  $(1 - v/V)$ . The probability,  $P_0$ , for having *no* sphere center in a volume  $v$  after having placed  $N$  spheres independently into the container of volume  $V$  is given by  $[(V - v)/V]^N = [1 - (nv)/N]^N$ . As  $N$  and  $V$  are increased, holding  $n$  and  $v$  fixed, we find

$$P_0 = \lim_{N \rightarrow \infty} \left(1 - \frac{nv}{N}\right)^N = \exp(-nv) . \quad (3.13)$$

In an analogous fashion the probability for finding  $i$  centers in the volume  $v$  is

$$\begin{aligned} P_i &= \lim_{N \rightarrow \infty} \frac{N!}{i!(N-i)!} [(V - v)/V]^{N-i} [v/V]^i \\ &= \frac{(nv)^i}{i!} \exp(-nv) , \quad \text{for } i = 1, 2, \dots \end{aligned} . \quad (3.14)$$

This discrete probability law is the Poisson distribution valid for the *Poisson point process* placing points at random into a volume.

$$P_i = \frac{(nv)^i}{i!} \exp(-nv) \quad \text{Poisson distribution} \quad (3.15)$$

The probability that there are *no* points in a volume of radius  $\ell$  in  $d$ -dimensional space is

$$P_0(\ell) = \exp\{-c_d n \ell^d\} , \quad (3.16)$$

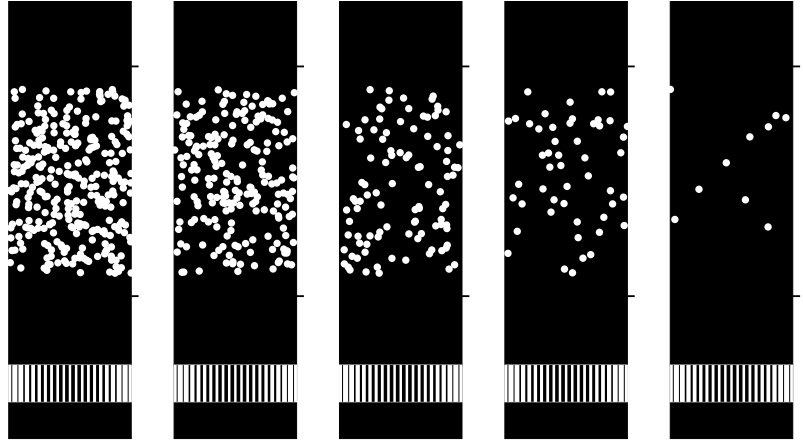


Figure 3.19: Quasi two-dimensional models of porous media used in permeability measurements. Fluid can flow in the black regions. The grid at the entrance is used to distribute the flow evenly over the channel cross section.

where the geometrical factor  $c_d$  is  $2, \pi$  and  $4\pi/3$  for one, two and three dimensions respectively. As a function of  $\ell$  equation (3.16) simply gives the fraction of distances between neighbors (that is, the distance between their centers) that are greater than  $\ell$ . Thus, the fraction of distances between points  $x < \ell$  is

$$P(x < \ell) = 1 - \exp\{-c_d n \ell^d\}. \quad (3.17)$$

This is also the *probability* to find a distance  $x < \ell$ . By differentiating this expression we find the probability distribution of distances (probability density) between particles

$$p(\ell) = d \cdot c_d \cdot n \cdot \ell^{d-1} \exp\{-c_d n \ell^d\}. \quad (3.18)$$

This result can be clarified by another derivation. To simplify the notation let us discuss the three-dimensional case. Let there be  $n = N/V$  particles per unit volume. The probability  $p(r)dr$  that the nearest neighbor to a particle occurs at a distance in the range  $[r, r+dr]$  must be the product of the probability that there are no particles within a sphere of radius  $r$  and that there is one particle in the spherical shell between  $r$  and  $r+dr$ .

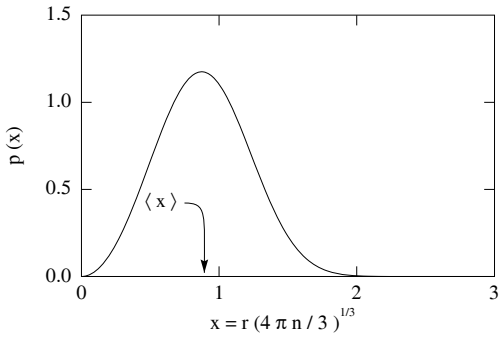


Figure 3.20: The probability density for the reduced distance  $x = r(4\pi n/3)^{1/3}$  to the nearest sphere in a three-dimensional Poisson porous medium with a number density  $n$  of spheres.

Therefore the function  $p(r)$  must satisfy the relation:

$$p(r) = \left(1 - \int_0^r p(r) dr\right) 4\pi r^2 n . \quad (3.19)$$

Taking the derivative of this equation with respect to  $r$ , we find

$$\frac{d}{dr} \left( \frac{p(r)}{4\pi r^2 n} \right) = -4\pi r^2 n \frac{p(r)}{4\pi r^2 n} , \quad (3.20)$$

which may be integrated

$$\int_1^{p(r)/4\pi r^2} \frac{d(p(r)/4\pi r^2)}{p(r)/4\pi r^2} = - \int_0^r 4\pi r^2 dr , \quad (3.21)$$

and we find

$$p(r) = 4\pi r^2 n \exp\{-4/3\pi r^3 n\} . \quad (3.22)$$

We find that the average distance to the nearest neighbor is

$$\langle r \rangle = \int_0^\infty r p(r) dr = \Gamma(4/3) \left( \frac{3}{4\pi n} \right)^{1/3} , \quad (3.23)$$

where  $\Gamma$  is the Gamma-function. The probability density for the distance to the nearest sphere in three-dimensions is shown in figure 3.20.

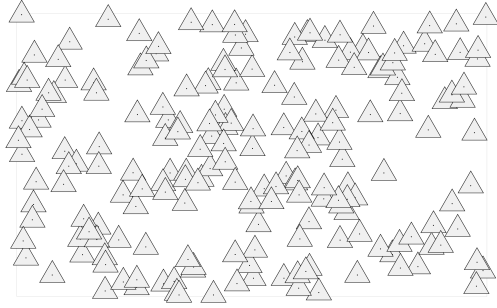


Figure 3.21: The porosity of aligned equilateral triangles with centers placed by a Poisson process.

### 3.5.2 Porosity of Overlapping (hyper) Spheres

As is usual in statistics, simpler expressions may be found by phrasing the questions carefully. Following Weissberg<sup>42</sup> and Strieder and Aris<sup>43</sup> we note that the porosity  $\phi$  is the probability that a random point is *not* contained by any sphere in the medium. Thus the porosity equals the probability that a randomly selected point in the porous medium has no sphere *center* within a distance  $a$  equal to the sphere radius. Therefore  $\phi$  is given by equation (3.13) with  $v = 4\pi a^3/3$  in three dimensions,

$$\phi = \exp \left\{ -n \frac{4\pi a^3}{3} \right\}, \quad d = 3. \quad (3.24)$$

This argument holds in any dimension for random packings of penetrable (hyper) spheres. The correct result in two-dimensions is

$$\phi = \exp \left\{ -n \pi a^2 \right\}, \quad d = 2. \quad (3.25)$$

We have checked that this formula works quite well even for rather small models as shown in figure 3.19.

### 3.5.3 Porosity of Overlapping Triangles

The subtlety of the argument just given is often overlooked. Therefore I introduce another example that is less trivial than the packing of disks. Consider the packing of aligned equilateral triangles illustrated in figure 3.21.

The centers of the triangles have the same positions as shown for the discs in figure 3.18, and they have the same area as the discs in that figure. Is the porosity the same? The argument again consists of several steps: (1) The porosity  $\phi$  is the probability that a point chosen at random is not inside one of the triangles. Equivalently, the porosity is the probability that a given fixed point is in pore space for an ensemble of realizations of the porous medium. (2) For any given point there is an exclusion region that cannot contain any of the triangle centers if the point is to be in pore space. The shape of the region is illustrated in figure 3.22; it is an inverted triangle that has the same area  $v_e$ , as the the triangles it excludes. (3) Choose a random point inside the volume  $V$ , that is, the area  $A$  illustrated in figure 3.22. (4) draw the exclusion volume  $v_e$ , that is, the inverted triangle. (5) Generate samples of Poisson porous media by placing  $N = nA$  aligned equilateral triangles on the area  $A$ , at random. (6) The probability that no triangle overlaps the exclusion volume is  $P_0 = \exp(-nv_e)$ . (7) By (1) we conclude that the porosity for the Poisson Porous medium of equilateral triangles is  $\phi = \exp(-nv_e)$ .

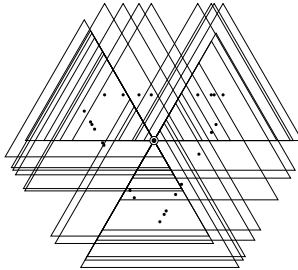


**Figure 3.22:** The centers of equilateral triangles (place by a Poisson point process) that touch, but do not cover a point selected at random.

### 3.5.4 Void-Void Correlation Function

The geometry of a porous medium is completely specified by the *characteristic function*  $\chi$

$$\chi(\mathbf{r}) = \begin{cases} 1 & \text{if } \mathbf{r} \in \text{pore space}, \\ 0 & \text{if } \mathbf{r} \in \text{solid matrix}. \end{cases} \quad (3.26)$$

The characteristic function cannot be determined in practice but a partial description can be obtained by considering various averages of  $\chi$ .<sup>42, 43, 45</sup> The characteristic function of the pore space clearly contains too much information to be of any practical interest except for well defined small models or periodic structures. The simplest average property is the *porosity*  $\phi$ , that is, the void fraction, given by

$$\phi = \langle \chi(\mathbf{r}) \rangle = \frac{1}{V} \int_V \chi(\mathbf{r}) d^3 r. \quad (3.27)$$

Information about the *structure* of the porous medium is contained in average of  $\chi(\mathbf{x})\chi(\mathbf{x} + \mathbf{r})$  with respect to  $\mathbf{x}$  for *fixed* separation  $\mathbf{r}$ . The resulting

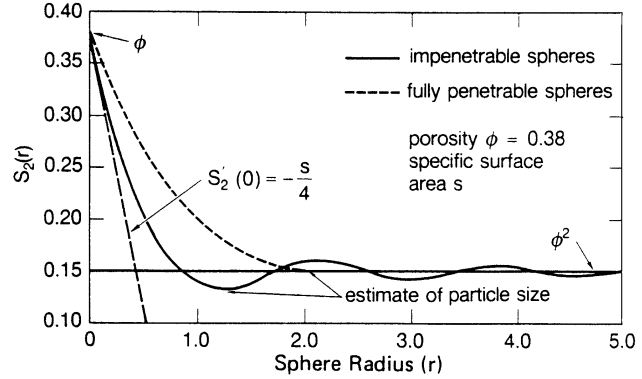


Figure 3.23: Two-point void-void correlation functions for model materials composed of penetrable and impenetrable spheres. Quantities that can be determined directly from the shape of the two-point correlation function include: (1) porosity, (2) specific surface area, and (3) mean particle size (if the size distribution is narrow so that exclusion volume effects are important). After Berryman and Blair [1].

Figure 3.23: Two-point void-void correlation functions for model materials composed of penetrable and impenetrable spheres.

average is the *void-void correlation function*  $G(\mathbf{r})$  defined by

$$G(\mathbf{r}) = \frac{1}{V} \int_V d^3x \chi(\mathbf{x})\chi(\mathbf{x} + \mathbf{r}). \quad (3.28)$$

The correlation function  $G(\mathbf{r})$  is the probability that a line segment, having a length and direction given by  $\mathbf{r}$ , placed at random in the porous medium will have *both* its ends in the pore space.

For a Poisson porous medium of spheres the probability that no sphere center is within a distance  $a$  from the end points of the line segment  $\mathbf{r}$  thrown at random into the medium is

$$G(\mathbf{r}) = e^{-nV_r} = \begin{cases} \exp \left[ -n \frac{4\pi a^3}{3} \left( 1 + \frac{3r}{4a} - \frac{r^3}{16a^3} \right) \right], & r < 2a, \\ \exp \left[ -n \frac{8\pi a^3}{3} \right] & , r > 2a. \end{cases} \quad (3.29)$$

where  $V_r$  is the volume covered by two spheres of radius  $a$  separated by a distance  $r = |\mathbf{r}|$ . Thus  $G(\mathbf{r})$  is the conditional probability (density) that for given a point in pore space, then the point at a distance  $\mathbf{r}$  is also in pore space.

The void-void correlation function satisfies several general relations (see references []): From the definition it follows immediately that

$$G(0) = \frac{1}{V} \int_V d^3x \chi(x)\chi(x) = \frac{1}{V} \int_V d^3x \chi(x) = \phi, \quad (3.30)$$

since  $\chi(x)^2 = \chi(x)$ .

In the limit  $r \rightarrow \infty$  the probability for being in the pore space at  $x$  is uncorrelated with the probability for being in the pore space at  $x + r$  and therefore we have

$$G(r \rightarrow \infty) = \phi^2. \quad (3.31)$$

These relations are satisfied by  $G(r)$  in equation (3.29) for the Poisson porous media.

There is an interesting relation between  $G(r)$  and the *specific surface*,  $S$ , the pore surface per unit volume

$$S = \frac{\text{Surface of pore space}}{\text{Total sample volume}}. \quad (3.32)$$

It can be shown that the following relation holds in general<sup>44, 47</sup>

$$S = -4 \left. \frac{\partial G(r)}{\partial r} \right|_{r=0}. \quad (3.33)$$

Note that Weissberg's expression, equation (3.29), satisfies the relations (3.30) and (3.31) and gives the following result for the specific surface for a *random packing of penetrable spheres*:

$$S = 4\pi a^2 n\phi = -\frac{3}{a}\phi \ln \phi, \quad (3.34)$$

where we have used equation (3.24) to express  $n$  in terms of the porosity. This result is also obtained by the following argument.<sup>43</sup> The specific surface of the spheres is  $S = 4\pi a^2 n$ . But only a fraction of this surface is exposed due to the overlap of spheres. The probability that a point in the surface is a neighbor to the void space is  $\phi$ , and equation (3.34) results.

Various results for relating to the void-void correlation function are illustrated in figure 3.23.

## Chapter 4

# Laminar Flow in Channels and Tubes

The Navier-Stokes equations that describe hydrodynamics have a relatively simple form. However, they are non-linear, a fact that gives rise to serious mathematical difficulties that tend to obscure the simple underlying physics. In this chapter I therefore discuss some simple examples of fluid flow that may be understood without the full mathematical apparatus. The simplification arises for very slow flows.

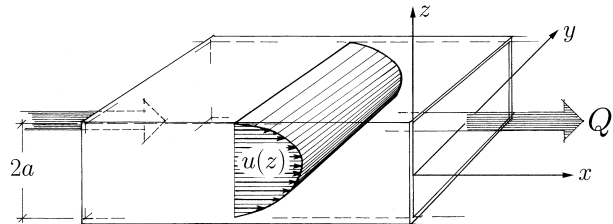


Figure 4.1: Flow in a channel. A flux  $Q$  per unit channel width gives rise to a parabolic velocity profile  $u(z)$  of the fluid along the  $x$ -direction.

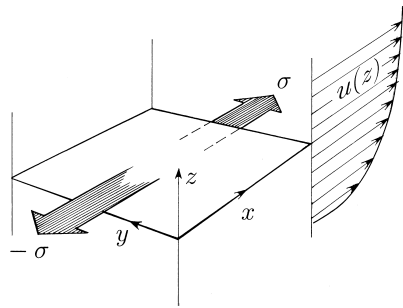


Figure 4.2: The shear forces per unit area,  $\sigma$ , due to a velocity gradient.

## 4.1 Laminar Flow in a Channel

One of the simplest hydrodynamic flow problems is the low velocity flow of a fluid through a channel of thickness  $2a$ , and a width so large that it may be considered to be infinite. In such a case the flow as indicated in the figure below, will be one-dimensional in the sense that the flow velocity  $\mathbf{u} = (u, 0, 0)$ , has a component only in the  $x$ -direction, and this component is a function of  $z$  only,  $\mathbf{u} = \mathbf{u}(z)$ .

We expect the velocity of the fluid to have its largest value at the center of the channel and decrease to zero at the walls. This expectation is based on our experience that fluids have a dissipation mechanism — the *viscosity* — that opposes velocity gradients. Qualitatively speaking, the faster fluid ( $z > z_0$ ) drags the slower fluid ( $z < z_0$ ) along (see figure 4.2) so that there is a force  $\sigma$  per unit area at  $z_0$ , acting in the direction of the flow. Similarly the slow fluid acts on the fast flow with an equal force but in the opposite direction.

It was *Newton's* assumption<sup>1</sup> that the stress, that is, (force/unit area),

<sup>1</sup>Newton (see []), in section IX of Book II: ‘Circular motion of Fluids’, opens with a ‘Hypothesis’, which reads: ‘... The resistance arising from the want of lubricity in the parts of a fluid is, other things being equal, proportional to the velocity with which the parts of the fluid are separated from one another ....’ Newton’s *defectus lubricitatis* is what we today call internal friction or viscosity. As discussed by Dowson,<sup>49</sup> viscosity is a word with an interesting roots: The Greek word *οἰξός* for misteltoe is related to viscosity since misteltoe berries contain a sticky substance, *viscin*, that was used as glue on twigs to catch birds. The word came to the modern form though Latin *viscositas*. Newton demonstrated that the idea that a viscous fluid in space could not explain the observed motion of the planets.

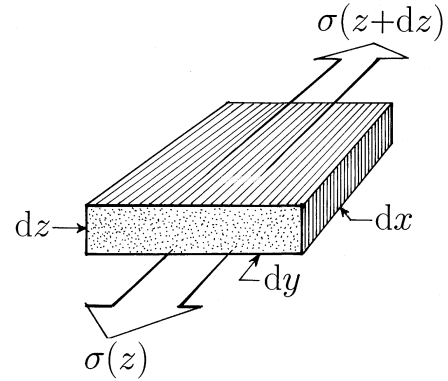


Figure 4.3: The shear forces acting on a volume element.

is given by

$$\sigma = \mu \frac{\partial u_x}{\partial z} \equiv \sigma_{xz}. \quad (4.1)$$

Where we have introduced the notation  $\sigma_{xz}$ , to indicate that the force (per unit area) acts in the  $x$ -direction on a surface that has a surface normal in the  $z$ -direction. Fluids that do not satisfy this *assumption* are called non-Newtonian fluids. The constant of proportionality,  $\mu$ , in equation (4.1), is called the *viscosity* of the fluid. From the equation we see that  $\mu$  has the dimension

$$[\mu] = \frac{\text{force/area}}{\text{velocity/distance}} = \text{Ns m}^{-2} = \text{Pas}, \quad (4.2)$$

in the SI system. The corresponding unit in the cgs system is poise = dyn s/cm<sup>2</sup>. The viscosity of water at 20 °C is 0.01 poise = 1 cP. In many situations the *kinematic viscosity*  $\nu$  defined by  $\nu = \mu/\rho$  with the dimension  $[\nu]=\text{m}^2/\text{s}$  is the more useful quantity.

Now consider the forces on a volume element as indicated in figure 4.3. The net force in the  $x$ -direction due to the viscosity terms is<sup>2</sup>

$$\left[ \mu \left( \frac{\partial u}{\partial z} \right)_{z+dz} - \mu \left( \frac{\partial u}{\partial z} \right)_z \right] dx dy dz = \mu \left( \frac{\partial^2 u}{\partial z^2} \right) dx dy dz. \quad (4.3)$$

The fluid is driven through the channel by a difference in the pressure at the entrance and at the exit of the channel. Supposing that the pressure

<sup>2</sup>There should also be forces in the  $z$ -direction, otherwise the fluid element will rotate. We will give a more complete derivation in the following sections.

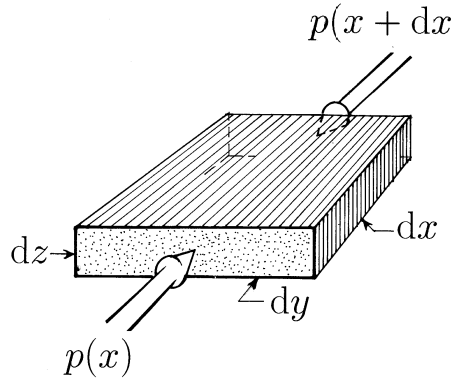


Figure 4.4: The forces on a fluid element due to a pressure gradient.

varies only in the  $x$ -direction the forces due to the pressure gradient act as indicated in figure 4.4. The net force on the fluid element due to the pressure gradient is then

$$[p(x) - p(x + dx)] dydz = - \left( \frac{\partial p}{\partial x} \right) dx dy dz. \quad (4.4)$$

With stationary flow each volume element flows without acceleration so that there is no net force on the volume element. Therefore we must require the following balance equation

$$\mu \left( \frac{\partial^2 u}{\partial z^2} \right) - \frac{\partial p}{\partial x} = 0. \quad (4.5)$$

Introducing the pressure gradient  $G$  by

$$G = - \frac{\partial p}{\partial x} = \frac{p(0) - p(L)}{L} = \frac{\Delta p}{L}. \quad (4.6)$$

Assuming that  $u$  is independent of  $y$ - and  $z$ , we see that the solution of equation (4.5) gives the velocity profile:

$$u(z) = \frac{G}{2\mu} (a^2 - z^2). \quad (4.7)$$

This is the classical parabolic velocity profile of flow in a channel, and we see that it is consistent with the boundary condition  $u(z = \pm a) = 0$ , at the surface of the channel.

The average speed of the flow is easily found by the expression

$$\langle u \rangle = \frac{1}{2a} \int_{-a}^a u(z) dz = \frac{a^2}{3\mu} \cdot G = \frac{2}{3} u_{\max}. \quad (4.8)$$

The volume of fluid passing through the channel per unit time and per unit length in the  $y$ -direction is then

$$Q = \int_{-a}^a u dz = \frac{2a^3}{3\mu} \frac{\Delta p}{L}. \quad (4.9)$$

## 4.2 Lubrication

### 4.2.1 Reynolds' Description of Lubrication

In a classical paper Osborne Reynolds<sup>50</sup> introduced the central ideas that form the foundation of the theory of lubrication.<sup>51</sup> Reynolds first gave a qualitative discussion, with very clear illustrations, before he proceeded with the analytical calculations using Stokes' equations. Reynolds' illustrations require detailed explanations that are best given in his own words. The problem he addressed is defined in figure 4.5. There are several special cases. First let the plates be parallel move AB to the left with a velocity  $U$ , see figure 4.6. Reynolds explained: ‘...there will be a tangential resistance

$$F = \mu \frac{U}{h}$$

per unit area, and the tangential velocity will vary uniformly from  $U$  at AB to zero at CD. Thus if FG be taken to represent  $U$ , then PN will represent the velocity in the fluid at P. The slope of the line EG therefore may be



Figure 4.5: Two nearly parallel surfaces separated by a viscous fluid. AB and CD are perpendicular sections of great extent compared with the distance  $h$  separating the surfaces, both surfaces being of unlimited length in the direction perpendicular to the paper (after Reynolds [1]).

Figure 4.5: Two nearly parallel surfaces separated by a viscous fluid. AB and CD

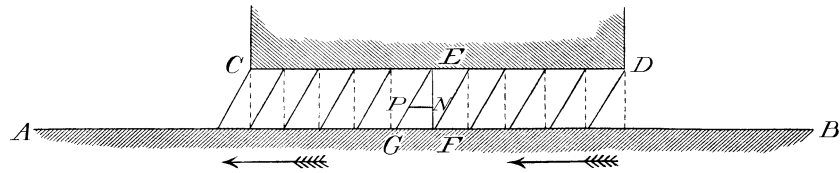


Figure 4.6: Case 1: Two parallel surfaces separated by a viscous fluid. AB moves to the left with a velocity  $U$  (after Reynolds [1]).

Figure 4.6: Case 1: Two parallel surfaces separated by a viscous fluid. AB moves to the left with a velocity  $U$  (after Reynolds [1])

taken to represent the force  $F$ , and the direction of the tangential force on either side is the same as if EG were in tension. The sloping lines therefore represent the condition of motion and stress throughout the film.'

He then went on to discuss another special case, see figure 4.7. 'The fluid has to be squeezed out between the surfaces, and since there is no motion at the surface, the horizontal velocity outward will be greatest half-way between the surfaces, nothing at O the middle of CD, and greatest at the ends. If at a certain stage of motion (shown by the dotted line, figure 4.7) the space between AB and CD be divided in 10 equal parts by vertical lines (figure 4.7, dashed vertical lines), and these lines supposed to move with the fluid, they will shortly after assume the positions of curved lines (figure 4.7), in which the areas included between each pair of curved lines is the same as in the dotted figure. In this case, as in Case 1, the distance QP will represent the motion at any point P, and the slope of lines

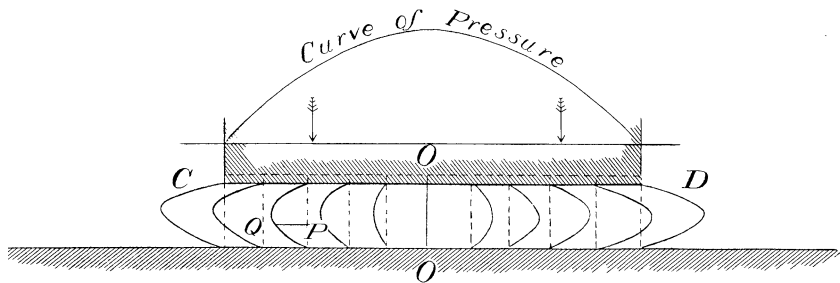


Figure 4.7: Case 2: Two parallel surfaces separated by a viscous fluid approaching with no tangential motion (after Reynolds [1]).

Figure 4.7: Case 2: Two parallel surfaces separated by a viscous fluid approaching with no tangential motion (after Reynolds [1])

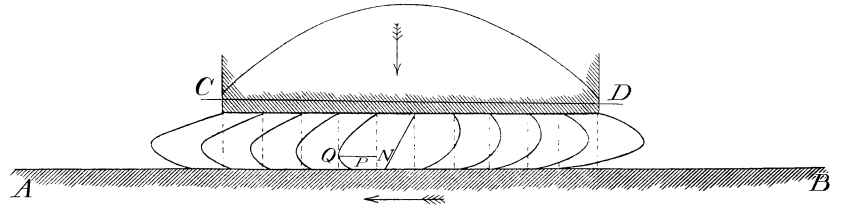


Figure 4.8: Case 3: Two parallel surfaces separated by a viscous fluid approaching with tangential motion (after Reynolds [1]).

Figure 4.8: Case 3: Two parallel surfaces separated by a viscous fluid approaching

will represent the tangential forces in the fluid as if the lines were stretched elastic strings. It is immediately seen that the fluid will be pulled toward the middle of CD by the viscosity as though by the stretched elastic lines, and hence that the pressure will be greatest at O and fall off towards the ends C and D, and would be approximately represented by the curve at the top of the diagram'

The next case Reynolds discussed was a *superposition* of the two previous cases, that is, parallel surfaces approaching with tangential motion. Since the Stokes' equations, which are the hydrodynamic equations for lubrication, are linear equations the solutions satisfy the superposition principle. This third case is illustrated in figure 4.8. 'The lines representing the motion in Cases 1 and 2 may be superimposed by adding the distances PQ in figure 4.7 to the distances in figure 4.6.

The result will be as shown in figure 4.8, in which the lines represent in the same way as before the stresses in the fluid where the surfaces are approaching with tangential motion.

In this case the distribution of pressure over CD is nearly the same as in Case 2, and the mean tangential forces will be the same as in Case 1. The distribution of the friction over CD will, however, be different. This is shown by the inclination of the curves at the points where they meet the surface. Thus on CD the slope is greater on the left and less on the right, which shows that the friction will be greater on the left and less on the right than in Case 1. On AB the slope is greater on the right and less on the left, as is also the friction.'

Now we come to the case of practical interest, that is, the situation illustrated in figure 4.9 'Surfaces inclined with tangential movement only'. 'AB is in motion as in Case 1, and CD is inclined as in figure 4.9. The effect will be nearly the same as in the compound movement (Case 3).

For if corresponding to the uniform movement  $U$  of AB the velocity of the fluid varied uniformly from the surface AB to CD, then the quantity carried across any section PQ would be  $PQ \times \frac{1}{2}U$ , and consequently would be proportional to PQ; but the quantities carried across all sections must be the same, as they surfaces do not change their relative distances; therefore there must be a general outflow from any vertical section PQ, P'Q' given by  $\frac{1}{2}U(PQ - P'Q')$ . This outflow will take place to the right and left of the section of greatest pressure. Let this be  $P_1Q_1$ , then the flow past any other section PQ  $\frac{1}{2}U(PQ - P_1Q_1)$ , to the right or left according as PQ is to the right or left of  $P_1Q_1$ . Hence at this section the motion will be one of uniform variation, and to the right and left lines showing the motion will be nearly as in figure 4.8. This is shown in figure 4.10. The pressure of the intervening film of fluid would cause a force tending to separate the

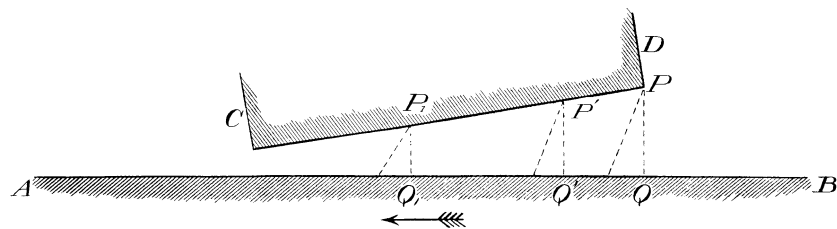


Figure 4.9: Case 4: Two inclined surfaces separated by a viscous fluid with tangential motion (after Reynolds [1]).

Figure 4.9: Case 4: Two inclined surfaces separated by a viscous fluid with tangential motion (after Reynolds [1]).

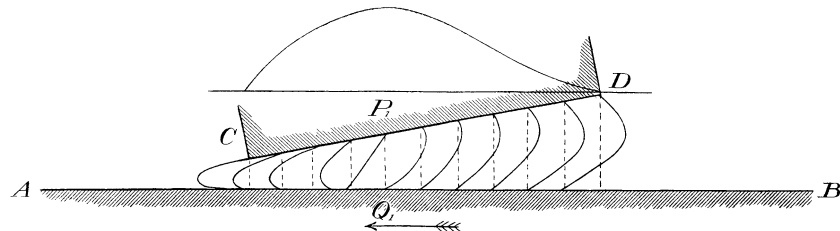


Figure 4.10: Case 4: Two inclined surfaces separated by a viscous fluid with tangential motion. The top curve represents the pressure, whereas the flow lines represent fluid velocities and stresses (after Reynolds [1]).

Figure 4.10: Case 4: Two inclined surfaces separated by a viscous fluid with tangential motion. The top curve represents the pr

surfaces. The mean line or resultant of this force would act through some point O. This point O does not necessarily coincide with P<sub>1</sub> the point of maximum pressure. For equilibrium of the surface AB, O will be in the line of the resultant external force urging the surfaces together, otherwise the surface ACD would change its inclination.

The resultant pressure must also be equal to the resultant external force perpendicular to AB (neglecting the obliquity of CD). If the surfaces were free to approach the pressure would adjust itself to the load, for nearer the surfaces the greater would be the friction and consequent pressure for the same velocity, so that the surfaces would approach until the pressure balanced the load.

As the distance between the surfaces diminished O would change its position, and therefore, to prevent an alteration of inclination, the surface CD must be constrained so that it could not turn around.

It is to be noticed that continuous lubrication between the plane surfaces can only take place with continuous motion in one direction, which is the direction of continuous inclination of the surfaces.

With reciprocating motion, in order that there may be continuous lubrication, the surfaces must be other than plane.'

Reynolds then discussed the lubrication of revolving cylindrical surfaces as used for railroad wheel bearing. This will, however, take us too far from the subject of simple hydrodynamics for the purposes of flow in porous media. Suffice to say that Reynolds' paper defined a new scientific field of great practical importance. I have quoted Reynolds qualitative discussion to show that complicated hydrodynamics may sometimes be understood without the complicated equations.

#### 4.2.2 Lubrication — an Analysis

As an example of the analytical treatment of lubrication let us consider the situation illustrated in figure 4.6. I follow Batchelor's treatment in [], and take the positive  $x$ -axis to be to the left in figure 4.10 with the  $z$ -axis vertical.

Let the bottom plate move with velocity  $U$  in the positive  $x$ -direction relative to the fixed top plate, that is, to the left in figure 4.10. The flow again satisfies equation (4.5) and the solution

$$u = \frac{h-z}{h} U - \frac{z(h-z)}{2\mu} \left( \frac{\partial p}{\partial x} \right). \quad (4.10)$$

Here  $h$  is the plate separation. This solution satisfied the *no slip boundary condition* which sets  $\mathbf{u} = 0$  at the stationary wall, and  $\mathbf{u} = (U, 0, 0)$  at the moving wall AB. This type of flow has a constant<sup>3</sup> velocity gradient  $\partial u / \partial z = -U/h$ , and we conclude from the definition (4.1) that the force per unit area along the wall surface is  $\sigma = \mu U/h$ .

The volume flow rate through this channel is (per unit channel length)

$$Q = \int_0^h u(z) dz = \left( \frac{h}{2} U - \frac{h^3}{12\mu} \left( \frac{\partial p}{\partial x} \right) \right). \quad (4.11)$$

Now consider the situation illustrated in figure 4.10 where the fixed block has a slight angle  $\alpha = (h_D - h_C)/L$  relative to the moving bottom plate, that is,  $dh = -\alpha dx$ . Here  $h_C$  and  $h_D$  are the heights of the block CD at C and D respectively and  $h_D > h_C$ . The pressure,  $p(x)$ , is now a nonlinear function of position. The pressure in the fluid at the entry and at the exit of the narrow lubricating channel must vanish, that is,  $p(0) = p(L) = 0$ . At some position  $x_0$  in the channel the pressure has an extreme value  $p_0 = p(x_0)$ . For incompressible flow the volume flow rate of the fluid is constant and since by definition  $dp/dx|_{x_0} = 0$  at  $x_0$  it follows from equation (4.11) that

$$Q_0 = \frac{h_0}{2} U - \frac{h_0^3}{12\mu} \left. \frac{\partial p}{\partial x} \right|_{x_0} = \frac{h}{2} U - \frac{h^3}{12\mu} \frac{\partial p}{\partial x},$$

and it follows (since  $\left. \frac{\partial p}{\partial x} \right|_{x_0} = 0$ ) that

$$h^3 \frac{\partial p}{\partial x} = 6\mu U (h - h_0). \quad (4.12)$$

We may integrate this equation using that  $dp/dx = -\alpha dp/dh$  to obtain the result

$$p = \frac{6\mu U}{\alpha} \left( \frac{1}{h} - \frac{1}{h_D} - \frac{h_0}{2h^2} + \frac{h_0}{2h_D^2} \right). \quad (4.13)$$

Here  $h_0 = h(x_0)$  may be determined by noting that  $p(h_C) = 0$ , which when inserted into equation (4.13) gives

$$h_0 = 2 \frac{h_C h_D}{h_C + h_D}. \quad (4.14)$$

---

<sup>3</sup>The  $\frac{\partial p}{\partial x}$  term is given by equation (4.12) and vanishes when  $h = h_0$ , that is, the block is parallel with the surface.

We may now calculate the vertical force on the block per unit width of the block:

$$F_{\perp} = \int_0^L p(x)dx = -\alpha^{-1} \int_{h_D}^{h_C} p(h)dh . \quad (4.15)$$

By partial integration this integral may be transformed into

$$F_{\perp} = -\frac{1}{\alpha} \int_{h_1}^{h_2} h \frac{dp}{dh} dh . \quad (4.16)$$

Using equation (4.12) the vertical force, on both surfaces, is found to be

$$F_{\perp} = \frac{6\mu U}{\alpha^2} \left\{ \ln \left( \frac{h_D}{h_C} \right) - 2 \left( \frac{h_D - h_C}{h_D + h_C} \right) \right\} . \quad (4.17)$$

This expression is seen to give a force lifting the fixed block provided that  $h_1 > h_2$ , that is,  $\alpha < 0$ . Let  $\Delta h = h_D - h_C$  and  $\langle h \rangle = (h_D + h_C)/2$ . Then for  $(\Delta h/\langle h \rangle) \ll 1$  the logarithm in equation (4.17) may be expanded and the lifting force expressed by

$$F_{\perp} \simeq \frac{\mu U}{2\alpha^2} \cdot \left( \frac{\Delta h}{\langle h \rangle} \right)^3 , \quad \text{for} \quad \frac{|\Delta h|}{\langle h \rangle} \ll 1 . \quad (4.18)$$

Thus if a heavy load is supported by a lubricating film on a moving surface the film must be thin. Increasing the viscosity of the lubricant and increasing the velocity also increases the load carrying capability.<sup>4</sup>

The drag force on AB may be calculated using equation (4.12) in equation (4.10) to evaluate the velocity gradient  $\frac{\partial u}{\partial z}$

$$F_{\parallel} = \int_0^L \mu \left( \frac{\partial u}{\partial z} \right)_{z=0} = -\frac{2\mu U}{\alpha} \left\{ 2 \ln \left( \frac{h_D}{h_C} \right) - 3 \left( \frac{h_D - h_C}{h_D + h_C} \right) \right\} . \quad (4.19)$$

The drag force on the block CD is:

$$F_{\parallel} = - \int_0^L \mu \left( \frac{\partial u}{\partial z} \right)_{z=0} = -\frac{2\mu U}{\alpha} \left\{ \ln \left( \frac{h_D}{h_C} \right) - 3 \left( \frac{h_D - h_C}{h_D + h_C} \right) \right\} . \quad (4.20)$$

The two tangential forces are not equal and opposite because the normal force on one plane has a small component parallel to the other plane. In the limit of small  $\Delta h/\langle h \rangle$  we find in both cases that:

$$F_{\parallel} \simeq \frac{\mu U}{\alpha} \frac{\Delta h}{\langle h \rangle} . \quad (4.21)$$

---

<sup>4</sup>See Batchelor [], p. 220.

The ratio of the drag force to the lifting force is an effective coefficient of friction:

$$\mu_{\text{friction}} = \frac{F_{\parallel}}{F_{\perp}} = \alpha g(h_D/h_C) \simeq 2\alpha \left( \frac{\langle h \rangle}{\Delta h} \right)^2. \quad (4.22)$$

The ratio of the drag force along the surface to the lifting force independent of velocity and viscosity, and depends only on the angle  $\alpha$  and a function,  $g$ , of the ratio  $h_D/h_C$  which in the limit  $\Delta h/\langle h \rangle \ll 1$ , has the simple form given in equation (4.22). In the discussion given above we assumed  $\alpha$  to be fixed. However, for a block that is free to slide under a given load, both  $\alpha$  and  $\langle h \rangle$  will adjust. If  $\Delta h/\langle h \rangle \simeq 1$ , then the coefficient of friction has an order of magnitude of  $\alpha \simeq \langle h \rangle/L$ , which can be made arbitrarily small by reducing  $\langle h \rangle$ . In practice the surfaces are not atomically smooth but have a self-affine fractal surface roughness, and contact between the surfaces arise on the atomistic level.

### 4.3 Laminar Flow in a Pipe

The flow in a tube with a cylindrical cross section at low velocities was investigated experimentally by Hagen<sup>52</sup> (1838) and by Poiseuille<sup>53</sup> (1840) and justified theoretically by G. G. Stokes<sup>54</sup> (1845). The flow is called *Hagen-Poiseuille* flow. In this case we must assume that the flow in a tube of length  $L$  is everywhere directed along the axis of the tube and that the magnitude of the velocity  $u(r)$ , depends only on the distance,  $r$ , from the axis. Again we consider the forces on a volume element that now has the form indicated in figure 4.11.

The net force due to the viscosity is now

$$\begin{aligned} & \mu \left[ \left( \frac{\partial u}{\partial r} \right)_{r+dr} (r + dr) - \left( \frac{\partial u}{\partial r} \right)_r r \right] d\varphi dx \\ &= \mu \left[ \left( r \frac{\partial u}{\partial r} \right)_{r+dr} - \left( r \frac{\partial u}{\partial r} \right)_r \right] d\varphi dx \quad (4.23) \\ &= \mu \frac{\partial}{\partial r} \left( r \frac{\partial u}{\partial r} \right) dr d\varphi dx \end{aligned}$$

The pressure contributes a term given by:

$$[p(x) - p(x + dx)]rd\varphi dr = Grd\varphi drdx \quad (4.24)$$

Equating these two terms gives a differential equation for the velocity

$$\mu \frac{\partial}{\partial r} \left( r \frac{\partial u}{\partial r} \right) = r \frac{\partial p}{\partial x} = -Gr. \quad (4.25)$$

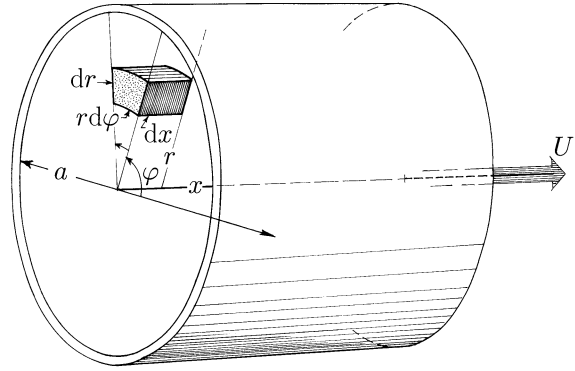


Figure 4.11: The fluid element in pipe flow.

If we try the solution

$$u(r) = -\frac{G}{4\mu}r^2 + A \ln r + B , \quad (4.26)$$

it is easily seen to satisfy the flow equation (4.25). However, we must choose  $A = 0$ , in order to avoid an infinite velocity at the center of the tube. Also if we make the reasonable assumption that the velocity is zero exactly at the tube wall we obtain the result

$$u(r) = \frac{G}{4\mu}(a^2 - r^2) = u_{\max} (1 - (r/a)^2) . \quad (4.27)$$

The velocity profile is parabolic with a maximum velocity given by

$$u_{\max} = \frac{Ga^2}{4\mu} . \quad (4.28)$$

There are a few quantities that we will need later which are easily calculated for this type of flow. The volume flow rate  $Q$  is given by

$$Q = \int_0^a u 2\pi r dr = \frac{\pi G}{8\mu} a^4 = \frac{\pi a^4}{8\mu} \left( -\frac{\partial p}{\partial x} \right) , \quad (4.29)$$

as is easily seen by evaluating the integral. This dependence of the mass flow rate  $Q$  on the pressure gradient  $G = |\Delta p|/L$  was established experimentally by G. Hagen<sup>52</sup> (1838) and by J. L. M. Poiseuille<sup>53</sup> (1840) and

derived theoretically by G. G. Stokes (1845). The Hagen-Poiseuille result was originally<sup>53</sup> written in the form

$$Q = B(1 + \alpha T + \beta T^2)hD^4/L \quad \text{Hagen-Poiseuille} \quad (4.30)$$

where  $D = 2a$  was the tube diameter,  $B$  a constant, and  $h$  the ‘head’, that is, the pressure difference over the length  $L$ .  $T$  was the temperature and  $\alpha$  and  $\beta$  coefficients found by fitting to the results obtained at various temperatures. The temperature dependence is due to the decrease of viscosity with increasing temperature and is consistent with modern results for water to within one-half percent.

Since  $Q$  depends on the cylinder radius,  $a$ , to the 4-th power we see that the pressure drop required to drive a given flow through a pore increases dramatically with decreasing radius.

The average flow velocity, that is, the velocity  $\langle u \rangle$  that would give the same  $Q$ , but with a constant velocity over the cross section of the tube is determined from the relation

$$Q = \pi a^2 \langle u \rangle, \quad (4.31)$$

with the result

$$\langle u \rangle = \frac{G}{8\mu} a^2 = \frac{1}{2} u_{\max}, \quad (4.32)$$

where  $u_{\max}$  is the maximum velocity in the tube, that is,  $u(r=0)$ . Note that this result differs from the result in equation (4.8) for channel flow.

For a tube with elliptical cross-section the flow equations may also be solved exactly. The resulting velocity profile<sup>5</sup>

$$u = \frac{(p_2 - p_1)}{2\mu L} \frac{a^2 b^2}{a^2 + b^2} \left(1 - \frac{y^2}{a^2} - \frac{z^2}{b^2}\right). \quad (4.33)$$

Here  $a$  and  $b$  are the minor and major axis of the ellipsoidal cross section of the tube. The discharge is found to be

$$Q = \frac{\pi(p_2 - p_1)}{4\mu L} \frac{a^3 b^3}{a^2 + b^2}. \quad (4.34)$$

It therefore follow that the average flow velocity,  $\langle u \rangle$  is given in terms of the maximum velocity

$$u_{\max} = \frac{(p_2 - p_1)}{2\mu L} \frac{a^2 b^2}{a^2 + b^2}, \quad (4.35)$$

---

<sup>5</sup>See Landau & Lifshitz *Fluid Mechanics*<sup>55</sup> p. 53.

by the expression

$$\langle u \rangle = \frac{1}{2} u_{\max}. \quad (4.36)$$

It is remarkable that this relation is *independent* of the ellipticity of the channel.

## Chapter 5

# The Hydrodynamic Equations

The basic equations of hydrodynamics rely on a continuum description of the systems of interest. A central role is played by conserved variables. For instance, in single component fluids the conservation of matter directly leads to the *continuity equation*. The conservation of energy as described by the first law of thermodynamics gives another equation. In more complicated systems the rotational motion of molecules and the conservation of angular momentum gives more equations. For fluid dynamics, however, the most important equation is *Newton's equation* relating the acceleration to the forces, that is, the conservation of momentum. In the following sections we shall derive the simplest form of the hydrodynamic equations.

### 5.1 The Continuity Equation

Consider a volume element *fixed* in space that has volume  $V$  and a surface  $S$  as indicated in figure 5.1. On every surface element of area  $dS$  we have an *outward* normal  $\mathbf{n}$  so that we may write the surface element as  $d\mathbf{S} = \mathbf{n}dS$ . The flow of the fluid is described by giving the velocity  $\mathbf{u} = \mathbf{u}(\mathbf{r}, t)$ , as function of position  $\mathbf{r}$ , and time  $t$ . This is the *Euler description*. A different description is obtained if one specifies the position,  $\mathbf{r}$ , of given fluid elements as a function of time by specifying  $\mathbf{r}(\mathbf{r}_0, t)$  given that it started at  $\mathbf{r}_0$  at time  $t_0$ . This is the *Lagrange description* and it is directly related to the *Euler description*.

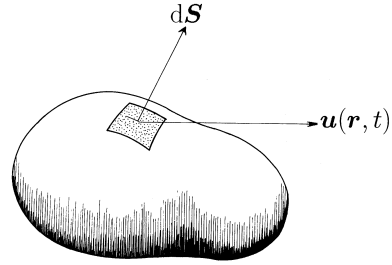


Figure 5.1: A fixed volume element in a velocity field  $\mathbf{u}$

With the fluid density given by  $\rho$  the *mass flux* is  $\mathbf{j} = \rho\mathbf{u}$ , which has the dimension  $[j] = \text{kg/m}^2\text{s}$ . The local mass flux out of the volume  $V$  is  $\mathbf{j}\cdot d\mathbf{S}$ . The rate of change of mass in the volume element is given by the difference in the mass flow into and the flow out of the volume:

$$\frac{d}{dt} \int_V \rho dV = - \int_S \rho \mathbf{u} \cdot d\mathbf{S} \quad (5.1)$$

Rate of increase of mass of fluid within  $V$       Rate of addition of mass across the surface  $S$

Here the fluid density is  $\rho = \rho(\mathbf{r}, t)$ . The volume is  $V$  and  $S$  its surface.  $d\mathbf{S}$  is an infinitesimal surface element with a direction given by the surface normal. In the limit of an infinitesimal volume element this equation becomes

$$\frac{\partial \rho}{\partial t} = - \lim_{V \rightarrow 0} \frac{1}{V} \int_S \rho \mathbf{u} \cdot d\mathbf{S} = - \nabla \cdot (\rho \mathbf{u}), \quad (5.2)$$

where we have used the definition<sup>1</sup> of the divergence operator  $\nabla \cdot$ . Thus the conservation of matter, equation (5.1), is equivalent to the differential equation

$$\frac{\partial \rho}{\partial t} + (\nabla \cdot \rho \mathbf{u}) = 0$$

(5.3)

which is the *continuity equation*.

## 5.2 Conservation of Momentum

The local volume flow of a fluid across the surface element  $dS$  is  $(\mathbf{n} \cdot \mathbf{u})dS$ . The *momentum per unit volume* of fluid is  $\rho\mathbf{u}$  and therefore we conclude

---

<sup>1</sup> Gauss's divergence theorem states that if  $V$  is a closed region with surface  $S$  then  $\int_V (\nabla \cdot \mathbf{u}) dV = \int_S (\mathbf{n} \cdot \mathbf{u}) dS$ , where  $\mathbf{n}$  is the outwardly directed unit normal vector.

that  $(\mathbf{n} \cdot \mathbf{u})\rho \mathbf{u} dS$  is the rate at which momentum is carried across the surface  $dS$  because of the fluid flow. This expression may be rearranged as  $[\mathbf{n} \cdot \rho \mathbf{u} \mathbf{u}]dS$ , and the quantity  $\rho \mathbf{u} \mathbf{u}$  is the *momentum flux*, that is, the momentum per unit area per unit time, convected with the fluid flow. The momentum flux is a tensor  $\{\rho \mathbf{u} \mathbf{u}\}$  a fact we emphasize with the notation<sup>2</sup>  $\{\dots\}$ .

In addition to the momentum transport by flow there will be momentum transfer due to molecular motion and interactions that will give rise to forces that change the momentum in the volume  $V$ .

In the simplest case of an *ideal fluid*, that is, for fluid flow where we may neglect *energy dissipation*, the force on the fluid element is simply given by the *pressure* and the the conservation of *momentum* corresponds to *Newton's law*:

$$\frac{d}{dt} \int_V \rho u dV = - \int_S \{\rho \mathbf{u} \mathbf{u}\} \cdot d\mathbf{S} - \int_S p dS + \int_V \rho \mathbf{g} dV$$

Rate of increase of momentum of fluid in $V$	Rate of addition of momentum across $S$ by convection	Force on fluid in $V$ by pressure	Force on fluid in $V$ by gravity
--	---	-----------------------------------	----------------------------------

(5.4)

Here  $\mathbf{g}$  is the acceleration of gravity. The Gauss divergence theorem applies also to scalars and tensors so that we have  $\int_S p d\mathbf{S} = \int_V [\nabla p] dV$  and  $\int_S \{\rho \mathbf{u} \mathbf{u}\} \cdot d\mathbf{S} = \int_V [\nabla \cdot \{\rho \mathbf{u} \mathbf{u}\}] dV$  so we obtain an equation involving only volume integrals. In the limit  $V \rightarrow 0$  we find *Euler's equation* for an ideal fluid ( that is, without viscosity):

$$\frac{\partial}{\partial t} [\rho \mathbf{u}] + [\nabla \cdot \{\rho \mathbf{u} \mathbf{u}\}] = -[\nabla p] + [\rho \mathbf{g}]$$

(5.5)

This equation was obtained by Euler (1755). Let us rewrite this equation into another form making use of the equation of continuity. First we remember the relation for the divergence of the dyadic  $\mathbf{ab}$ :

$$[\nabla \cdot \mathbf{ab}] = [\mathbf{a} \cdot \nabla \mathbf{b}] + \mathbf{b}(\nabla \cdot \mathbf{a}), \quad (5.6)$$

which is easily derived by writing the expression in Cartesian coordinates

---

<sup>2</sup>In this section we follow reference [] and use ( ) to indicate scalars such as  $(\mathbf{u} \cdot \mathbf{n})$ . A vector result of a multiplication is indicated by square brackets [ ] as in  $[\mathbf{n} \cdot \mathbf{u} \mathbf{u}]$  where  $\mathbf{u} \mathbf{u}$  is the *dyadic product*, that is, a second order *tensor* which for an arbitrary vector  $\mathbf{x}$  gives  $\{\mathbf{u} \mathbf{n}\} \cdot \mathbf{x} = \mathbf{u}(\mathbf{n} \cdot \mathbf{x})$ . Here we have used the notation  $\{\dots\}$  to denote second-order tensors.

defined by the *unit vectors*  $\mathbf{e}_i$  with  $i = 1, 2, 3$ .

$$\begin{aligned}
 \mathbf{ab} &= \sum_{jk} \mathbf{e}_j a_j b_k \mathbf{e}_k \\
 \nabla &= \sum_i \frac{\partial}{\partial x_i} \mathbf{e}_i \\
 [\nabla \cdot \mathbf{ab}] &= \sum_{ijk} \frac{\partial}{\partial x_i} \mathbf{e}_i \cdot \mathbf{e}_j a_j b_k \mathbf{e}_k \\
 &= \sum_{ik} \left( \frac{\partial}{\partial x_i} a_i b_k \right) \mathbf{e}_k \\
 &= \sum_i \left( \frac{\partial a_i}{\partial x_i} \right) \mathbf{b} + \sum_{ik} a_i \left( \frac{\partial b_k}{\partial x_i} \right) \mathbf{e}_k \\
 &= \mathbf{b}(\nabla \cdot \mathbf{a}) + [\mathbf{a} \cdot \nabla \mathbf{b}]
 \end{aligned} \tag{5.7}$$

Using this result we find that

$$[\nabla \cdot [\rho \mathbf{u}] \mathbf{u}] = [\rho \mathbf{u} \cdot \nabla \mathbf{u}] + \mathbf{u}(\nabla \cdot [\rho \mathbf{u}]) , \tag{5.8}$$

Here we may now use the equation of continuity (5.3) and find that

$$[\nabla \cdot [\rho \mathbf{u}] \mathbf{u}] = [\rho \mathbf{u} \cdot \nabla \mathbf{u}] - \mathbf{u} \frac{\partial \rho}{\partial t} . \tag{5.9}$$

This result may now be reinserted into equation (5.5) to give the Euler equation in another form:

$\rho \frac{\partial}{\partial t} \mathbf{u} + (\rho \mathbf{u} \cdot \nabla) \mathbf{u} = -[\nabla p] + \rho \mathbf{g}$

Euler (5.10)

valid for ideal fluids, that is, fluids flow for which dissipation may be neglected, and thus the viscosity is ignored.

### 5.2.1 The Substantive Derivative

In order to discuss the effect of acceleration on fluid elements (the Lagrange point of view) we must remember that when we specify the velocity field  $\mathbf{u}$  the particles in a fluid element may accelerate because the velocity field changes, that is,  $\partial \mathbf{u} / \partial t \neq 0$ , and also because the particles arrive at positions with a different velocity, that is,  $\partial \mathbf{u} / \partial \mathbf{r} \neq 0$ . For simplicity consider the variation of some scalar quantity such as the temperature  $T$  or density  $\rho$ . The change in temperature of a fluid element is given by

$$\delta T = \frac{\partial T}{\partial t} \delta t + \frac{\partial T}{\partial x} \delta x + \frac{\partial T}{\partial y} \delta y + \frac{\partial T}{\partial z} \delta z , \tag{5.11}$$

and consequently we have

$$\frac{\delta T}{\delta t} = \frac{\partial T}{\partial t} + \frac{\partial T}{\partial x} \frac{\delta x}{\delta t} + \frac{\partial T}{\partial y} \frac{\delta y}{\delta t} + \frac{\partial T}{\partial z} \frac{\delta z}{\delta t} . \tag{5.12}$$

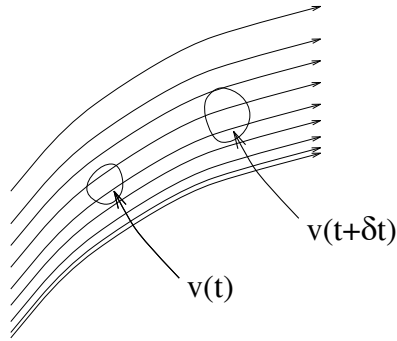


Figure 5.2: A small fluid element of volume  $v$  is convected and deformed by the velocity field  $\mathbf{u}(\mathbf{r}, t)$ . Ignoring diffusion the mass inside  $v(t)$  does not change.

Now we choose  $(\partial x / \partial t, \partial y / \partial t, \partial z / \partial t)$  to be given by the velocity  $\mathbf{u}$ , that is, we evaluate the change in  $T$  at a position in space that is precisely the position occupied by the fluid element at a later time due to the *convection* prescribed by the velocity field  $\mathbf{u}$  (the Lagrangian point of view). Since we get an equation of the form (6.5) for each and every component of a tensor the general effect is described by introducing the *substantive derivative*

$$\boxed{\frac{D}{Dt} = \frac{\partial}{\partial t} + \mathbf{u} \cdot \nabla} \quad (5.13)$$

*Newton's equation* specifies that the rate of change of the momentum equals the force. The mass in a small (Lagrangian) volume  $v$  is  $m = \rho v$ , and the momentum of this mass is  $m\mathbf{u}(\mathbf{r}, t)$ . This mass is convected with the fluid, therefore the rate of change of the momentum is  $mD\mathbf{u}(\mathbf{r}, t)/Dt$ . The choice of the small Lagrangian volume is arbitrary, therefore the rate of change of momentum, per unit volume is  $\rho D\mathbf{u}(\mathbf{r}, t)/Dt$ , which is given by

$$\boxed{\rho \frac{D\mathbf{u}}{Dt} = \rho \frac{\partial \mathbf{u}}{\partial t} + \rho \mathbf{u} \cdot \nabla \mathbf{u}} \quad (5.14)$$

which is also the left hand side of Euler's equation (5.10). The force density is

$$\mathbf{f} = -\nabla p + \mathbf{f}_\mu + \mathbf{F}, \quad (5.15)$$

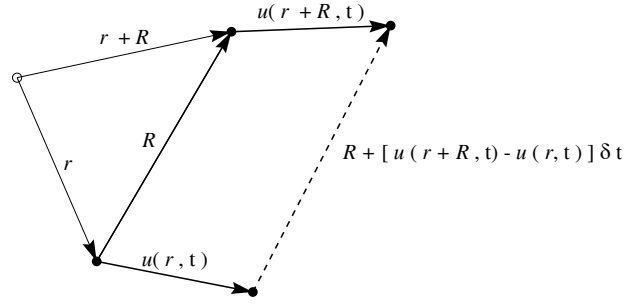


Figure 5.3: The velocity field at neighboring positions.

where  $\mathbf{f}_\mu$  is the viscous force, to be discussed later. We conclude that Newton's equation of motion leads to:

$$\boxed{\rho \frac{\partial}{\partial t} \mathbf{u} + (\rho \mathbf{u} \cdot \nabla) \mathbf{u} = -[\nabla p] + \mathbf{f}_\mu + \rho \mathbf{g}} . \quad (5.16)$$

Here the first term on the right hand side is simply the effect of a pressure gradient discussed earlier. The last term represents forces due to fields such as gravity  $\mathbf{F} = m\mathbf{g}$ . The middle term is due to viscosity. This term requires special attention and we discuss it in the following section.

### 5.2.2 The Rate of Strain Tensor

Consider two points in a fluid separated by a vector distance  $\mathbf{R}$  as indicated in figure 5.3. We expect the dissipation and the viscosity in a fluid to be related to the change in *relative* position of the fluid particles since there is no dissipation for a fluid at rest, in uniform translation or rotation. The change in relative position can be expressed by the *substantive derivative* of the square distance between neighboring fluid particles:

$$\frac{D}{Dt}(\mathbf{R})^2 = \sum_{i=1}^3 2R_i \frac{DR_i}{Dt} . \quad (5.17)$$

After a time increment  $\delta t$  the particles originally at  $\mathbf{r}$  and at  $\mathbf{r} + \mathbf{R}$  are separated by

$$\mathbf{R}(t + \delta t) = [\{\mathbf{r} + \mathbf{R}(t)\} + \delta t \mathbf{u}(\mathbf{r} + \mathbf{R}(t), t)] - [\mathbf{r} + \delta t \mathbf{u}(\mathbf{r}, t)] . \quad (5.18)$$

Therefore the change in  $\mathbf{R}$  is

$$\delta\mathbf{R} = [\mathbf{u}(\mathbf{r} + \mathbf{R}, t) - \mathbf{u}(\mathbf{r}, t)] \delta t. \quad (5.19)$$

But we may write

$$u_i(\mathbf{r} + \mathbf{R}) = u_i + \sum_{j=1}^3 \frac{\partial u_i}{\partial x_j} R_j, \quad (5.20)$$

and find

$$\frac{DR_i}{Dt} = \frac{\delta R_i}{\delta t} = \sum_{j=1}^3 \frac{\partial u_i}{\partial x_j} R_j. \quad (5.21)$$

We therefore conclude that

$$\frac{1}{2} \frac{1}{R^2} \frac{DR^2}{Dt} = \sum_{i,j=1}^3 \left( \frac{R_i}{R} \right) e_{ij} \left( \frac{R_j}{R} \right), \quad (5.22)$$

where we have introduced the *rate of strain tensor*  $e$  given by

$$e_{ij} = \frac{1}{2} \left( \frac{\partial u_i}{\partial x_j} + \frac{\partial u_j}{\partial x_i} \right). \quad (5.23)$$

This tensor has the same form as the strain tensor well known from the theory of elasticity. However, for hydrodynamics the local displacements are replaced by the local fluid velocities. equation (5.22) is a quadratic form, and we may take the limit  $R \rightarrow 0$  without difficulty.

If the velocity is a constant, as is the case when the fluid in its container moves rigidly, then  $e = 0$ , and no dissipation is expected. If instead, the container and the fluid rotates as a rigid body we again expect no dissipation. In this case with a given angular velocity  $\boldsymbol{\Omega}$ , the velocity field is given by

$$\mathbf{u} = \boldsymbol{\Omega} \times \mathbf{r} = \Omega(-y, x, 0), \quad (5.24)$$

and we again find that all the components of  $e = 0$ . We therefore conclude that we expect the dissipation to depend only on  $e$ .

### 5.3 The Stress Tensor

In order to describe forces on fluid elements we introduce the *stress tensor* in the same way as in the theory of elasticity. As illustrated in figure 5.4 the stress tensor  $\boldsymbol{\sigma}$  specifies the force  $\sigma_{ij}$  per unit area in the  $i$ -direction

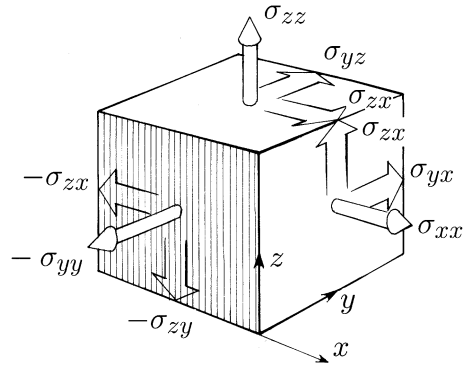


Figure 5.4: The various components of the stress tensor.

on a surface with a normal in the positive  $j$ -direction. Since tensors are invariant under rotations of the coordinate system we can easily obtain the forces on a surface element oriented in any direction. The fundamental assumption is that for *Newtonian fluids* the stress tensor  $\boldsymbol{\sigma}$  is proportional to the rate of strain tensor  $\mathbf{e}$ :

$$\sigma_{ij} = \sum_{kl} \Lambda_{ijkl} e_{kl} . \quad (5.25)$$

This is Newton's assumption, and it has the same form for elastic solids, only that here the fourth order viscosity tensor  $\boldsymbol{\Lambda}$  replaces the fourth order elastic constant tensor  $\mathbf{C}$  in the theory of elasticity. The tensor  $\boldsymbol{\Lambda}$ , is characteristic of the *isotropic* fluid and therefore it must have the symmetry of the fluid *at rest*. This condition greatly reduces the number of independent components of the  $3 \times 3 \times 3 \times 3 = 81$  component  $\boldsymbol{\Lambda}$  tensor. There are only three independent coefficients:

$$\Lambda_{ijkl} = \lambda \delta_{ij} \delta_{kl} + \xi \delta_{ik} \delta_{jl} + \chi \delta_{il} \delta_{jk} . \quad (5.26)$$

Therefore we may write the stress tensor in the form

$$\boxed{\sigma_{ij} = \lambda \delta_{ij} (e_{11} + e_{22} + e_{33}) + (\xi + \chi) e_{ij}} = \lambda \delta_{ij} \nabla \cdot \mathbf{u} + 2\mu e_{ij} \quad (5.27)$$

Here we have expressed the viscosity  $\mu$  in terms of the phenomenological constants  $\xi$  and  $\chi$  by

$$\mu = \frac{1}{2}(\xi + \chi) , \quad (5.28)$$

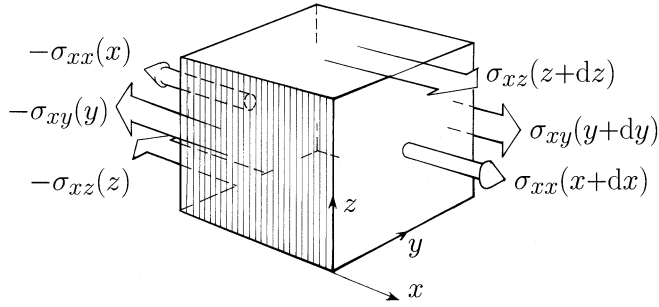


Figure 5.5: The stresses on a volume element.

and used that  $\nabla \cdot \mathbf{u} = e_{11} + e_{22} + e_{33}$ . The  $\lambda$  term is the *bulk viscosity* and it is related to dissipation effects that arise when the density changes as for instance in longitudinal sound waves.

Now consider the forces in the  $x$ -direction on a small volume element due to viscous stresses as indicated in figure 5.5. The pressure terms are written explicitly in equation (5.16), but could have been included in the stress terms. We find by summing the contributions of the viscous stresses on all the 6 sides of the volume element that the total viscous force in the  $x$ -direction is

$$\begin{aligned} F_{\mu,x} &= (\sigma_{xx}(x+dx) - \sigma_{xx}(x))dydz \\ &+ (\sigma_{xy}(y+dy) - \sigma_{xy}(y))dxdz \\ &+ (\sigma_{xz}(z+dz) - \sigma_{xz}(z))dxdy. \end{aligned} \quad (5.29)$$

The force per unit volume is therefore

$$f_{\mu,x} = \frac{\partial \sigma_{xx}}{\partial x} + \frac{\partial \sigma_{xy}}{\partial y} + \frac{\partial \sigma_{xz}}{\partial z}. \quad (5.30)$$

For an arbitrary direction the above argument gives

$$\begin{aligned} f_{\mu,i} &= \sum_{j=1}^3 \frac{\partial}{\partial x_j} \sigma_{ij} = \sum_{j=1}^3 \frac{\partial}{\partial x_j} (\lambda \delta_{ij} (e_{11} + e_{22} + e_{33}) + (\xi + \chi) e_{ij}) \\ &= \lambda \sum_{j=1}^3 \frac{\partial}{\partial x_j} \delta_{ij} \nabla \cdot \mathbf{u} + \mu \sum_{j=1}^3 \frac{\partial}{\partial x_j} \frac{\partial u_i}{\partial x_j} + \mu \sum_{j=1}^3 \frac{\partial}{\partial x_j} \frac{\partial u_j}{\partial x_i}, \\ &= \lambda \frac{\partial}{\partial x_i} \nabla \cdot \mathbf{u} + \mu \sum_{j=1}^3 \frac{\partial^2 u_i}{\partial x_j^2} + \mu \frac{\partial}{\partial x_i} \sum_{j=1}^3 \frac{\partial u_j}{\partial x_j} \\ &= (\lambda + \mu) \frac{\partial}{\partial x_i} \nabla \cdot \mathbf{u} + \mu \nabla^2 u_i \end{aligned} \quad (5.31)$$

The *viscous force* per unit fluid volume  $\mathbf{f}_\mu$  is therefore given by

$$\boxed{\mathbf{f}_\mu = \mu \nabla^2 \mathbf{u} + (\mu + \lambda) \nabla \nabla \cdot \mathbf{u}} \quad (5.32)$$

If the fluid is incompressible it follows that  $\partial\rho/\partial t = 0$ , and then the continuity equation gives  $\nabla\cdot\mathbf{u} = 0$ . In this case the viscous force is given by the simple expression

$$\mathbf{f}_\mu = \mu\nabla^2\mathbf{u} . \quad (5.33)$$

## 5.4 The Navier-Stokes Equation

The rate of change of momentum density equation (5.14) is equal to the force per unit volume equation (5.15), according to Newton's equation of motion. With the viscous force given by equation (5.32) the fluid equations of motion are

$$\rho\frac{D\mathbf{u}}{Dt} = \rho\frac{\partial\mathbf{u}}{\partial t} + \rho\mathbf{u}\cdot\nabla\mathbf{u} = -\nabla p + \mu\nabla^2\mathbf{u} + (\mu + \lambda)\nabla\nabla\cdot\mathbf{u} + \mathbf{F} , \quad (5.34)$$

with the continuity equation given by

$$\frac{\partial\rho}{\partial t} + \nabla\cdot\rho\mathbf{u} = 0 . \quad (5.35)$$

These equations simplify to the *Navier-Stokes equations*<sup>57, 58</sup> if the fluid is incompressible. In this case  $\partial\rho/\partial t = 0$ , and the continuity equation requires the velocity field to be divergence free

$$\nabla\cdot\mathbf{u} = 0 , \quad \text{for incompressible fluids.} \quad (5.36)$$

In this case the dynamical equations simplify to

$$\rho\frac{\partial\mathbf{u}}{\partial t} + \rho\mathbf{u}\cdot\nabla\mathbf{u} = -\nabla p + \mu\nabla^2\mathbf{u} + \mathbf{F} \quad \text{Navier-Stokes}$$

(5.37)

This equation is a second order partial differential equation and it has the major complication of being *non-linear* by the  $\mathbf{u}\cdot\nabla\mathbf{u}$  term. In many problems the external force  $\mathbf{F} = 0$ , and the fluid motion is caused by imposed pressure differences or relative movement of boundaries. Generally fluid flow takes place in a field of gravity which can not be ignored. If the density is uniform, the gravitational force is balanced by a vertical pressure gradient that is present whether or not the fluid is moving and that does not interact with any flow. This hydrostatic balance can be subtracted out of the dynamical equation and the problem reduced to one without body forces. This assumes, of course, that the fluid region is supported at the bottom, and that there are no free surfaces at which waves can develop.

The equations (5.36) and (5.37) effectively are one scalar and one vector equation, which constitute a total of 4 equations for the determination

of one scalar quantity, the pressure  $p$ , and one vector quantity, the velocity field  $\mathbf{u}$ . The number of unknowns is thus correctly matched by the number of equations. The pressure must necessarily be an intrinsic variable in any hydrodynamic problem for there to be enough variables to satisfy the basic laws of mechanics. In addition the conservation of energy leads to one more equation which we do not discuss here.

## 5.5 Boundary Conditions

In order to obtain solutions of the Navier Stokes equations we need sufficient boundary conditions to specify the problem at hand. Boundary conditions cannot be derived from the continuum equations — they are microscopic in origin. The first condition that typically enters a fluid dynamics problem is the condition that the fluid does not penetrate the container wall (assuming the wall to be non-porous). Therefore the fluid velocity normal to the wall moving with velocity  $\mathbf{U}$  must satisfy

$$\mathbf{u} \cdot \mathbf{n} = \mathbf{U} \cdot \mathbf{n}, \quad (5.38)$$

where  $\mathbf{n}$  is the unit normal to the surface. Often the frame of reference is chosen such that the wall is at rest, thus the boundary condition becomes

$$\mathbf{u} \cdot \mathbf{n} = 0, \quad (5.39)$$

Another condition often used is the *no-slip boundary condition* stating that there is no relative tangential velocity between a rigid wall and the fluid immediately next to it. Formally this condition is written

$$\mathbf{u} \times \mathbf{n} = \mathbf{U} \times \mathbf{n}, \quad (5.40)$$

or with the walls at rest

$$\mathbf{u} \times \mathbf{n} = 0, \quad (5.41)$$

This condition has no fundamental justification and there are many instances where it does not apply. The question as to the correctness of the no-slip boundary condition must be decided by experiment for the case at hand. In most of our discussion we will treat problems for which the no-slip boundary condition is known to apply.

The stress on a surface is determined from the stress tensor  $\boldsymbol{\sigma}$ , given in equation (5.27) Thus if we have a wall at  $y = 0$ , and the velocity has components  $\mathbf{u} = (u, v, w)$ , the force (per unit area) at the wall is

$$\mathbf{F}_{\text{wall}} = \mu \left\{ \left( \frac{\partial u}{\partial y} + \frac{\partial v}{\partial x} \right), 2 \left( \frac{\partial v}{\partial y} \right), \left( \frac{\partial w}{\partial y} + \frac{\partial v}{\partial z} \right) \right\}_{y=0}, \quad (5.42)$$

but the continuity equation gives the relation

$$\frac{\partial v}{\partial y} = -\frac{\partial u}{\partial x} - \frac{\partial w}{\partial z}, \quad (5.43)$$

so that if the no-slip condition  $u = v = w = 0$  at  $y = 0$ , applies

$$\mathbf{F}_{\text{wall}} = \mu \left\{ \left( \frac{\partial u}{\partial y} \right), 0, \left( \frac{\partial w}{\partial y} \right) \right\}_{y=0}. \quad (5.44)$$

Thus the viscous force acts tangentially along the surface. The only normal force is due to the pressure.

Other commonly used boundary conditions refers to free surfaces where there is no stress from the other side. If there is no wall, so that the surface is free, the boundary condition must state that no forces can act across the free surface and we must require that the pressure to be continuous  $p_1 = p_2$ , and the stress to vanish at the surface  $\sigma_{y=0} = 0$ . In this case the hydrostatic pressure may vary because of waves on the surface and therefore the hydrostatic pressure cannot be separated in the dynamical equations.

Often boundary conditions are applied at infinity. For instance, for flow around a single sphere one will specify the uniform velocity at large distances

$$\mathbf{u} \rightarrow \mathbf{u}_0 \text{ as } r \rightarrow \infty. \quad (5.45)$$

## 5.6 The Reynolds Number and Scaling

The *Navier-Stokes equation* equation (5.37) may be written

$$\frac{\partial \mathbf{u}}{\partial t} + \mathbf{u} \cdot \nabla \mathbf{u} = -\frac{1}{\rho} \nabla p + \nu \nabla^2 \mathbf{u}. \quad (5.46)$$

for the situation that there are no body forces and the flow is given by the boundary conditions. Here we have introduced the *kinematic viscosity*  $\nu$  defined by:

$$\nu = \frac{\mu}{\rho}. \quad (5.47)$$

The kinematic viscosity has dimensions  $[\nu] = \text{m}^2/\text{s}$ , which is the same as for a diffusion constant. The kinematic viscosity is  $0.15 \text{ cm}^2/\text{s}$  for air and  $0.01 \text{ cm}^2/\text{s}$  for water. The kinematic viscosity is the only *molecular* property of the fluid that enters. If the density is constant, as it is for incompressible fluids, then the only difference between the flow of water and the flow of air is the kinematic viscosity.

For a sphere of diameter  $\ell$  moving through an infinite fluid with velocity  $U$  the only variables that can affect the flow field are  $\nu$ ,  $\ell$  and  $U$ . Therefore we expect different flow regimes to be characterized by different values of some dimensionless combination of the relevant physical parameters. The conventional choice of such a dimensionless combination is the *Reynolds number*  $Re$ , given by

$$\boxed{Re = \frac{U\ell}{\nu} \quad \text{Reynolds number}} \quad (5.48)$$

The dimensions of the quantities used here are  $[U] = \text{m/s}$ ,  $[\ell] = \text{m}$  and  $[\nu] = \text{m}^2/\text{s}$ , thus it is easy to see that the Reynolds number is indeed a dimensionless quantity. For flow in a tube of diameter  $d$  the length scale in  $Re$  is replaced by  $d$ . In general  $\ell$  is taken to be a characteristic length set by the boundary conditions of the problem. Of course, we could have taken the tube length  $L$  instead of the diameter  $d$ , to set the length scale. We could also have chosen  $\ell$  to be the radius of curvature  $R$  if the tube is bent. Different choices only change the numerical value of  $Re$ , and does not alter the fact that we expect different types of flow depending on whether  $Re$  is very small or very large. In the figure 5.6 we see that at  $Re \sim 2300$ , there is a marked increase in the flow through a tube for a given pressure gradient. This increase in flow means that the velocity profile changes drastically and becomes the turbulent flow characteristic of high Reynolds numbers.<sup>3</sup>

Another example of the effect of changing the Reynolds number is seen in figure 5.7 where the flow past a cylinder is visualized by letting a dye flow out at the down stream point of the cylinder. For low flow velocities,  $Re < 30$ , the fluid streams nicely past the cylinder. As the flow rate is increased, the flow becomes unstable with beautiful periodic oscillations in the flow field emerge. Finally at high Reynolds numbers the flow pattern becomes chaotic or turbulent.

Flows of biological interest are often at very *low* Reynolds numbers. For instance bacteria have typical dimensions of less than 1  $\mu\text{m}$ , and consequently the Reynolds number of bacteria swimming in water must be very small indeed (with  $U < 1 \text{ mm/s}$ , we have  $Re < 10^{-3}$ ). On the other hand,

---

<sup>3</sup>The dimensionless pressure is  $\hat{p} = p/\rho U^2$  (see equation (5.52)), and the Reynolds number is  $Re = \rho U d / \mu$ , where  $d$  is the tube diameter. By multiplying the dimensionless pressure by  $Re^2$  we find another form of the dimensionless pressure:  $\tilde{p} = \hat{p} Re^2 = p \rho d^2 / \mu^2$ . The dimensionless pressure difference between the ends of the tube may be written  $(\tilde{p}_1 - \tilde{p}_2)d/L = (p_1 - p_2)d^3 \rho / \mu^2 L$ . Here the dimensionless factor  $d/L$  was used so that the dimensionless pressure difference will be independent of tube length. This form of the dimensionless pressure difference consist only of easily measurable quantities, and is the form used in figure 5.6.

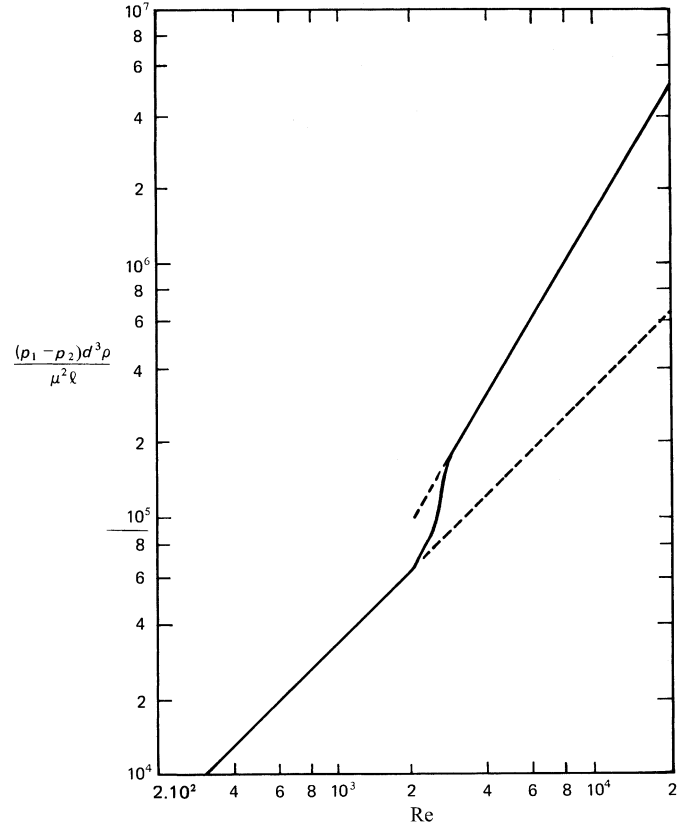


Figure 5.6: The normalized pressure drop  $\Delta p d^3 \rho / L \mu^2$  over a pipe of diameter  $d$  and length  $L$  as a function  $Re$ . The transition from low Reynolds number laminar flow to turbulent flow at high Reynolds numbers near  $Re \approx 3000$  is clearly visible. (After Tritton, 1988; reference [1]).

Figure 5.6: The normalized pressure drop  $\Delta p d^3 \rho / L \mu^2$  over a pipe of diameter  $d$  and length  $L$  as a function  $Re$ .

flows on a geophysical scale such as winds or ocean currents, often are characterized by *high* Reynolds numbers simply because the typical distances are very large — say hundreds of km, and therefore unsteady and turbulent motion is to be expected. For boat with a 15 m mast sailing in a (strong)  $U = 10$  m/s wind, the Reynolds number is  $10^6$ .

In the Navier-Stokes equation (5.46) let us measure lengths in terms of

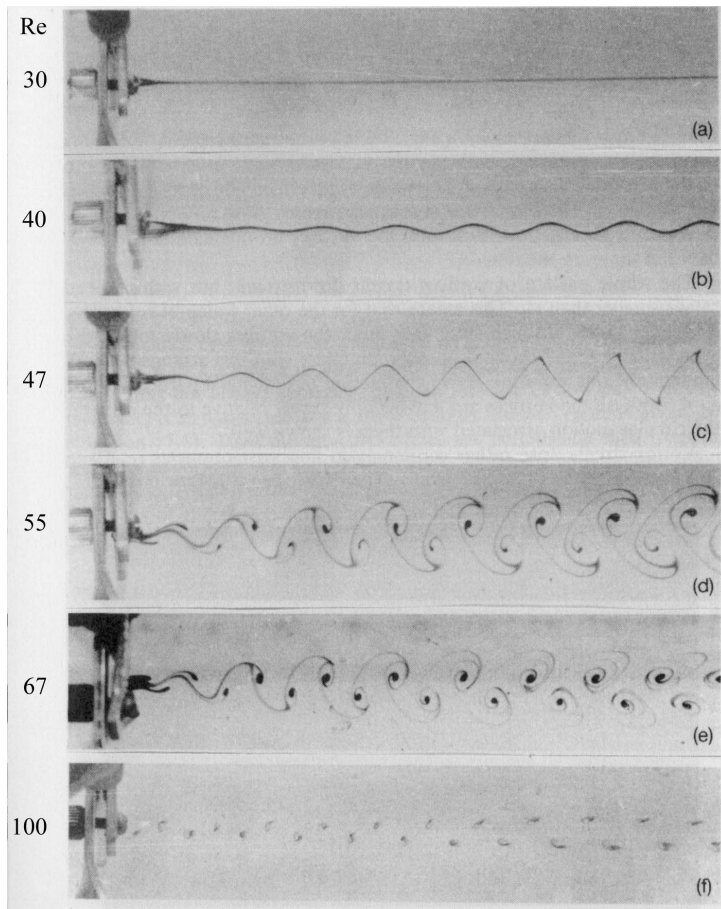


Figure 5.7: The flow around a cylinder as function of  $Re$ . (After Tritton, 1988; reference [1]).

Figure 5.7: The flow around a cylinder as function of  $Re$ . (After Tritton, 1988; reference [1]).

$\ell$  velocities in terms of  $U$  so that we introduce the dimensionless variables:

$$\hat{\mathbf{r}} = \mathbf{r}/\ell, \quad \hat{\mathbf{u}} = \mathbf{u}/U, \quad \hat{t} = tU/\ell. \quad (5.49)$$

Then the Navier-Stokes equation takes the form

$$\frac{\partial \hat{\mathbf{u}}}{\partial \hat{t}} + \hat{\mathbf{u}} \cdot \hat{\nabla} \hat{\mathbf{u}} = -\hat{\nabla} \hat{p} + \frac{1}{\text{Re}} \hat{\nabla}^2 \hat{\mathbf{u}}. \quad (5.50)$$

Here the reduced pressure is  $\hat{p} = p/(\rho U^2)$ . Let us return to the flow around a moving sphere. From equation (5.50) it follows that the velocity field can only depend on  $\hat{\mathbf{r}}$  and  $\text{Re}$ :

$$\mathbf{u}(\mathbf{r}, U, \ell) = U \mathbf{f} \left( \frac{\mathbf{r}}{\ell}, \text{Re} \right), \quad (5.51)$$

where  $\mathbf{f}$  is a (vector) function that depends on the geometry of the boundary conditions. For a sphere in a flow of velocity  $U$  the vector function  $\mathbf{f}$  behaves in such a way that the sphere has no effect on the flow field when  $|\mathbf{r}/\ell| \rightarrow \infty$  and  $\text{Re} \rightarrow 0$ . This equation (5.51) is Reynolds' *law of similarity* and it follows that the geometry of the flow is identical for spheres of different diameters and at different velocities and at various kinematic viscosities are all the same if the Reynolds number is the same.

The reduced pressure,  $\hat{p} = p/\rho U^2$ , can only depend on  $\mathbf{r}/\ell$  and  $\text{Re}$ :

$$p = \rho U^2 f \left( \frac{\mathbf{r}}{\ell}, \text{Re} \right), \quad (5.52)$$

where  $f$  is a scalar function of its arguments.

It is interesting to note that the *force* on the sphere moving with a velocity  $U$  depends *not* on  $\mathbf{r}$  but only on  $\text{Re}$  and  $\ell$ . The force must have the dimension of a pressure times area and it follows that the force on the sphere must have the following scaling:

$$F = \rho U^2 \ell^2 f \left( \frac{\mathbf{r}}{\ell} \Big|_{|\mathbf{r}|=\ell}, \text{Re} \right) = \rho U^2 \ell^2 f(\text{Re}), \quad (5.53)$$

consistent with Stoke's law derived in the next section.

In the limit of very low  $\text{Re}$ , the last term in equation (5.50) dominates over nonlinear term, which can be ignored, and leads to the *Stokes equation* valid for low Reynolds number *stationary* flow.

$$\nabla p - \mu \nabla^2 \mathbf{u} = 0, \quad \text{Re} \ll 1 \quad \text{Stokes}$$

(5.54)

This equations is used for *creeping flow* mostly for systems where the characteristic length scale is *microscopic* as it is for porous media and for the motion of micro-organisms.

In the limit of very high Reynolds numbers. viscosity is ignored and the Navier-Stokes equation simplifies to

$$\frac{\partial \mathbf{u}}{\partial t} + \mathbf{u} \cdot \nabla \mathbf{u} = -\frac{1}{\rho} \nabla p, \quad \text{Re} \gg 1 \quad \text{Euler} \quad (5.55)$$

which is *Euler's equation* first obtained by L. Euler (1755). This equation is used when viscosity can be ignored as in fully developed turbulence. This equation is *scale-invariant* under a rescaling by an *arbitrary* positive factor  $b$  so that

$$\mathbf{r} \rightarrow b \cdot \mathbf{r}; \mathbf{u} \rightarrow b^H \cdot \mathbf{u}; t \rightarrow b^{1-H} \cdot t; p/\rho \rightarrow b^{2H} p/\rho \quad (5.56)$$

When these transformed variables are inserted into Euler's equation it follows that the scaling factor  $b$  cancels in the resulting equation and the untransformed equation is recovered. This transformation is valid for arbitrary  $H$ . In the famous Kolmogorov (1941) theory,<sup>60,61</sup> global scale invariance (in a statistical sense) is implicitly assumed and the exponent  $H = \frac{1}{3}$  is singled out by an energy argument; a more 'refined' argument was given by Kolmogorov<sup>62</sup> in 1962. The regime where this scaling is valid is called the *inertial range* of *fully developed turbulence*.

## 5.7 Stokes Flow past a Sphere

The creeping motion described by equation (5.54) was used by Stokes to calculate the drag force on a sphere moving in a viscous fluid. This calculation allows the measurement of fluid viscosity by observing the fall velocity of spheres in fluids. Consider a sphere of radius  $a$  fixed at the origin in a fluid moving downward that has the velocity  $\mathbf{U}_0 = -U_0 \mathbf{e}_z$  far from the sphere (see figure 5.8).

The Stokes equation is

$$\nabla p - \mu \nabla^2 \mathbf{u} = 0, \quad (5.57)$$

and it is natural to choose polar coordinates for this problem. In polar coordinates with unit vectors  $\mathbf{e}_z, \mathbf{e}_\theta, \mathbf{e}_\varphi$  the uniform flow field is given by:

$$\mathbf{U} = U_r \mathbf{e}_r + U_\theta \mathbf{e}_\theta + U_\varphi \mathbf{e}_\varphi, \quad (5.58)$$

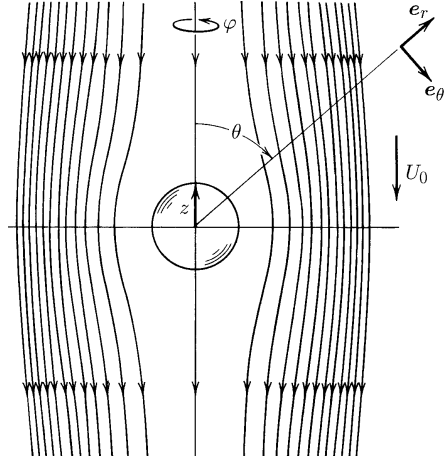


Figure 5.8: Flow around a sphere with fluid velocity  $-U_0 \mathbf{e}_z$  far from the sphere.

where the orthogonal set of unit vectors  $\mathbf{e}_r$ ,  $\mathbf{e}_\theta$  and  $\mathbf{e}_\varphi$  specify the directions for the field components given by

$$\begin{aligned} U_r &= -U_0 \cos \theta, \\ U_\theta &= U_0 \sin \theta, \\ U_\varphi &= 0. \end{aligned} \quad (5.59)$$

(see also equations (8.5) and (8.6))

In polar coordinates the pressure term in equation (5.57) is

$$\nabla p = \left( \frac{\partial p}{\partial r} \right) \mathbf{e}_r + \left( \frac{1}{r} \frac{\partial p}{\partial \theta} \right) \mathbf{e}_\theta + \left( \frac{1}{r \sin \theta} \frac{\partial p}{\partial \varphi} \right) \mathbf{e}_\varphi. \quad (5.60)$$

whereas the Laplace term in equation (5.57) is quite complicated:

$$\begin{aligned}
 [\nabla^2 \mathbf{u}]_r &= \frac{\partial}{\partial r} \left( \frac{1}{r^2} \frac{\partial(r^2 u_r)}{\partial r} \right) + \frac{1}{r^2 \sin \theta} \frac{\partial}{\partial \theta} \left( \sin \theta \frac{\partial u_r}{\partial \theta} \right) \\
 &+ \frac{1}{r^2 \sin^2 \theta} \frac{\partial^2 u_r}{\partial \varphi^2} - \frac{2}{r^2 \sin \theta} \frac{\partial u_\theta \sin \theta}{\partial \theta} - \frac{2}{r^2 \sin \theta} \frac{\partial u_\varphi}{\partial \varphi} \\
 [\nabla^2 \mathbf{u}]_\theta &= \frac{1}{r^2} \frac{\partial}{\partial r} \left( \frac{1}{r^2} \frac{\partial u_\theta}{\partial r} \right) + \frac{1}{r^2} \frac{\partial}{\partial \theta} \left( \frac{1}{\sin \theta} \frac{\partial(u_\theta \sin \theta)}{\partial \theta} \right) \\
 &+ \frac{1}{r^2 \sin^2 \theta} \frac{\partial^2 u_\theta}{\partial \varphi^2} - \frac{2}{r^2} \frac{\partial u_r}{\partial \theta} - \frac{2 \cot \theta}{r^2 \sin \theta} \frac{\partial u_\varphi}{\partial \varphi} \\
 [\nabla^2 \mathbf{u}]_\varphi &= \frac{1}{r^2} \frac{\partial}{\partial r} \left( r^2 \frac{\partial u_\varphi}{\partial r} \right) + \frac{1}{r^2} \frac{\partial}{\partial \theta} \left( \frac{1}{\sin \theta} \frac{\partial(u_\varphi \sin \theta)}{\partial \theta} \right) \\
 &+ \frac{1}{r^2 \sin^2 \theta} \frac{\partial^2 u_\varphi}{\partial \varphi^2} + \frac{2}{r^2 \sin \theta} \frac{\partial u_r}{\partial \varphi} + \frac{2 \cot \theta}{r^2 \sin \theta} \frac{\partial u_\theta}{\partial \varphi}
 \end{aligned} \tag{5.61}$$

After some calculations, using these expressions, one finds that

$$\begin{aligned}
 u_r &= -U_0 \cos \theta \left( 1 - \frac{3a}{2r} + \frac{a^3}{2r^3} \right) \\
 u_\theta &= U_0 \sin \theta \left( 1 - \frac{3a}{4r} - \frac{a^3}{4r^3} \right) \\
 p &= p_0 + \frac{3}{2} \frac{\mu U_0 a}{r^2} \cos \theta
 \end{aligned} \tag{5.62}$$

is a solution of the Stokes equation that satisfies the boundary condition of zero velocity at the surface of the sphere and has the correct velocity at a large distance from the sphere. Here  $p_0$  is the ambient pressure.

The *stress* from the pressure on the sphere in the direction of flow is

$$(p|_{r=a} - p_0) \cos \theta = \frac{3\mu U_0}{2a} \cos^2 \theta. \tag{5.63}$$

The stress along the surface has only one component in the  $\theta$  direction having a magnitude of  $(\partial u_\theta / \partial r)$ . This stress has a component in the flow direction given by

$$\mu \frac{\partial u_\theta}{\partial r} \Big|_{r=a} \sin \theta = \frac{3\mu U_0}{2a} \sin^2 \theta. \tag{5.64}$$

The total force per unit area in the flow direction is therefore

$$f_z = \frac{3\mu U_0}{2a} (\cos^2 \theta + \sin^2 \theta) = \frac{3\mu U_0}{2a}. \tag{5.65}$$

The combined effect of pressure and viscous stress on the surface of the sphere, in the direction of the flow, is independent of  $\theta$  and the integrated drag force is therefore given by  $F_D = 4\pi a^2 f_z$ , which may be written

$$F_D = 6\pi\mu a U \quad \text{Stokes law} \quad (5.66)$$

This is the famous *Stokes law* for the drag force on a sphere of radius  $a$  moving with a velocity  $U$ .

With the Reynolds number defined by  $\text{Re} = (\rho U a)/\mu$  we see that Stokes law may be written as

$$F_D = 6\pi \cdot (\rho U^2 a^2) \cdot \frac{1}{\text{Re}} , \quad (5.67)$$

which has the similarity form given in equation (5.64). Einstein<sup>63,64</sup> used this expression with his theory for the viscosity of sugar-solutions to estimate the Avogadro's number  $N_A \simeq 6.56 \cdot 10^{23} \text{ mol}^{-1}$  (the correct value is  $N_A = 6.022045 \cdot 10^{23} \text{ mol}^{-1}$ ). Equation (5.66), which is a result of continuum hydrodynamics, has been reproduced using molecular-dynamics simulations<sup>65</sup> of a 'Lenard-Jones' fluid, and shown to hold even for spheres comparable to molecular dimensions.

The expression for the drag force has been improved<sup>66</sup> for  $\text{Re} < 1$  using perturbation expansions

$$F_D = 6\pi\mu a U \left[ 1 + \frac{3}{16}\text{Re} + \frac{9}{160}\text{Re}^2 \ln \text{Re} + \dots \right] . \quad (5.68)$$

Experiments<sup>67</sup> show that an eddy forms behind the sphere at  $\text{Re} \simeq 24$ . The eddy and wake start to oscillate at  $\text{Re} \simeq 130$  but the flow remains *laminar* up to  $\text{Re} \simeq 200$ . With further increase in  $\text{Re}$  turbulence gradually builds up.

The Stokes equation neglects completely the convection of momentum in the original Navier-Stokes equation (the nonlinear term). C. W. Oseen<sup>68,69</sup> pointed out that this neglect is not justified and proposed the equations (now called *Oseen equation*) for stationary flow

$$\rho(\mathbf{U} \cdot \nabla)\mathbf{u} = -\nabla p + \mu\nabla^2\mathbf{u} \quad \text{Oseen equation} \quad (5.69)$$

which replaces  $(\mathbf{u} \cdot \nabla)$  in the Navier-Stokes equation (5.37) by  $(\mathbf{U} \cdot \nabla)$  where  $\mathbf{U}$  is the velocity of the sphere. The first order correction is then

$$F_D = 6\pi\mu a U \left[ 1 + \frac{3}{8}\text{Re} \dots \right] . \quad (5.70)$$

as shown already by Oseen<sup>70,68</sup> and further improved upon later (see a discussion by Mazur & Weisenborn reference []).

A small bubble of radius  $a$  rising in a fluid of density  $\rho$  is spherical when small. Stokes law does not apply since the boundary condition is changed at the surface of the bubble. The result for the drag force is (see for instance reference [])

$$F_D = 4\pi\mu a U \quad \text{for bubble .} \quad (5.71)$$

Note that this result is *independent* of the surface tension. The drag force of a bubble is only  $\frac{2}{3}$  of that experienced by a solid sphere. However, if the boundary conditions are modified for example by proteins or surfactants that accumulate at the bubble water interface the boundary conditions are effectively changed to the non-slip boundary condition.

For small finite Re inertial forces will deform the bubble and the resulting shape is a balance among viscous, inertial and surface tension forces. Taylor & Arcivos<sup>72</sup> have shown that the shape may be given by radial function

$$R(\theta) = a \left[ 1 - \frac{5}{96} \text{Re Ca} (3 \cos^2 \theta - 1) \right], \quad (5.72)$$

where Ca is the *capillary number* defined by  $\text{Ca} = \mu U / \sigma$ . The expression is valid for  $\text{Re} \ll 1$  and  $\text{ReCa} \ll 1$  and shows that the rising bubble tends to become a ellipsoid flattened transverse to the flow.

# Chapter 6

## Darcy's Law

Permeability and the proportionality of flow with pressure gradient was first established<sup>73</sup> by Henry Darcy (1856) in connection with his design and execution of the municipal water supply systems for the city of Dijon. His results are widely used for investigating all types of water flow through porous media, such as underground flow to wells, flow in soils being irrigated, and the permeability of dam foundations. The flow of oil in reservoirs has been found to follow Darcy's law, and the unit of permeability is designated as the darcy. Darcy's experimental setup is shown in figure 6.1.

A homogeneous filter bed of sand of height  $L$  is bounded by planes of area  $A$ . By varying the flow rate and measuring the pressure differences Darcy found that the volume flow rate  $Q$ , with units  $\text{m}^3/\text{s}$ , was related to the head difference  $h_1 - h_2$  by

$$Q = K' A(h_1 - h_2)/L , \quad (6.1)$$

where  $K'$  is a constant that depends on the type of sand used. The pressure at the bottom is  $p_2 = \rho g h_2$  and the pressure at the inlet level is  $p_1 = \rho g h_1 - \rho g L$ . In the last expression the term  $\rho g L$  represents the hydrostatic pressure drop in going from (2) to (1). The difference in pressure at the two ends of the filter bed is

$$(p_1 - p_2) = \rho g(h_1 - h_2) - \rho g L . \quad (6.2)$$

Therefore the observed relation may be rewritten (with  $K = K'/\rho g$ ) as

$$Q = KA(-(p_2 - p_1)/L + \rho g) . \quad (6.3)$$

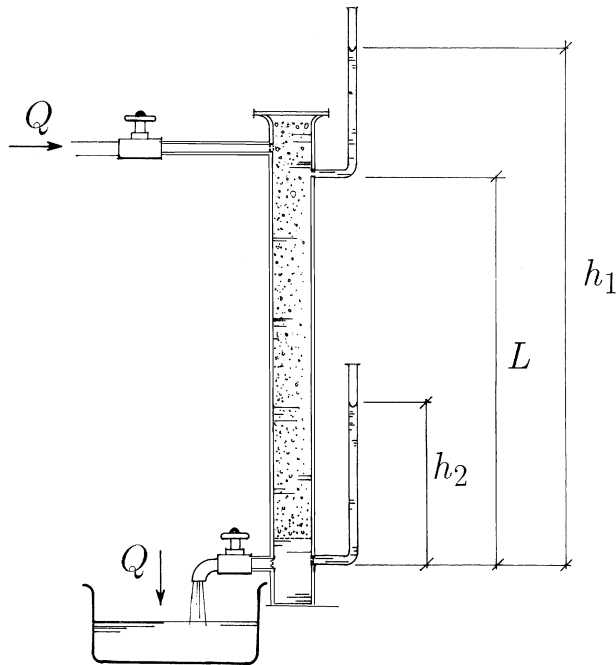


Figure 6.1: Darcy's experiment on water permeability.

This equation is one formulation of *Darcy's law*. The flow  $Q$  is zero if the pressure difference exactly equals the hydrostatic pressure difference so that  $p_2 - p_1 = \rho g L$ . In this case  $h_2 = h_1$  and the head difference vanishes. Note that the flow moves in the direction of lower *piezometric head*  $h$ , as measured by water filled manometers—not in the direction of decreasing pressure (the pressure increases with depth).

Nutting (1930) introduced<sup>74</sup> the *permeability*  $k$ , by the relation

$$K = k/\mu , \quad (6.4)$$

where  $\mu$  is the fluid viscosity. The permeability is characteristic of the porous medium, whereas the fluid viscosity enters separately in the constant  $K$  of Darcy's law. The permeability  $k$  is dimensionally determined by equation (6.3)

$$[k] = \frac{[Q][L][\mu]}{[A][p]} = \text{m}^2 . \quad (6.5)$$

Substance	Permeability Range		Literature reference
	$k$ in $\text{cm}^2$		
Berl saddles	$1.310^{-3}$ to $3.910^{-3}$		Carman (1938) []
Wire crimps	$3.810^{-5}$ to $1.010^{-4}$		Carman (1938)
Black slate powder	$4.910^{-10}$ to $1.210^{-9}$		Carman (1938)
Silica powder	$1.310^{-10}$ to $5.110^{-10}$		Carman (1938)
Sand (loose beds)	$2.010^{-7}$ to $1.810^{-8}$		Carman (1938)
Soils	$2.910^{-9}$ to $1.410^{-7}$		Aronovice and Donnan (1946) []
Sandstone ('oil sand')	$5.010^{-12}$ to $3.010^{-8}$		Muskat (1937) []
Limestone, dolomite	$2.010^{-11}$ to $4.510^{-10}$		Locke and Bliss (1950) []
Brick	$4.810^{-11}$ to $2.210^{-9}$		Stull and Johnson (1940) []
Bituminous concrete	$1.010^{-9}$ to $2.310^{-7}$		McLaughlin and Goetz (1955) []
Leather	$9.510^{-10}$ to $1.210^{-9}$		Mitton (1945) []
Cork board	$3.310^{-6}$ to $1.510^{-5}$		Brown and Bolt (1942) []
Hair felt	$8.310^{-6}$ to $1.210^{-5}$		Brown and Bolt (1942)
Fiberglass	$2.410^{-7}$ to $5.110^{-7}$		Wiggins et al. (1939) []
Cigarette	$1.110^{-5}$ to $1.210^{-5}$		Brown and Bolt (1942)
Agar-agar	$2.010^{-10}$ to $4.410^{-9}$		Pallmann and Duel (1945) []

Table 6.1: Permeability of various substances (after Scheidegger, 1974)

Hence the dimension of  $k$  is area. The oil industry, however, uses the unit<sup>1</sup> 'darcy'. For a substance with a permeability of 1 darcy a pressure gradient of 1 atm/cm produces a flow of 1  $\text{cm}^3/\text{s}$  through a cross section of 1  $\text{cm}^2$  for a fluid of viscosity is 1 cp (as for water). With this definition we find that

$$1\text{darcy} = 9.87 \cdot 10^{-9} \text{cm}^2 \simeq (1\mu\text{m})^2 . \quad (6.6)$$

In table 6 the permeability of various substances are given.

---

<sup>1</sup>This name first was first suggested by Wyckoff et al. (1933) see reference [].

## 6.1 Differential Form of Darcy's Equation

Darcy's law is easily<sup>78</sup> generalized to infinitesimal layers. With the volume flux (volume per area and time) defined by

$$U = Q/A , \quad (6.7)$$

we find that equation (6.3) may be written in the limit  $L \rightarrow 0$  as

$$\mathbf{U} = -\frac{k}{\mu}(\nabla p - \rho \mathbf{g}) , \quad \text{Darcy's law}$$

(6.8)

where we have used  $(p_2 - p_1)/L \rightarrow \nabla p$  for  $L \rightarrow 0$ , and  $\mathbf{g} = (0, 0, -g)$ . The volume flux is in the direction of the pressure gradient if the effect of gravity is neglected—as for horizontal flow. Note that  $\mathbf{U}$ , the *filtration velocity*, has the dimension m/s. This filtration velocity is also called the Darcy velocity, seepage velocity or specific discharge. Note again that with the  $z$ -axis vertical and up, we find that for  $\mathbf{U} = 0$  that  $\frac{\partial p}{\partial z} + \rho g = 0$ , which gives  $p(z) = p(0) - \rho g z$  as expected.

Darcy's law alone does not specify the flow, it must be supplemented by the continuity equation. The continuity equation for a fluid moving in a porous medium is different from the continuity equation (5.1) for hydrodynamic flow. Instead the continuity equation takes the form:

$$\frac{d}{dt} \int_V \phi \rho dV = - \int_S \rho \mathbf{U} \cdot d\mathbf{S}$$

Rate of increase of mass of fluid within  $V$ 
Rate of addition of mass across the surface  $S$

(6.9)

The porosity  $\phi$  on the left hand side of equation (6.9) accounts for the fact that the fluid is excluded from the matrix. On the right hand side we have the Darcy velocity  $\mathbf{U}$  instead of the fluid velocity  $\mathbf{u}(\mathbf{r}, t)$ , as it expresses the volume flow per unit area and time. In the limit  $V \rightarrow 0$  we obtain the continuity equation for flow in porous media in the form

$$\frac{\partial \phi \rho}{\partial t} + \nabla \cdot (\rho \mathbf{U}) = 0$$

(6.10)

Of course, this continuity equation is only valid on length scales much above the pore scale since both the porosity  $\phi$  and the Darcy velocity  $\mathbf{U}$  are defined as average quantities over some (macroscopic) region. Thus the limit  $V \rightarrow 0$  is not to be taken too seriously. The averaging procedures required are in fact subtle and controversial; for a good discussion see the

	Porous Flow	Electric Flow
potential	$p$	$V$
current	$U$	$j$
transport equation	$\mathbf{U} = -\frac{k}{\mu} \nabla p$	$\mathbf{j} = -\sigma \nabla V$
transport coefficient	$k/\mu$	$\sigma$

Table 6.2: Analogy between porous and electric stationary flow.

classic book by Jacob Bear (reference [1]) and Bear and Bachmat (reference [2]).

The Darcy equation (6.8) and the continuity equation (6.10) may be combined to give a dynamic equation

$$\frac{\partial \phi \rho}{\partial t} = \nabla \cdot \left\{ \rho \frac{k}{\mu} (\nabla p - \rho \mathbf{g}) \right\}. \quad (6.11)$$

In order to solve this equation, even in the simplest situations, we need boundary conditions and an equation of state that relates the density to the pressure, that is, we need  $\rho(p)$ . Equation (6.11) is nonlinear unless simplifications apply.

For incompressible fluids in porous media with  $\phi$  and  $k$  constant, the dynamical equation (6.11) simplifies for the stationary flow to the *Laplace equation* for the pressure:

$$\nabla^2 p = 0. \quad (6.12)$$

This equation is well known from many fields of physics, from electrostatics, elasticity theory, diffusion, currents in electrolytes etc. For electrical conduction the analogous quantities are listed in table 6.2. The electrical potential  $V$  is analogous to the pressure  $p$ , the conductivity  $\sigma$  is analogous to  $k/\mu$ , the electric current is analogous to the Darcy flow, and Ohm's law is analogous to Darcy's law. Note that also the boundary conditions must be taken into account when the analogy is discussed. We shall return to a more detailed discussion of this later.

It is possible to linearize<sup>88</sup> equation (6.11) if the fluid has a constant compressibility,  $\kappa$ , that is, the density is given by an equation of state of the form

$$\rho = \rho_0 \exp[\kappa(p - p_0)], \quad \kappa = \rho^{-1} \partial \rho / \partial p. \quad (6.13)$$

Using this expression in equation (6.11) we find

$$\frac{\partial \rho}{\partial t} = \nabla \cdot \{ D(\nabla \rho - \kappa \rho^2 \mathbf{g}) \}, \quad (6.14)$$

where the ‘diffusion constant’  $D$  for the density is given by

$$D = \frac{k}{\phi\mu\kappa} . \quad (6.15)$$

This type of equation enters the discussion when gas expands in a porous medium and in *pressure tests* used in oil production. If the gravity term in equation (6.14) can be ignored (as in horizontal flow), then the equation becomes a simple linear diffusion equation for the density and the mathematical methods and intuition developed for diffusion equations and heat conduction can be used.

## Chapter 7

# Models for Flow in Porous Media

In order to understand the physical basis of Darcy's law many models have been suggested and discussed in the literature. The simplest of these models is the capillary model, which we discuss in the next section. For idealized models where spheres are placed in a regular lattice array the hydrodynamic equations can be solved and accurate numerical results have been obtained. Finally the analogy to electric flow in inhomogeneous substances will be discussed.

### 7.1 The Capillary Model

$$Q = \frac{\pi a^4}{8\mu} \frac{\Delta p}{L}, \quad (7.1)$$

where the pressure gradient is  $\frac{\partial p}{\partial x} = -\Delta p/L$  and  $\Delta p$  is the magnitude of the pressure drop. The effective or average velocity in the pore is (see equation (4.32))

$$\langle u \rangle = \frac{Q}{\pi a^2} = \frac{a^2}{8\mu} \frac{\Delta p}{L}. \quad (7.2)$$

With  $n$  pores per unit area the flow rate is

$$U = Qn = n \frac{\pi a^4}{8\mu} \frac{\Delta p}{L} = n\pi a^2 \langle u \rangle. \quad (7.3)$$

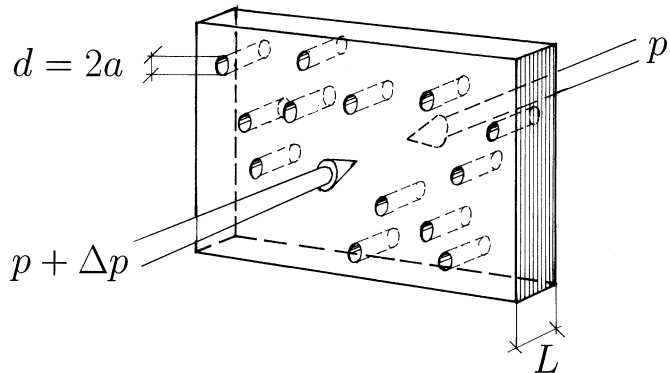


Figure 7.1: Filter consisting of capillaries.

If we consider the membrane to be an infinitesimal cross-section of a porous medium as indicated in figure 7.1 then we see that the flow per unit area and time is given by

$$U = \frac{k}{\mu} \frac{\Delta p}{L}, \quad (7.4)$$

which in fact is Darcy's law with the permeability  $k$  given by

$$k = n \frac{\pi a^4}{8}. \quad (7.5)$$

Thus the capillary model leads directly to Darcy's law and gives an explicit expression for the permeability that depends only on the pore geometry. However, this model clearly is inadequate because it supports flow only in a single direction. There have been many attempts to generalize this model but without much success. The most important aspect of the model is that it shows that the *separation* of the fluid viscosity and the pore geometry in Darcy's law has the form  $K = k/\mu$ .

### 7.1.1 $k$ expressed in terms of macroscopic quantities

For a porous medium consisting of an assembly of tortuous capillaries the permeability in equation (7.5) may be expressed in terms of macroscopically measurable quantities such as the porosity  $\phi$  and the specific surface  $S$ . The rewritten expression is in practice used to correlate observations of permeability with sample porosity.

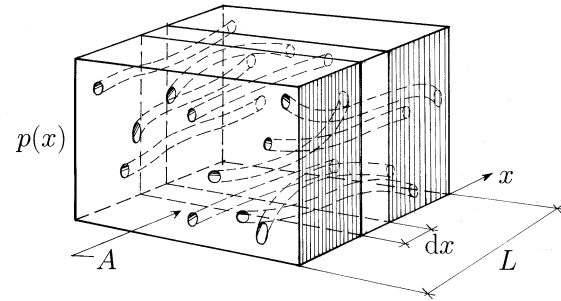


Figure 7.2: Model of a porous medium as stack of membranes.

The porosity of the sample illustrated in figure 7.2 is

$$\phi = nA \frac{\pi a^2 L}{AL} = n\pi a^2 , \quad (7.6)$$

Combining this result with equation (7.3) we find that

$$U = \phi \langle u \rangle , \quad (7.7)$$

Thus the volume flow velocity or filtration velocity,  $U$ , is less than the average pore velocity  $\langle u \rangle$  by a factor  $\phi$ . This result was first pointed out in 1863 by Dupuit.<sup>91</sup>

Using the expression for  $\phi$ , we may eliminate  $n$  in equation (7.5) and the permeability  $k$  may be written

$$k = \frac{\phi a^2}{8} . \quad (7.8)$$

The *specific surface area*  $S$  is the pore surface area per unit volume. This is a quantity that may be relatively easily measured by several methods. Clearly  $S$  is a quantity characteristic for a porous substance just as the porosity is. For the capillary model  $S$  is

$$S = \frac{(nA)2\pi aL}{LA} = n2\pi a , \quad (7.9)$$

where  $A$  is the cross section and  $L$  the length of the sample. The expression for  $S$  may be combined with the expression (7.6) for the porosity to eliminate  $n$  and we find

$$S = 2\frac{\phi}{a} . \quad (7.10)$$

Shape	$K_0$	Remarks
1. circle	2.0	Poiseuille's law
2. Ellipses		—
Major axis = twice minor axis	2.13	—
Major axis = 10 by minor axis	2.45	—
3. Rectangles		—
Length = breadth, i.e., square	1.78	—
Length = 2 by breadth	1.94	—
Length = 10 by breadth	2.65	—
Length is infinite	3.0	—
4. Equilateral triangle	1.67	—
5. Pipes with Cores		—
Core set concentrically	2.0–3.0	—
Core set eccentrically	1.7–3.0	Eccentricity < 0.7
Core set eccentrically	1.2–2.0	Eccentricity > 0.7

Table 7.1: Values of  $K_0$  for streaming flow in various cross-sections (after Carman, 1937).

The specific surface is an inverse length and we expect  $S^{-1}$  to be a typical pore size for any porous medium.

Using equations (7.8) and (7.10) the permeability may be written in terms of the macroscopically measurable quantities  $\phi$  and  $S$ :

$$k = \frac{\phi^3}{2S^2} = \frac{\phi^3}{K_0 S^2}. \quad (7.11)$$

Clearly, the factor  $K_0 = 2$ , in the relation above comes from the geometry of the pores. The results for capillaries of various cross sections in table 7.1 have been given by Carman.<sup>92</sup> This table shows that the shape of the cross-section of the capillaries has very little effect on the permeability.  $K_0$  ranges only between the limits 1.2 and 3. It is interesting to note that  $K_0 = 2$  does not necessarily denote a circular cross-section, nor even a shape resembling a circle.

Equation (7.11) is valid for a porous medium consisting of capillary tubes of equal radius as in a Nuclepore filter. The permeability expression in equation (7.11) is expressed in a form involving only *porosity*,  $\phi$ , and *specific surface*,  $S$ , which both are routinely measured for rock samples in

the oil industry. Thus it is interesting to compare equation (7.11) with experimental results.

## 7.2 Kozeny Expression for $k$

In order to extend equation (7.11) to a real porous substance with known porosity,  $\phi$ , and specific surface area,  $S$ , one must in some way account for the fact that the path of fluid elements is not straight. This is done by introducing an effective length  $L_e$ . There are two effects to consider:

*Firstly* the pressure drop  $\Delta p$  acts over the effective capillary length<sup>93</sup>  $L_e$  instead of the actual sample length so that we may write the flow in any one of the *effective* capillaries as

$$Q = \frac{\pi a^4}{8\mu} \frac{L}{L_e} \frac{\Delta p}{L}, \quad (7.12)$$

as in equation (7.1) with  $L_e$  replacing  $L$ .

*Secondly* the relation between the flow per unit area  $U$ , and  $Q$  is modified since the number of ‘capillaries’ per unit area must satisfy the equation

$$nA\pi a^2 L_e = \phi A L, \quad (7.13)$$

which simply equates two expressions for the pore volume. Combining equations (7.11) and (7.13) we find that  $U = nQ$  is given by Darcy’s equation in the form

$$U = \frac{\phi a^2}{8T^2 \mu} \frac{\Delta p}{L}, \quad (7.14)$$

so that the permeability is given by

$$k = \frac{\phi a^2}{8T^2}. \quad (7.15)$$

The ratio of effective length to sample length is called the *tortuosity*

$$T = \frac{L_e}{L}. \quad (7.16)$$

The tortuosity also determines other properties of porous media and it is commonly deduced from measurements of the electric resistivity of samples saturated with an electrolyte. The specific surface area is given<sup>1</sup> by

---

<sup>1</sup>Two expressions for specific surface for the tortuous capillary model gives  $nA2\pi aL_e = SLA$ , gives  $S = 2\phi/a$  as before

equation (7.9), as before, and we may therefore write the permeability in as

$$k = \frac{\phi^3}{KS^2}, \quad (7.17)$$

where the *Kozeny constant* should be given by the *Carman relation*

$$K = K_0 \left( \frac{L_e}{L} \right)^2 = K_0 \mathcal{T}^2, \quad (7.18)$$

instead of Kozeny's result equation (7.11). The expression for the specific permeability finally becomes

$$k = \frac{\phi^3}{K_0 \mathcal{T}^2 S^2} \quad \text{Carman-Kozeny}$$

(7.19)

Equations similar to this one, containing  $S$  and  $\phi$ , are commonly called Carman-Kozeny equations.

Carman<sup>92</sup> observed that a dye streak injected in a packing of spheres typically made an angle of  $45^\circ$  to the flow direction, and he concluded that  $\mathcal{T} = L_e/L = \sqrt{2}$ , is the proper value for the tortuosity and therefore the Kozeny constant is estimated to be 4. Experimentally the Carman-Kozeny constant  $K$  is approximately 5, as shown in figure 7.3, for random packings of spheres.

For beds of spheres packed to various porosities, the specific surface area is

$$S = 3(1 - \phi)/a. \quad (7.20)$$

With this result, the Carman-Kozeny expression (7.17) for the permeability, takes the form<sup>2</sup>

$$k = \frac{a^2}{9K} \frac{\phi^3}{(1 - \phi)^2}. \quad (7.21)$$

A most important aspect of this equation is the  $\phi^3/(1 - \phi)^2$  dependence. This factor is in agreement with experiments, as discussed by Carman,<sup>92</sup> and also with numerical solutions<sup>95</sup> of the Stokes equations for lattice packings of spheres when the porosity is less than 0.5.

---

<sup>2</sup>For Poisson porous media we find  $k = \frac{a^2}{9K_0 \mathcal{T}^2} \frac{\phi^3}{(\phi \ln \phi)^2}$ , where we have used that  $S = 4\pi a^2 \phi n$  and  $\ln \phi = -n(4\pi/3)a^3$  gives  $S = 3a^{-1}\phi \ln \phi$ .

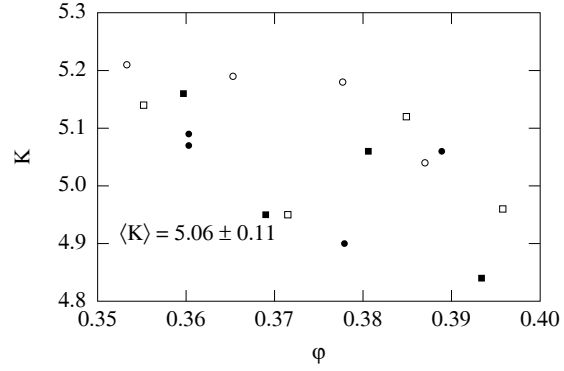


Figure 7.3: Carman-Kozeny constant  $K$ . Schriever's data<sup>94</sup> for small glass spheres of diameter  $d$ . (○):  $d = 1.025\text{ mm}$ ; (●):  $d = 0.528\text{ mm}$ ; (□):  $d = 0.443\text{ mm}$ ; (■):  $d = 0.252\text{ mm}$ . The average is  $K = 5.06 \pm 0.11$  (after Carman 1937).

### 7.2.1 Flow at finite Reynolds Numbers in Porous Media

Carman<sup>92</sup> reviewed and discussed the earlier results in terms of dimensionless groups first introduced by Blake<sup>96</sup> (1922), and Stanton and Pannell<sup>97</sup> (1914). In a discussion of flow in porous media the first dimensionless group to consider is the *Reynolds number*

$$\text{Re} = \frac{\rho \langle u \rangle m}{\mu}. \quad (7.22)$$

Here the characteristic length scale was taken to be  $m$  the so called *hydraulic radius* defined by

$$m = \frac{\text{cross-section normal to flow}}{\text{perimeter presented to flow}}. \quad (7.23)$$

For a circular pipe of radius  $a$  one finds  $m = a/2$ . For pipes of uniform cross-section an alternate expression for  $m$  is

$$m = \frac{\text{volume of fluid}}{\text{surface presented to fluid}}. \quad (7.24)$$

If this expression is applied to a porous medium, the hydraulic radius is also given by

$$m = \frac{\phi}{S}, \quad (7.25)$$

which is Kozeny's assumption. With the relation  $U = \phi\langle u \rangle$  it follows that the Reynolds number for porous flow is given by

$$\text{Re} = \frac{\rho U}{\mu S} . \quad (7.26)$$

A second dimensionless group is the *resistance coefficient*  $\psi$

$$\psi = \frac{F}{\rho\langle u \rangle^2} . \quad (7.27)$$

This is the ratio of the frictional force  $F$ , per unit area of the pore surface and a kinetic energy of the flow per unit volume. The frictional force is obtained by noting that in the volume  $V = AL$  the work done per unit time by the pressure drop,  $U\Delta p A$ , must equal the energy dissipated at the pore surface:

$$U\Delta p A = F \langle u \rangle S V , \quad (7.28)$$

where the fluid is taken to move at the velocity  $\langle u \rangle$  in the pore. This gives the frictional force as

$$F = \frac{U}{\langle u \rangle S} \frac{\Delta p}{L} = \frac{\phi}{S} \frac{\Delta p}{L} . \quad (7.29)$$

The resistance coefficient can therefore be written in a form involving easily measured quantities, using  $U = \phi\langle u \rangle$ ,

$$\psi = \frac{\phi^3}{\rho U^2 S} \frac{\Delta p}{L} . \quad (7.30)$$

In figure 7.4 the resistance coefficient  $\psi$ , is plotted as a function of the Reynolds number for many experiments on beds of spheres.

It should be noted that in figure 7.4 the Reynolds number is twice  $\text{Re}$  defined in equation (7.26), whereas the resistance coefficient is 4 times the resistance coefficient in equation (7.30) as used by Carman. Such numerical differences in the definition of dimensionless groups are common in hydrodynamics. As is seen from figure 7.4 the plot of experimental results with the dimensional groups  $\psi$ , and  $\text{Re}$ , give a very nice data collapse with all the experimental results on a single curve.

More recent correlations and dimensional arguments have been reviewed<sup>14</sup> by Dullien (1992). Dullien introduces the *friction factor*

$$f_p = \frac{D_p}{\rho U^2} \frac{\Delta p}{L} \quad (7.31)$$

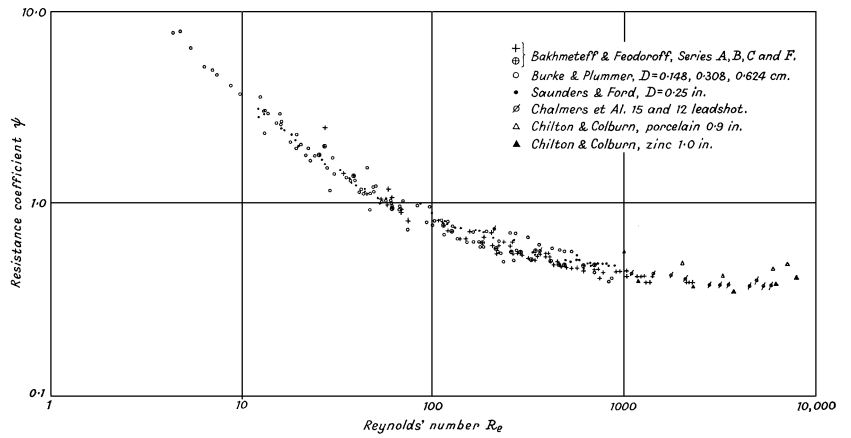


Figure 7.4: Resistance coefficient as a function of Reynolds number for beds of spheres, (after Reference [1]).

Figure 7.4: Resistance coefficient as a function of Reynolds number for beds of sph

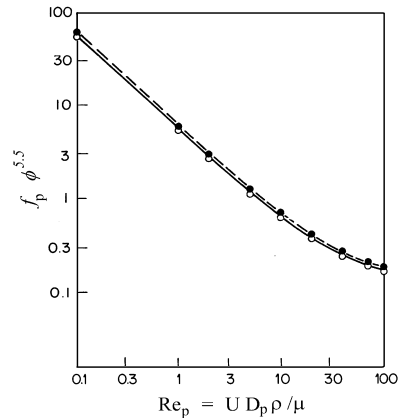


Figure 7.5: The particle scaled friction factor,  $f_p \phi^{5.5}$ , as a function of particle Reynolds number  $Re_p$  (from [1] after [1]).

Figure 7.5: The particle scaled friction factor,  $f_p \phi^{5.5}$ , as a function of particle Re

and the particle Reynolds number

$$\text{Re}_p = \frac{D_p U \rho}{\mu}. \quad (7.32)$$

Here  $D_p$  is the ‘surface average sphere diameter.’ In terms of these expressions the permeability is given by  $k = D_p^2 / \text{Re}_p f_p$ . Rumpf and Gupte found<sup>99</sup> for random packings of spheres with  $0.35 < \phi < 0.7$ , and  $10^{-2} < \text{Re}_p < 10^2$  (seen figure 7.5) that the experimental results are well fitted by the expression

$$f_p = c \frac{5.6}{\text{Re}_p} \phi^{-5.5}, \quad (7.33)$$

with  $c = 1.00$  and  $1.05$  for narrow and wide size distributions of the spheres respectively.

We note that equation (7.33), with the definitions (7.31) and (7.32), may be rewritten as

$$U = \frac{D_p^2 \phi^{5.5}}{5.6 c \mu} \frac{\Delta p}{L}, \quad (7.34)$$

is Darcy’s law. Therefore the permeability is given by

$$k_{RG} = \frac{D_p^2 \phi^{5.5}}{5.6 c}, \quad (7.35)$$

according to Rumpf and Gupte. They found that the porosity function  $f(\phi) = \phi^{-5.5}$ , fits the data best. A number of other porosity functions have been fitted to observations, see table 7.2.

From table 7.2 it is clear that a number of power-law type relations fit observations equally well. It is well known that fits of power laws to experimental data in a limited range gives unreliable results for the exponent. It is not to be expected that there is a general correlation between the permeability and porosity. A closed cell foam may have a large porosity and a negligible water permeability. Rocks with large poorly connected pores will have an unusually low permeability for a given porosity. Thus we conclude that factors other than the porosity  $\phi$  influence the permeability strongly. The comparison between the Carman-Kozeny result and the Rumpf and Gupte result is seen in figure 7.5.

### 7.2.2 Reynolds Number Dependence of the Permeability

From the curves in the figures 7.4–7.6, it is clear that there is a change in behavior near  $\text{Re} = 1$ , from the low velocity *creeping flow* to the nonlinear

$1/f(\phi)$	Author
$(1 - \phi)^2/\phi^3$	Blake (1922), Kozeny (1927), Carman (1937)
$(1 - \phi)^2/\phi$	Zunker (1920)
$[(1 - \phi)^{1.3}/(\phi - 0.13)]^2$	Terzaghi (1925)
$[1.115(1 - \phi)/\phi^{1.5}][(1 - \phi)^2 + 0.018]$	Rapier (1949)
$69.43 - \phi$	Hulbert and Feben (1933)
$\phi^{-3.3}$	Slichter (1898)
$\phi^{-1.0}$	Krüger (1918)
$\phi^{-6.0}$	Hatch (1934), Mavies and Wilsey (1936)
$\phi^{-4.0}$	Fehling (1939)
$\phi^{-4.1}$	Rose (1945)
$\phi^{-5.5}$	Rumpf and Gupte (1971)

Table 7.2: Different porosity functions for low Reynolds number flow. After Rumpf and Gupte (1971).

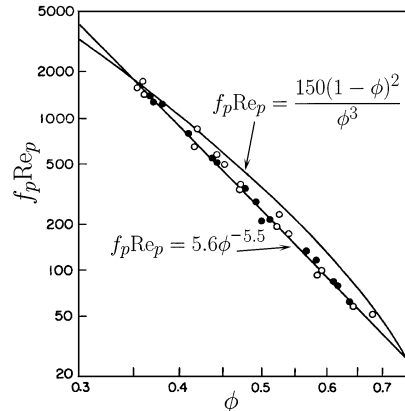


Figure 7.6: Comparison of the Rumpf and Gupte porosity function  $Re_p f_p = D^2/k = 5.6\phi^{-5.5}$  as a function of porosity,  $\phi$ . The Carman-Kozeny equation (7.21) gives  $Re_p f_p = K36(1 - \phi)^2/\phi^3$ . (from [] after []).

Figure 7.6: Comparison of the Rumpf and Gupte porosity function  $Re_p f_p = D^2/k$

regime where the inertial  $\mathbf{u} \cdot \nabla \mathbf{u}$  term in the Navier-Stokes equation becomes important and finally to the *turbulent* flow in the high velocity region. The phenomenological equation proposed by Forchheimer<sup>100</sup> (1901) to describe this crossover is

$$\frac{\Delta p}{L} = \alpha \mu U + \beta \rho U^2. \quad (7.36)$$

The coefficient  $\alpha$  must be identified with the inverse permeability  $1/k$ , in order to obtain Darcy's law at low Reynolds numbers. The so-called inertia parameter  $\beta$ , has the dimension  $[\beta] = \text{m}^{-1}$ , that is an inverse length. The Forchheimer equation may be written in a dimensionless form by rearranging equation (7.36), to give the form suggested by Ahmed and Sunada,<sup>101</sup>

$$\frac{\Delta p}{L \beta \rho U^2} = 1 + \frac{\alpha \mu}{\beta \rho U}, \quad (7.37)$$

where the last term on the right hand side is an inverse Reynolds number. With this form a very large set of experimental results collapse on a single curve as shown in figure 7.7.

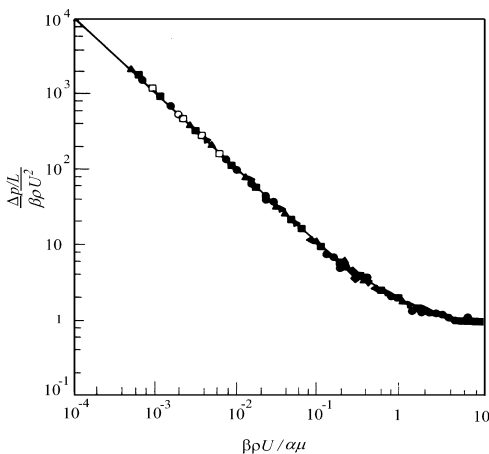


Figure 7.7: Dimensionless correlation based on the Forchheimer equation (from [ ] after [ ]).

Figure 7.7: Dimensionless correlation based on the Forchheimer equation (from [ ] after [ ]).

## Chapter 8

# Conduction through Porous Media

J. C. Maxwell<sup>102</sup> in *A Treatise on Electricity and Magnetism* (Vol 1, pp. 398–411) solves the general problem of electric flow in a inhomogeneous medium by a method that today would be called a position-space renormalization method, or a variant of the effective medium theory. His method and results are applicable to any problem where the property under discussion satisfies Laplace's equation with the same boundary conditions. Maxwell's law of mixtures is therefore appropriate also for flow in porous media that satisfies the Laplace equation (6.12) for  $p$  (see also table 6.2). We shall follow his discussion and consider the flow of electricity in a medium with resistivity  $\rho$  that has embedded in it spheres of a material with resistivity  $\rho_1$ .

### 8.1 A Single Sphere

The electric field  $\mathbf{E}$ , is related to the current density  $\mathbf{j}$ , by Ohm's law:

$$\mathbf{j} = \rho^{-1} \mathbf{E}. \quad (8.1)$$

Here  $\rho$ , is the specific resistance of the material. The continuity equation for the conservation of electric charge gives the result that at *steady state* (low frequency) the current density is without divergence

$$\nabla \cdot \mathbf{j} = 0, \quad (8.2)$$

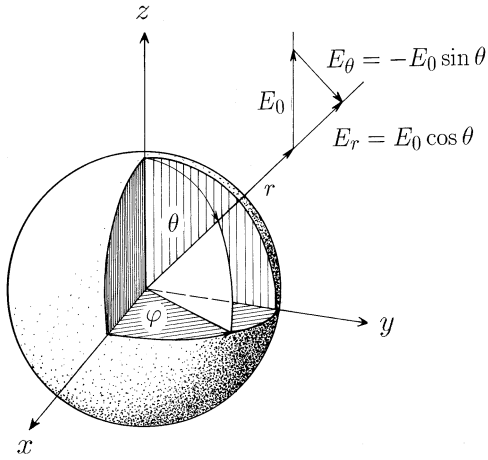


Figure 8.1: Polar coordinates for a single sphere

and the electric field is given by the gradient of the electric potential  $V$ :

$$\mathbf{E} = -\nabla V . \quad (8.3)$$

Therefore combining equations (8.1) and (8.3), we find that the potential must satisfy Laplace's equation

$$\nabla^2 V = 0 . \quad (8.4)$$

There are two conditions that the distribution of currents must fulfill in general:

1. The potential must be continuous across boundaries.
2. The currents must be continuous across boundaries.

As an example of these conditions let us suppose that the surface separating two media is spherical and of radius  $a$ . The specific resistivity being  $\rho_1$  within and  $\rho$  outside of the surface.

### 8.1.1 Homogeneous Electric Fields

Introducing polar coordinates (see figure 8.1) with the  $z$ -axis along the external homogeneous field of magnitude  $E_0$ , we find

$$\mathbf{E} = E_r \mathbf{e}_r + E_\theta \mathbf{e}_\theta + E_\varphi \mathbf{e}_\varphi , \quad (8.5)$$

where the orthogonal set of unit vectors  $\mathbf{e}_r$ ,  $\mathbf{e}_\theta$  and  $\mathbf{e}_\varphi$  specify the directions for the field components given by

$$\begin{aligned} E_r &= E_0 \cos \theta \\ E_\theta &= -E_0 \sin \theta \\ E_\varphi &= 0 \end{aligned} \quad (8.6)$$

In polar coordinates the gradient of a potential  $V$  is

$$\nabla V = \left( \frac{\partial V}{\partial r} \right) \mathbf{e}_r + \left( \frac{1}{r} \frac{\partial V}{\partial \theta} \right) \mathbf{e}_\theta + \left( \frac{1}{r \sin \theta} \frac{\partial V}{\partial \varphi} \right) \mathbf{e}_\varphi. \quad (8.7)$$

From this expression it follows that the potential for a uniform field in polar coordinates  $\mathbf{E}_0 = -\nabla V$  is given by

$$V = -E_0 r \cos \theta. \quad (8.8)$$

This is, of course, a trivial result since in Cartesian coordinates the electric field is  $\mathbf{E} = E_0(0, 0, 1) = -\nabla V = (\partial V / \partial x, \partial V / \partial y, \partial V / \partial z)$  so that  $\partial V / \partial z = -E_0$  and therefore  $V = -E_0 z$  apart from an arbitrary additional constant. Since  $z = r \cos \theta$  in polar coordinates equation (8.8) follows.

The divergence of the field  $\mathbf{E}$  is in polar coordinates given by:

$$\nabla \cdot \mathbf{E} = \frac{1}{r^2} \frac{\partial}{\partial r} (r^2 E_r) + \frac{1}{r \sin \theta} \frac{\partial}{\partial \theta} (\sin \theta E_\theta) + \frac{1}{r \sin \theta} \frac{\partial}{\partial \varphi} (E_\varphi). \quad (8.9)$$

It follows that the homogeneous field in equation (8.6) satisfies the equation  $\nabla \cdot \mathbf{E} = 0$  as required by equation (8.2). Thus the potential equation (8.8) satisfies the Laplace equation (8.4).

### 8.1.2 Electric Dipole Fields

The potential

$$V = Br^{-2} \cos \theta, \quad (8.10)$$

leads with equation (8.7) to an electric dipole field given by

$$\mathbf{E} = (2Br^{-3} \cos \theta) \mathbf{e}_r + (Br^{-3} \sin \theta) \mathbf{e}_\theta. \quad (8.11)$$

The dipole potential and the field are illustrated in figure 8.2. It is easy to show (using equation (8.9)) that this field satisfies the equation  $\rho \nabla \cdot \mathbf{j} = \nabla \cdot \mathbf{E} = -\nabla^2 V = 0$

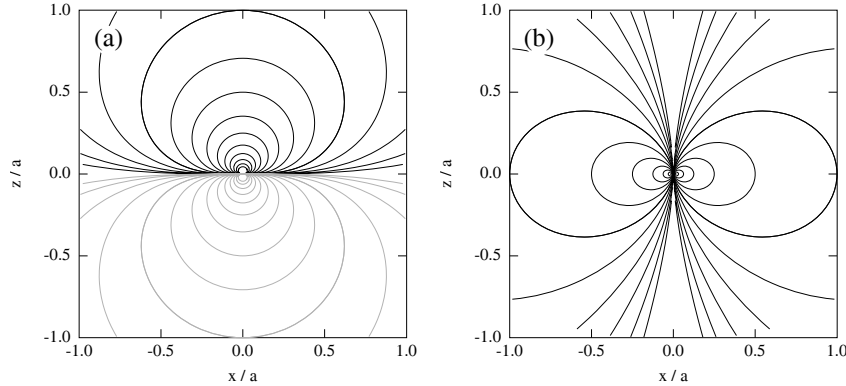


Figure 8.2: (a) – Equi-potential lines for the dipole potential  $V = Br^{-2} \cos \theta$  (in units of  $B/a^2$ ) as a function of position in reduced coordinates  $x/a$  and  $z/a$ , where  $a$  is a characteristic length scale (radius of a metallic sphere)  $V > 0$  for  $z > 0$  and  $V < 0$  for  $z < 0$  (gray curves). The contour through  $(0, 1)$  has  $V = V_0 = B/a^2$  the contours inside this contour have  $V = V_0 \times 2^n$  for  $n = 1, \dots, 9$ . Contours outside  $V_0$  have the same shape but fall partly outside the frame and have  $n = -1, \dots, -4$ . The contour through  $(0, -1)$  has  $V = -V_0$ . (b) – Electric field lines for the dipole potential as a function of position in reduced coordinates  $x/a$  and  $z/a$ . A positive ‘test-particle’ that follows the field lines starting on the  $z = 0$  axis would move down. The field lines shown have  $\mathbf{E}(x = a, z = 0) = (0, -E_n)$ , with  $E_n = 2^n \times Ba^{-3}$ . The field lines through  $(\pm 1, 0)$  have  $n = 0$ , those inside these field-line have increasing fields ( $n = 1, \dots, 5$ ), those outside have decreasing fields ( $n = -1, \dots, -5$ ).

### 8.1.3 A Sphere in a Homogeneous Field

Consider a sphere of radius  $a$  and resistivity  $\rho_1$  in an external medium of resistivity  $\rho$  in a homogeneous electric field  $\mathbf{E}_0$ . The potential must satisfy Laplace’s equation, which is a linear differential equation. Therefore any linear combination of solutions of the Laplace’s equation is also a solution. The boundary conditions are that the current through the interface is continuous, and that the potential is continuous at the interface. The solution, which satisfies the boundary conditions, is a superposition of a homogeneous field and a dipole field.

INSIDE THE SPHERE we try the following solution of the Laplace equation

equation (8.4)

$$V_1(r, \theta) = (A_1 r + B_1 r^{-2}) \cos \theta , \quad \text{for } 0 < r < a . \quad (8.12)$$

But we must require that the potential is finite everywhere inside the sphere; thus  $B_1 = 0$ . The potential inside the sphere must therefore have the form

$$V_1(r, \theta) = -E_1 r \cos \theta , \quad \text{for } r < a , \quad (8.13)$$

where  $E_1$  is the magnitude (to be determined later) of the *uniform* electric field inside the sphere.

OUTSIDE THE SPHERE we again try the superposition of a homogeneous and a dipole field:

$$V(r, \theta) = (Ar + Br^{-2}) \cos \theta , \quad \text{for } r > a . \quad (8.14)$$

But as  $r \rightarrow \infty$ , we must obtain asymptotically the applied uniform field and consequently we find that

$$V(r, \theta) = (-E_0 r + Br^{-2}) \cos \theta , \quad (8.15)$$

where  $B$  is to be determined from the boundary conditions.

CONTINUITY OF THE POTENTIAL at the surface of the sphere gives by matching  $V$  at the surface of the sphere the relation

$$E_1 = E_0 - B/a^3 . \quad (8.16)$$

CONTINUITY OF THE CURRENT through the interface gives

$$\rho_1^{-1} \mathbf{n} \cdot \mathbf{E}_1 = \rho^{-1} \mathbf{n} \cdot \mathbf{E} , \quad \text{at } r = a , \quad (8.17)$$

where  $\mathbf{n} = \mathbf{e}_r$  is the surface normal of the sphere,  $\mathbf{E} = -\nabla V$  and  $\mathbf{E}_1 = -\nabla V_1$ . Thus we may write

$$\frac{1}{\rho_1} E_{1r}(a, \theta) = \frac{1}{\rho} E_r(a, \theta) . \quad (8.18)$$

Using the expressions for the fields that follow from the potentials in equations (8.13) and (8.15) we find that

$$\frac{1}{\rho_1} E_1 \cos \theta = \frac{1}{\rho} (E_0 + 2B/a^3) \cos \theta . \quad (8.19)$$

Substituting equation (8.16) here, we find

$$\frac{1}{\rho_1} (E_0 - B/a^3) = \frac{1}{\rho} (E_0 + 2B/a^3) , \quad (8.20)$$

which leads to an explicit expression for  $B$

$$B = a^3 \frac{\rho - \rho_1}{\rho + 2\rho_1} E_0 . \quad (8.21)$$

If we now replace  $B$  in equation (8.16) we find that the field inside the sphere is *homogeneous* and given by

$$E_1 = E_0 \left( 1 - \frac{\rho - \rho_1}{\rho + 2\rho_1} \right) = \frac{3\rho_1}{\rho + 2\rho_1} E_0 , \quad \text{for } r < a . \quad (8.22)$$

The field *outside* the sphere consists of a superposition of an homogeneous field and a dipole field:

$$\begin{aligned} \mathbf{E} = & E_0 \cos \theta \left\{ 1 + 2 \left( \frac{a}{r} \right)^3 \frac{\rho - \rho_1}{\rho + 2\rho_1} \right\} \mathbf{e}_r \\ & + E_0 \sin \theta \left\{ -1 + \left( \frac{a}{r} \right)^3 \frac{\rho - \rho_1}{\rho + 2\rho_1} \right\} \mathbf{e}_\theta . \end{aligned} \quad (8.23)$$

If  $\rho_1/\rho \rightarrow 0$ , we have the case of a conducting sphere in an insulating medium, and  $E_1 = 0$ , as expected. If, on the other hand,  $\rho_1 \rightarrow \infty$ , we have the case of an insulating sphere in a conductor and in this case  $E_1 = \frac{3}{2}E_0$ , the well known Lorentz<sup>103</sup> result.

#### 8.1.4 Many Spheres

If there are  $n$  spheres of radius  $a$ , and resistivity  $\rho_1$ , placed in a medium whose resistivity is  $\rho$ , at such a distance from each other that their effects in disturbing the course of current may be taken to be independent of each other, then if these spheres are all contained within a sphere of radius  $a'$ , the potential at a great distance from the center of this sphere will be in the form

$$V = (-E_0 r + nBr^{-2}) \cos \theta , \quad \text{for } a \ll a' \ll r , \quad (8.24)$$

where  $B$  is given by equation (8.21)

The filling factor of the material (1) in the large sphere of radius  $a'$  is

$$c = (1 - \phi) = n(a/a')^3 , \quad (8.25)$$

as indicated in figure 8.3. Therefore the potential can be written

$$V = -E_0 r \left\{ 1 + c \left( \frac{a'}{r} \right)^3 \frac{\rho_1 - \rho}{2\rho_1 + \rho} \right\} \cos \theta . \quad (8.26)$$

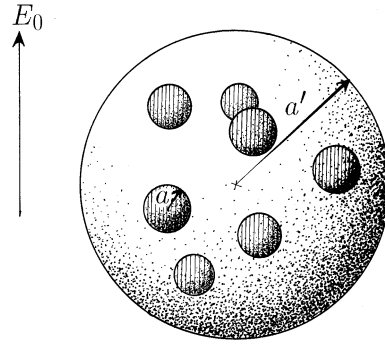


Figure 8.3: A spherical inhomogeneous conductor in a uniform external field.

Now if the whole sphere of radius  $a'$ , had been made of a material of resistivity  $\rho_{\text{eff}}$ , the potential outside the sphere would be

$$V = -E_0 r \left( 1 + (a'/r)^3 \frac{\rho_{\text{eff}} - \rho}{2\rho_{\text{eff}} + \rho} \right) \cos \theta. \quad (8.27)$$

The effective resistivity is determined by the requirement that equations (8.26) and (8.27) should be equivalent to one another and we obtain the relation

$$c \frac{\rho_1 - \rho}{2\rho_1 + \rho} = \frac{\rho_{\text{eff}} - \rho}{2\rho_{\text{eff}} + \rho}, \quad (8.28)$$

which may be solved for the effective resistivity<sup>1</sup>

$$\rho_{\text{eff}} = \rho \frac{2\rho_1 + \rho + c(\rho_1 - \rho)}{2\rho_1 + \rho - 2c(\rho_1 - \rho)}. \quad (8.29)$$

This is *Maxwell's law of mixtures* (1881). It is identical to Rayleigh's<sup>104</sup> (1892) result for the effective resistance of a lattice of spheres embedded in a matrix of a different conductivity in the limit  $c \ll 1$ . Maxwell's law is valid for anything that satisfies Laplace's equation, for instance elastic constants, thermal resistivities, diffusion constants, dielectric constants, porous media permeabilities.

It is useful to rewrite the expression for  $\rho_{\text{eff}}$  in terms of the conductivity  $\sigma = 1/\rho$ :

$$\sigma_{\text{eff}} = \sigma \frac{2\sigma + \sigma_1 - 2c(\sigma - \sigma_1)}{2\sigma + \sigma_1 + c(\sigma - \sigma_1)}. \quad (8.30)$$

---

<sup>1</sup>It is tempting to set up a self consistency relation by letting  $\rho = \rho_{\text{eff}}$ . But this leads to  $\rho_{\text{eff}} = \rho_1$ !

Let us consider a few limiting cases.

- If the spheres and the medium have the same resistivity  $\rho_1 = \rho$ , we find the expected result  $\rho_{\text{eff}} = \rho$ .
- If the spheres are ‘superconducting’ (more precisely, have  $\rho_1 = 0$ ) the effective resistivity is

$$\rho_{\text{eff}} = \rho(1 - c)/(1 + 2c) , \quad (8.31)$$

which is seen to become equal to the matrix resistivity if the volume fraction of the superconductor vanishes. On the other hand if the volume fraction approaches unity the effective resistivity correctly vanishes. However, this divergence should have occurred at the latest at the maximal filling factor for the close packed array of spheres  $\phi = 0.74048$ , and for random packings of spheres at  $\phi = 0.637$ . Considering that Maxwell’s formula is derived under the assumption  $c \ll 1$ , it does remarkably well even at high filling factors.

- If the spheres are insulating  $\rho_1 = \infty$ , then the effective resistivity is

$$\rho_{\text{eff}} = \rho \frac{2 + c}{2 - 2c} , \quad (8.32)$$

and this correctly diverges as the volume fraction of the insulator approaches one.

- In the limit of low filling factors Maxwell’s law of mixtures becomes

$$\rho_{\text{eff}} = \rho(1 + 3c \frac{\rho_1 - \rho}{2\rho_1 + \rho} + \dots) . \quad (8.33)$$

We may also consider a few simple cases illustrated in figure 8.4. for non-spherical arrangements of the two materials. For the case of parallel slabs perpendicular to the flow we have effectively a set of series resistors with resistances

$$R_1 = \rho_1 c L / A \quad \text{and} \quad R_2 = \rho(1 - c)L / A \quad (8.34)$$

so that the effective resistivity becomes

$$\rho_{\perp} = \rho \frac{\rho - c(\rho - \rho_1)}{\rho} , \quad (8.35)$$

for the parallel case the material may be distributed in any way what so ever and the two parallel resistances are

$$R_1 = \rho_1 L / cA \quad \text{and} \quad R_2 = \rho L / (1 - c)A \quad (8.36)$$

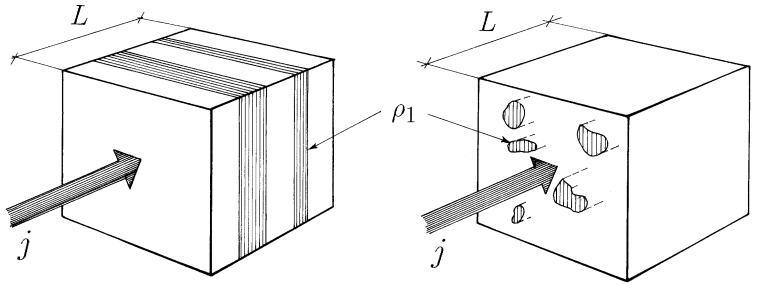


Figure 8.4: Two simple configurations of mixed conductors.

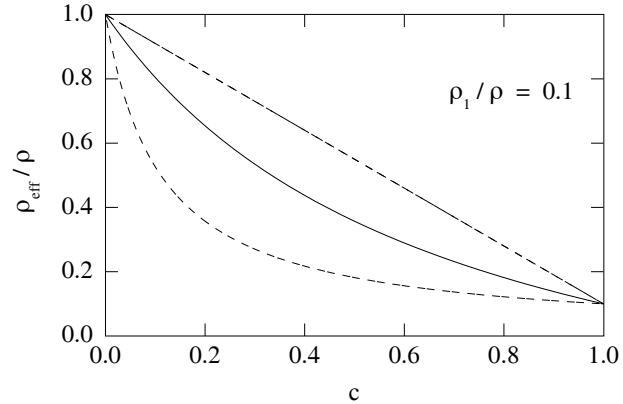


Figure 8.5: The effective resistivity as function of the volume fraction of the low resistivity fraction. Maxwell's result is intermediate between the situation where the sample consists of layers perpendicular to the current (top curve) and the situation where the current is parallel to the inhomogeneities (bottom curve).

thus the effective resistivity for the parallel conductor case becomes

$$\rho_{\parallel} = \rho \frac{\rho_1}{\rho_1 + c(\rho - \rho_1)} . \quad (8.37)$$

Since these expressions differ considerably in detail from the Maxwell's law of mixtures, it is to be expected that the detailed particle shape and size distribution will affect the Maxwell law in practice. A comparison of the

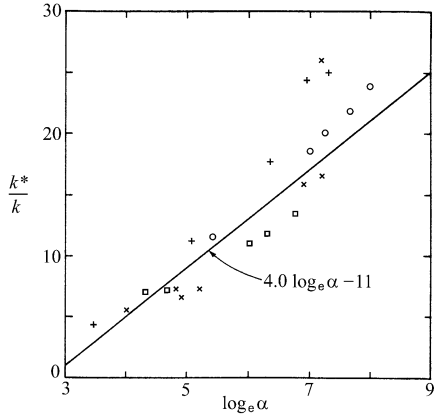


Figure 8.6: Comparison of the Batchelor & O'Brien formula to experimental results.

mixture laws for  $(\rho_1/\rho) = 0.1$ , is shown in figure 8.5.

Batchelor and O'Brien<sup>105</sup> have derived an expression for the electrical conduction through a statistically uniform granular material, in the limit of high volume fractions of the conducting material and with  $\rho/\rho_1 \ll 1$ . They find that the effective resistivity is then given by

$$\rho_{\text{eff}} = \rho \left( 1 + 4 \ln \frac{\rho}{\rho_1} \right). \quad (8.38)$$

The logarithmic divergence in the conductivity is well brought out in the experimental results shown in figure 8.6.

## Chapter 9

# Hydrodynamic Flow in Periodic Media

The discussion of flow through periodic arrays has a long history and the first serious attempt was made by Rayleigh<sup>104</sup> who solved the equations for flow of electricity through a periodic array of cylinders or spheres, in terms of an expansion in the filling factor,  $c = 1 - \phi$ , of the obstacles as a small parameter. Rayleigh recovered Maxwell's result (8.29) as the first order term and found the next order term by numerical methods. Rayleigh's method has since been pursued and recently evaluated numerically to very high orders. In this section we will discuss the solution of the hydrodynamic flow equations in a system of regularly spaced spheres.

In the limit of low Reynolds numbers the Navier-Stokes equations for incompressible stationary flow simplify to the linear *Stokes equations*

$$\nabla p = \mu \nabla^2 \mathbf{u} + \mathbf{F}, \quad \nabla \cdot \mathbf{u} = 0, \quad (9.1)$$

where the last equation is the continuity equation for stationary flow. The force  $\mathbf{F}$  is the volume force density that we will use as a periodic point force in order to satisfy the boundary conditions. The non-slip boundary conditions insists on vanishing velocities at interfaces with surface normal  $\mathbf{n}$  and they may be expressed as follows:

$$\mathbf{n} \cdot \mathbf{u} = 0, \quad \text{and} \quad \mathbf{n} \times \mathbf{u} = 0. \quad (9.2)$$

We consider the flow around a set of  $N$  spheres of radius  $a$  placed on a lattice defined by the lattice points

$$\mathbf{R}_n = n_1 \mathbf{a} + n_2 \mathbf{b} + n_3 \mathbf{c}, \quad (9.3)$$

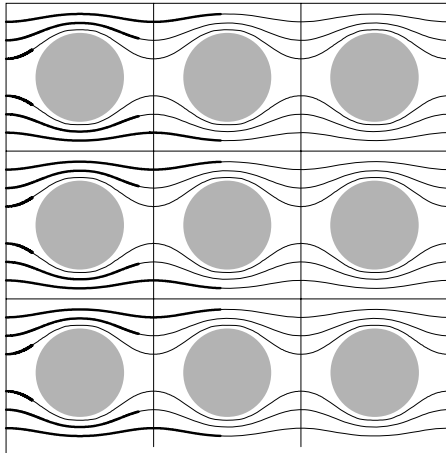


Figure 9.1: Streamlines in a periodic lattice of cylinders. The heavy lines show the trace of particles that start simultaneously at the left and follow the streamlines. The square lattice (thin lines) has one cylinder in each unit cell.

where  $\mathbf{a}$ ,  $\mathbf{b}$ ,  $\mathbf{c}$ , are the vectors defining the unit cell, and  $\mathbf{n} = (n_1, n_2, n_3)$  are integer indices ( $n_i = 0, \pm 1, \pm 2, \dots$ ). The velocity field must be a periodic function with the period of the lattice

$$\mathbf{u}(\mathbf{r} + \mathbf{R}_\mathbf{n}) = \mathbf{u}(\mathbf{r}), \quad (9.4)$$

for any point  $\mathbf{r}$ . For a complete description of the velocity field it is sufficient to obtain the velocity field in a single unit cell, the velocity elsewhere can then be obtained using equation (9.4). For the sake of discussion we may take the average flow to be in the  $x$ -direction as illustrated in figure 9.1. The flux through the system is the same through every unit cell, and the volume flow per unit area and time is given by

$$\mathbf{U} = \frac{1}{V} \int_V \mathbf{u} d^3 r. \quad (9.5)$$

The Darcy velocity is simply the velocity field averaged over of the unit cell with volume  $V = \mathbf{a} \cdot (\mathbf{b} \times \mathbf{c})$ . The fact that  $\mathbf{u}$  has a non-vanishing average is consistent with the periodicity of  $\mathbf{u}$  (a constant  $\mathbf{u}$  is periodic with any period).

The pressure  $p$  has an average non-periodic gradient in addition to the

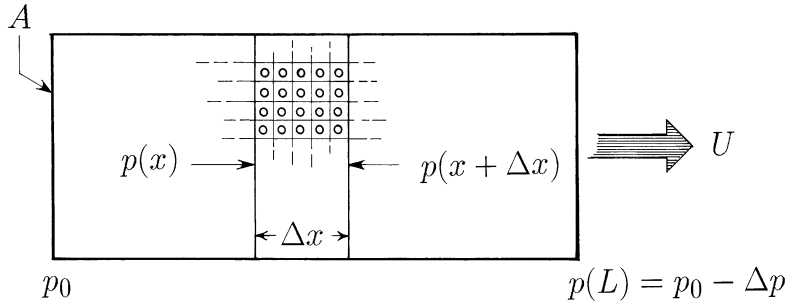


Figure 9.2: The pressure due to the pressure gradient over an array

periodic part

$$p(\mathbf{r}) = -\mathbf{G} \cdot \mathbf{r} + p'(\mathbf{r}), \quad (9.6)$$

where  $p'(\mathbf{r})$  is the periodic part of the pressure satisfying the relation

$$p'(\mathbf{r} + \mathbf{R}_n) = p'(\mathbf{r}). \quad (9.7)$$

The pressure gradient,  $\mathbf{G}$ , is parallel to the average velocity  $\mathbf{U}$ . Let

$$\mathbf{G} = \langle -\nabla p \rangle = \frac{\Delta p}{L}(1, 0, 0), \quad (9.8)$$

so that there is a pressure drop  $\Delta p = |\Delta p|$ , over the length  $L$ , of the sample as illustrated in figure 9.2. The pressure drop over the sample is directly related to the net force acting on the spheres. The force due to a pressure gradient on the volume element illustrated in figure 9.2 is

$$F_p = \{p(x) - p(x + \Delta x)\}A = G\Delta x A, \quad (9.9)$$

in the direction of flow. Here  $A$  is the cross-section of the fluid element. Since the fluid flow is stationary, this force must be exactly balanced by the force acting on the fluid due to its interaction with the spheres. Because of the periodicity it is enough to consider the volume element to be a single unit cell.  $F_p$  is independent of  $y$  by symmetry. It follows that the force acting on each sphere has the direction of the average flow  $\mathbf{U}$  and a magnitude given by

$$F_s = GV = \frac{\Delta p}{L}V. \quad (9.10)$$

By the definition of the fluid *stress tensor*  $\boldsymbol{\sigma}$ , which here includes the hydrostatic pressure term  $-p\delta_{ij}$ , the force per unit area acting on a surface

element with normal direction  $\mathbf{n}$  is

$$\mathbf{f} = \mathbf{n} \cdot \boldsymbol{\sigma} . \quad (9.11)$$

The force  $\mathbf{F}_s$  acting on a sphere is therefore also given by the surface integral of  $\mathbf{f}$  over the sphere surface  $S$ :

$$\mathbf{F}_s = \int_S \mathbf{f} dS = \int_S \boldsymbol{\sigma} \cdot d\mathbf{S} = \mathbf{G}V . \quad (9.12)$$

The force acting on each sphere will move them unless the spheres are packed in a lattice structure, that is, SC, FCC, HCP,.... Higher porosities, in which the spheres do not touch each other can be obtained in *fluidized beds*. In a fluidized bed the upward flow of a fluid just compensates the settling of the spheres due gravity. As the flow rate increases the packing density decreases in such a way that the pressure drop over the packing is just enough to lift all the spheres. Experiments<sup>106</sup> on small spheres (0.6  $\mu\text{m}$  in diameter in water) show the spheres in a fluidized bed forms a FCC lattice because of weak electrostatic interactions between the spheres. The expansion of the fluidized bed with increasing flow velocity is accurately described by the theory presented in this chapter.<sup>1</sup>

The Stokes equation (9.1) is a linear differential equation therefore the force on the spheres must be proportional to the average velocity  $\mathbf{U}$ . The Stokes drag on a sphere is also proportional to velocity (see equation (5.66)) and we may therefore introduce a *drag coefficient*  $C_D$ , by the relation<sup>2</sup>

$$\mathbf{F}_s = C_D \mathbf{F}_{\text{Stokes}} = C_D 6\pi\mu a \mathbf{U} . \quad (9.13)$$

Moreover,  $\mathbf{F}_s$  is related to the pressure gradient by equation (9.10) so we may write equation (9.13) in the form of *Darcy's equation*

$$\mathbf{U} = \frac{V}{6\pi\mu a C_D} \mathbf{G} . \quad (9.14)$$

The unit cell volume  $V$  can be expressed in terms of the sphere radius  $a$ , and the *filling factor*  $c$  or the porosity  $\phi$ , by

$$V = \frac{4\pi a^3}{3c} = \frac{4\pi a^3}{3(1 - \phi)} . \quad (9.15)$$

---

<sup>1</sup>Fluidized beds may exhibit complicated dynamics involving bubbles of low density regions moving within high density surroundings. Such bubbles are commonly observed when a gas is the suspending fluid.

<sup>2</sup>Demonstrate that  $\mathbf{F}_s$  and  $\mathbf{U}$  have the same direction

The permeability,  $k = V/6\pi a C_D$ , is therefore related to the drag coefficient  $C_D$  by

$$k = \frac{2a^2}{9C_D c} = \frac{2a^2}{9C_D(1-\phi)} \quad (9.16)$$

This for the permeability should be compared to the Carman-Kozeny expression (7.21)

$$k_{\text{C-K}} = \frac{a^2}{9K} \frac{\phi^3}{(1-\phi)^2}. \quad (9.17)$$

Where the constant  $K \simeq 5$  for random packings of spheres. Equations (9.14) and (9.15) lead to a drag coefficient  $C_D = 10(1-\phi)/\phi^3$  corresponding to the Carman-Kozeny permeability expression.

## 9.1 The Fundamental Solution

### 9.1.1 Periodic Functions and Lattice Fourier Sums

It is well known in solid state physics that any periodic function  $f(\mathbf{r})$  with the periodicity of the lattice may be written as a discrete *lattice Fourier sum*

$$f(\mathbf{r}) = \sum_{\mathbf{q}} f_{\mathbf{q}} e^{-i\mathbf{q}\cdot\mathbf{r}}. \quad (9.18)$$

Here  $\mathbf{q}$  is a vector to a point in the *reciprocal lattice* defined by the unit cell vectors

$$\mathbf{a}^* = \frac{2\pi}{V}(\mathbf{b} \times \mathbf{c}), \quad \mathbf{b}^* = \frac{2\pi}{V}(\mathbf{c} \times \mathbf{a}), \quad \mathbf{c}^* = \frac{2\pi}{V}(\mathbf{a} \times \mathbf{b}). \quad (9.19)$$

Here  $\mathbf{q}$  is given by

$$\mathbf{q} = m_1 \mathbf{a}^* + m_2 \mathbf{b}^* + m_3 \mathbf{c}^*, \quad (9.20)$$

for  $m_1, m_2$  and  $m_3$  positive or negative integers. The reciprocal lattice unit vectors and the direct lattice unit vectors are orthogonal:

$$\begin{aligned} \mathbf{a}^* \cdot \mathbf{a} &= \mathbf{b}^* \cdot \mathbf{b} &= \mathbf{c}^* \cdot \mathbf{c} &= 2\pi, \\ \mathbf{a}^* \cdot \mathbf{b} &= \mathbf{a}^* \cdot \mathbf{c} &= \dots &= 0. \end{aligned} \quad (9.21)$$

and the unit cell in the reciprocal lattice has a volume

$$V^* = \mathbf{a}^* \cdot (\mathbf{b}^* \times \mathbf{c}^*) = \frac{(2\pi)^3}{V}, \quad (9.22)$$

where  $V = \mathbf{a} \cdot (\mathbf{b} \times \mathbf{c})$  is the unit cell volume for the periodic lattice.

To show that  $f(\mathbf{r})$  is indeed periodic express  $f(\mathbf{r} + \mathbf{R}_n)$  as a lattice Fourier sum

$$\begin{aligned} f(\mathbf{r} + \mathbf{R}_n) &= \sum_{\mathbf{q}} f_{\mathbf{q}} e^{-i\mathbf{q}\cdot\mathbf{r}} e^{-i\mathbf{q}\cdot\mathbf{R}_n} \\ &= \sum_{\mathbf{q}} f_{\mathbf{q}} e^{-i\mathbf{q}\cdot\mathbf{r}} = f(\mathbf{r}) . \end{aligned} \quad (9.23)$$

Here we have made use of the fact that

$$e^{-i\mathbf{q}\cdot\mathbf{R}_n} = 1 , \quad (9.24)$$

since  $\mathbf{q}\cdot\mathbf{R}_n = (m_1\mathbf{a}^* + m_2\mathbf{b}^* + m_3\mathbf{c}^*)(n_1\mathbf{a} + n_2\mathbf{b} + n_3\mathbf{c}) = 2\pi(m_1n_1 + m_2n_2 + m_3n_3) = 2\pi M$ , where  $M$  is an integer.

A lattice Kronecker  $\delta$ -function in the reciprocal space is defined by the integral

$$\frac{1}{NV} \int d^3\mathbf{r} e^{i(\mathbf{q}-\mathbf{Q})\cdot\mathbf{r}} = \delta_{\mathbf{q},\mathbf{Q}} . \quad (9.25)$$

Here the sample volume is  $NV$  and  $N$  is the number of unit cells. The vectors  $\mathbf{q}$  and  $\mathbf{Q}$  are vectors in reciprocal space, and  $\mathbf{q}$  is on the reciprocal lattice. However, the integral is non-zero<sup>3</sup> only if  $\mathbf{Q} = \mathbf{q}$  and they are both on the reciprocal lattice, that is, they have the form (9.20). The lattice Kronecker  $\delta$ -function,  $\delta_{\mathbf{q},\mathbf{Q}}$ , is defined by

$$\delta_{\mathbf{q},\mathbf{Q}} = \begin{cases} 1 & , \mathbf{Q} = \mathbf{q} , \text{on reciprocal lattice,} \\ 0 & , \mathbf{Q} \neq \mathbf{q} . \end{cases} \quad (9.26)$$

The Fourier coefficients  $f_{\mathbf{q}}$  in equation (9.18) are given by

$$f_{\mathbf{q}} = \frac{1}{NV} \int d^3\mathbf{r} f(\mathbf{r}) e^{i\mathbf{q}\cdot\mathbf{r}} . \quad (9.27)$$

To see this express  $f(\mathbf{r})$  in the integral above using equation (9.18), then use equation (9.25) to get

$$\sum_{\mathbf{Q}} f_{\mathbf{Q}} \frac{1}{NV} \int d^3\mathbf{r} e^{i(\mathbf{q}-\mathbf{Q})\cdot\mathbf{r}} = \sum_{\mathbf{Q}} f_{\mathbf{Q}} \delta_{\mathbf{q},\mathbf{Q}} = f_{\mathbf{q}} . \quad (9.28)$$

We will also need the lattice-periodic  $\delta$ -function defined by:

$$\Delta(\mathbf{r} - \mathbf{r}') = \sum_{\mathbf{n}} \delta(\mathbf{r} - \mathbf{r}' + \mathbf{R}_n) . \quad (9.29)$$

---

<sup>3</sup>For a cubic lattice with  $NV = L^3$  we have with  $k = (\mathbf{Q} - \mathbf{q})_x$  that the integral in equation (9.25) is the product of three integrals of the form  $\frac{1}{L} \int_{-L/2}^{L/2} dx e^{ikx} = \frac{1}{ikL} (e^{ikL/2} - e^{-ikL/2}) = \frac{2}{kL} \sin(kL/2)$ . This integral vanishes with increasing  $L$ , that is, for  $kL \rightarrow \infty$ , unless  $kL \rightarrow 0$ , which requires  $k$  to vanish. When  $k = 0$  the integral equals one.

The Fourier amplitudes  $\Delta_{\mathbf{q}} = 1/V$  are constant and independent of  $\mathbf{q}$  as can bee seen from the general expression (9.27)

$$\begin{aligned}\Delta_{\mathbf{q}} &= \frac{1}{NV} \int d^3 \mathbf{r} \Delta(\mathbf{r} - \mathbf{r}') e^{i\mathbf{q} \cdot (\mathbf{r} - \mathbf{r}')} \\ &= \sum_{\mathbf{n}} \frac{1}{NV} \int d^3 \mathbf{x} \delta(\mathbf{x} + \mathbf{R}_n) e^{i\mathbf{q} \cdot \mathbf{x}} \\ &= \sum_{\mathbf{n}} \frac{1}{NV} e^{i\mathbf{q} \cdot \mathbf{R}_n} = \frac{1}{V}.\end{aligned}\quad (9.30)$$

We may therefore write the lattice-periodic  $\delta$ -function as

$$\Delta(\mathbf{r} - \mathbf{r}') = \frac{1}{V} \sum_{\mathbf{q}} e^{-i\mathbf{q} \cdot (\mathbf{r} - \mathbf{r}')}. \quad (9.31)$$

### 9.1.2 The Stokes Equation in Reciprocal Space

The velocity  $\mathbf{u}$ , the pressure gradient  $\nabla p$ , and the force  $\mathbf{F}$  are periodic functions with the periodicity of the lattice so we may write them as Fourier lattice sums:

$$\begin{aligned}\mathbf{u}(\mathbf{r}) &= \sum_{\mathbf{q}} \mathbf{u}_{\mathbf{q}} e^{-i\mathbf{q} \cdot \mathbf{r}}, \\ -\nabla p &= \sum_{\mathbf{q}} \mathbf{G}_{\mathbf{q}} e^{-i\mathbf{q} \cdot \mathbf{r}}, \\ \mathbf{F}(\mathbf{r}) &= \sum_{\mathbf{q}} \mathbf{F}_{\mathbf{q}} e^{-i\mathbf{q} \cdot \mathbf{r}}.\end{aligned}\quad (9.32)$$

With these expressions the Stokes equation (9.1) takes the form

$$\mu q^2 \mathbf{u}_{\mathbf{q}} = \mathbf{G}_{\mathbf{q}} + \mathbf{F}_{\mathbf{q}}, \quad (9.33)$$

Here the force Fourier amplitude  $\mathbf{F}_{\mathbf{q}}$  is given by

$$\mathbf{F}_{\mathbf{q}} = \frac{1}{NV} \int d^3 \mathbf{r} e^{i\mathbf{q} \cdot \mathbf{r}} \mathbf{F}(\mathbf{r}). \quad (9.34)$$

In Fourier space the continuity equation  $\nabla \cdot \mathbf{u} = 0$  has the form

$$\mathbf{q} \cdot \mathbf{u}_{\mathbf{q}} = 0. \quad (9.35)$$

Since the pressure gradient is the gradient of a scalar it follows that the curl of the gradient must vanish or

$$\mathbf{q} \times \mathbf{G}_{\mathbf{q}} = 0. \quad (9.36)$$

For  $q = 0$ , the solution of equation (9.33) is

$$\mathbf{G}_0 = -\mathbf{F}_0. \quad (9.37)$$

The average force from the spheres acting on the fluid is  $F_0$ , and opposes the pressure gradient as required for stationary flow.

For  $\mathbf{q} \neq 0$  we find, by multiplying equation (9.33) by  $\mathbf{q}$ , that

$$\mu q^2 \mathbf{q} \cdot \mathbf{u}_q = \mathbf{q} \cdot \mathbf{G}_q + \mathbf{q} \cdot \mathbf{F}_q . \quad (9.38)$$

The continuity equation (9.35) leads to the conclusion that the left hand side of equation (9.38) vanishes. Since  $\mathbf{G}_q$  is parallel to  $\mathbf{q}$ , as seen from equation (9.36), it follows that the gradient amplitudes are given by

$$\mathbf{G}_q = -q^{-2} \mathbf{q} \mathbf{q} \cdot \mathbf{F}_q . \quad (9.39)$$

Inserting this result into equation (9.33), we find the Fourier amplitudes of the velocity field

$$\mathbf{u}_q = \frac{1}{\mu} \left\{ \frac{\mathbf{1}}{q^2} - \frac{\mathbf{q}\mathbf{q}}{q^4} \right\} \cdot \mathbf{F}_q , \quad (\mathbf{q} \neq 0) . \quad (9.40)$$

Note that equation (9.40) makes explicit the expectation that the velocities are proportional to the applied forces. The velocity may now be written

$$\mathbf{u}_q = \chi_q \cdot \mathbf{F}_q . \quad (9.41)$$

Here the (tensor) *linear response function* is

$$\boxed{\chi_q = \frac{1}{\mu} \left\{ \frac{\mathbf{1}}{q^2} - \frac{\mathbf{q}\mathbf{q}}{q^4} \right\} , \quad (\mathbf{q} \neq 0)} \quad (9.42)$$

The velocity field in real space is, using equation (9.32), given by

$$\begin{aligned} \mathbf{u}(\mathbf{r}) &= \mathbf{U} + \sum'_q \chi_q \cdot \mathbf{F}_q e^{-i\mathbf{q} \cdot \mathbf{r}} \\ &= \mathbf{U} + \sum'_q \chi_q e^{-i\mathbf{q} \cdot \mathbf{r}} \frac{1}{NV} \int d^3 \hat{\mathbf{r}} e^{i\mathbf{q} \cdot \hat{\mathbf{r}}} \mathbf{F}(\hat{\mathbf{r}}) , \end{aligned} \quad (9.43)$$

where  $\mathbf{U}$  is the  $\mathbf{q} = 0$ , or uniform component of the velocity field. The prime in the sum  $\sum'_q$  denotes a summation that excludes the term  $\mathbf{q} = 0$ . The relation (9.43) may be written in the form

$$\mathbf{u}(\mathbf{r}) = \mathbf{U} + \frac{1}{NV} \int d^3 \hat{\mathbf{r}} \chi(\mathbf{r} - \hat{\mathbf{r}}) \cdot \mathbf{F}(\hat{\mathbf{r}}) , \quad (9.44)$$

where the *linear response function* or *Green's function* for the problem at hand is given by the Fourier lattice sum

$$\chi(\mathbf{r} - \hat{\mathbf{r}}) = \sum'_q \chi_q e^{-i\mathbf{q} \cdot (\mathbf{r} - \hat{\mathbf{r}})} . \quad (9.45)$$

This Green's function specifies the velocity at a point  $\mathbf{r}$  if periodic forces of unit magnitude are applied in all the points  $\mathbf{r}' + \mathbf{R}_n$ . More precisely,

let  $\mathbf{f}$  be the force (of unit magnitude) applied at  $\mathbf{r}'$  and at all the points  $\mathbf{r}' + \mathbf{R}_n$ . This *periodic point force* may be written

$$\mathbf{F}(\mathbf{r}) = \Delta(\mathbf{r} - \mathbf{r}')\mathbf{f} = \sum_n \delta(\mathbf{r} - \mathbf{r}' - \mathbf{R}_n)\mathbf{f}. \quad (9.46)$$

The integral in equation (9.44) is easily evaluated with this force and we find that

$$\mathbf{u}(\mathbf{r}) = \mathbf{U} + \frac{1}{V}\chi(\mathbf{r} - \mathbf{r}') \cdot \mathbf{f}, \quad (9.47)$$

and  $\chi(\mathbf{r} - \mathbf{r}')$  is therefore the change in velocity at  $\mathbf{r}$  given unit periodic force at  $\mathbf{r}'$ .

The *fundamental solution* (9.47) of the *Stokes equation*, can with equations (9.45) and (9.42) be written as

$$\mathbf{u} = \mathbf{U} + \frac{1}{\mu} (S_1 \mathbf{f} + \nabla \mathbf{f} \cdot \nabla S_2), \quad (9.48)$$

which in Cartesian coordinates has the form

$$u_i = U_i + \frac{1}{\mu} \left( f_i S_1 + \sum_j f_j \frac{\partial^2 S_2}{\partial x_i \partial x_j} \right). \quad (9.49)$$

The two sums  $S_1$  and  $S_2$  are given by

$$\begin{aligned} S_1 &= \frac{1}{V} \sum'_q q^{-2} e^{-i\mathbf{q} \cdot (\mathbf{r} - \mathbf{r}')}, \\ S_2 &= \frac{1}{V} \sum'_q q^{-4} e^{-i\mathbf{q} \cdot (\mathbf{r} - \mathbf{r}')}. \end{aligned} \quad (9.50)$$

As pointed out by Hasimoto<sup>107</sup> these sums are solutions of the equations

$$\begin{aligned} \nabla^2 S_2 &= -S_1, \\ \nabla^2 S_1 &= -\left(\Delta(\mathbf{r} - \mathbf{r}') - \frac{1}{V}\right). \end{aligned} \quad (9.51)$$

The last equation shows that  $S_1$  is equivalent to the electrostatic potential of a lattice composed of positive unit charges surrounded by uniform cloud of negative charge that neutralizes them. This uniform background charge corresponds to the mean pressure gradient in the present problem, and rescues the lattice sums from diverging. The sums were evaluated by Ewald<sup>108</sup> in his calculation of the *Madelung energy* of ionic crystals.

## 9.2 Lattice of Small Spheres

Hasimoto<sup>107</sup> discussed the boundary condition of vanishing velocity  $\mathbf{u}$  at the surface of periodically arranged spheres with radius  $a$ . It is sufficient for small *filling factors* of the spheres ( $c \ll 1$ ) to evaluate the sums  $S_1$  and  $S_2$  limit  $r \rightarrow 0$ . Burgers<sup>109</sup> has shown that the point force  $\mathbf{f}$  can to a good approximation be obtained from equation (9.49), if the mean velocity on the sphere vanishes.

$$\langle \mathbf{u} \rangle = (4\pi a^2)^{-1} \int_S \mathbf{u} dS = 0 . \quad (9.52)$$

Thus the *non-slip boundary condition* is violated in this approximation. The result for the force  $\mathbf{F}_s = -\langle \mathbf{f} \rangle$ , is

$$\mathbf{F}_s = C_D 6\pi\mu a \mathbf{U} , \quad (9.53)$$

with the *drag coefficient*  $C_D$ , given by

$$C_D^{-1} = \begin{cases} 1 - 1.7601c^{1/3} + c - 1.5593c^2 + \dots & \text{sc} \\ 1 - 1.791c^{1/3} + c - 0.329c^2 + \dots & \text{bcc} \\ 1 - 1.791c^{1/3} + c - 0.302c^2 + \dots & \text{fcc} \end{cases} \quad (9.54)$$

Here we have included Hasimoto's terms, which take the boundary conditions into account to order  $a^6$ , for the simple cubic lattice (sc), the body centered lattice (bcc), and the face centered close packed lattice (fcc).

From the drag coefficient we obtain the permeability from equation (9.16), and in figure 9.3 we have plotted Hasimoto's result for  $k$  as a function of the filling factor  $c$ .

It is interesting to note that to leading order in the filling factor,  $c$ , the drag coefficient  $C_D$ , and therefore the permeability  $k \sim 1/(C_D c) = (1/c)(1 - 1.791c^{1/3} \dots)$ , have a correction term that is proportional to  $c^{1/3}$  or the inverse distance between the spheres. This result should be compared to *Maxwell's law of mixtures* equation (8.30), which to leading order in  $c$  for the effective conductivity is

$$\sigma_{\text{eff}} = \sigma(1 - 1.5c + \dots) , \quad (9.55)$$

for insulating spheres in a matrix of conductivity  $\sigma$ . The difference in these two results is, of course, due to the presence of the viscosity term and the fact that there is no equivalent to the non-slip boundary condition in the electric conduction problem.

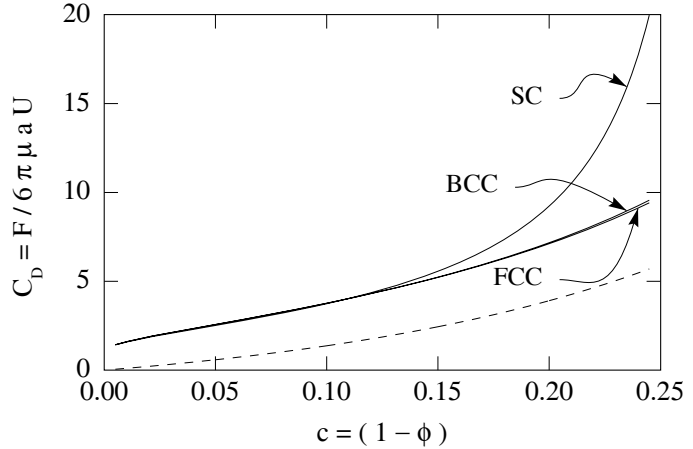


Figure 9.3: The drag coefficient  $C_D$  as a function of filling factor,  $c = (1 - \phi)$ , for packing of spheres in the simple cubic (SC), the body-centered cubic (BCC), and face-centered cubic (FCC) lattices. The results are obtained in an approximation valid at small filling factors (see equation (9.54)) (Hasimoto reference [ ]). The dashed curve corresponds to the Carman-Kozeny expression (9.17) with  $K = 5$ .

Figure 9.3: The drag coefficient  $C_D$  as a function of filling factor,  $c = (1 - \phi)$ , for

### 9.3 The General Case

The case where the filling factor,  $c = (1 - \phi)$ , is *not* small and the spheres almost touch is not easily handled by the systematic series expansions of the type pioneered by Rayleigh.<sup>104</sup> McPhedran and McKenzie<sup>110</sup> have calculated the conductivity of lattices of spheres to order  $c^{22/3}$ , and found good agreement with experiment even for filling factors where the spheres almost touch. Sangani and Acrivos<sup>111</sup> have used the method of generalized functions to obtain conductivities to order  $c^9$  for any conductivity ratio of the spheres to the matrix. They have also extended Hasimoto's calculation of the permeability by similar methods to order  $c^{10}$ . Their results agree well with those obtained by Zick and Homsy.<sup>95</sup> The method introduced by Zick and Homsy for the *Stokes flow* in a lattice of spheres consists of giving the problem an integral formulation, and then applying a numerical *Galerkin method* that gave them very accurate results even when the spheres touch.

The non-slip boundary condition requires the velocity to vanish on the surface of the spheres. It therefore follows from equation (9.44) that the

periodic force  $\mathbf{F}(\mathbf{r})$  must satisfy the integral equation

$$\mathbf{U} = -\frac{1}{V} \int_V d^3 \hat{\mathbf{r}} \chi(\mathbf{r} - \hat{\mathbf{r}}) \cdot \mathbf{F}(\hat{\mathbf{r}}), \quad \text{with } \mathbf{r} \text{ on } S. \quad (9.56)$$

Since  $\chi$  and  $\mathbf{F}$  are periodic it is sufficient to integrate over the unit cell and drop the number of unit cells factor  $N$  in front of the integral. The force  $\mathbf{F}$  acting on the fluid is restricted to the surface of the spheres and there it is the negative of the force acting on the sphere. Therefore we may write the integral equation as

$$\mathbf{U} = -\frac{1}{V} \int_V d^3 \hat{\mathbf{r}} \chi(\mathbf{r} - \hat{\mathbf{r}}) \cdot \mathbf{f}(\hat{\mathbf{r}}), \quad \text{with } \mathbf{r} \text{ on } S. \quad (9.57)$$

Here the surface stress vector  $\mathbf{f}$  is given by the fluid stress tensor

$$\mathbf{f} = \boldsymbol{\sigma} \cdot \mathbf{n}, \quad (9.58)$$

where the fluid stress tensor now includes the pressure, that is,

$$\sigma_{ij} = -p\delta_{ij} + \mu \left( \frac{\partial u_i}{\partial x_j} + \frac{\partial u_j}{\partial x_i} \right). \quad (9.59)$$

Using equations (9.42) and (9.45) for  $\chi$ , we obtain for  $\mathbf{r}$  and  $\hat{\mathbf{r}}$  on  $S$

$$\mathbf{U} = -\frac{1}{V} \sum'_{\mathbf{q}} (q^{-2} - q^{-4} \mathbf{q} \cdot \mathbf{q}) e^{-i\mathbf{q} \cdot \mathbf{r}} \int_S e^{i\mathbf{q} \cdot \hat{\mathbf{r}}} \mathbf{f}(\hat{\mathbf{r}}) dS. \quad (9.60)$$

This is the integral equation derived by Zick and Homsy.<sup>95</sup> The domain of the integral equation is the two-dimensional surface of a sphere whereas the domain of the differential equations is the three-dimensional fluid region. This gives the integral equation a great advantage over the differential equations with regard to the size of the numerical problem. The integral equation has only three unknowns, the three components of the surface stress vector. Also, the conversion of the differential equations to the integral equation automatically satisfies all the periodicity and boundary conditions.

Zick and Homsy used a complete, but not orthogonal, set of basis functions of the form

$$\varphi_{pqt} = x^p y^q z^t, \quad (9.61)$$

to obtain a representation of the integral equation. They truncated the resulting set of linear equations at order  $M = p + q + t = 12$ , and solved the resulting set of equations numerically for the cubic lattices.

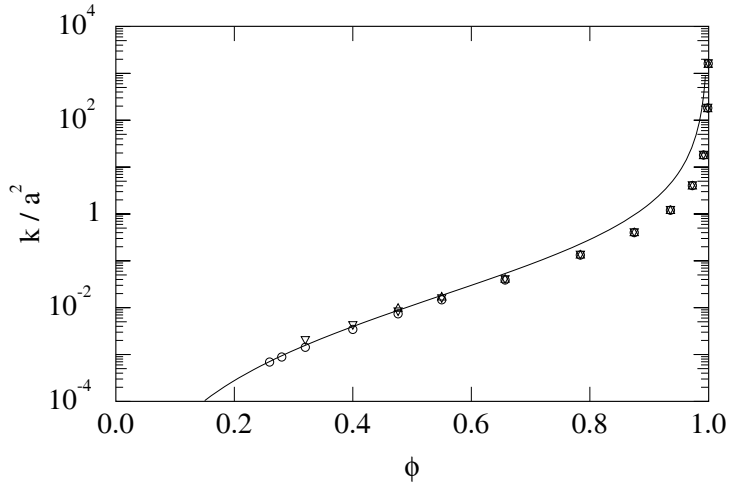


Figure 9.4: The permeability  $k$  of cubic lattice packings of spheres as a function of the filling factor  $c = (1 - \phi)$ . Calculated by Zick and Homsy.<sup>95</sup> The curve is the Carman-Kozeny result (see equation (9.17) with  $K = 5$ ).

In figure 9.4 we have plotted their result for the permeability  $k$  as function of the filling factor  $c = (1 - \phi)$ . In this figure we have also given the Carman-Kozeny expression equation (7.21) for the permeability, with the Carman-Kozeny constant  $K = 5$ . For high filling factors the Carman-Kozeny result is very good, but it over-estimates the permeability at low filling factors, that is, at high porosities. At low filling factors  $c < 0.2$ , Zick and Homsy's results are indistinguishable from those of Hasimoto.<sup>107</sup>

These results for the periodic arrays of spheres are very satisfactory and agree within a few percent with experimental results. The case of random sphere packings, however, is still open and requires further work. The most interesting question is whether the randomness of the packing changes the permeability porosity relationship in a qualitative way. We will return to this question after an introduction of the percolation concepts.

# Chapter 10

## Capillary Action

‘A tube, the bore of which is so small that it will only admit a hair (*capilla*), is called a capillary tube. When such a tube of glass, open at both ends, is placed vertically with its lower end immersed in water, the water is observed to rise in the tube, and to stand within the tube at a higher level than the water outside. The action between the capillary tube and the water has been called Capillary Action, and the name has been extended to many other phenomena which have been found to depend on properties of liquids and solids similar to those which cause water to rise in capillary tubes’

Thus begins J. C. Maxwell’s famous article<sup>112</sup> in Encyclopedia Britannica (1876). The understanding of the surface phenomena involved in capillary rise has contributions from many of the great names in science starting with Leonardo da Vinci, considered to be the discoverer of capillary action. Maxwell goes on as follows:

‘The forces which are concerned in these phenomena are those which act between neighbouring parts of the same substance, and which are called forces of cohesion, and those which act between portions of matter of different kinds, which are called forces of adhesion. These forces are quite insensible between two portions of matter separated by any distance which we can directly measure’

Here we have a macroscopic phenomenon, easy to observe as in capillary rise, that depends on the interactions on the atomic, or molecular, level. Maxwell’s article was written before science had clear concepts concerning atoms, molecules, and heat—concepts we now take for granted. Capillary phenomena were investigated by Hooke,<sup>113</sup> Newton, Young, Laplace, Gay-Lussac, Gauss, Poisson, Faraday, Rayleigh, Kelvin,

van der Waals, Boltzmann, Gibbs, and many others. The development of the early ideas and experiments are very nicely described in Maxwell's article. A readable introduction in Rowlinson and Widom's book<sup>114</sup> *Molecular Theory of Capillarity* also describes the evolution of the ideas of how capillary phenomena can be understood in terms of molecular interactions.

Capillary phenomena such as surface tension, adhesion, adsorption, surface films, wetting, flotation, detergency, emulsions, foams, are important in many practical situations in daily life, in industry, in oil recovery and production. The use of soap and detergents in washing depends on capillary phenomena. Capillary phenomena represent a very large field of science and engineering. Excellent books on the subject are Adamson's standard reference:<sup>115</sup> *Physical Chemistry of Surfaces*, the book by Rowlinson and Widom<sup>114</sup> already mentioned, and Israelachivili's book<sup>116</sup> *Intermolecular and Surface Forces*. de Gennes<sup>117</sup> has written a clear, review of many aspects of surface tension, wetting and spreading.

In the following sections we discuss fundamental aspects of interface dynamics, surface tension and contact angle required for a discussion of the simultaneous flow of several fluids in porous media, so called multiphase flow. The formation of bubbles in fluids and droplets in vapors are important in oil production, therefore we discuss nucleation theory in an introductory way.

## 10.1 Mechanical Theory of Capillary Action

The capillary rise indicates that there is an attractive interaction between the molecules of water and the glass walls, but the range of these interactions are ‘insensible’, that is, they are truly microscopic. For instance, the rise does not depend on the thickness of the glass.

Young, Laplace, and others imagined that there is an attractive force between the molecules that depends on distance and vanishes beyond a microscopic distance  $\delta$ . We follow the argument given in Rowlinson and Widom's book.<sup>114</sup> Imagine that a fluid (water) is cut by a plane and the two parts moved away a distance  $\ell$  as illustrated in figure 10.1. Assume that the molecules in the fluid interact with an attractive force, as we just discussed, which has a range  $\delta$  given by:

$$f(s < \delta) < 0, \quad f(s \geq \delta) = 0. \quad (10.1)$$

Let the number density of molecules be  $\rho$  in the fluid. Consider the volume elements  $dx dy dr$ , and  $s^2 \sin \theta ds d\theta d\varphi$  illustrated in figure 10.1. The total

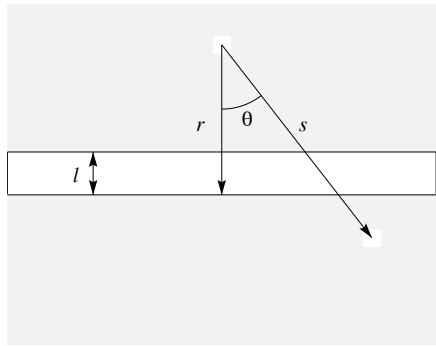


Figure 10.1: A fluid is imagined to be cut by a horizontal plane and separated a distance  $\ell$ . The force between molecules in the fluid element  $dxdydr$  and  $s^2 \sin \theta ds d\theta d\varphi$  is  $f(s)$  for each pair molecules in the two volume elements. The total force is obtained by integration (after reference [1]).

Figure 10.1: A fluid is imagined to be cut by a horizontal plane and separated a distance  $\ell$ . The force between molecules in the

force,  $F(\ell)$ , of attraction (per unit area) between the two parts is in the direction normal to the surface, as the horizontal components cancel. The attractive force (per surface element  $dxdy$ ) is given by

$$\begin{aligned} F(\ell) &= -\rho^2 \int_{\ell}^{\delta} dr \int_r^{\delta} ds s^2 f(s) \int_0^{\cos^{-1}(r/s)} d\theta \sin \theta \cos \theta \int_0^{2\pi} d\varphi \\ &= -\pi \rho^2 \int_{\ell}^{\delta} dr \int_r^{\delta} ds (s^2 - r^2) f(s) . \end{aligned} \quad (10.2)$$

Here the  $\cos \theta$  term comes in because we only need the vertical component of the attraction. The upper limit of integration is obtained by noting that the  $\theta_{\max}$  is given by  $\cos \theta_{\max} = r/s$ . The force is given in terms of a potential as

$$f(s) = -\frac{d\phi}{ds} , \text{ or } \phi(s) = \int_s^{\delta} ds' f(s') , \text{ and } \phi(s \geq \delta) = 0 . \quad (10.3)$$

The force between the two halves of the fluid may then be written:<sup>1</sup>

$$F(\ell) = -2\pi\rho^2 \int_{\ell}^{\delta} dr r(r-\ell) \phi(r) . \quad (10.4)$$

The force of attraction between the two fluid halves (per unit area) in the limit of vanishing separation is

$$K = F(0) = -2\pi\rho^2 \int_0^{\delta} dr r^2 \phi(r) = -\frac{1}{2}\rho^2 \int_{|r|\leq\delta} d^3\mathbf{r} \phi(r) . \quad (10.5)$$

The constant  $K$ , introduced by Laplace is positive since  $\phi(r)$  was assumed to be negative, that is, the same sign as  $f(s)$  in equation (10.1). The Laplace constant  $K$  has units of (force/area), that is, pressure, and  $K$  is often called the Laplace pressure. The problem with only attractive classical forces is, of course, that there is nothing to stop the system from collapsing. An internal ‘pressure’ is required for such a collapse not to happen, and Laplace concluded that this (large) pressure had to equal  $K$  in magnitude.

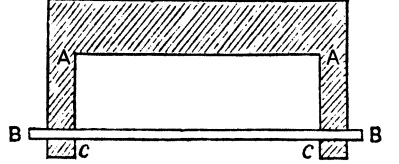
The work done to separate the two fluid halves (per unit area) is

$$H = \int_0^{\delta} d\ell F(\ell) = -\pi\rho^2 \int_0^{\delta} d\ell \ell^3 \phi(\ell) . \quad (10.6)$$

This work to create *two* surfaces is the increase in energy of the system and therefore we may associate an energy  $\sigma$ , per unit area, with the surface — the surface energy.

$$\sigma = \frac{1}{2}H = -\frac{1}{8}\rho^2 \int d^3\mathbf{r} r \phi(r) = -\frac{1}{2}\pi\rho^2 \int_0^{\delta} dr r^3 \phi(r) . \quad (10.7)$$

Dupré described an experiment in which the surface energy  $\sigma$  can be measured (see figure ??). If the metal piece (BB) in figure ?? is moved so as to increase the area  $a \times b$  by increasing the distance  $b = AB$ , a work  $Fdb = \sigma a db$  is done. Here  $F$  is the force on the metal piece (BB) of length  $a$ . We may con-



<sup>1</sup>Integrate the last integral in equation (10.2) by parts to give  $-|_r^{\delta}(s^2 - r^2)\phi(s) + \int_r^{\delta} ds 2s\phi(s) = 2\int_r^{\delta} ds s\phi(s)$ . In the resulting expression, integrate the first integral by parts to give:  $F(\ell) = -2\pi\rho^2 \int_{\ell}^{\delta} dr \int_r^{\delta} ds s\phi(s) = -2\pi\rho^2 (\{|_{\ell}^{\delta} r \int_r^{\delta} ds s\phi(s)\} + \int_{\ell}^{\delta} dr r^2 \phi(r))$ , which reduces to equation (10.4).

sider  $\sigma$  to be either the surface-energy per unit area or the surface-tension per unit contour. Maxwell<sup>112</sup> defined surface tension as follows:

Definition.—*The tension of a liquid surface across any line on the surface is normal to the line, and is the same for all directions of the line, and is measured by the force across an element of the line divided by the length of that element.*

## 10.2 Curved Surfaces

When the surface is curved, surface tension leads to a difference in pressure between the two phases in contact. The pressure on the concave side exceeds the pressure on the convex side by  $\Delta p$  given by Young-Laplace's equation<sup>2</sup>

$$\boxed{\Delta p = \sigma \left( \frac{1}{R_1} + \frac{1}{R_2} \right)} \quad \text{Young-Laplace} \quad (10.8)$$

Here  $R_1$  and  $R_2$  are the principal radii of curvature of the interface. The Young-Laplace equation is consistent with experimental observations. The interface separating two fluid regions that have a constant pressure difference, and uniform pressure in each phase, must be a surface of constant curvature, that is,  $\frac{1}{R_1} + \frac{1}{R_2} = 2/C$ , where  $C$  is a constant.

The Laplace pressure inside a drop of radius  $R$  may be found by considering changes in the internal energy of the fluid due to a change in surface area. The internal cohesive energy density<sup>3</sup>  $\Phi$  is

$$\Phi = \frac{1}{2} \rho^2 \int_{|\mathbf{r}| \leq \delta} d^3 r \phi(r). \quad (10.9)$$

Here the integral has a range  $\delta$  around the point under consideration. At a flat surface the energy density  $\Phi_A = \frac{1}{2}\Phi_I$ , is only half the energy density in the interior of the fluid, since there are no particles to interact with in the half-sphere of radius  $\delta$  outside the fluid. The Laplace pressure  $K$  in

---

<sup>2</sup>This equation has been attributed to Young (1804)<sup>118</sup> and was rediscovered independently one year later by Laplace.<sup>119</sup> However, Young stated that: *It is well known, and it results immediately from composition of forces, that where a line is equably distended, the force that it exerts, in a direction perpendicular to its own, is directly as its curvature; and the same is true for a surface of simple curvature; but where the curvature is double, each curvature has its appropriate effect, and the joint forces must be as the sum of the curvatures of any two perpendicular directions.*

<sup>3</sup>Since the density is required there is a  $\rho^2$ , instead of only  $\rho$  in equation (10.9).

equation (10.5) may be interpreted as the difference  $2\Phi_A - 2\Phi_I$  since

$$K = -2\pi\rho^2 \int_0^\delta dr r^2 \phi(r) = -\Phi_I = 2\Phi_A - 2\Phi_I . \quad (10.10)$$

However, if the fluid surface is curved, as in a drop of radius  $R$  surrounded by its vapor, the surface term must be modified to be given by

$$\Phi_A = \pi\rho^2 \int_0^\delta dr r^2 \phi(r) \int_0^{\cos^{-1}(r/2R)} d\theta \sin\theta . \quad (10.11)$$

This result may be written

$$\Phi_A(R) = \Phi_A(\infty) + \frac{\sigma}{R} , \quad (10.12)$$

where  $\sigma$  is given by equation (10.7). We then may write the Laplace pressure  $K(R)$  for the curved surface in terms of the Laplace pressure,  $K$ , of the flat interface given by equation (10.5) as follows:  $K(R) = 2\Phi_A(R) - 2\Phi_I = 2\Phi_A(R) - 2\Phi_A(\infty) + (2\Phi_A(\infty) - 2\Phi_I)$ , and finally we have

$$K(R) = K + \frac{2\sigma}{R} . \quad (10.13)$$

The increase in pressure due to the curvature is the last term, and if instead of a spherical drop have as surface with two radii of curvature a more lengthy argument gives the Young-Laplace equation (10.8).

The argument made here was based on mechanical force and energy considerations. However, we should really use concepts from thermodynamics and statistical physics since we are interested in surfaces at finite temperatures. We will therefore no longer follow the historical development of the ideas, but rather follow the thermodynamic arguments as presented in Landau and Lifshits' book<sup>120</sup> *Statistical Physics*, and in the review<sup>121</sup> of *wetting* by M. Schick.

### 10.3 Surface Tension Thermodynamics

The understanding of surface tension and processes that change the surface such as capillary waves, detergents, condensation, evaporation, and nucleation phenomena require thermodynamic concepts and relations not ordinarily covered in introductory courses in thermodynamics and statistical physics. I have summarized some of the relevant thermodynamic concepts in the appendix A.

Consider for instance a drop of water surrounded by water vapor. The drop will evaporate, stay in (metastable) equilibrium, or grow depending on the thermodynamic conditions given by temperature, pressure, solutes in the drop, and chemical potentials. It is simplest to work in an ensemble that has a variable number of particles.

We start by considering the interface between a fluid and its vapor, such as a drop of water in a cloud. We will also discuss the probability for the creation of a drop in a super-saturated vapor. Then we discuss the solid-liquid-vapor system which leads to a discussion of wetting, contact angles and other properties characteristic of three-phase systems.

### 10.3.1 Reversible Work, and Surface Tension

Let us discuss the interface between two ‘bodies’, that is, two fluids, a fluid and a gas, a fluid and a solid, or two solids that are in contact over an interface area  $A$ . Let the interface increase by a small amount  $\delta A$ , for instance by changing the shape of a drop in another fluid.

The *reversible work*<sup>4</sup> in such a process is proportional to  $\delta A$ :

$$\delta\mathcal{R}_{\min} = \sigma\delta A . \quad (10.14)$$

The reversible work depends on the thermodynamic conditions for the system. For processes at constant pressure, temperature and number of molecules,  $\delta\mathcal{R}_{\min} = \delta G$ , where  $G$  is the Gibbs free-energy of the system as a whole. In a system where the chemical potential  $\mu$ , volume  $V$  and the temperature  $T$  are fixed, we have  $\delta\mathcal{R}_{\min} = \delta\Omega$ , where  $\Omega$  is the thermodynamic ‘Landau potential.’ If  $\sigma < 0$  equation (10.14) states that a negative reversible work has to be supplied in order to increase the interface by  $\delta A$ . But this means that the system would be able to do work on the surroundings by increasing its surface, the surface would grow indefinitely—the two phases would mix. Hence, for the interface to exist at all we must have  $\sigma > 0$ . Equation (10.14) corresponds to the expression  $\delta\mathcal{R}_{\min} = -P\delta V$  for the reversible work done in a change of volume of a system.

For a system of two phases of the same substance in a given volume,  $V$ , separated by an interface of area  $A$ , containing  $N$  molecules, the first law of thermodynamics equation (A.58) takes the form

$$dE = TdS + \mu dN + \sigma dA . \quad (10.15)$$

---

<sup>4</sup>That is, the minimum work required to perform the change, or the negative of maximum work the system can perform on its surroundings.

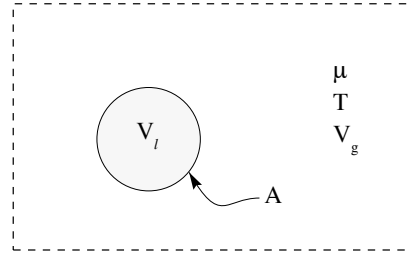


Figure 10.2: A liquid drop, volume  $V_l$  and area  $A$  in its vapor at a fixed chemical potential  $\mu$  and temperature  $T$ .

Here the internal energy is  $E$ , the entropy is  $S$ , the temperature is  $T$ , the chemical potential is  $\mu$ , and  $\sigma$  is the surface-tension. The surface term enters simply as an additional work term. At equilibrium the temperature and the chemical potential are uniform in the system and therefore equal for the two phases.

However, since the pressure is *not* uniform in a system with curved interfaces between the two phases of the same substance, it is more convenient to work with the ‘Landau potential’  $\Omega = E - TS - \mu N = -PV$  relating the independent variables  $T$ ,  $\mu$  (and the volume  $V$ ) instead of the energy  $E$  with the independent variables  $S$ ,  $N$  and volume (see section A.9). The first law may be written in terms of  $\Omega$  as (see equation (A.68))

$$d\Omega = -SdT - Nd\mu + \sigma dA . \quad (10.16)$$

For a system in an *external bath* that fixes the temperature  $T = T_0$  the chemical potential  $\mu = \mu_0$ , the reversible work is the change in  $\Omega$ , see equation (A.67). Note that for a fluid in equilibrium with its own vapor the chemical potential is the same in the two phases, and the chemical potential is not independent of temperature but given by an *equation of state*  $\mu = \mu_{\text{coex}}(T)$ . The surface tension for such a system is therefore a function of only one independent variable, either the temperature or the chemical potential.

### 10.3.2 Thermodynamic Surface Quantities

The thermodynamic potentials may be separated into ‘volume’ and surface terms. For the system illustrated in figure 10.2 we have

$$V_\ell + V_g = V \quad \text{The total volume is } V \quad (10.17)$$

$$n_\ell V_\ell + n_g V_g = N \quad \text{The number of molecules is } N \quad (10.18)$$

Here  $n_\ell(\mu, T)$  and  $n_g(\mu, T)$  are the number densities of molecules in the liquid and in the gas phase respectively. In writing equations (10.17) and (10.18) we have assumed that there is no extra volume associated with the surface, that is,  $V_s = 0$ ; and there is no excess number of particles in the surface, that is,  $N_s = 0$ . Here we use subscript  $s$  to indicate surface quantities and  $0$  for bulk quantities.

At fixed  $T$  and  $\mu$  equation (10.16) gives  $d\Omega = \sigma dA$ , which may be integrated to give  $\Omega_s = \sigma A$  and for the complete system we have<sup>5</sup>

$$\Omega = \Omega_0 + \Omega_s = \Omega_0 + \sigma A \quad (10.19)$$

$$\Omega_0 = -P_\ell V_\ell - P_g V_g \quad (10.20)$$

The surface entropy  $S_s$  the Helmholtz- and Gibbs- surface free-energy  $F_s$  and surface energy  $E_s$  are given by

$$S_s = - \left( \frac{\partial \Omega_s}{\partial T} \right)_{\mu, A} = - \frac{d\sigma}{dT} A \quad (10.21)$$

$$F_s = \Omega_s + \mu N_s = \sigma A \quad \text{since } N_s = 0 \quad (10.22)$$

$$G_s = F_s + PV_s = \sigma A \quad \text{since } V_s = 0 \quad (10.23)$$

$$E_s = F_s + TS_s = \left( \sigma - T \frac{d\sigma}{dT} \right) A \quad (10.24)$$

Thus  $\sigma$  is the Helmholtz or Gibbs surface free-energy per unit surface area.

## 10.4 The Young-Laplace Law

For a drop of fluid in its own vapor at given temperature  $T$  and chemical potential  $\mu$ , the total Landau potential of the system is given by equa-

---

<sup>5</sup>This argument ignores the possibility that the interface moves. A small drop in a vapor has translational, rotational and vibrational degrees of freedom that contribute to the free energy as a whole in a way not directly related to the surface free energy  $\sigma$ .

tions (10.19) and (10.20), that is,

$$\Omega = -P_\ell V_\ell - P_g V_g + \sigma A . \quad (10.25)$$

Since  $V = V_\ell + V_g$ , and because in equilibrium the two phases must have the same chemical potential  $\mu = \mu_\ell(P_\ell, T) = \mu_g(P_g, T)$ , it follows that the pressures are uniform in each phase (but  $P_\ell \neq P_g$ ), and equation (10.25) becomes

$$\Omega = -P_\ell V_\ell - P_g(V - V_\ell) + \sigma A . \quad (10.26)$$

Now, let the droplet have a volume  $V_\ell = 4\pi R^3/3$  and area  $A = 4\pi R^2$ , and consider a small change in radius  $\delta R$ , because molecules condense on the droplet, then we find that

$$\delta\Omega = \left( \frac{\partial\Omega}{\partial R} \right)_{T,\mu,V} \delta R = \{-(P_\ell - P_g)4\pi R^2 + \sigma 8\pi R\} \delta R . \quad (10.27)$$

Note that  $P_\ell$  should not be considered a function of  $V_\ell$ , since  $P_\ell$  is given as the solution of  $\mu_\ell(P_\ell, T) = \mu$ , for processes at fixed  $\mu$  and  $T$ . Similarly  $P_g$  is fixed. The Landau potential will decrease as the system approaches thermal equilibrium at fixed  $\mu, T$  and  $V$  (see section A.9) and  $\delta\Omega = 0$  at equilibrium. Solving equation (10.27) with  $\delta\Omega = 0$  gives the Young-Laplace law as in equation (10.8).

$$P_\ell - P_g = \frac{2\sigma}{R} \quad \text{Young-Laplace}$$

(10.28)

The derivation that led to equation (10.8) was based on mechanical arguments. Here we have obtained the same result with general thermodynamic arguments. However,  $\sigma$  is now a free-surface energy, not just the energy.

#### 10.4.1 The Vapor Pressure of a Drop

The chemical potential in the liquid and in the vapor must be equal at equilibrium, therefore the pressures satisfy the equations

$$\mu_\ell(P_0, T) = \mu_g(P_0, T) \quad R \rightarrow \infty \quad (10.29)$$

$$\mu_\ell(P_\ell, T) = \mu_g(P_g, T) \quad R \text{ finite} \quad (10.30)$$

If the pressures do not deviate much from the equilibrium vapor pressure  $P_0$ , then we may expand the chemical potentials as follows (with  $i = \ell$  or  $g$ ):

$$\mu_i(P_i, T) = \mu_i(P_0, T) + \left( \frac{\partial\mu_i}{\partial P_i} \right)_T \delta P_i + \dots \quad (10.31)$$

We note that the chemical potential is the Gibbs free-energy per particle (see equation (A.72)), and therefore, using equation (A.71), the *molecular volume* is  $v_i = \left(\frac{\partial \mu_i}{\partial P_i}\right)_T$ , and it follows that

$$(P_\ell - P_0)v_\ell = (P_g - P_0)v_g . \quad (10.32)$$

This equation may be combined with the Young-Laplace equation (10.28) to give expressions for the pressures independently

$$P_\ell - P_0 = \frac{2\sigma}{R} \frac{v_g}{v_g - v_\ell} \simeq \frac{2\sigma}{R} \quad (10.33)$$

$$P_g - P_0 = \frac{2\sigma}{R} \frac{v_\ell}{v_g - v_\ell} \simeq \frac{2\sigma v_\ell P_0}{R kT} \quad (10.34)$$

where the approximations use that typically  $v_\ell \ll v_g$  and that the vapor has a low pressure so that the ideal gas law may be used to give  $v_g = kT/P_g \simeq kT/P_0$ . The pressure inside the drop,  $P_\ell$ , is slightly larger than the pressure difference given by the Young-Laplace equation (10.28) since the vapor pressure of the drop is larger than the vapor pressure of a flat interface, which is  $P_0$ .

The vapor pressure of a drop of radius  $R$  is given by equation (10.34) was first derived by Kelvin<sup>122</sup>

$$\boxed{P_g - P_0 = \frac{2\sigma}{R} \frac{v_\ell}{v_g - v_\ell} \quad \text{Kelvin}} \quad (10.35)$$

Thus the vapor pressure of a small drop exceeds that of a flat surface. The approximate expression for the vapor pressure in equation (10.34) may be written in the form first obtained by Helmholtz<sup>123</sup> using the concept of free-energy introduced by his father

$$\boxed{\ln S = \ln \frac{P_g}{P_0} = \frac{2\sigma v_\ell}{kTR} \quad \text{Helmholtz}} \quad (10.36)$$

where have used the approximation  $(P_g - P_0)/P_0 \simeq \ln(P_g/P_0)$ .

The Helmholtz equation is more accurate than the Kelvin equation for very small droplets as can be seen by the following derivation. For very small droplets ( $R = 1\text{--}10$  nm, say), the approximation (10.31) must be improved. We note first that the chemical potential of an ideal gas has the form

$$\boxed{\mu = kT \ln P + \chi(T) \quad \text{ideal gas ,}} \quad (10.37)$$

where  $\chi(T)$  is only a function of temperature (see Landau and Lifshitz<sup>120</sup> equation 42.6). Therefore we may write

$$\mu_g(P_g, T) - \mu_g(P_0, T) = kT \ln(P_g/P_0) \quad (10.38)$$

to the extent that the vapor behaves as an ideal gas even at high pressures. For the liquid phase we may write

$$\begin{aligned} \mu_\ell(P_\ell, T) - \mu_\ell(P_0, T) &= \left( \frac{\partial \mu_\ell}{\partial P_\ell} \right)_T \Big|_{P_0} (P_\ell - P_0) \\ &\quad + \frac{1}{2} \left( \frac{\partial^2 \mu_\ell}{\partial P_\ell^2} \right)_T \Big|_{P_0} (P_\ell - P_0)^2 + \dots \\ &= v_\ell(P_\ell - P_0) \left( 1 + \frac{1}{2} \kappa_\ell(P_\ell - P_0) + \dots \right) \end{aligned} \quad (10.39)$$

Here we have used that  $v_\ell = (\partial \mu_\ell / \partial P_\ell)_T$  and therefore the second order term is simply the isothermal compressibility of the liquid

$$\kappa_\ell = \frac{1}{v_\ell} \left( \frac{\partial v_\ell}{\partial P_\ell} \right)_T. \quad (10.40)$$

For liquids with a small compressibility we may approximate the left hand side of equation (10.39) by  $v_\ell(P_\ell - P_0)$  and we find setting  $\mu_\ell(P_\ell, T) - \mu_\ell(P_0, T)$  equal to the expression in equation (10.38)

$$\ln(P_g/P_0) = \frac{v_\ell(P_\ell - P_0)}{kT}. \quad (10.41)$$

We may write  $(P_\ell - P_0) \simeq (P_\ell - P_g) = 2\sigma/R$ , when  $(P_g - P_0) \ll (P_\ell - P_0)$ . With this approximation equation (10.41) becomes the Helmholtz equation (10.36).

## 10.5 Nucleation

Nucleation phenomena dominate the dynamics of first-order phase transitions. For droplets to nucleate the vapor must be super-saturated, that is, the pressure of the vapor,  $P_g$ , must exceed the equilibrium vapor pressure of a flat surface,  $P_0$ . We define the *super-saturation* as  $S = P_g/P_0 > 1$ . In cavitation, or boiling vapor, bubbles nucleate in the liquid phase and the fluid is said to be superheated. The nucleation of gas bubbles in porous rock during oil production can create serious practical problems. Daniel Gabriel Fahrenheit was the first to observe and describe<sup>124</sup> supercooling of

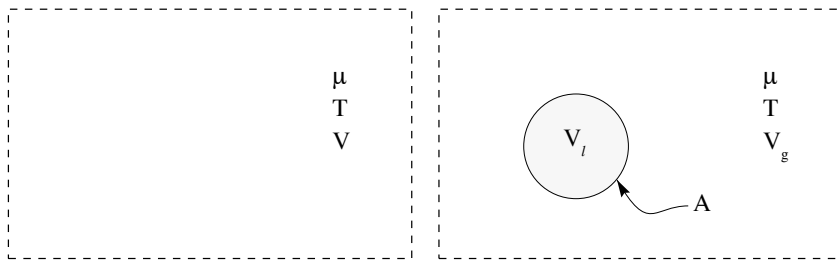


Figure 10.3: Nucleation of liquid drop, volume  $V_l$  and area  $A$  in its vapor at a fixed chemical potential  $\mu$  and temperature  $T$  in a fixed volume  $V$  (a) The system before the fluctuation that nucleates a drop (b) The system with a drop at equilibrium with the surrounding vapor.

water in small capillaries.<sup>6</sup> The first to take both experimental and theoretical interest in nucleation problems<sup>123</sup> was Helmholtz (1886). Gibbs (1878) discussed the reversible work<sup>125</sup> necessary to form a critical cluster. Nucleation theory has many non-trivial aspects that has led to much controversy in the literature. Here I shall discuss only elementary aspects, more details may be found in reference [] .

Nucleation is a non-equilibrium process. By random collisions molecules may form a small cluster that may continue to grow or evaporate. The thermodynamic potential  $\Omega$  will decrease for the system until it has reached its minimum value consistent with the thermodynamic constraints of given  $V$ ,  $\mu$  and  $T$ . Even in thermal equilibrium there are *fluctuations* in which  $\Omega$  increases. The probability to have a fluctuation is

$$\boxed{Pr \sim \exp(-\mathcal{R}_{\min}/k_B T) \sim \exp(-\Delta\Omega/k_B T)} \quad (10.42)$$

Here  $\mathcal{R}_{\min}$  is the minimum work required to change the system to a new state with a specified fluctuation. The reversible work for the system with given  $V$ ,  $\mu$  and  $T$  equals the change in the Landau potential (see equation (A.67));  $\mathcal{R}_{\min} = \Delta\Omega$  required to create the fluctuation. If we instead

<sup>6</sup>Fahrenheit was born in Danzig but studied in Holland and worked in Amsterdam. Fahrenheit was the first to make a mercury thermometer, and he also used alcohol thermometers. He used three fixed points: (1): 0 degrees for a mixture of ice, water and salt; (2): 32 degrees for a mixture of ice and water; (3): 96 degrees at the body temperature of a ‘healthy’ person in the mouth or under the arm. Fahrenheit used rain-water in a 1 inch bulb he evacuated in the manner used by him to make thermometers. Fahrenheit found that the water was liquid at 15 degrees, that is,  $-9.4^\circ C$ , and solidified immediately if he broke the tip of the capillary attached to the bulb to admit air.

discuss nucleation for given  $P$ ,  $N$  and  $T$ , then we should use the Gibbs free energy to give  $\mathcal{R}_{\min} = \Delta G$  (see equation (A.53)). The general results will be the same since we may consider the open system with  $V$ ,  $\mu$  and  $T$  given, to be a small subsystem of a much larger system at given  $P$ ,  $N$  and  $T$ . The chemical potential of the vapor equals the prescribed chemical potential, that is,  $\mu_g(P_g, T) = \mu$ , and therefore we may consider  $P_g = P$  to be fixed. The Landau potential is  $\Omega = -PV$  before the appearance of a droplet; and it is  $\Omega = -P \cdot (V - V_\ell) - P_\ell V_\ell + \sigma A$  after the formation of the droplet. The change in Landau potential in a fluctuation that creates a droplet is therefore given by<sup>7</sup>

$$\mathcal{R}_{\min} = \Delta\Omega = -(P_\ell - P)V_\ell + \sigma A . \quad (10.43)$$

For a spherical droplet of radius  $R$  we have  $V_\ell = \frac{4\pi}{3}R^3$  and  $A = 4\pi R^2$  and therefore

$$\mathcal{R}_{\min} = \Delta\Omega = -(P_\ell - P) \frac{4\pi}{3}R^3 + \sigma 4\pi R^2 . \quad (10.44)$$

Note again that since we consider processes at fixed  $\mu$  and  $T$ , it follows that  $P_\ell$  is fixed, that is,  $P_\ell$  does not vary with  $R$ , and is given as the solution of  $\mu_\ell(P_\ell, T) = \mu$ .<sup>8</sup> Similarly  $P = P_g$  is fixed and given as the solution of  $\mu_g(P_g, T) = \mu$ . Since the pressure inside the droplet is always larger than the pressure outside the droplet, because of surface tension, we see that there will be a gain in Landau potential proportional to the droplet volume. The surface tension term in equation (10.44) is always positive and proportional to droplet area. For small droplets—and all droplets have to start as small droplets—the  $R^2$  is much larger than the  $R^3$ -term in equation (10.44), and therefore the formation of a small droplet, or nucleus, always requires reversible work, and an increase in the appropriate free-energy. There is a critical size of the nucleus for which  $\mathcal{R}_{\min}$  has a maximum value. We find that  $d\mathcal{R}_{\min}/dR = 0$  for

$$R^* = \frac{2\sigma}{P_\ell - P} , \quad (10.45)$$

which we recognize as the Young-Laplace equation (10.28). If the droplet radius is the critical radius then the droplet is in metastable equilibrium

---

<sup>7</sup>For very small droplets we need correction terms that take into account the fact that droplets have translational, rotational and vibrational degrees of freedom (see reference [1] for a discussion)

<sup>8</sup>Why does  $P_\ell$  not depend on  $R$ ? If we had  $\mu_\ell(P_\ell, T, R) = \mu$  we would get a different result for  $\mathcal{R}_{\min}$ . However, the point is that the chemical potential of the fluid depends only on temperature and pressure through the equation of state of the liquid, and it is irrelevant how the pressure is applied, and thus  $\mu_\ell$  is independent of  $R$ .

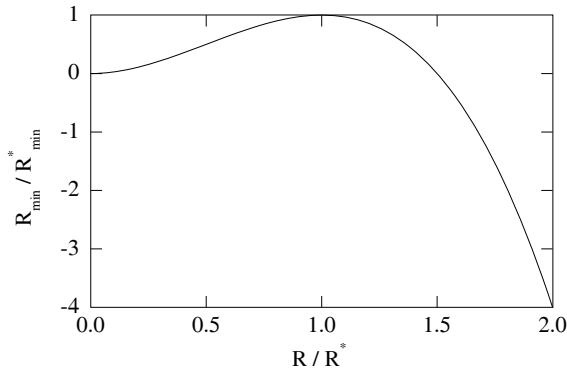


Figure 10.4: The reversible work  $\mathcal{R}_{\min}$  required to form a drop of radius  $R$  in a system with given temperature and chemical potential. The radius is measured in units of the critical radius  $R^*$ , and the reversible work is measured in units of  $\mathcal{R}_{\min}^*$

with its vapor and we find

$$\mathcal{R}_{\min}^* = \Delta\Omega^* = \frac{4}{3}\pi\sigma R^{*2} = \frac{16\pi}{3} \frac{\sigma^3}{(P_\ell - P)^2}, \quad (10.46)$$

where the superscript \* indicates values for the *critical nucleus*.

We may write the reversible work required to form a cluster of any size as

$$\mathcal{R}_{\min}/\mathcal{R}_{\min}^* = -2 \left( \frac{R}{R^*} \right)^3 + 3 \left( \frac{R}{R^*} \right)^2. \quad (10.47)$$

This result shows that the reversible work or  $\Delta\Omega$  can always be plotted in the dimensionless form, as illustrated in figure 10.4, whatever the supersaturation is.

## 10.6 Nucleation Kinetics

Droplets in a vapor grow by the acquisition of molecules from the vapor. The number of molecules that hit a surface per unit area and time,  $\nu$  with units  $[\nu]=\text{m}^{-2} \text{s}^{-1}$ , is given by

$$\nu = \frac{N}{V} \sqrt{\frac{k_B T}{2\pi m}} = \frac{P}{\sqrt{2\pi m k_B T}}, \quad (10.48)$$

where the pressure  $P = Nk_B T$  is the pressure of an ideal gas of  $N$  molecules at temperature  $T$ , and  $m$  is the molecular mass.

The expression for the collision frequency  $\nu$  follows from the Maxwell distribution of velocities:

$$dN_v = \frac{N}{V} \frac{m^{3/2}}{(2\pi m k_B T)^{3/2}} \exp \left\{ -m(v_x^2 + v_y^2 + v_z^2)/2k_B T \right\} dv_x dv_y dv_z . \quad (10.49)$$

Here  $v_x, v_y, v_z$ , is the molecular velocity in the  $x, y$  and  $z$ -directions respectively, and  $dN_v$  is the number of molecules that have velocities in the range  $[v_x, v_x + dv_x]$ ,  $[v_y, v_y + dv_y]$ , and  $[v_z, v_z + dv_z]$ , normalized to  $N/V$  particles per unit volume. From this expression we may calculate the number of molecules,  $\nu$  that hit the wall per unit area and time. Let the  $z$ -axis be perpendicular to the wall. The number particles,  $\nu\tau$ , that reach the wall in time  $\tau$ , must come from a distance  $z \leq v_z\tau$ . These particles come from a volume that has unit area as the base and a height  $v_z\tau$ . Integrating over  $v_z$  we find that

$$\nu\tau = \frac{N}{V} \iint_{-\infty}^{\infty} dv_x dv_y \int_0^{\infty} dv_z v_z \tau \frac{m^{3/2}}{(2\pi m k_B T)^{3/2}} \exp \left\{ -m(v_x^2 + v_y^2 + v_z^2)/2k_B T \right\} . \quad (10.50)$$

The result of this integration is equation (10.48).

The mass of a drop that contains  $n$  molecules, is  $nm$ , such a drop has a volume  $V(n)$  and a surface area  $A(n)$  that is given in terms of the molecular volume,  $v$ , by

$$V(n) = nv = \frac{4}{3}\pi R^3 , \quad A(n) = 4\pi R^2 = 4\pi \left( \frac{3nv}{4\pi} \right)^{2/3} . \quad (10.51)$$

Therefore the rate at which a droplet grows from  $n$  to  $n+1$  in size is given by the *transition rate*

$$W(n+1|n) = \nu \hat{A}(n) , \quad \text{for } n \rightarrow n+1 . \quad (10.52)$$

Here  $\hat{A}(n) = 4\pi(R(n) + a)^2$  is the ‘capture’-area of the drop, that is, the effective area of the surface when a molecule of radius  $a$  touches the surface. Droplets diminish in size by evaporation, so with an *evaporation frequency*  $\alpha(n)$  we have the transition rate for  $n+1$  to  $n$  in size given by

$$W(n|n+1) = \alpha(n+1) \hat{A}(n) , \quad \text{for } n+1 \rightarrow n . \quad (10.53)$$

Note that the effective capture areas for the processes  $n \rightarrow n-1$  and  $n \rightarrow n+1$  are the same.

Detailed balance in (metastable) equilibrium requires that

$$W(n|n+1)c_0(n+1) = W(n+1|n)c_0(n) . \quad (10.54)$$

and we find that the evaporation rate is given by the impingement frequency and  $c_0(n)$ , that is, the equilibrium concentration of droplets:

$$\alpha(n+1) = \nu \frac{c_0(n)}{c_0(n+1)}. \quad (10.55)$$

The equilibrium concentration of droplets,  $c_0(n)$  that have size  $n$ , is proportional to the probability  $Pr$  (see equation (10.42)) to find a droplet of size  $n$  for a given volume and chemical potential  $\mu$ . Therefore we have

$$c_0(n) \sim \exp(-\mathcal{R}_{\min}/k_B T) = \exp(-\Delta\Omega/k_B T). \quad (10.56)$$

and

$$c_0(n) \sim \exp \left\{ -[-2(R/R^*)^3 + 3(R/R^*)^2] \frac{\frac{4}{3}\pi\sigma R^{*2}}{k_B T} \right\}. \quad (10.57)$$

In the interval  $\Delta t$  the concentration of droplets of size  $n$  at time  $t$ ,  $c(n, t)$  changes to

$$c(n, t + \Delta t) = c(n, t) + \Delta t [W(n|n-1)c(n-1, t) - W(n-1|n)c(n, t) + W(n|n+1)c(n+1, t) - W(n+1|n)c(n, t)].$$

If  $\delta t$ , is small, and  $n \gg 1$  then we may approximate the equation above by a differential equation. Using the detailed balance equation (10.54) we rewrite the equation:

$$\begin{aligned} \frac{\partial}{\partial t} c(n, t) &= W(n|n-1)c_0(n-1) \left\{ \frac{c(n-1)}{c_0(n-1)} - \frac{c(n)}{c_0(n)} \right\} \\ &\quad + W(n+1|n)c_0(n) \left\{ \frac{c(n+1)}{c_0(n+1)c(n)/c_0(n)} - \frac{c(n)}{c_0(n)} \right\}. \end{aligned}$$

Now we approximate the differences in the braces by derivatives:

$$\begin{aligned} \frac{\partial}{\partial t} c(n, t) &= -W(n|n-1)c_0(n-1) \frac{\partial}{\partial n} \frac{c(n, t)}{c_0(n)} \Big|_{n-1} \\ &\quad + W(n+1|n)c_0(n) \frac{\partial}{\partial n} \frac{c(n, t)}{c_0(n)} \Big|_n. \end{aligned}$$

Again we have the difference of two terms, the first evaluated at  $n-1$  and the second at  $n$ . This difference may be approximated by the *nucleation equation* is a special case of the general Fokker-Planck equation (E.15):

$$\frac{\partial}{\partial t} c(n, t) = \frac{\partial}{\partial n} \left( D(n)c_0(n) \frac{\partial}{\partial n} \frac{c(n, t)}{c_0(n)} \right) \quad (10.58)$$

Here,  $c(n, t)$  is the concentration of droplets of size  $n$  at time  $t$ . The size ‘diffusion constant’  $D(n)$  is given by the Einstein relation in equations (E.11) and (E.20) as

$$D(n) = \frac{1}{2}a^2\Gamma = \nu\hat{A}(n) \quad (10.59)$$

since the mean square jump distance is 1, and the jump rate is  $\Gamma = 2\nu\hat{A}(n)$ .

Equation (10.58) is a continuum equation of the form

$$\frac{\partial}{\partial t}c(n, t) + \frac{\partial}{\partial n}J(n) = 0, \quad (10.60)$$

where the *nucleation rate* or flux is given by

$$J(n) = -Dc_0\frac{\partial}{\partial n}\left(\frac{c}{c_0}\right) = -D\frac{\partial c}{\partial n} + \frac{D}{k_B T}cf(n). \quad (10.61)$$

Here the “force”,  $f(n)$  is given by the derivative of the potential  $\Delta\Omega$  in equation (10.43)

$$f(n) = -\frac{\partial\Delta\Omega}{\partial n}. \quad (10.62)$$

The nucleation rate therefore consists of two terms: the diffusion term  $-D\frac{\partial c}{\partial n}$ , and the *drift term*  $+\left[\frac{D}{k_B T}f\right]c$ . The term in square brackets is the “drift velocity” and has the form of a *mobility*  $\mu$  times a force. The mobility satisfies the second Einstein relation

$$\mu = \frac{D}{k_B T}, \quad \text{Einstein relation II} \quad (10.63)$$

In a stationary state,  $c(n, t) = c_s(n)$  and  $\frac{\partial c_s}{\partial t} = 0$ , the nucleation rate,  $J(n) = J_s$  is independent of  $n$  is given by

$$J_s = -D(n)c_0(n)\frac{\partial}{\partial n}\left(\frac{c_s(n)}{c_0(n)}\right). \quad (10.64)$$

To achieve a stationary state in an open system we fix the external potential of the vapor  $\mu = \mu_0$  so that we have a supersaturation. As droplets nucleate and grow they will reach some macroscopic size at which they are removed from the system. For such a system the sub-critical clusters are in quasi-equilibrium with the monomer concentration; therefore we have that  $c_s(n)/c_0(n) \rightarrow 1$  when  $n \ll n^*$ . Similarly, clusters much larger than the critical size  $n^*$  grow rapidly so that  $c_s(n)/c_0(n) \rightarrow 0$  for  $n \gg n^*$ . We note

that cluster size is  $n = (4\pi v/3)R^3$ , where  $v$  is the molecular volume. It follows from the expressions equations (10.46) and (10.47) that the Landau potential may be written

$$\Delta\Omega = \Delta\Omega^* \left\{ -2(n/n^*) + 3(n/n^*)^{2/3} \right\}. \quad (10.65)$$

Here,  $n^* = (4\pi v/3)(R^*)^3$ , is the critical size, and  $\Delta\Omega^*$  is given by equation (10.46). We may expand  $\Delta\Omega$  in a Taylor series around the critical size:

$$\Delta\Omega = \Delta\Omega^* + \frac{\partial\Delta\Omega}{\partial n} \Big|_{n^*} (n - n^*) + \frac{1}{2} \frac{\partial^2\Delta\Omega}{\partial n^2} \Big|_{n^*} (n - n^*)^2 + \dots. \quad (10.66)$$

Here the first order term vanishes since the critical size is found by requiring  $\partial\Delta\Omega/\partial n = 0$ . The second order term may be used to find the width,  $\Delta$ , of the critical region by setting:

$$\Delta\Omega(n = n^* \pm \frac{1}{2}\Delta) = \Delta\Omega^* - k_B T. \quad (10.67)$$

This gives the width of the critical region as

$$\Delta = 2n^*(3k_B T/2\Delta\Omega^*)^{\frac{1}{2}}. \quad (10.68)$$

We note that  $\frac{\partial}{\partial n} \left( \frac{c_s(n)}{c_0(n)} \right) \simeq 1/\Delta$ . With this approximation the nucleation rate is given by

$$J_s = \frac{D(n^*)}{\Delta} c_0(n^*). \quad (10.69)$$

The nucleation rate,  $J_s$ , that is, the number of droplets formed per unit volume and per unit time, depends exponentially on the supersaturation via  $c_0^* = \exp(-\frac{4}{3}\pi\sigma R^2/k_B T)$  (see equation (10.57)). Changes in the nucleation rate is therefore most easily affected by changing  $\Delta\Omega^*$  since  $c_0^* \sim \exp(-\Delta\Omega^*)$ .

## 10.7 Young's Law

Drops of water on solid surfaces is a familiar phenomenon. Depending the properties of the solid surface the drop may take a variety of shapes, as illustrated in figure 10.5, that depend on the contact angle.

The *equilibrium angle of contact*  $\theta_0$  is a thermodynamic variable that depends on three surface free energies:

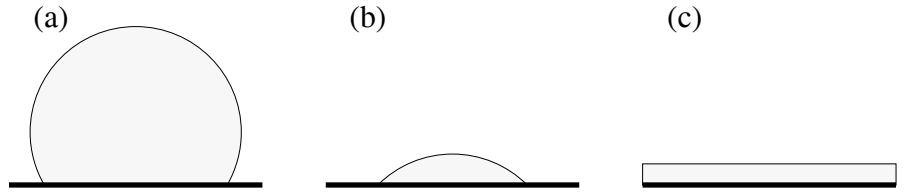


Figure 10.5: A small drop in equilibrium on a horizontal surface. (a) and (b) correspond to partial wetting with an equilibrium contact angle in the range  $0 < \theta < \pi$ . (c) corresponds to complete wetting and the drop spreads to a film in between the liquid and the vapor.

$\sigma_{\ell,g}$  the free energy per unit area of the liquid-gas interface, that is, the liquid vapor interface.

$\sigma_{s,\ell}$  the solid-liquid free energy per unit area.

$\sigma_{s,g}$  the solid-gas (or vapor) free energy per unit area. In general molecules from the vapor adsorb onto the solid surface and  $\sigma_{s,g}$  refers to that equilibrium situation.

The equilibrium contact angle is given by Young's law:

$$\boxed{\sigma_{s,g} = \sigma_{s,\ell} + \sigma_{\ell,g} \cos \theta_0} \quad \text{Young} \quad (10.70)$$

Young<sup>118</sup> did not formulate his 'law' in mathematical terms. In the beginning of his paper he states:

But it is necessary to premise one observation, which appears to be new, and which is equally consistent with theory and with experiment; that is, that for each combination of a solid and a fluid, there is an appropriate angle of contact between the surfaces of the fluid exposed to air and to the solid. This angle, for glass and water, and in all cases where a solid is perfectly wetted by a fluid, is evanescent: for glass and mercury, it is about  $140^\circ$ , in common temperatures, and when the mercury is moderately clean.

Here he claims priority to the concept of an angle of contact. He clearly states that the angle of contact is characteristic of the fluid (water or mercury), 'air' and the solid (glass). He also implies that purity is relevant.

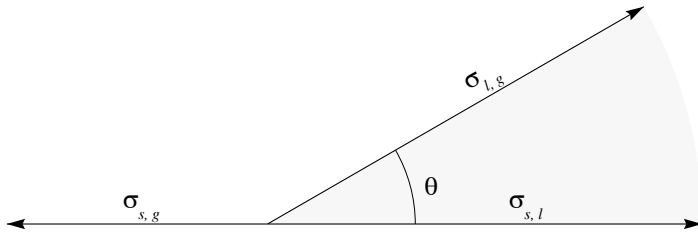


Figure 10.6: The balance of forces at the vapor-liquid-solid intersection is consistent with Young's law.

There are several ways to derive Young's law. The most common method is to interpret the surface free energy as a tension. Following Maxwell's definition (see page 10.1) the surface tension is the *force* across a line per unit length. Mechanical equilibrium then requires that the forces along the solid surface balance (see figure 10.6) and equation (10.70) follows.

The forces should balance also in the vertical direction. This is, however, not possible, since with the given geometry one needs to compensate the upward component  $\sigma_{\ell,g} \sin \theta_0$  by a downward component that must finally come from the solid, and the problem with the force argument is that it really assumes that the solid is non-deformable. Thus we are lead to the more general case of a drop resting on a deformable medium—such as another fluid. The conclusion from such a discussion is that equation (10.70) is indeed correct in the limit of a non-deformable solid (see reference [] for a discussion).

### 10.7.1 Angle of Contact Thermodynamics

The angle of contact can be understood as a thermodynamic variable that reaches the value  $\theta_0$  in thermal equilibrium. For the system illustrated in figure 10.7 the total Landau potential is

$$\begin{aligned}\Omega &= -P_\ell V_\ell - P_g(V - V_\ell) + \sigma_{\ell,g} A_{\ell,g} + \sigma_{s,\ell} A_{s,\ell} + \sigma_{s,g}(A - A_{s,\ell}) \quad (10.71) \\ &= \Omega_v - (P_\ell - P_g)V_\ell + \sigma_{\ell,g} A_{\ell,g} + (\sigma_{s,\ell} - \sigma_{s,g})A_{s,\ell}.\end{aligned}$$

where  $\Omega_v = -P_g V + \sigma_{s,g} A$  is the Landau potential in the absence of the drop. This expression for  $\Omega$  differs from equation (10.25) by the additional surface terms. Here the volumes and areas of the drop resting on the

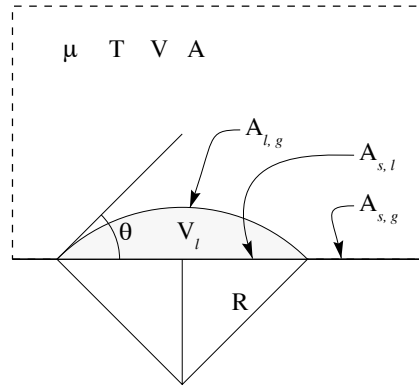


Figure 10.7: A drop resting on a solid surface at given chemical potential  $\mu$  and temperature  $T$ . The open system has volume  $V$  and wall area  $A$  accessible to the vapor. The drop has radius of curvature  $R$  and angle of contact  $\theta$ .

surface may be expressed in terms of the radius  $R$  of the spherical cap and the angle of contact  $\theta$ , or the variable  $u = \cos \theta$ .

$$\begin{aligned} A_{s,\ell} &= \pi(R \sin \theta)^2 &= \pi R^2(1 - u^2) && u = \cos \theta , \\ A_{\ell,g} &= \int_0^\theta 2\pi R \sin \tilde{\theta} R d\tilde{\theta} = 2\pi R^2 \int_{\cos \theta}^1 du & &= 2\pi R^2(1 - u) , \\ V_\ell &= \pi R^3 \int_0^\theta \sin^3 \tilde{\theta} d\tilde{\theta} = \pi R^3 \int_{\cos \theta}^1 du (1 - u^2) & &= \pi R^3(\frac{2}{3} - u + \frac{1}{3}u^3) . \end{aligned}$$

We have already shown that the pressure difference is given by the Young-Laplace law (10.28):  $P_\ell - P_g = 2\sigma_{\ell,g}/R$ , which when used with the expressions above leads to the following expression for  $\Omega$ :

$$\Omega = \Omega_v + \frac{2}{3}\pi R^2 \sigma_{\ell,g}(1 - u^3) + \pi R^2(\sigma_{s,\ell} - \sigma_{s,g})(1 - u^2) . \quad (10.72)$$

In thermal equilibrium at fixed  $\mu$  and  $T$  we must have  $(\partial\Omega/\partial u)_{\mu,T} = 0$ , a condition that with equation (10.72) leads directly to Young's law (10.70). Thus we may consider the contact angle  $\theta$  to take on a value  $\theta_0$  in thermal equilibrium.

## 10.8 Capillary Rise

A fluid rises to a height  $h$  in a capillary if the contact angle is less than  $\pi/2$ . The Young-Laplace pressure across the meniscus is

$$P_g - P_\ell = \frac{2\sigma_{l,g}}{R} = 2\sigma_{\ell,g} \cos \theta/a , \quad (10.73)$$

with the highest pressure being on the vapor side. This pressure difference must be equal to the difference in hydrostatic pressure in the two phases given by

$$P_\ell(h) = p_0 - \rho_\ell gh , \quad P_g(h) = p_0 - \rho_g gh . \quad (10.74)$$

Here  $g$  is the acceleration of gravity, and  $p_0$  is the reference pressure. Inserting these results in equation (10.73) we find that the fluid will rise to a height given by

$$h = 2\sigma_{\ell,g} \cos \theta / (\rho_\ell - \rho_g) ga \quad (10.75)$$

The capillary rise  $h < 0$  if the fluid is non-wetting, that is,  $\theta > \pi/2$ , which is the case for mercury in glass capillaries. Often the notion of a *capillary length*  $\lambda$  (or capillary constant) is introduced. The rise of a fluid in capillary wetted by the fluid is

$$\lambda^2 = 2\sigma_{\ell,g} / g\Delta\rho = ha \quad \text{capillary constant} \quad (10.76)$$

Here  $\Delta\rho = \rho_\ell - \rho_g$ . The capillary length  $\lambda$  determines the length scale of most capillary phenomena. For water  $a = 3.93$  mm at  $0^\circ$  C, and decreases with increasing temperature, becoming zero at the critical point.

## Chapter 11

# Viscous Fingering in the Hele-Shaw Cell

A Hele-Shaw cell consists of two transparent plates separated a distance  $b$ . Hele-Shaw<sup>127</sup> studied the flow of water around various objects placed in the cell. He visualized the flow *streamlines* by injecting a dye to produce colored streamlines. These experiments verify directly that the fluid flow in a Hele-Shaw cell with a small  $b$  is the ‘creeping flow’ characteristic for low Reynolds numbers. If the plate separation is increased turbulent flow with confused stream-lines arise at moderate flow velocities.

The velocity in an infinitely wide channel  $\mathbf{U} = \langle \mathbf{u} \rangle$  was discussed in section 4.1 with the main result in equation (4.8). This equation may be written in the form of the Darcy equation (6.8) for flow in the Hele-Shaw cell illustrated in figure 11.1

$$\mathbf{U} = -\frac{k}{\mu} \nabla(p + \rho \hat{g} z), \quad (11.1)$$

component of the acceleration of gravity along the  $z$ -coordinate of the cell. For a cell placed in the horizontal position we therefore have  $\hat{g} = 0$ . The viscosity of the fluid is  $\mu$  and the permeability of the Hele-Shaw cell is

$$k = \frac{b^2}{12}. \quad (11.2)$$

Note that the velocity in equation (11.1) is the *average* velocity over the thickness of the cell. For incompressible fluids the equation of continuity

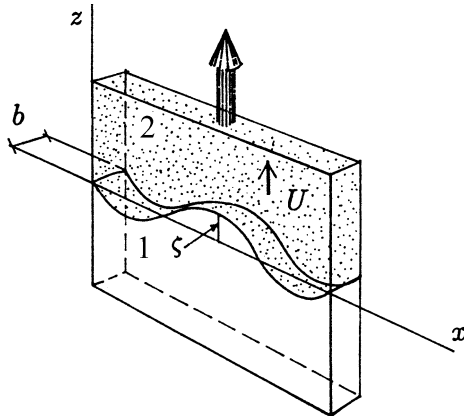


Figure 11.1: Geometry of the Hele-Shaw channel.

gives

$$\nabla \cdot \mathbf{U} = -\frac{k}{\mu} \nabla^2(p + \rho \hat{g} z) = 0. \quad (11.3)$$

The Laplace equation (11.3) is characteristic of potential problems encountered in electrostatics, in diffusion problems and many other fields and consequently we call flows controlled by equation (11.3) for potential flow. A solution of the flow problem in addition requires the boundary conditions to be specified.

We will discuss the situation illustrated in figure 11.1, where a fluid (1) displaces another fluid (2). The interface between the two fluids is controlled by capillary forces when the fluids are at rest and there is a pressure difference between the two fluids at the interface

$$(p_1 - p_2) = \sigma \left( \frac{1}{R_x} + \frac{1}{R_y} \right), \quad (11.4)$$

where  $\sigma$  is the interfacial tension between the two fluids. The two radii of curvature  $R_x$  and  $R_y$ , describe the interface locally as indicated in figure 11.2. We define the radii of curvature to be positive if they have their center in fluid (1). We find  $R_y = b/2 \cos \theta$ , where  $\theta$  is the contact angle between fluid (2) and the plates of the Hele-Shaw cell. We will assume that  $R_x \gg R_y$ . We have that  $p_1 > p_2$  when the fluids are at rest and (2) is the wetting fluid.

Now let us inject the fluid (1) at a constant rate  $\bar{U}$  at  $z = -\infty$  and withdraw fluid (2) at the same rate at  $z = \infty$ . The interface between

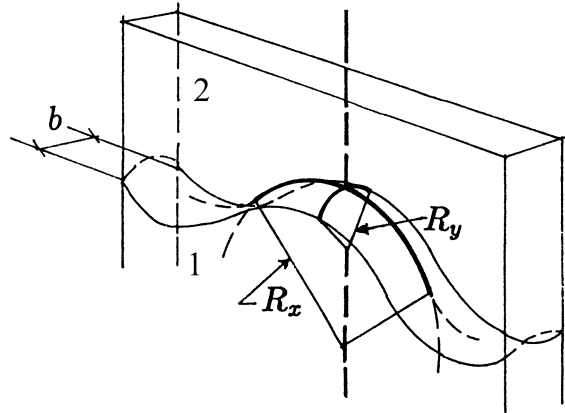


Figure 11.2: Geometry of the fluid–fluid interface.

the two fluids will then move with a velocity  $\bar{\mathbf{U}} = (0, 0, \bar{U})$  along the  $z$ -axis. However, it turns out that the interface is *unstable* if the viscosity of the driving fluid is smaller than the viscosity of the fluid being driven. Engelberts and Klinkenberg<sup>128</sup> coined the term *viscous fingering* in relation to their observation of such instabilities when water drives oil out of a porous medium. Flow in porous media also follow the equations (11.1) and (11.3), and therefore the flow in Hele-Shaw cells are often used to model the flow in porous media. However, as we shall see there are important differences and the validity of using the Hele-Shaw cell a model of flow in porous media remains an open question.

The theory of viscous fingering was developed and compared to experiments independently by Saffman and Taylor<sup>129</sup> and by Chuoke, van Meurs and van der Poel.<sup>130</sup> Recently there has been a growing interest in the field and many new theoretical and experimental results have been published; see reference [] for a review and my book<sup>132</sup> *Fractals* for a discussion of *fractal viscous fingering*.

The physics of the viscous fingering lies in the geometry of the moving boundary. Assume that a pressure difference is maintained over the length of a finite Hele-Shaw cell. The pressure in the air is constant since we ignore its viscosity, and the largest pressure gradient appear at the longest finger. Thus a finger that gets ahead of the rest of the interface will move faster than the rest and grow further—this is clearly an unstable situation.

## 11.1 Linear Stability Analysis

To analyze the stability of the moving interface we first note that in a frame of reference moving with the interface at a velocity  $\bar{U}\mathbf{e}_z$  in the  $z$ -direction, a small *perturbation*,  $\mathbf{u}$ , in the velocity satisfies a modified version of equation (11.1) for each of the fluids<sup>1</sup> ( $i = 1, 2$ ):

$$\mathbf{u}_i = -\nabla\chi_i . \quad (11.5)$$

Here we have introduced the *velocity potential*

$$\chi_i = \frac{k_i}{\mu_i} \left( p_i + P_i(t) + \frac{\mu_i}{k_i} \bar{U} z + \rho_i \hat{g} z \right) , \quad (11.6)$$

which then satisfies the Laplace equations

$$\nabla^2\chi_i = 0 . \quad (11.7)$$

The velocity potential  $\chi_i$  gives the fluid velocity directly by equation (11.5). The velocity potential is linear in pressure, in the driving velocity  $\bar{U}$ , and in the gravity term. In addition the velocity potential is linear in an arbitrary time dependent pressure term  $P_i(t)$  that must be determined from the boundary condition that at the interface we must have  $\mathbf{u}_1 = \mathbf{u}_2 = (\partial\zeta/\partial t)$ , where  $\zeta(t)$  is the interface position.

In order to test the stability of the advancing interface we follow standard practice<sup>129,130</sup> and assume that the straight interface is perturbed by a sinusoidal displacement so that in the frame of reference moving with the average velocity  $\bar{U}$  the position of the interface is given by the real part of

$$\zeta = \epsilon \exp(\gamma t + iqx) , \quad (11.8)$$

as illustrated in figure 11.1. The wavelength of the perturbation is  $\lambda = 2\pi/q$ . The growth rate of the perturbation is  $\gamma$ . For a stable interface the perturbation  $\zeta$  will decay in time and  $\gamma < 0$ . If the growth rate is positive  $\gamma > 0$ , a perturbation of infinitesimal amplitude  $\epsilon$  will grow exponentially. We shall limit ourselves to a discussion of the onset of instability and assume the perturbation to be *infinitesimal* and neglect terms of order  $\epsilon^2$  and higher.

The velocity of the interface in the moving frame must equal the fluid velocities so that we have the boundary conditions

$$\frac{\partial\zeta}{\partial t} = - \left( \frac{\partial\chi_1}{\partial z} \right)_{z=\zeta} = - \left( \frac{\partial\chi_2}{\partial z} \right)_{z=\zeta} . \quad (11.9)$$

---

<sup>1</sup>For the Hele-Shaw cell  $k_1 = k_2 = b^2/12$ . In 2-dimensional porous media the permeabilities may differ, since the displacement may be incomplete, and we retain the notation  $k_1$  and  $k_2$ .

As is easily seen the following solutions of the Laplace equations (11.7)

$$\begin{aligned}\chi_1 &= -\frac{\gamma}{q}\epsilon \exp(+qz + iqx + \gamma t), \\ \chi_2 &= +\frac{\gamma}{q}\epsilon \exp(-qz + iqx + \gamma t),\end{aligned}\quad (11.10)$$

satisfy the boundary conditions given in equation (11.9) to first order in  $\epsilon$ . The velocity potential of the perturbation  $\chi_1 \rightarrow 0$  as  $z \rightarrow -\infty$  and  $\chi_2 \rightarrow 0$  as  $z \rightarrow \infty$ , so that the perturbation is localized at the interface.

We now insert equation (11.6) with  $z = \zeta$  into the pressure equation (11.4) using the expressions for  $\zeta$  and  $\chi_i$  to get

$$\begin{aligned}\frac{\mu_1}{k_1}\chi_1(\zeta) - \frac{\mu_2}{k_2}\chi_2(\zeta) + \left\{ \left( \frac{\mu_2}{k_2} - \frac{\mu_1}{k_1} \right) \bar{U} - (\rho_1 - \rho_2)\hat{g} \right\} \zeta \\ - P_1(t) + P_2(t) = \sigma \left( \frac{1}{R_x} + \frac{1}{R_y} \right).\end{aligned}\quad (11.11)$$

We note that for  $q\zeta \ll 1$  we may to order  $\epsilon$  write  $\chi_1(\zeta) \simeq -\frac{\gamma}{q}\epsilon \exp(iqx + \gamma t)$  and a similar expression for  $\chi_2$ . Note also that for  $q\zeta \ll 1$  we find that the radius of curvature in the  $x$ -direction is given by  $1/R_x \simeq -(\partial^2\zeta/\partial x^2)$ , and we have  $R_y \sim b/2 \cos \theta$ , so that we may write

$$(p_1 - p_2) = P_c - \sigma \frac{\partial^2 \zeta}{\partial x^2}, \quad (11.12)$$

where we have introduced the *capillary pressure*  $P_c = 2\sigma \cos \theta/b$ . It follows from equation (11.11) that in the limit  $\epsilon \rightarrow 0$

$$-P_1 + P_2 = P_c = 2\sigma \cos \theta/b,$$

Thus the stationary pressure difference between the two fluids is given by the capillary pressure  $P_c$ . The remaining terms in equation (11.11) all contain a factor  $\epsilon \exp(iqx + \gamma t)$ , which may be eliminated, and we rewrite equation (11.11) as follows:

$$\gamma \left( \frac{\mu_2}{k_2} + \frac{\mu_1}{k_1} \right) - \left\{ \left( \frac{\mu_2}{k_2} - \frac{\mu_1}{k_1} \right) \bar{U} - (\rho_1 - \rho_2)\hat{g} \right\} q + \sigma q^3 = 0. \quad (11.13)$$

For  $q > 0$  it follows from equation (11.13) that  $\gamma > 0$ , and the interface is unstable for  $\mu_2 > \mu_1$  if  $\bar{U} > U_c$  where the critical velocity is given by

$$U_c = \left( \frac{\hat{g}(\rho_1 - \rho_2)}{\frac{\mu_2}{k_2} - \frac{\mu_1}{k_1}} \right). \quad (11.14)$$

Note that  $U_c < 0$  for  $\rho_2 > \rho_1$  when  $\mu_2 > \mu_1$  and the system is unstable even at  $\bar{U} = 0$ . Also, in the absence of gravity effects the interface is unstable at any velocity since  $U_c = 0$ .

We find from equation (11.13) that the interface is unstable for disturbances with a wavelength  $\lambda = 2\pi/q$  satisfying the relation

$$\lambda > \lambda_c = 2\pi \left( \frac{\sigma}{\left( \frac{\mu_2}{k_2} - \frac{\mu_1}{k_1} \right) (\bar{U} - U_c)} \right)^{1/2}. \quad (11.15)$$

Ignoring gravity effects we find that the interface is always stable if the driving fluid has a higher viscosity than the fluid being driven.

When the interface is unstable we have a real *critical wavelength*  $\lambda_c$ , which may be used to write equation (11.13) for the *growth rate*  $\gamma$  in a dimension-less (scaled) form:

$$\gamma = \frac{1}{\tau} \left\{ \left( \frac{\lambda_c}{\lambda} \right) - \left( \frac{\lambda_c}{\lambda} \right)^3 \right\}. \quad (11.16)$$

The units of the growth rate  $\gamma$  is  $\tau^{-1}$ , where the time scale  $\tau$  is defined by

$$\tau = \frac{\lambda_c}{2\pi A(\bar{U} - U_c)}. \quad (11.17)$$

Here we use the viscosity ratio (Atwood ratio) introduced by Tryggvason and Aref,<sup>133</sup> given by

$$A = \frac{\frac{\mu_2}{k_2} - \frac{\mu_1}{k_1}}{\frac{\mu_2}{k_2} + \frac{\mu_1}{k_1}} \xrightarrow{k_1=k_2} \frac{\mu_2 - \mu_1}{\mu_2 + \mu_1}. \quad (11.18)$$

For a fluid of negligible viscosity, as is the case when air displaces an oil or glycerol, we have  $A \sim 1$ , and when two fluids of identical viscosity displace each other we have  $A \rightarrow 0$ . In the latter case the characteristic time  $\tau$  diverges and the instability will take an infinite time to develop.

The equation (11.16) suggests that we scale distance with  $\lambda_c$  and time with  $\tau$  giving the dimensionless time  $t'$  and the dimensionless distances  $x', z'$  given by<sup>2</sup>

$$x', z' = \frac{x}{\lambda_c}, \frac{z'}{\lambda_c} \quad \text{and} \quad t' = \frac{t}{\tau}. \quad (11.19)$$

---

<sup>2</sup>Tryggvason and Aref (1983) introduce similar dimensionless quantities related to ours by  $t'_{TA} = t'/\sqrt{24}$  and  $x'_{TA} = 2\pi x'/\sqrt{24}$

Tryggvason and Aref<sup>133</sup> have shown that the equations of motion for the interface in the scaled time and distances  $t', x'$  are in fact *independent* of the surface tension  $\sigma$  so that the structure of the interface depends only on the viscosity ratio  $A$ . However, this scaling region is obtained only for the case that  $\lambda_c \ll W$ . In the region where  $\lambda_c \sim W$  the lateral boundary conditions control the instability and in this region the natural length scale is the width  $W$  of the Hele-Shaw channel. The proper time-scale in this case is  $W/\bar{U}$ .

It is easy to show, by setting  $d\gamma/d\lambda = 0$  in equation (11.16), that the maximum growth rate is obtained by perturbations with a wavelength

$$\lambda_m = \sqrt{3}\lambda_c .$$

We therefore expect that in experiments in a Hele-Shaw channel of width  $W$  an initially straight interface will develop *viscous fingers* with a characteristic period  $\lambda_m$ . Using the expression (11.2) for the permeability and assuming that the viscosity of the driving fluid is negligible,  $\mu_1 \ll \mu_2$ , as is the case when glycerol is displaced by air, we find for a horizontal cell that we expect fingers with a period given by

$$\lambda_m = \pi b \sqrt{\frac{\sigma}{\bar{U}\mu}} = \frac{\pi b}{\sqrt{\text{Ca}}} . \quad (11.20)$$

Here we have introduced the dimensionless *capillary number* Ca defined by

$$\text{Ca} = \frac{\bar{U}\mu}{\sigma} , \quad (11.21)$$

which measures the ratio of viscous to capillary forces.

## 11.2 Observations of Viscous Fingers

Saffman and Taylor<sup>129</sup> and Chuoke, van Meurs and van der Poel<sup>130</sup> not only developed the theory of viscous fingering in a Hele-Shaw channel they also studied viscous fingering experimentally. We show fingering patterns for air displacing glycerol observed by Saffman and Taylor in figure 11.3. The initial air–glycerol interface had irregularities at the start of the experiments.<sup>3</sup> Note that the observed wavelength of approximately 2.2 cm is quite close to the wavelength of maximum instability  $\lambda_m = \sqrt{3}\lambda_c = 2.1$  cm.

Similar fingers were observed by Chuoke et al. as shown in figure 11.4 the finger structure was quite close to the most unstable wavelength  $\lambda_m$ .

---

<sup>3</sup>Many more experiments are possible. Much new work on perturbed fingers. We should repeat the experiment using Vidar's fluids

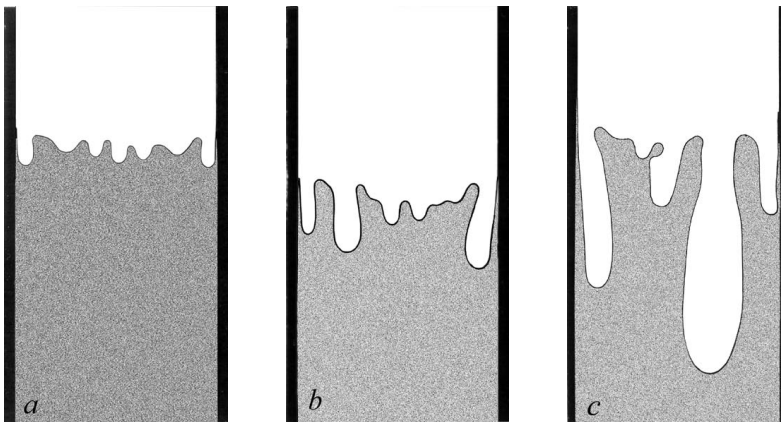


Figure 11.3: Viscous fingering in a vertical cell where air displaces glycerol from the top and downwards.  $\bar{U} = 0.1 \text{ cm/s}$  and  $\lambda_c = 1.2 \text{ cm}$ . (a) – Early stage with observed average  $\lambda \simeq 2.2 \text{ cm}$ . (b) – Later stage: Fingers tend to space themselves. (c) – Late stage: Longer fingers inhibit the growth of neighbors (after Saffman and Taylor reference []).

Figure 11.3: Viscous fingering in a vertical cell where air displaces glycerol from the top and downwards.  $\bar{U} = 0.1 \text{ cm/s}$  and  $\lambda_c = 1.2 \text{ cm}$ .

Saffman and Taylor also made a detailed study of the shape of a single finger in a long horizontal channel as shown in figure 11.5.

The tendency for fingers to develop equidistant spacings irrespective of the channel width  $W$ , suggests that one should study the hydrodynamics of a single finger with periodic lateral boundary conditions. Saffman and Taylor found that for negligible viscosity of the driving fluid,  $\mu_1 \ll \mu_2$ , and with a neglect of the influence of radius of curvature  $R_x$  on the pressure difference (that is,  $R_x \gg b$ ) the bubble profile is given by (see figure 11.5)

$$z = \frac{1 - \delta}{\pi} \ln \left\{ \frac{1}{2} \left( 1 + \cos \frac{\pi x}{\delta} \right) \right\}. \quad (11.22)$$

Here the width of the finger is  $W\delta$  so that  $\delta$  is the fractional finger width. The velocity of the finger is  $U^* = U\delta$ . The relative width of the finger is, however, *not* given by their equations and is therefore arbitrary.

Saffman and Taylor concluded from their experiments on Hele-Shaw cells that

...as the speed of flow for any given fluid increases,  $\delta$  rapidly decreases to  $\delta = \frac{1}{2}$ , and remains close to this value over a large

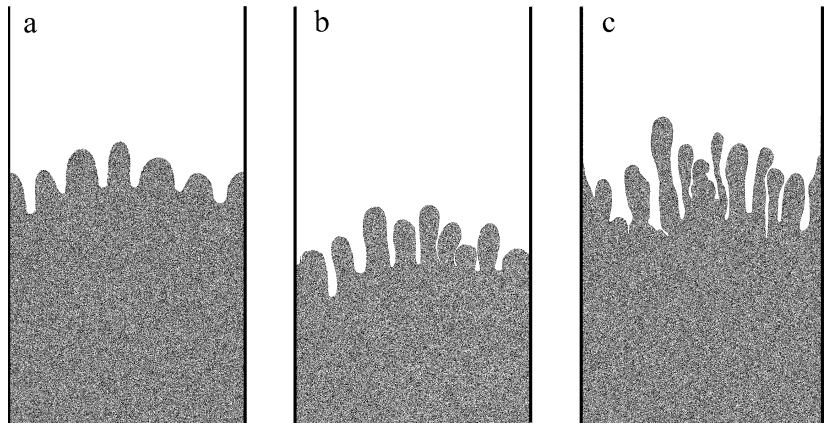


Figure 11.4: Water-glycerol solution (dark)  $\mu_1 = 0.552 \text{ poise}$ ,  $\rho_1 = 1.21 \text{ g/cm}^3$  moved upward and displaced oil  $\mu_2 = 1.39 \text{ poise}$ ,  $\rho_2 = 0.877 \text{ g/cm}^3$ . The system was tilted an angle of  $44^\circ 25'$ . The bulk interfacial tension was  $\sigma = 33 \text{ dyne/cm}$ , and the oil weted the walls. The critical velocity was  $U_c = 0.23 \text{ cm/s}$ . (a) –  $\bar{U} = 0.41 \text{ cm/s}$ ,  $\lambda_m = 3.5 \text{ cm}$  observed  $\lambda = 3.5 \text{ cm}$ . (b) –  $\bar{U} = 0.87 \text{ cm/s}$ ,  $\lambda_m = 2.6 \text{ cm}$  observed  $\lambda = 2.4 \text{ cm}$ . (c) –  $\bar{U} = 1.66 \text{ cm/s}$ ,  $\lambda_m = 1.6 \text{ cm}$  observed  $\lambda = 1.7 \text{ cm}$  (Chuoke et. al. 1959).

range of speeds, till at high speeds of flow the tongue or finger of the advancing fluid itself breaks down and divides into smaller fingers.

They suggested that the shape of the meniscus depends only on  $U_{\text{tip}}\mu/\sigma$ , which is the capillary number  $\text{Ca}$  in equation (11.21) using the tip velocity  $U_{\text{tip}}$  as the characteristic velocity. As shown in figure 11.6 the observed relative finger width  $\delta$  as function of the capillary number  $\text{Ca}$  fall on a single curve giving a very satisfying data collapse for the experiments on single fingers propagating in a Hele-Shaw channel.

Saffman and Taylor had no explanation for the selection of  $\delta = 0.5$  at high  $\text{Ca}$ . Also they note that an analysis of the stability of finger solutions given in equation (11.22) indicate that they are *unstable* for all values of  $\delta$ . This instability of the finger solution was confirmed by McLean and Saffman.<sup>134</sup>

Pitts<sup>135</sup> observed that the advancing finger left a thin layer of the viscous wetting fluid on the glass plates. Attempting to account for this effect Pitts made an *ad hoc* assumption for the boundary conditions and

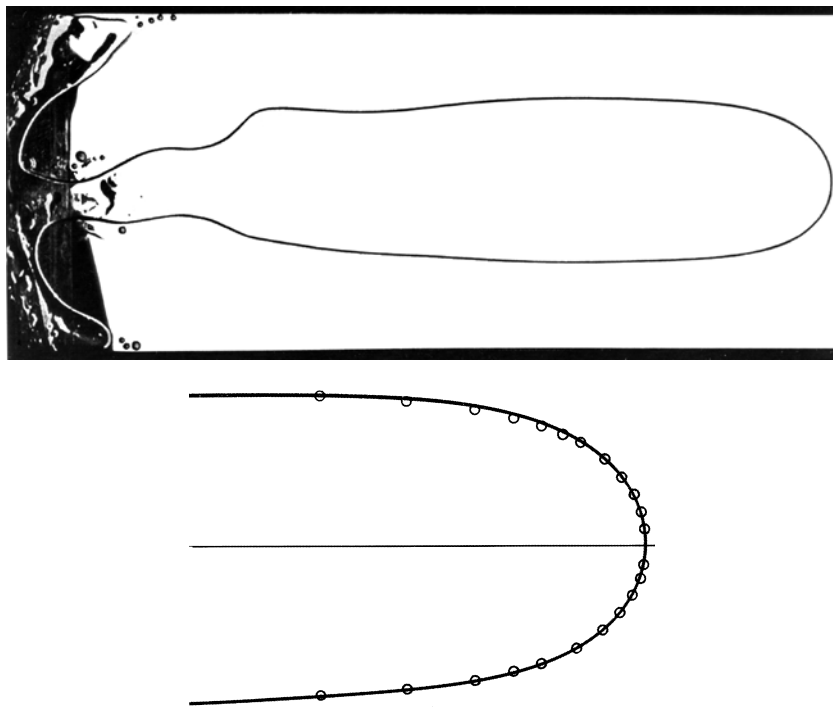


Figure 11.5: (a) – An air finger advancing into glycerol in a Hele-Shaw channel  $b = 0.09 \text{ cm}$  and  $W = 10.26 \text{ cm}$ . The finger started at a small bubble injected before the experiment. (b) – Comparison of the shape of the finger tip in (a) and the theoretical expression indicated by  $\circ$  (after Saffman and Taylor reference [1]).

Figure 11.5: (a) – An air finger advancing into glycerol in a Hele-Shaw channel  $b = 0.09 \text{ cm}$  and  $W = 10.26 \text{ cm}$ . The finger start

found an equation for the finger shape given by equation (11.22) but with  $\delta$  replacing  $1 - \delta$  in front of the logarithm. He finds that this modified expression fits the experimental results very well indeed. Pitts further made the assumption that the radius of curvature (for  $\cos \theta = 1$ ), of the advancing meniscus is  $R_y = b/2m$  with  $m > 1$  instead of  $m = 1$  as was assumed above. Also assuming that  $m$  is independent of the velocity  $\bar{U}$ , or the capillary number  $\text{Ca}$ , he found that his own experimental results and those by Saffman and Taylor (1958) are very well described by

$$\lambda \ln \left( \frac{\lambda}{1 - \lambda} \right) = b \frac{\pi}{12} (m - 1) \text{Ca}^{-1},$$

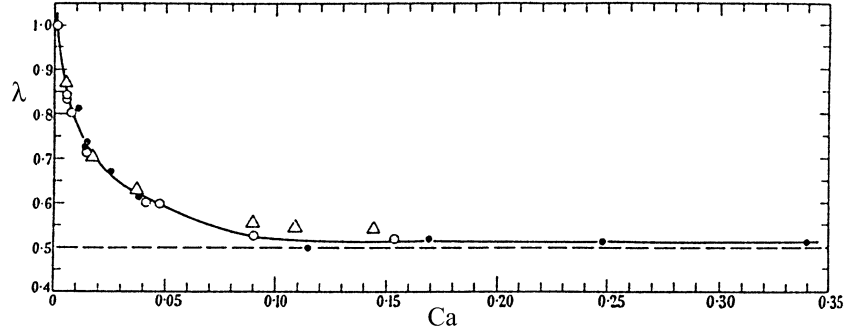


Figure 11.6: The relative width  $\delta$  of a water finger advancing in oil as function of the capillary number  $\text{Ca} = U_{\text{tip}}\mu/\sigma$  where  $U_{\text{tip}}$  is the tip velocity.  $\circ$  and  $\triangle$  Shell Talpa  $\mu = 4.5 \text{ poise}$ .  $\bullet$  Shell Dalia  $\mu = 0.30 \text{ poise}$  (after Saffman and Taylor reference [1]).

Figure 11.6: The relative width  $\delta$  of a water finger advancing in oil as function of

when  $m = 1.26$  is chosen. Unfortunately, no justification of the assumptions made by Pitts is available.

### 11.3 The Nonlinear Regime

The development of viscous fingers in the Hele-Shaw cell beyond the initial (linear) stability analysis can not be studied by analytical methods. Tryggvason and Aref<sup>133</sup> have solved the two-dimensional flow equations for the Hele-Shaw cell numerically. They represent the interface by a vortex sheet and compute the evolution of this vortex sheet using a variant of the vortex-in-cell method.

It is convenient in the numerical calculations to work with a Hele-Shaw channel of unit width and they use the scaled units  $\tilde{x} = x/W$  and  $\tilde{t} = tW/U_*$ , where they use a velocity defined by  $U_* = A(\bar{U} - U_c)$ . They also introduce the non-dimensional surface-tension coefficient:

$$B = \frac{\sigma b^2}{12U_*\bar{\mu}W^2} = \left( \frac{\lambda_c}{2\pi W} \right)^2 = \frac{1}{A\text{Ca}^*} \left( \frac{b}{W} \right)^2. \quad (11.23)$$

Here the average viscosity  $\bar{\mu} = \frac{1}{2}(\mu_1 + \mu_2)$ , and the capillary number  $\text{Ca}^*$  is a modification of equation (11.21) so that  $\text{Ca}^* = \bar{\mu}(\bar{U} - U_c)/\sigma$ .

However, as pointed out by Tryggvason and Aref<sup>133</sup> the equations of motion for the interface is independent of the surface-tension coefficient  $B$  if one instead uses the scaling given in equation (11.19). Therefore their numerical results may be taken to be valid for any surface tension ratio, and the important parameter is the viscosity ratio  $A$ .

In their calculations they choose to start with an interface consisting of an arbitrary collection of small-amplitude waves of various wavelengths. The surface tension was chosen such that the most unstable wavelength (according to linear stability theory) was about eight grid spacings. As seen from the second relation in equation (11.23) this is all that is needed in order to specify  $B$ . For the numerical results reproduced in the figures 11.7 to 11.9 the important control parameter is therefore the viscosity ratio  $A$ .

When the viscosity ratio  $A = 0$ , we still have a fingering instability as shown in figure 11.7. This fingering instability is driven by the density difference of the two fluids and from equations (11.14) and (11.15) it follows that for this case the critical wave length is  $\lambda_c = 2\pi(\sigma/\hat{g}(\rho_2 - \rho_1))^{1/2}$ . Therefore this instability occurs only if the upper fluid is denser than the lower fluid. The interface is very complex but has an up-down symmetry that is in fact apparent in the equations when  $A = 0$ . The fingers tend to become very thin and have rather small bubbles at the end. It is likely that some of these bubbles will eventually detach and propagate into the more viscous fluid. Such a detachment is not allowed by the program used by Tryggvason and Aref.<sup>4</sup>

As the viscosity ratio is increased one finds that the interface is less chaotic, and the driving low viscosity fluid penetrates more deeply into the high viscosity fluid. There is a slight tendency to splitting of the low viscosity fingers. On the other hand fingers tend to merge, and could possibly collapse to produce a reduced number of fingers with increasing time if such topology changes had been allowed by the algorithm used. The numerical results in figure 11.9 for  $A = 1$  have a striking resemblance to the experimental results shown in figure 11.3 and 11.5.

---

<sup>4</sup>There are papers by Kadanoff that claim that drops cannot detach in two-dimensional problems. I suggest that lattice gas simulations will allow detachment due to fluctuations.

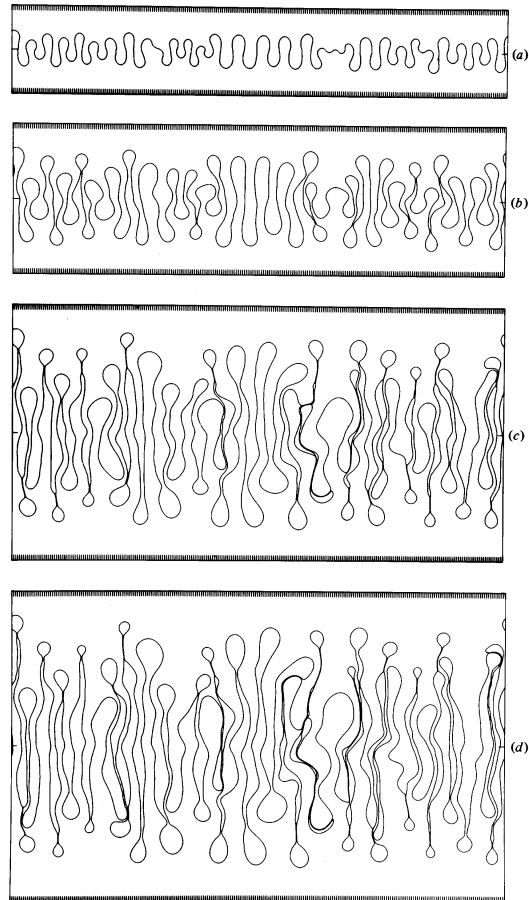


Figure 11.7: The evolution of the mixing layer with  $A = 0$  and  $B = 1.25 \cdot 10^{-5}$ . Note that this corresponds to gravity driven — not viscous fingering. Note the up-down symmetry. (Tryggvason and Aref 1983).

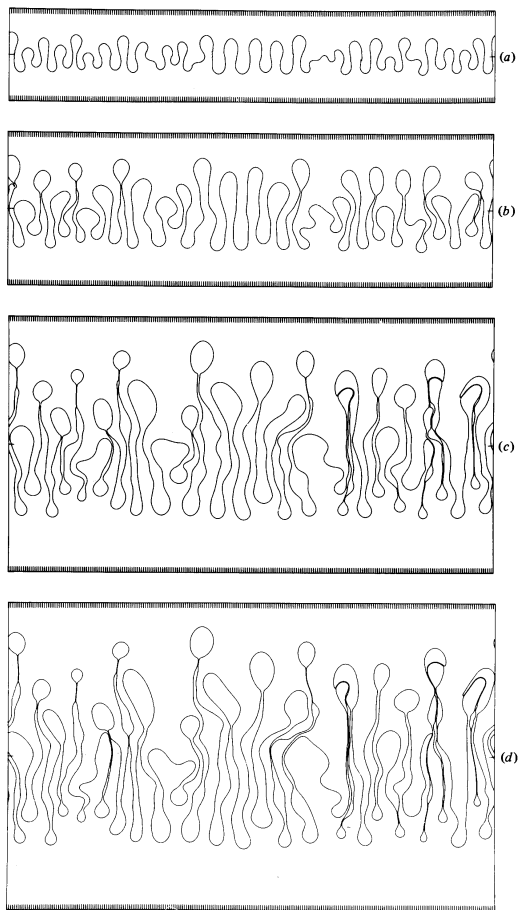


Figure 11.8: The evolution of viscous fingers with  $A = 0.5$  and with the same initial condition and value of  $B$  as in the previous figure. (Tryggvason and Aref 1983).

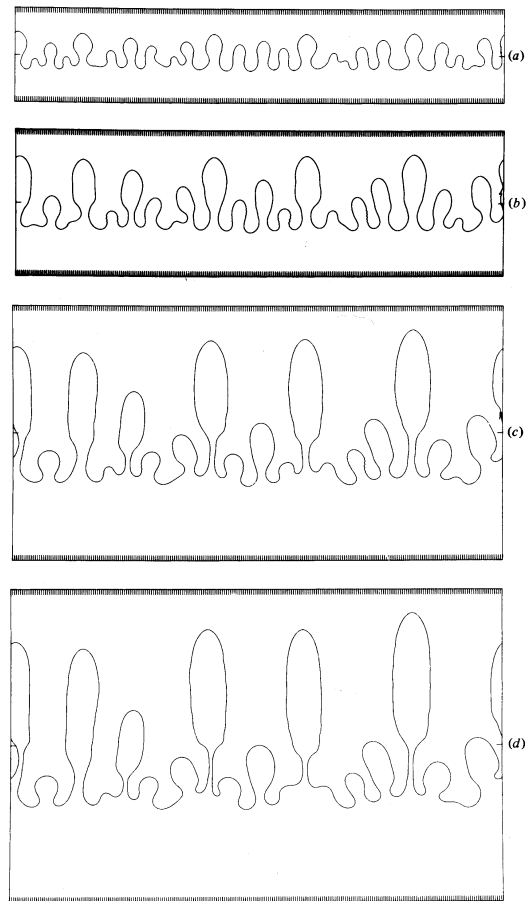


Figure 11.9: The evolution of viscous fingers with  $A = 1$  and with the same initial condition and value of  $B$  as in the previous two figures (Tryggvason and Aref 1983).

## 11.4 Experiments on Viscous Finger Dynamics

In a set of elegant experiments Maher<sup>136</sup> studied the evolution of viscous fingers as function of the viscosity ratio  $A$ . Maher used the unique features of the properties of binary mixtures at the near the critical unmixing temperature  $T_c$ . The binary mixture of isobutyric acid and water has at the critical composition a critical temperature  $T_c = 26.12^\circ C$  and separates into two immiscible phases one rich in water and one rich in isobutyric acid. At the critical temperature two phases can no longer be distinguished and therefore we have  $\rho_1 = \rho_2$ ,  $\mu_1 = \mu_2$  and  $\sigma = 0$ . In terms of the reduced temperature  $\epsilon = (T_c - T)/T_c$  the viscosity coefficient is  $A = 0.053\epsilon^\beta$  and the interface tension coefficient is  $B = 0.024\epsilon^{2\nu-\beta}$ . The critical exponents are  $\beta = 0.31$  and  $\nu = 0.61$ . Therefore, Maher obtained very small values of  $A$  by simply varying the temperature and thereby for the first time obtained viscous fingering results in this regime as shown in figure 11.10.

The observed fingering pattern (shown in figure 11.7) is similar to those obtained numerically by Tryggvason and Aref for  $A = 0$ . Also the expected variation of finger width  $\lambda_c$  with  $A$  and  $B$  was observed. Note again that the experimental results for  $A \sim 0$  correspond to a gravity driven system. In fact the results in figure 11.10 were obtained by inverting a small cell ( $45 \times 45 \times 1 mm$ ) which had come to equilibrium at a temperature slightly below  $T_c$ .

Maher also performed fingering experiments by displacing paraffin oil with water using  $A = 0.93$  and  $B = 8.3 \cdot 10^{-4}$ . His results are shown in figure 11.11.

Again the experimental results and the numerical results obtained by Tryggvason and Aref for  $A = 1$  see figure 11.9, are strikingly similar.

Maher in addition observed that the dimensionless length of the mixing region  $\theta' = \text{width}/\lambda_c$  depends on the dimensionless time  $t' = t/\tau$  as follows:

$$\theta' = (t')^a . \quad (11.24)$$

The observed exponent  $a = 1.6$  had some scatter but gave a good approximation for both the high and the low  $A$  values. The numerical results by Tryggvason and Aref for  $\theta'$  vs  $t'$  falls reasonably well on a power law with  $a = 1.85$  for  $A = 1$ . For  $A = 0$  their results give  $a \sim 1.85$  for  $t' < 25$  and then crosses over to  $a \sim 1.3$ . There is no theoretical prediction for the width of the mixing zone, and the result in equation (11.24) may not hold in detail. However, both theory and experiments on the Rayleigh-Benard

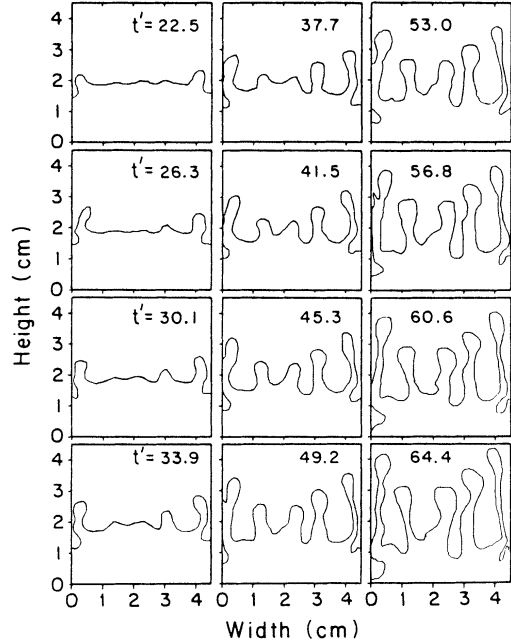


Figure 11.10: Time series of fingering patterns for isobutyric acid plus water.  $A = 0.015$ ,  $B = 6.6 \cdot 10^{-4}$ . The dimensionless time,  $t'$ , is indicated for each frame. (Maher 1985).

and on the Taylor instability have shown that the amplitudes of the instabilities grow with time in a power-law fashion similar to equation (11.24), and with  $a = 1.5$ .

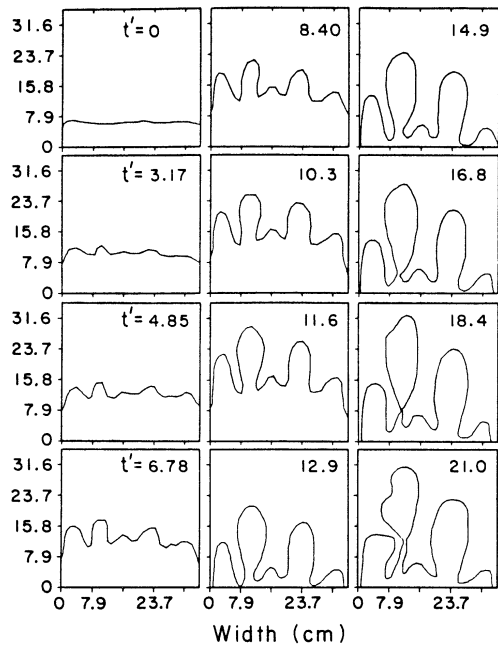


Figure 11.11: Time series of fingering patterns for paraffin oil plus water.  
 $A = 0.93$ ,  $B = 8.3 \cdot 10^{-4}$ .

## Chapter 12

# Multiphase Flow

The displacement of one fluid by another is of central interest in oil production, ground water management and in many industrial processes. From a scientific point of view the basic equations describing *multi-phase flow* in porous media are not known — it is difficult to understand that a problem of such importance technologically so far has been left almost exclusively to engineering. Current engineering practice in reservoir engineering concentrates on reservoir simulation based on an extension of Darcy's equation (6.8)

$$\mathbf{U} = -\frac{k}{\mu}(\nabla p - \rho \mathbf{g}), \quad (12.1)$$

to include two-phase flow. Darcy's equation has been well established both experimentally and theoretically as a good description of single phase flow through porous media of arbitrary geometry. It is the extension to multiphase flow that is in question, not the single phase flow case. There is a wealth of new phenomena that arise when two or more fluids flow simultaneously in porous media.

Consider a homogeneous porous medium with permeability  $k$  and porosity  $\phi$  saturated with a fluid (say oil) denoted by an index (o) so that its viscosity is denoted by  $\mu_o$ . Complicated displacement fronts form when another fluid (w), say water, with viscosity  $\mu_w$  is injected into the oil filled porous medium.

A slow injection of a non-wetting fluid<sup>1</sup> displacing a wetting fluid results in *invasion percolation*. Such a displacement process is called *drainage*

---

<sup>1</sup>For the sake of discussion assume that water does not wet the matrix whereas the resident oil does. In practice reservoirs are often water-wet, not oil-wet, or have 'mixed' wetting.

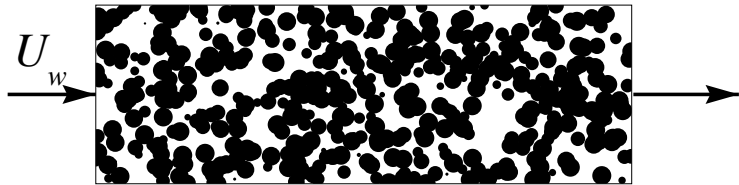


Figure 12.1: Water injected at a flux  $U_w$  flows in a porous sample in a steady state when no oil is produced, and the capillary interface is fixed on the pore level. The flow of water is then described by Darcy's equation but with a reduced permeability  $kk_w$ . (The figure shows a cross-section of a three-dimensional Poisson porous medium, which percolates in three dimensions but not in the cross-section).

in the petroleum literature. Invasion percolation is a process that leads to *fractal fronts*. If instead the displacement occurs at very high rates, and the invading phase has a much lower viscosity than the defending phase, one observes *fractal viscous fingering*. Fractal processes are generally modeled by *algorithmic models* not by differential equations and it is not known to what extent fractal displacement processes may be described by differential equations.

At first only the defending phase (o) is produced at the other end until the invading phase breaks through and both phases are produced. Finally one may reach a *steady state* where the original ‘defending’ oil phase is not moving any more and pores filled by oil remain fixed. Thus water (w) flows in an *effective porous medium* that does not have the full pore space available for flow. Thus the flow of water has a *filtration velocity* given by

$$\mathbf{U}_w = -k \frac{k_w}{\mu_w} \nabla p_w , \quad (12.2)$$

when gravity effects are ignored. Here  $k_w$  is the *relative permeability* of water. There are no problems with this formulation as long as there is no change of the oil-water interface geometry, that is, the process is truly stationary. The relative permeability depends on *saturation*

$$S = S_w = \frac{\text{water volume}}{\text{pore volume}} . \quad (12.3)$$

If all the oil is displaced so that  $S = 1$ , we expect  $k_w = 1$ . In the case that water cannot dislodge the oil we expect  $k_w = 0$  as long as  $S \leq S_{wc}$  where  $S_{wc}$  is the *percolation threshold* for water flow.

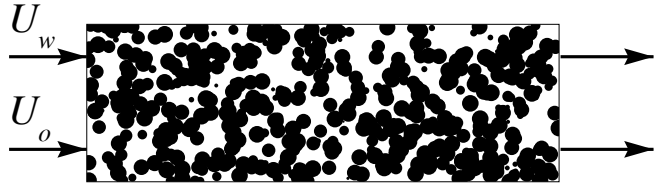


Figure 12.2: Water injected at a flux  $U_w$  and oil injected with a flux  $U_o$  flows in a porous sample in a steady state with the simultaneous production of oil and water. If the capillary interface is fixed on the pore level then both phase may be described by Darcy's equation but with a reduced permeabilities  $kk_w$  and  $kk_o$ , that may in addition depend on viscosities.

We may also consider the case where both oil and water are injected into the sample at fixed rates  $\mathbf{U}_w$  and  $\mathbf{U}_o$ , or at fixed pressure differences  $\Delta p_w$  and  $\Delta p_o$  across the sample, and a stationary state is reached in which both phases are produced at the other end and no changes occur at the pore level. Thus each of the phases see its flow constrained by a combination of the matrix and the pore space occupied by the other phase. Here we expect the following equations to apply:

$$\mathbf{U}_w = -k \frac{k_w}{\mu_w} \nabla p_w , \quad (12.4)$$

$$\mathbf{U}_o = -k \frac{k_o}{\mu_o} \nabla p_o . \quad (12.5)$$

I emphasize that the pressure in the oil,  $p_o$ , is not equal to the pressure in the water phase  $p_w$  and the difference is given by the *capillary pressure*. The wetting fluid tends to occupy the small pores whereas the non-wetting fluid tends to occupy the large pores. If there is no flow then the menisci between the two fluids must adjust so that the pressure difference is everywhere given by

$$p_c = (p_w - p_o) = \sigma \left( \frac{1}{R_1} + \frac{1}{R_2} \right) . \quad (12.6)$$

Here  $R_1$  and  $R_2$  are the principal radii of curvature,  $\sigma$  the interface tension. In practice contact-angle hysteresis and variable wetting properties prevents thermodynamic equilibrium to be reached, and a meta-stable equilibrium is reached in steady. When pressure gradients are applied fluid flow begins and the capillary equilibrium is shifted, pores become invaded and menisci adjust until eventually a new stationary state is reached. Since the pressures  $p_w$  and  $p_o$  now are functions of position we conclude that the

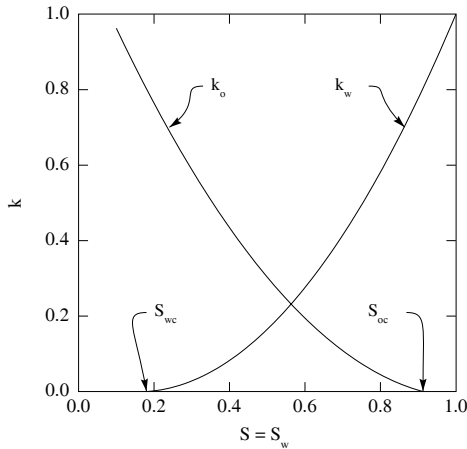


Figure 12.3: Effect of water saturation  $S = S_w$ , on the relative permeability to water  $k_w$  and oil  $k_o$  in unconsolidated sands (after Buckley and Leverett [1] figure 1). There is no permeability for water below the critical water saturation  $S_{wc} \approx 0.19$ , and there is no permeability to oil for water saturation above  $S_{oc} \approx 0.91$ , that is, for oil-saturation below the residual oil saturation  $S_{or} = 1 - S_{oc}$ .

Figure 12.3: Effect of water saturation  $S = S_w$ , on the relative permeability to water  $k_w$  and oil  $k_o$  in unconsolidated sands (after

capillary pressure is dependent on position as well. Both the relative permeabilities and the capillary pressure will depend on saturation  $S = S_w$ , and  $S_o = 1 - S$ .

The relative permeabilities as a function of (water) saturation,  $S_w$ , are usually plotted as in figure 12.3. The relative permeability plot has some general features. At the irreducible water saturation,  $S_{wc}$ , the permeability of water vanishes, only oil may flow, we may say that the water saturation is below the *percolation threshold* for water. For water saturations above the critical value  $S_{oc} = (1 - S_{or})$  oil is at its residual saturation  $S_{or}$ .

The relative permeabilities must be measured, and the measurement procedures completely specified since the measured relative permeabilities will depend on saturation *history*, that is, the permeability is not a function of saturation alone. For analytical purposes many forms for the relative permeability have been suggested and fit to experimental observations. The relative permeabilities can be measured by steady state experiments similar to what was just described. Many methods are used in engineering prac-

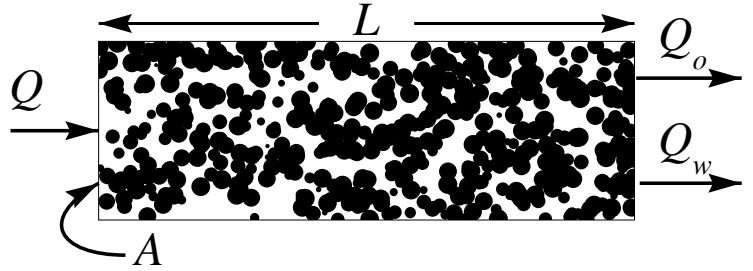


Figure 12.4: One-dimensional flow in a porous medium with cross section  $A$  and length  $L$ . Water (w) is injected with a flow rate  $Q$  and displaces oil (o) from the reservoir rock.

tice in order to measure relative permeabilities, or to estimate them from empirical formulae (see reference [ ]). As an example consider the equations obtained by Corey<sup>138, 139</sup> for drainage oil and gas relative permeabilities, that is, for the displacement of oil by gas,

$$k_o = (S_{oe})^4, \quad (12.7)$$

$$k_g = (1 - S_{oe})^2 \times (1 - S_{oe}^2), \quad (12.8)$$

$$S_{oe} = (S_o - S_{or})/(1 - S_{or}). \quad (12.9)$$

Here  $S_{or} = S_{oc}$  is the *residual oil saturation*, that is, the percolation threshold for the flow of oil.

## 12.1 Buckley-Leverett Displacement

Buckley and Leverett start their famous paper<sup>137</sup> ‘Crude oil has no inherent ability to expel itself from the pores of the reservoir rocks in which it is found; rather, it must be forcibly ejected or displaced by the accumulation of other fluids.’ They introduced as simple one-dimensional solution to the flow equations (12.4) and (12.5) in which the displacement process leads to a sharp shock front. With the generalized Darcy equations (12.4) and (12.5) we may attempt to use them also outside the stationary regime. For this purpose we need mass balance equations that track the changes in saturation. In figure 12.4 we sketch a one-dimensional displacement

process.

$$U_w = Q_w/A = -k \frac{k_w}{\mu_w} \nabla p_w , \quad (12.10)$$

$$U_o = Q_o/A = -k \frac{k_o}{\mu_o} \nabla p_o , \quad (12.11)$$

$$S_w + S_o = 1 . \quad (12.12)$$

The continuity equations for the two fluids may be written

$$\begin{aligned} \phi A \frac{\partial S_w}{\partial t} + \frac{\partial Q_w}{\partial x} &= 0 , \\ \phi A \frac{\partial S_o}{\partial t} + \frac{\partial Q_o}{\partial x} &= 0 . \end{aligned} \quad (12.13)$$

We also need the capillary pressure equation with  $S = S_w$

$$p_c(S) = p_w - p_o . \quad (12.14)$$

Here we treat only the simplest case where we assume  $p_c(S)$  to be independent of position:

$$\frac{\partial p_c(S)}{\partial x} = 0 . \quad (12.15)$$

The continuity equations may be combined to note that the total flow  $Q = Q_w + Q_o$  is independent of position.

We may introduce *fractional flows* as follows:

$$\begin{aligned} f_w &= Q_w/Q , \\ f_o &= Q_o/Q = 1 - f_w . \end{aligned} \quad (12.16)$$

Using these expressions with equations (12.10)–(12.12) we find

$$f_w = \frac{-k \frac{k_w}{\mu_w} \frac{\partial p_w}{\partial x}}{-k \frac{k_w}{\mu_w} \frac{\partial p_w}{\partial x} - k \frac{k_o}{\mu_o} \frac{\partial p_o}{\partial x}} . \quad (12.17)$$

But from equations (12.14) and (12.15) it follows that  $\frac{\partial p_w}{\partial x} = \frac{\partial p_o}{\partial x}$  and therefore we may write the fractional flow as:

$$f = f_w = \frac{Q_w}{Q_w + Q_o} = \frac{1}{1 + \frac{k_o}{k_w} \frac{\mu_w}{\mu_o}} . \quad (12.18)$$

The fractional flow  $f = f_w$  is then given by equation (12.13) (see Buckley and Leverett's<sup>137</sup> equation (1))

$$\phi A \frac{\partial S}{\partial t} + Q \frac{\partial f}{\partial x} = 0 . \quad (12.19)$$

Here we consider  $f$  to be a *given* known function of  $S$ , and we intend to find the saturation  $S(x, t)$  as a function of position and time. We note that

$$\frac{\partial f(S)}{\partial x} = \left( \frac{df}{dS} \right) \frac{\partial S}{\partial x} . \quad (12.20)$$

The ‘piston flow velocity’

$$U_0 = \frac{Q}{\phi A} , \quad (12.21)$$

is the velocity expected if there is no smearing of the front, that is, the invading fluid displaces the defending fluid without any mixing in a purely one-dimensional displacement process. With this notation we arrive at the *Buckley-Leverett equation*

$$\boxed{\frac{\partial S}{\partial t} + U(S) \frac{\partial S}{\partial x} = 0} \quad (12.22)$$

where the front velocity at saturation  $S$  is:

$$\boxed{U(S) = U_0 \left( \frac{df}{dS} \right)} \quad (12.23)$$

is the velocity at a given saturation level  $S$ . Figure 12.5 shows the fractional flow and  $df/dS$  as a function of saturation for a case discussed by Buckley and Leverett<sup>137</sup> where  $\mu_o/\mu_w = 2$

From the equation (12.23) it is possible to propagate an initial saturation profile  $S(x, t_0)$  to a new profile  $S(x, t + \Delta t)$  using the expression

$$\Delta x = \frac{Q \Delta t}{\phi A} \frac{df(S)}{dS} . \quad (12.24)$$

As shown in figure 12.6 the initial saturation is propagated to form an unstable distribution in which  $S(x)$  becomes multiple valued. This ambiguity is resolved by insisting on the mass balance

$$Q \Delta t / \phi A = \int_0^{x_f} dx \{ S(x, t_0 + \Delta t) - S(x, t_0) \} . \quad (12.25)$$

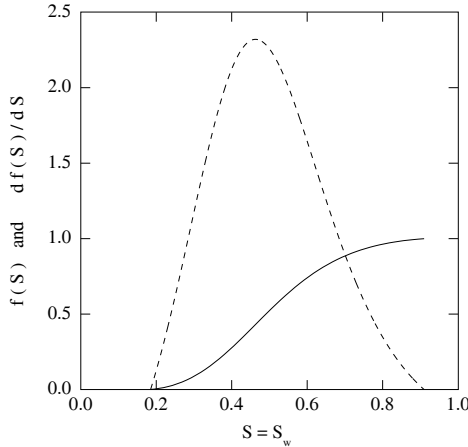


Figure 12.5: Effect of water saturation  $S = S_w$ , on the fractional flow  $f = f_w$  (full line) and the Buckley-Leverett front velocity  $U(S)/U_0 = df/dS$  (dashed line). The curves were calculated on the basis of the relative permeability curves shown in figure 12.3 (after Buckley and Leverett [figure 1] with  $\mu_o/\mu_w = 2$ .

Figure 12.5: Effect of water saturation  $S = S_w$ , on the fractional flow  $f = f_w$  (full line) and the Buckley-Leverett front velocity

And a shock front arises at  $x_f$ . Of course, one may solve the differential equation (12.19) numerically, also including capillary effects and gravity, but the Buckley-Leverett shock survives in general and the strong saturation gradients really indicate that the generalized Darcy equations are inadequate.

## 12.2 Two-Phase Flow in a Capillary

The flow of two fluids in a capillary may be found exactly if one fluid (2) wets the wall and the other fluid (1) forms a cylindrical region concentric with the tube axis. This geometry represents an unstable situation since surface tension will tend to break up the cylindrical fluid (1) into drops.<sup>2</sup>

<sup>2</sup>The surface free-energy per unit length of the cylindrical interface between the two fluids is  $A_{\text{cyl}} = 2\pi R$ . The same volume  $i$  converted into drops, of maximal radius  $a$  has an area  $A_{\text{drop}} = 2\pi(R/a)^2/a$ . Therefore we have  $\sigma A_{\text{cyl}}/\sigma A_{\text{drop}} = (3/2)(R/a) < 1$  if  $R < 2a/3$ . Thus the cylindrical arrangement is unstable with respect to the formation of droplets. This instability is driven by the surface tension. Even in the case,  $2/3 < R < 1$ ,

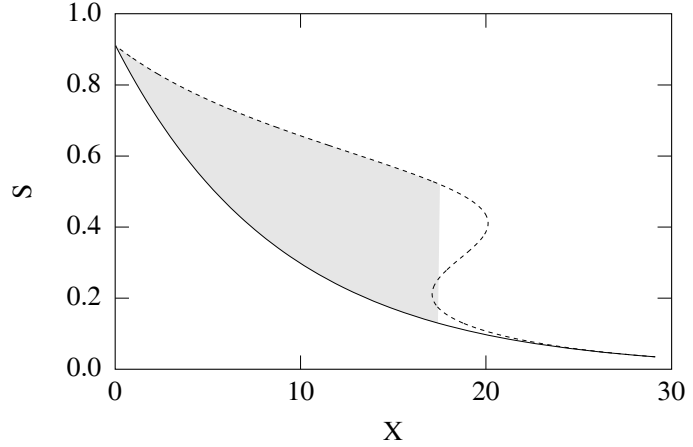


Figure 12.6: The initial water saturation  $S(x, t_0)$  as a function of position (full line). After a time step  $\Delta t$  such that  $Q\Delta t/\phi A = 5$  the saturation profile (dashed curve) is propagated by equation (12.23) to the unstable profile (dashed curve). Mass balance limits the profile (shaded region), and a shock front at  $x_f$  results.

However, the simple cylindrical geometry permits us to solve the Stokes equations for the flow exactly<sup>3</sup> and the simple solution allows us to illustrate some general aspects of two-phase flow. We find that the equations for this simple two-phase flow is *not* consistent with the generalized Darcy equations (12.4) and (12.5).

Consider two-phase fluid flow through a pipe of radius  $a$ . Fluid (1), with viscosity  $\mu_1$ , is assumed to occupy the region  $0 < r < R$  and the other fluid (2), with viscosity  $\mu_2$ , occupies the region  $R < r < a$ . Find the velocities and flow rates of fluid (1) and (2). We will write the results in terms of the *saturation* of phase (1)  $S = S_1$  where

$$S = (R/a)^2. \quad (12.26)$$

The pressure in the two fluids may be different and the capillary pressure,

---

we find that the cylindrical geometry may reduce its surface free-energy, by creating droplets that have a cylindrical shape of radius  $a$ , with spherical end-caps, that will conserve volume (per unit length) and decrease the interface area per unit length.

<sup>3</sup>In fact the stationary solution of the Stokes equation is also a solution of the Navier-Stokes equation for flow that is cylindrically symmetric, because the  $\mathbf{u} \cdot \nabla \mathbf{u} = 0$  in that case.

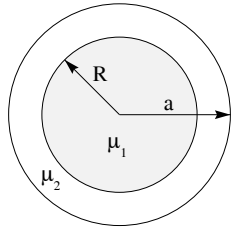


Figure 12.7: Two-fluid flow in a capillary. The fluid (1) occupies a cylindrical region of radius  $r \leq a$ .

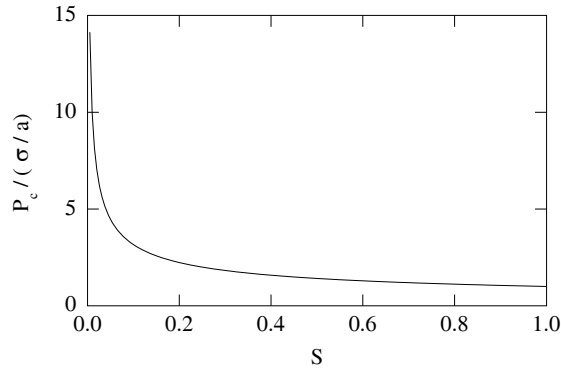


Figure 12.8: The capillary pressure,  $P_c$ , as a function of saturation,  $S$ , for two-phase flow in a capillary.

that is, the difference in pressure between the concave and the convex sides of the interface, is given by

$$p_c = (p_1 - p_2) = \sigma/R = \frac{\sigma}{a\sqrt{S}} , \quad (12.27)$$

Here the radius of curvature along the capillary is infinite and does not contribute to the capillary pressure. The capillary pressure for this system is shown in figure 12.8.

Each fluid must satisfy equation (4.25) for each fluid independently:

$$\mu_1 \frac{\partial}{\partial r} \left( r \frac{\partial u_1}{\partial r} \right) = r \frac{\partial p_1}{\partial x} \quad 0 < r < R \quad (12.28)$$

$$\mu_2 \frac{\partial}{\partial r} \left( r \frac{\partial u_2}{\partial r} \right) = r \frac{\partial p_2}{\partial x} \quad R < r < a \quad (12.29)$$

The solution have the form (see equation (4.26)):

$$u_1(r) = A_1(a^2 - r^2) + C_1, \quad 0 < r \leq R \quad (12.30)$$

$$u_2(r) = A_2(a^2 - r^2) + B_2 \ln r + C_2, \quad R < r \leq a \quad (12.31)$$

Substitution of equations (12.30) and (12.31) in equations (12.28) and (12.29) determines the amplitudes:

$$A_1 = \frac{1}{4\mu_1} G_1, \quad A_2 = \frac{1}{4\mu_2} G_2, \quad (12.32)$$

where we have introduced the gradients  $G_i = -(\partial p_i / \partial x)$ . pressure gradient

The boundary conditions determine the other constants:

(1)–The velocity must vanish at the tube wall:  $u_2(a) = 0$ :

$$u_2(a) = B_2 \ln a + C_2 = 0 \implies C_2 = -B_2 \ln a, \quad (12.33)$$

(2)–The velocity of the two fluids must be equal at  $r = R$ :  $u_1(R) = u_2(R)$ , which gives (using equation (12.33)):

$$\begin{aligned} A_1(a^2 - R^2) + C_1 &= A_2(a^2 - R^2) + B_2 \ln R + C_2 \\ &= A_2(a^2 - R^2) + B_2 \ln(R/a), \end{aligned} \quad (12.34)$$

and we obtain an expression for  $C_1$ :

$$C_1 = -(A_1 - A_2)(a^2 - R^2) + B_2 \ln(R/a). \quad (12.35)$$

(3)–The shear stress is continuous across interface:

$$\mu_1 \left( \frac{\partial u_1}{\partial r} \right) \Big|_R = \mu_2 \left( \frac{\partial u_2}{\partial r} \right) \Big|_R, \quad (12.36)$$

otherwise a volume element that contains the interface would rotate. Using equations (12.28) and (12.29) we find

$$B_2 = -2 \left( \frac{\mu_1}{\mu_2} A_1 - A_2 \right) R^2. \quad (12.37)$$

This result may be used with equation (12.35) to find

$$C_1 = -(A_1 - A_2)(a^2 - R^2) - 2 \left( \frac{\mu_1}{\mu_2} A_1 - A_2 \right) R^2 \ln(R/a). \quad (12.38)$$

Collecting the results for the constants we may write the solution

$$\begin{aligned} u_1 &= A_1(a^2 - r^2) - (A_1 - A_2)(a^2 - R^2) \\ &\quad - 2 \left( \frac{\mu_1}{\mu_2} A_1 - A_2 \right) R^2 \ln(R/a), \quad 0 < r \leq R \\ u_2 &= A_2(a^2 - r^2) - 2 \left( \frac{\mu_1}{\mu_2} A_1 - A_2 \right) R^2 \ln(r/a), \quad R < r \leq a \end{aligned} \quad (12.39)$$

The flow of each fluid may be found by integrating the expression

$$Q_i = \int_0^{2\pi} \int_0^a r dr d\varphi u_i(r), \quad (12.40)$$

to give

$$\begin{aligned} Q_1 &= \frac{1}{2} \pi a^4 A_1 \{S^2 - 2(\mu_1/\mu_2)^2 S^2 \ln S\} \\ &\quad + \frac{1}{2} \pi a^4 A_2 \{2S - 2S^2 + 2S^2 \ln S\} \end{aligned} \quad (12.41)$$

$$\begin{aligned} Q_2 &= \frac{1}{2} \pi a^4 A_1 (\mu_1/\mu_2) \{2S + 2S^2 \ln S - 2S^2\} \\ &\quad + \frac{1}{2} \pi a^4 A_2 \{1 - 4S + 3S^2 - 2S^2 \ln S\} \end{aligned} \quad (12.42)$$

In terms of the average flow velocities (Darcy velocity):  $U_i = Q_i/\pi a^2$  and with the *permeability*  $k = a^2/8$  we find that the generalization of the Darcy equation for two fluid flow for this case has the form:

$$U_1 = -k \frac{k_{11}}{\mu_1} \frac{\partial p_1}{\partial x} - k \frac{k_{12}}{\mu_2} \frac{\partial p_2}{\partial x} \quad (12.43)$$

$$U_2 = -k \frac{k_{21}}{\mu_2} \frac{\partial p_1}{\partial x} - k \frac{k_{22}}{\mu_2} \frac{\partial p_2}{\partial x} \quad (12.44)$$

Where we have introduced the symmetric *relative permeability matrix*:

$$\begin{aligned} k_{11} &= S^2 - (\mu_1/\mu_2) S^2 \ln S^2 \\ k_{12} &= 2S - 2S^2 + S^2 \ln S^2 \\ k_{21} &= 2S - 2S^2 + S^2 \ln S^2 \\ k_{22} &= 1 - 4S + 3S^2 - S^2 \ln S^2 \end{aligned} \quad . \quad (12.45)$$

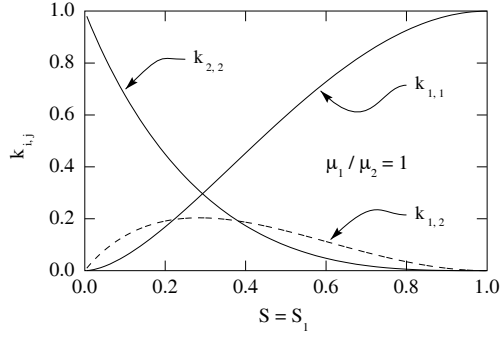


Figure 12.9: The relative permeabilities  $k_{11}$ ,  $k_{22}$  and the cross-term permeability  $k_{12}$  as a function of saturation  $S = S_1$  for  $\mu_1/\mu_2 = 1$ .

The cross-terms  $k_{12} = k_{21}$  represent the viscous coupling between the fluids. Such cross-terms have been observed in experiments on porous rocks<sup>140</sup> and in lattice gas simulations<sup>141, 142</sup> for two phase flow in porous media. We see that equations (12.41) and (12.42) with our expression for  $k_{ij}$  give  $U = U_1 + U_2 = -(k/\mu)(\partial p/\partial x)$  for  $\mu_1 = \mu_2 = \mu$ , that is, we recover Darcy's law for the total flow, when the two fluids have the same viscosity. Note that the cross terms both have  $1/\mu_2$  factor in equations (12.43) and (12.44). I chose this form because then  $k_{12} = k_{21}$  do not contain any viscosities, and exhibit the general symmetry required from the theory of irreversible processes.

The general form of transport equations in nonequilibrium statistical physics is<sup>120</sup>

$$J_i = \sum_j L_{ij} X_j . \quad (12.46)$$

Here  $X_i$  are the *generalized force* (given by  $X_i = -(\partial p_i / \partial x)$  in the present case),  $J_i$  are the *currents* ( $J_i = U_i$  here) and  $L_{ij}$  are the transport coefficients given by

$$L_{11} = k k_{11} / \mu_1 , \quad L_{12} = L_{21} = k k_{12} / \mu_2 , \quad L_{22} = k k_{22} / \mu_2 . \quad (12.47)$$

The general *Onsager relations* for the transport coefficients

$$\boxed{L_{ij} = L_{ji}} \quad \text{Onsager} \quad (12.48)$$

are satisfied for the flow equations (12.43) and (12.44) in the example discussed here.

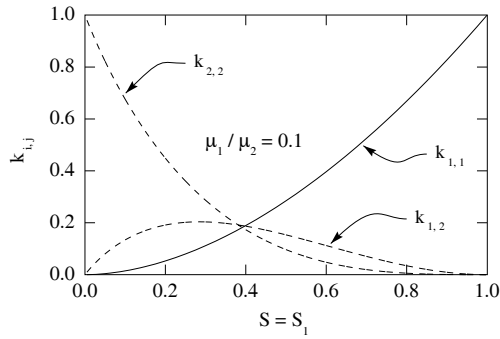


Figure 12.10: The relative permeabilities  $k_{1,1}$ ,  $k_{2,2}$  and the cross-term permeability  $k_{1,2}$  as a function of saturation  $S = S_1$  for  $\mu_1/\mu_2 = 0.1$ .

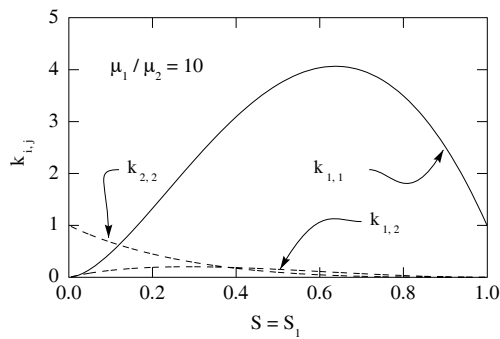


Figure 12.11: The relative permeabilities  $k_{11}$ ,  $k_{22}$  and the cross-term permeability  $k_{12}$  as a function of saturation  $S = S_1$  for  $\mu_1/\mu_2 = 10$ .

We find that the cross-term permeability for  $\mu_1/\mu_2 = 1$  is of the same order of magnitude as the relative permeabilities themselves (see figure 12.9). In this case we have a maximum  $k_{12} = 0.204$  for  $S = 0.285$ ; at this saturation we have  $k_{11} = 0.285$  and  $K_{22} = 0.308$ .

In the situation that  $\mu_1/\mu_2 < 1$ , that is, the viscosity of the fluid in the core is less than that of the fluid near the wall, we find that the relative permeabilities do not change much from the situation discussed above. In figure 12.10 we have illustrated the case  $\mu_1/\mu_2 = 0.1$ , which shows that the cross-term permeability is more important in this situation. Another

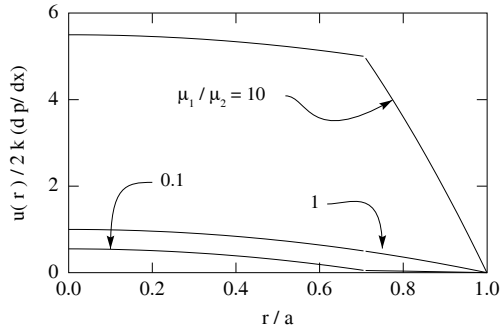


Figure 12.12: The velocity as a function of radius as a saturation of  $S = 0.5$  for several values of the viscosity ratio for the situation where  $dp_1/dx = dp_2/dx$ .

feature of this situation is that  $k_{11} \sim (1 - S)$  for  $S \rightarrow 1$ . The  $S^2 \ln S^2$  term in  $k_{11}$  disappears in the limit  $\mu_1/\mu_2 \rightarrow 0$  and we find the behavior similar to what is shown in figure 12.10.

The relative permeability curves change drastically when  $\mu_1 \gg \mu_2$  (I illustrate the case  $\mu_1/\mu_2 = 10$  in figure 12.11). In this limit the low-viscosity fluid near the wall ‘lubricates’ the flow of the high-viscosity fluid in the center of the capillary. The effect is that  $k_{11}$  becomes much larger than one, that is, a small gradient in  $p_1$  will give a much larger current than would be expected without lubrication.

In figure 12.12 I show the velocity as a function of radial position for  $S = 0.5$  at various viscosity ratios, in the situation where the gradients  $dp_i/dx$  in both phases are identical. The effect of lubrication is evident for  $\mu_1/\mu_2 = 10$ .

# Appendix A

## Thermodynamics

Here I summarize the basic thermodynamic concepts needed to discuss the thermodynamics of diffusion, capillarity and other systems of physical interest. Landau and Lifshits' *Statistical Physics book*<sup>120</sup> is a very concise and useful reference that I have used as a starting point for the following discussion.

### A.1 Entropy

Entropy is a fundamental concept in thermodynamics that can best be understood in terms of statistical mechanics. One may say that entropy is a measure of disorder. Consider a system that can be in a (large) number of possible states  $| i \rangle$ , that may be either classical states or quantum states of the system. The index  $i$ , may be thought of as a label of the energy of the system. The *entropy* of such a system is

$$S = -k_B \sum_i p_i \ln p_i = -k_B \langle \ln p_i \rangle \quad (\text{A.1})$$

Here  $p_i$  is the probability to find the system in the state  $| i \rangle$ , and  $k_B$  is the Boltzmann constant. The probabilities must be *normalized*:

$$\sum_i p_i = 1 . \quad (\text{A.2})$$

For a *large* system consisting of many particles, that is, a system that has many degrees of freedom, one finds for a given energy  $E$  that there is huge

number,  $W$ , of equally likely (quantum) states available for the system. The number of available states is called the statistical weight for the closed system. Formally we have  $p_i = 1/W$ , and we can write the entropy as:

$$S = k_B \ln W \quad \text{Boltzmann's entropy} \quad (\text{A.3})$$

The *entropy*  $S(E, V)$  of a *closed system*<sup>1</sup> depends on its energy  $E$  and volume  $V$  when the system is at equilibrium.

A closed system *not* in equilibrium will change with time in such a way that the entropy  $S$  increases with time until it reaches its maximum value in *thermal equilibrium*. This is often called the second law of thermodynamics (Clausius (1865)).

The entropy depends only on macroscopic variables, such as the volume, that constrain the system.

## A.2 Information

The definition of entropy in equation (A.1), is directly related to the definition of the information measure. As an example consider the probability distribution for the number of ‘eyes’ that come up when throwing a fair die. The probabilities of the six possible states  $|1\rangle, |2\rangle, \dots, |6\rangle$  are  $p_i$ , with  $i = 1, \dots, 6$ . Small variations  $\delta p_i$ , lead to a variation in  $S$  as defined in (A.1). The maximal value of  $S$  may be found, taking into account the constraint (A.2), using a *Lagrange parameter*  $k_B\lambda$ :

$$\begin{aligned} 0 &= \delta(S - k_B\lambda \cdot 1) = \delta \left( -\sum_{i=1}^6 k_B p_i \ln p_i - k_B \lambda \sum_{i=1}^6 p_i \right) \\ &= -k_B \sum_{i=1}^6 \left( \ln p_i + \frac{p_i}{p_i} + \lambda \right) \delta p_i \\ &\Rightarrow p_i = \exp(-1 - \lambda) \Rightarrow p_i = \frac{1}{6}. \end{aligned} \quad (\text{A.4})$$

Here we have chosen  $\lambda$  so that  $p_i$  satisfies equation (A.2). We see that requiring the information entropy to have its maximum value leads to the result that  $p_i = 1/6$ , independent of  $i$ —as expected for fair dice.

When we throw two dice, we have many more possibilities. As before, the ‘first’ die has the possible states  $\{|i\rangle\}$ , with  $i = 1, \dots, 6$ . The other die

---

<sup>1</sup>that is, an isolated system that cannot exchange work, heat or particles with its surroundings

has the states  $\{|j\rangle\}$  with  $j = 1, \dots, 6$ , of course. Counting the eyes for the pair of dice we have 36 possible outcomes  $\{|\alpha\rangle\}$ , with  $\alpha = 1, \dots, 36$  corresponding to the states  $|11\rangle, |12\rangle, \dots, |66\rangle$ . With the argument developed above we will find that  $p_\alpha = 1/36$ . It is important to note, however, that the statistical independence of the two dice allows another approach.

The states  $|\alpha\rangle = |i\rangle|j\rangle$  are in a product space of the two independent states  $|i\rangle$  and  $|j\rangle$ , much in the same way that the position of a point in the plane  $\mathbf{r} = (x, y)$ , is given in terms of the independent coordinates  $x$  and  $y$ ; or with our notation  $|\mathbf{r}\rangle = |x\rangle|y\rangle$ . The process of throwing the dice yields eyes that are statistically independent, and the probability,  $p_{ij}$ , that the first die has  $i$  eyes and the second has  $j$  eyes is the product of the probability  $p_i$  for the first die to show  $i$  eyes and  $p_j$ , which is the probability that the second die shows  $j$  eyes:

$$p_\alpha = p_{ij} = p_i p_j \quad \text{statistically independent} \quad (\text{A.5})$$

It follows that the entropy of the combined system may be written

$$\begin{aligned} S &= -k_B \sum_{ij} p_{ij} \ln p_{ij} = -k_B \sum_{ij} p_i p_j \ln p_i p_j \\ &= -k_B \sum_i p_i \ln p_i \sum_j p_j + -k_B \sum_j p_j \ln p_j \sum_i p_i \\ &= S_1 + S_2, \end{aligned} \quad (\text{A.6})$$

where we have used that probabilities are normalized:  $\sum_i p_i = \sum_j p_j = 1$ . We conclude that the (information) entropy of a system consisting of statistically independent parts is the sum of the entropies of the parts. Entropy is an extensive property, that is, entropy is proportional to system size.

### A.2.1 The Gibbs Distribution

The method used above may be extended to situations where there is more information available about the system. A typical problem in statistical physics is to determine the entropy for a system that has a given volume,  $V$ , and energy,  $E$ . For such a system with a *Hamiltonian*  $H$ , there are *energy eigenstates*  $|i\rangle$  that satisfies the Heisenberg equation

$$H|i\rangle = \varepsilon_i|i\rangle, \quad (\text{A.7})$$

where  $\varepsilon_i$ , is the energy of the eigen-state  $|i\rangle$ . Now if the system is in that state with probability  $p_i$ , then the energy of the system, or rather the

expectation value,  $\langle H \rangle$  of the Hamiltonian, is

$$E = \langle H \rangle = \sum_i \varepsilon_i p_i = \langle \varepsilon_i \rangle \quad (\text{A.8})$$

Here the sum is over all possible states. This expression is also valid for classical systems if one accepts the notation  $| i \rangle$ , to be used also for the continuum case with the sum being replaced by integrals over the coordinates specifying the state of the classical system in phase space.

At equilibrium the entropy has its maximum value consistent with the constraints on the system. As before we handle the constraints using the method of Lagrange multipliers. The constraint that the distribution must be normalized (A.2), has an associated (conjugate) Lagrange parameter  $k_B\lambda$ , whereas the constraint that the energy is given has the conjugate Lagrange parameter  $k_B\beta$ . With arbitrary variations  $\delta p_i$ , in the probabilities  $p_i$ , we require

$$\begin{aligned} 0 &= \delta \left( - \sum_i k_B p_i \ln p_i - k_B \lambda \sum_i p_i - k_B \beta \sum_i \varepsilon_i p_i \right) \\ &= -k_B \sum_i (\ln p_i + 1 + \lambda + \beta \varepsilon_i) \delta p_i \end{aligned} \quad (\text{A.9})$$

The expression within the parenthesis must vanish since the variations in  $\delta p_i$  are arbitrary, and as a result we find the *Gibbs distribution*

$$p_i = \frac{\exp(-\beta \varepsilon_i)}{\sum_i \exp(-\beta \varepsilon_i)} \quad (\text{A.10})$$

Here we have already determined the Lagrange parameter  $\lambda$  so that the distribution is normalized.

This is one of the most important formulas in statistical physics. Much of the work in this course is related with the use and understanding of this formula.

The remaining Lagrange parameter,  $\beta$ , can be found by inserting  $p_i$  in to the expression for the energy equation (A.8), and solving that equation for  $\beta$  as a function of  $E$ . This procedure can be followed only in the simplest of cases. However, as we shall see later, the Lagrange parameter  $\beta$  conjugate to the energy is in fact given by

$$\beta = \frac{1}{k_B T} \quad (\text{A.11})$$

The denominator in equation (A.9) is the *partition function*  $Z$  that plays a central role in statistical physics since all thermodynamic quantities may be calculated once  $Z$  is known. The partition function is given by

$$Z = \sum_i \exp(-\beta \varepsilon_i) \quad \text{partition function} \quad (\text{A.12})$$

## A.3 Temperature

Consider two systems (1) and (2), in thermal contact with each other but *insulated* from the surroundings, that is, they form a closed system. Both the entropy of the total system,  $S = S_1(E_1) + S_2(E_2)$ , and the energy,  $E = E_1 + E_2$ , are sum of their parts. The energy of a closed system is fixed and a small energy exchange between the two sub-systems must have the form  $\delta E_2 = -\delta E_1$ , therefore the change in entropy for the closed system may be written

$$\begin{aligned} \frac{dS}{dE_1} &= \frac{dS_1}{dE_1} + \frac{dS_2}{dE_2} \frac{dE_2}{dE_1} \\ &= \frac{dS_1}{dE_1} - \frac{dS_2}{dE_2} = 0. \end{aligned} \quad (\text{A.13})$$

It follows that  $dS_1/dE_1 = dS_2/dE_2$  for  $S$  to have its maximal value at fixed  $E$  and  $V$ .

The previous argument may be generalized to a system consisting of many parts. At equilibrium one concludes that  $dS/dE$  has the same value everywhere. Therefore one finds that *absolute temperature*  $T$ , defined as the change in the (equilibrium) entropy with energy

$$\frac{1}{T} = \left( \frac{\partial S}{\partial E} \right)_V \quad (\text{A.14})$$

is independent of position for a system in thermal equilibrium; it is also the same for two systems in equilibrium with each other, for example for a liquid in equilibrium with its vapor. In equation (A.14) we have explicitly written that the change is to take place at a fixed volume. Volume changes are discussed in the section A.4. For the closed system we may also consider the energy as a function of entropy  $E(S)$ , and equation (A.14) may therefore also be written as

$$T = \left( \frac{\partial E}{\partial S} \right)_V \quad (\text{A.15})$$

### A.3.1 Temperature in the Gibbs Distribution

We are now in the position that we may check the expression (A.11). We first note that  $\beta$  is a function of energy,  $E$ , for a given volume  $V$  and that the energy is given in terms of the distribution  $p_i$  by

$$E = \sum_i \varepsilon_i p_i = \sum_i \varepsilon_i Z^{-1} e^{-\beta \varepsilon_i} = - \left( \frac{\partial \ln Z}{\partial \beta} \right)_V . \quad (\text{A.16})$$

The equilibrium entropy may be expressed as

$$S(V, E) = -k_B \sum_i p_i \ln p_i = k_B \sum_i \beta \varepsilon_i p_i + k_B \sum_i p_i \ln Z . \quad (\text{A.17})$$

We note that  $\ln Z$  is independent of  $i$ , so we take it outside the sum. The probabilities are normalized, therefore we may write entropy as a function of volume and energy as follows:

$$S(V, E) = k_B \beta E + k_B \ln Z . \quad (\text{A.18})$$

with  $\beta = \beta(V, E)$ . Let us now use the formal expression for temperature given in equation (A.14)

$$\frac{1}{T} = \left( \frac{\partial S}{\partial E} \right)_V = k_B \beta + k_B E \left( \frac{\partial \beta}{\partial E} \right)_V + k_B \left( \frac{\partial \ln Z}{\partial \beta} \right)_V \left( \frac{\partial \beta}{\partial E} \right)_V = k_B \beta . \quad (\text{A.19})$$

Here we have used equation (A.16). We have therefore reached the conclusion that  $\beta = 1/k_B T$  in as announced by equation (A.11).

## A.4 Pressure

Following Landau and Lifshits we note that both the entropy and the energy are additive quantities, that is, they are proportional to system size, and therefore do not depend on the *shape* for systems in thermal equilibrium. We may consider the entropy to be a function of energy  $S(E)$ , or equivalently the energy to be a function of the entropy  $E(S)$ , for the closed system, that is, we have no external system or medium.

Now, consider a process in which the wall of the container moves slowly enough for the system to stay in internal thermal equilibrium. A force  $\mathbf{F}$  acts from the contents of the system on the container wall surface element,  $\delta \mathbf{s}$ . If the container wall moves a small distance,  $\delta \mathbf{r}$ , then work is done

on the surroundings given by  $\delta\mathcal{R} = \mathbf{F}\cdot\delta\mathbf{r}$ . But this work must equal the decrease  $\delta E$  in energy of the system

$$\delta E = -\mathbf{F}\cdot\delta\mathbf{r}. \quad (\text{A.20})$$

The change in volume in this process is  $\delta V = \delta\mathbf{s}\cdot\delta\mathbf{r}$ , and it follows that

$$\delta E = \left(\frac{\partial E}{\partial V}\right)_S \delta V = \left(\frac{\partial E}{\partial V}\right)_S \delta\mathbf{s}\cdot\delta\mathbf{r}. \quad (\text{A.21})$$

Since the displacement  $\delta\mathbf{r}$  is arbitrary, it follows from equations (A.20) and (A.21) that

$$\mathbf{F} = -\left(\frac{\partial E}{\partial V}\right)_S \delta\mathbf{s}. \quad (\text{A.22})$$

The force is perpendicular to the surface element and proportional to its area. Therefore the force per unit area, that is, the *pressure* is

$$P = -\left(\frac{\partial E}{\partial V}\right)_S \quad (\text{A.23})$$

A system in thermal equilibrium must also be in mechanical equilibrium. Imagine a closed system to be subdivided by an (imaginary) interface, then the pressure on both sides must be equal; we conclude that the pressure is constant everywhere for a system in thermal equilibrium. Here we should note that if the closed system consists of a drop with is vapor, then we have a *real* interface and we have *different* pressures in the two phases, but uniform pressure in each of the phases.

The energy  $E(S, V)$  of a closed system, in thermal equilibrium, is a function of entropy and volume, and a small change may, using equations (A.15) and (A.23), be written

$$dE = TdS - PdV \quad (\text{A.24})$$

This is a most important relation, often called the *first law* of thermodynamics. It follows that:

$$T = \left(\frac{\partial E}{\partial S}\right)_V, \quad P = -\left(\frac{\partial E}{\partial V}\right)_S. \quad (\text{A.25})$$

This first law may also be written

$$dS = \frac{1}{T}dE + \frac{P}{T}dV, \quad (\text{A.26})$$

and it follows that

$$\frac{P}{T} = \left(\frac{\partial S}{\partial V}\right)_E. \quad (\text{A.27})$$

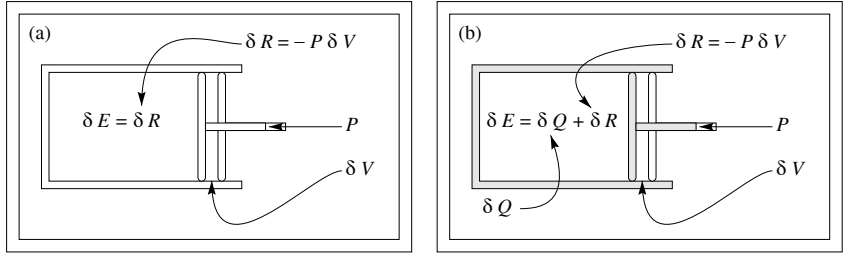


Figure A.1: A closed system consisting of a heat bath surrounding the system of interest. (a) – The surroundings work on a thermally insulated system by changing its volume by  $\delta V$ . The work done by the system is  $\delta\mathcal{R} = -P\delta V$ . The increase in energy of the system is  $\delta E = \delta\mathcal{R} = -P\delta V$ . (b) – The walls of the system conduct *heat* and in the process of changing the volume of the system the heat  $\delta Q$  enters the system, therefore the energy change is  $\delta E = \delta Q + \delta\mathcal{R}$ . Together the system and the surroundings form a closed system

## A.5 Work and Heat

Consider a closed system that consists of two parts—the ‘system’ and the surrounding *medium* or ‘*heat bath*’ (see figure A.1). First consider the situation in which the system is thermally insulated from the medium. If the volume of the system changes by  $\delta V$  then the medium, which has a pressure  $P$  (equal to the pressure of the medium), performs *work* on the system given by

$$\delta\mathcal{R} = -P\delta V . \quad (\text{A.28})$$

The work  $\mathcal{R}$  is conventionally taken to be positive when work is done on the system. In figure A.1a the volume change of the system is negative and the work done by the medium on the system is therefore positive. Since the system is thermally insulated from the medium the energy increase of the system is simply

$$\delta E = \delta\mathcal{R} = -P\delta V \quad (\text{A.29})$$

If the system is not thermally insulated from the medium, then the energy of the system may also change because energy in the form of heat,  $\delta Q$ , is transported by thermal conduction into the system from the medium. The energy change of the system can then be written

$$\delta E = \delta\mathcal{R} + \delta Q . \quad (\text{A.30})$$

For the system in figure A.1a the work is given by equation (A.29) and we can write the heat as

$$\delta Q = \delta E + P\delta V . \quad (\text{A.31})$$

If the process proceeds in such a way that the system is in internal thermal equilibrium ( $T$  is uniform and the same in the system and in the medium), then the energy of the system,  $E(S, V)$  is a function of the entropy of the system,  $S$ , and the system volume  $V$ , even if the system is *not* in equilibrium with its surrounding medium (but, of course, in internal equilibrium). In this situation we may use the first law of thermodynamics equation (A.24), since in (internal) equilibrium  $E(S, V)$  must be the same whether the system is closed or not. It follows then from equations (A.24) and (A.31) that

$$\boxed{\delta Q = T\delta S \quad \text{internal equilibrium}} \quad (\text{A.32})$$

The change of energy of a system that is not thermally insulated consists of two parts: the work,  $\delta R$ , done on the system and the heat  $\delta Q$  conducted to the system. However, the energy,  $E$ , cannot be divided into a ‘work part’ and a ‘heat part’ since both the amount of heat and the work done depend on the exact ‘path’ the process takes; the energy on the other hand depends only of the state and not of the path.

If the system is not in thermal equilibrium, but has uniform pressure and temperature (for instance, a chemical reaction may be incomplete, as in a battery that is not completely discharged), then the entropy increases with time independently of the heat gained from the medium. For such *irreversible processes* equation (A.32) is replaced by

$$\boxed{\delta Q < T\delta S \quad \text{not in internal equilibrium}} \quad (\text{A.33})$$

The process is irreversible since if one tries to get back to the initial state by letting the system work on the medium instead of the other way around, the entropy cannot return to its original value since the entropy has an independent increase in both processes.

## A.6 Maximum Work

Now consider a system that is thermally isolated, but can exchange work with its surroundings. Initially we assume that the various parts of the system is *not* in thermal equilibrium. For the sake of illustration consider the situation illustrated in figure A.2. The final state depends on how

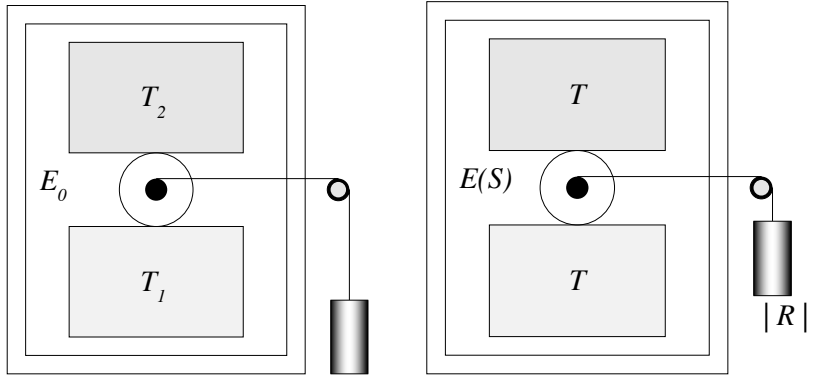


Figure A.2: A thermally isolated system contains two parts at different temperatures  $T_2 > T_1$ . The two parts are connected via a heat engine that may perform the work  $|\mathcal{R}|$  on the surroundings outside the system. as the system approaches equilibrium. (a) – Initially the energy of the system is  $E_0$ . (b) – Finally the two parts have the same temperature  $T$ , and an amount of work was done on the surroundings. The energy of the equilibrium system is a unique function of entropy,  $E(S)$ . Both  $E$  and  $S$  depends on how the equilibrium state was reached.

equilibrium was reached. The work done on the outside world in this process is

$$|\mathcal{R}| = E_0 - E(S) \quad \Rightarrow \left( \frac{\partial |\mathcal{R}|}{\partial S} \right) = - \left( \frac{\partial E}{\partial S} \right)_V = -T. \quad (\text{A.34})$$

where  $E_0$  is the energy of the system initially, and  $E(S)$  is the energy of the final equilibrium state. Since  $S$  cannot decrease for a thermally isolated system, it must increase, or at best remain constant, as the system approaches equilibrium. But from equation (A.34) we see that  $|\mathcal{R}|$  decreases with increasing  $S$ , thus the maximum work is done on the surroundings when  $S$  is constant, that is, for a reversible process.

### A.6.1 Carnot Process

Change the problem slightly: Determine the maximum work that can be obtained by transferring a small amount of energy,  $-\delta E$  from the hot,  $T_2$ , to the cold  $T_1$ , ‘reservoir’ in figure A.2. If the heat-engine does no work

and  $|\mathcal{R}| = 0$ , then the total entropy increases by

$$\delta S = \frac{-\delta E}{T_2} + \frac{+\delta E}{T_1} = \delta E \left( \frac{1}{T_1} - \frac{1}{T_2} \right), \quad (\text{A.35})$$

where we have used equation (A.14). Thus the entropy of the system increases when thermal equilibrium is reached without performing work on the surroundings. This is what happens when the two reservoirs are just brought into contact so that thermal conduction equilibrates the temperatures of the two reservoirs. From equation (A.35) it follows that energy(heat) flows from the hot reservoir to the cold reservoir as equilibrium is approached and the entropy increases. The process stops, with no further increase in entropy, when the two temperatures have become equal.

In order to extract the *maximum work* possible, the heat-engine must execute a reversible process, that is, the process must be cyclic, since the heat-engine should be in the same state before and after the work was extracted. Carnot discussed a process that has four stages:

1. The heat engine, at temperature  $T_2$ , is brought into contact with the reservoir at  $T_2$ , and receives the amount  $-\delta E_2$  *isothermally*.
2. The heat-engine is removed from the  $T_2$ -reservoir, thermally isolated and undergoes an *adiabatic expansion* until its temperature is decreased to  $T_1$ .
3. The heat-engine is put in thermal contact with the  $T_1$  reservoir, and gives off isothermally the energy  $\delta E_1$  at temperature  $T_1$ .
4. The heat-engine is removed from the  $T_1$ -reservoir, thermally isolated and undergoes an *adiabatic compression* until its temperature is increased to  $T_2$ . The cycle is then, and the four stages may be repeated.

The heat-engine performs work on the outside world during expansion, and receives work during contraction. The process just described is a Carnot process. During the first process the hot reservoir has a change in energy given by  $\delta E_2 = T_2 \delta S_2$ , which is negative, of course. Then during stage (3) the  $T_1$  reservoir taken to be receives an energy  $\delta E_1 = T_1 \delta S_1$ . Since the process is reversible, there is no change in entropy of the thermally insulated system so that  $\delta S_1 = -\delta S_2$ . Thus we find that the change of energy of the thermally insulated system is  $\delta E = \delta E_1 + \delta E_2 = T_1 \delta S_1 + T_2 \delta S_2 = (T_2 - T_1) \delta S_2$ . Since energy is conserved,  $\delta E + \mathcal{R} = 0$ , and  $\delta S_2 = \delta E_2 / T_2$  we find that the work done on the surroundings is given by

$$\mathcal{R}_{\max} = -\frac{T_2 - T_1}{T_2} \delta E_2 \quad (\text{A.36})$$

This work is positive when heat is taken from the hot reservoir (2) and given up to the cold reservoir (1). In this case  $\delta E_2 < 0$ , and we find that the maximum work that can be obtained from a heat engine, is

$$|\mathcal{R}|_{\max} = \frac{T_2 - T_1}{T_2} |\delta E_2| \quad (\text{A.37})$$

Here  $|\delta E_2|$  is the energy given up by the hot reservoir. The efficiency,  $|\mathcal{R}|_{\max}/|\delta E_2|$  of this process is given by

$$\eta_{\max} = (T_2 - T_1)/T_2 = (1 - T_1/T_2). \quad (\text{A.38})$$

This expression sets an upper limit for the amount of work that may be extracted by a heat-engine, of any design—practical, imagined or future! It does not matter whether steam, liquid metals, mercury vapor, plasmas or whatever is used as a working medium, this efficiency cannot be surpassed. The reason is that in this cyclic Carnot process the state of the heat engine is returned to the starting point at the beginning of each cycle. Therefore the energy of the whole system, engine and heat reservoirs, at the beginning of the cycle does not depend on the machine used. Of course, in any practical engine we have losses, so that the process is not truly reversible. Thus practical efficiencies are less than the efficiency of the ideal Carnot cycle.

I a refrigerator, heat,  $|T_1 \delta S_1|$  is taken from the cold reservoir and released at the hot reservoir; then the efficiency of an ideal refrigerator is  $\eta_{\min} = (T_2 - T_1)/T_1 = |\mathcal{R}|_{\min}/|T_1 \delta S_1|$ , where  $|\mathcal{R}|_{\min}$  is the minimum work required to take the heat  $\delta Q = |T_1 \delta S_1|$ , away from the cold reservoir.

Lord Kelvin realized that the Carnot cycle may be used to define an *absolute scale of temperature*—the scale used here. Since the efficiency  $\eta_{\max} \leq 1$  it follows that there is a lower limit of (equilibrium) of zero. The Kelvin scale therefore has a natural fixed point, absolute zero. Since  $\eta_{\max}$  depends only on the ratio  $T_1/T_2$ , there is an arbitrary scale factor that is fixed by setting  $T = 273.16$  K for the triple point of pure water. With this scale one degree on the Celsius scale equals one degree on the Kelvin scale.

## A.7 Work in an External medium

Let us discuss the system illustrated in figure A.3. It consists of the system of interest in thermal contact with the heat bath or medium. The system can also exchange work with an external object (illustrated by a spring) that is thermally insulated from both the system and the medium. The

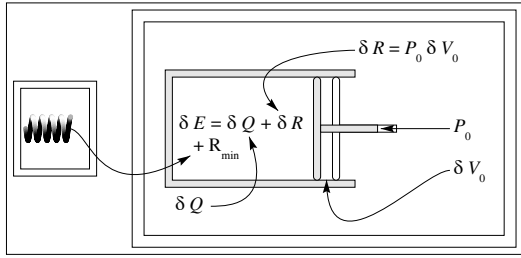


Figure A.3: A ‘medium’ with temperature  $T_0$ , pressure  $P_0$ , and volume  $V_0$  is in contact with a ‘system’ at temperature  $T$ , pressure  $P$ , and volume  $V$ . The system may also be worked upon by some external mechanism that is thermally insulated from both the medium and the system.

medium, that is, the heat bath, is considered to be huge in size and in internal thermal equilibrium so that when changes occur in the system the temperature  $T_0$  and pressure  $P_0$  of the medium are unaffected. The temperature,  $T$ , and the pressure,  $P$ , of the system may differ from  $T_0$ , and  $P_0$ , when the system is internal equilibrium but not in equilibrium with the surrounding heat bath. The system, the medium, and the object form a closed system for which the entropy can only increase or, at best, stay constant (the second law of thermodynamics).

In this case the energy change of the system (not necessarily small) is

$$\Delta E = \mathcal{R} + P_0 \Delta V_0 - T_0 \Delta S_0 . \quad (\text{A.39})$$

Here  $\mathcal{R}$  is the work done on the system by the external object,  $P_0 \Delta V_0$  is the work done on the system by the medium, and  $T_0 \Delta S_0$  is the heat transported from the medium to the system. Since the total volume is fixed we find that the change in volume of the system is  $\Delta V = -\Delta V_0$ . The second law of thermodynamics insists that the entropy of the closed system cannot decrease with time and therefore we have  $\Delta S_0 + \Delta S \geq 0$ , where  $\Delta S$  is the change in entropy of the system. Using these results we may rewrite equation (A.39) in the form

$$\mathcal{R} \geq \Delta E - T_0 \Delta S + P_0 \Delta V . \quad (\text{A.40})$$

Here the equality occurs for *reversible processes* in which the total entropy  $S + S_0$  is constant. The *minimum work* required to bring the system from one state to another is therefore

$\mathcal{R}_{\min} = \Delta(E - T_0 S + P_0 V)$

(A.41)

where we have placed the constant temperature  $T_0$  and pressure  $P_0$  of the medium after the variation  $\Delta$ . The reverse change, that is, the process that brings the system from its final state back to its initial state, will let the system work on the external object and *maximum work* is extracted for a reversible process. We have  $|\mathcal{R}_{\max}| = \mathcal{R}_{\min}$ .

For a system that is in internal equilibrium at each stage of the process that changes its state, we may use the first law:  $dE = TdS - PdV$  to find that the minimum work required to bring about a change  $dS$  and  $dV$  is

$$d\mathcal{R}_{\min} = (T - T_0)dS - (P - P_0)dV . \quad (\text{A.42})$$

If the body is not in equilibrium,<sup>2</sup> so that its state is not given by  $T$  and  $V$  alone, then for processes that occur at constant volume  $V$  and temperature  $T = T_0$ , the reversible work is

$$\mathcal{R}_{\min} = \Delta F = \Delta(E - TS) . \quad (\text{A.43})$$

Here we have introduced the *Helmholtz free energy*  $F$  defined as

$$F(T, V) = E - TS \quad \text{Helmholtz free energy} \quad (\text{A.44})$$

The minimum reversible work that is required to bring about a change in the state (from state (1) to state (2)) of the system at constant temperature and volume is the change in the Helmholtz free energy in going from state (1) to the other state (2). The reverse process, from (2) to (1) gives the maximum work that may be generated by the system.

For a system where there is no external work  $\mathcal{R} = 0$ , it follows from equation (A.40) that

$$\Delta(E - T_0S + P_0V) \leq 0 , \quad (\text{A.45})$$

and we conclude that  $E - T_0S + P_0V$  will decrease spontaneously until the equilibrium state is reached. The Helmholtz free energy is approaches a minimum value for processes that occurs at fixed temperature  $T$  and volume  $V$ .

We note that if the system undergoes a reversible isothermal change of state, then the first law has the form

$$d\mathcal{R} = dE - dQ = dE - TdS = d(E - TS) , \quad (\text{A.46})$$

---

<sup>2</sup>Here we may, for example, think of a system in which salt is slowly dissolved in water.

where now  $\mathcal{R}$  and  $Q$  are functions of the state since the ‘path’ was specified to be reversible and isothermal. It follows that

$$d\mathcal{R} = dF, \quad \text{where } F = E - TS. \quad (\text{A.47})$$

It follows that  $dF = dE - SdT - TdS$ , and substituting the first law in equation (A.24) we find that  $dE = TdS - PdV$ , and we conclude that

$$dF = -SdT - PdV \quad (\text{A.48})$$

From this equation it immediately follows that

$$S = -\left(\frac{\partial F}{\partial T}\right)_V, \quad P = -\left(\frac{\partial F}{\partial V}\right)_T \quad (\text{A.49})$$

The Helmholtz free energy  $F$  is a function of the thermodynamic state of the system, and is a function of  $T$ , and  $V$ , that is,  $F = F(T, V)$ .

The energy  $E$  may be found from  $E = F + TS$  as follows

$$E = F - T\left(\frac{\partial F}{\partial T}\right)_V = -T^2\left(\frac{\partial}{\partial T}\frac{F}{T}\right)_V. \quad (\text{A.50})$$

If we know  $F(T, V)$  for a system we therefore may find the energy  $E(S, V)$ , using derivatives and *vice versa*.

The Helmholtz free energy may be expressed in terms of the partition function  $Z$ , using that  $p_i = \exp\{-\beta\epsilon_i\}/Z$

$$\begin{aligned} F &= E - TS = E + k_B \sum_i p_i \ln p_i \\ &= E + k_B T \sum_i p_i [(-\beta\epsilon_i) - \ln Z] \\ &= E - E - k_B T \ln Z \\ &= -k_B T \ln Z. \end{aligned} \quad (\text{A.51})$$

The partition function  $Z$  plays a central role in statistical physics since the Helmholtz free energy is given by

$$F = -k_B T \ln Z, \quad \text{Helmholtz free energy} \quad (\text{A.52})$$

from which all other thermodynamic properties may be calculated.

If, instead the process proceeds at constant pressure and temperature, then we find from equation (A.41) that

$$\mathcal{R}_{\min} = \Delta G = \Delta(E - TS + PV). \quad (\text{A.53})$$

where we have introduced the *Gibbs free energy*  $G$  defined as

$$G(T, P) = E - TS + PV \quad \text{Gibbs free energy} \quad (\text{A.54})$$

Using the first law (A.24) we find that

$$dG = -TdT + VdP . \quad (\text{A.55})$$

If the system cannot work on an external object then equation (A.40) becomes

$$\Delta(E - T_0S + P_0V) \leq 0 . \quad (\text{A.56})$$

Thus in a process at  $P = P_0$  and  $T = T_0$ , the Gibbs free-energy (A.54) will decrease (spontaneously) until equilibrium is reached. Note that it has not been assumed that  $T$  and  $P$  are constant during the process, only that  $T = T_0$  and  $P = P_0$  at the beginning and at the end of the process that leads to equilibrium.

## A.8 The Number of Particles Dependence

The energy and entropy are proportional to system size so they must be proportional to the number,  $N$ , of particles for uniform systems. We can therefore write the energy of a closed system as

$$E = Nf(S/N, V/N) , \quad (\text{A.57})$$

since the volume is also additive. Here  $f$  is some function (depending on the type of system) of the *entropy per particle*  $s = S/N$  and *volume per particle*  $v = V/N$ , that is, the molecular volume.

In the discussion leading to equations (A.24) and (A.27) we did assume that the number of particles in the system was fixed. However, in comparing two systems, both in equilibrium, but with a small difference,  $dN$ , in the number of particles, the energy must also differ by a small amount  $dE = (\frac{\partial E}{\partial N})_{S,V} dN$ . Therefore the first law of thermodynamics (A.24) takes the form

$$dE = TdS - PdV + \mu dN \quad (\text{A.58})$$

Here the *chemical potential*  $\mu$  is defined as

$$\mu = \left( \frac{\partial E}{\partial N} \right)_{S,V} . \quad (\text{A.59})$$

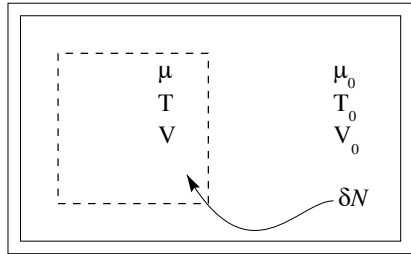


Figure A.4: A ‘medium’ with temperature  $T_0$ , chemical potential  $\mu_0$  and volume  $V_0$  is in contact with a ‘system’ at temperature  $T$ , chemical potential  $\mu$  volume  $V$ . The system is ‘open’ and permits exchange of particles, or molecules, between the system and the medium.

## A.9 The Landau Potential $\Omega$

Consider a system in a fixed volume  $V$ , that is in thermal contact with a ‘medium’ at temperature  $T_0$  and chemical potential  $\mu_0$  (we use subscript 0 to indicate quantities for the heat bath). Let the walls of the system permit the exchange of particles or molecules between the system and the surrounding medium. The system of interest with its surrounding heat bath form together a closed system.

In a process that changes the thermodynamic state of the system we have variations in entropy  $\Delta S$ , in energy  $\Delta E$  and so on that satisfy

$$\Delta S_0 + \Delta S \geq 0 \quad \text{2nd. law} \quad (\text{A.60})$$

$$\Delta E_0 + \Delta E = 0 \quad \text{conservation of energy} \quad (\text{A.61})$$

$$\Delta N_0 + \Delta N = 0 \quad \text{conservation of particles} \quad (\text{A.62})$$

$$\Delta V_0 = \Delta V = 0 \quad \text{fixed total volume} \quad (\text{A.63})$$

$$\Delta E_0 = T_0 \Delta S_0 + \mu_0 \Delta N_0 \quad \text{1st. law equation (A.58).} \quad (\text{A.64})$$

We have insisted that the volume of the system is fixed, so in equation (A.63) we have dropped the  $PdV$  term in the first law in the form of equation (A.58). The equations above may be combined to give

$$\Delta(E - T_0 S - \mu_0 N) \leq 0 \quad (\text{A.65})$$

From this equation it follows that the *Landau potential*  $\Omega$  defined by<sup>3</sup>

$$\boxed{\Omega(T, \mu) = E - TS - \mu N} \quad \text{Landau potential} \quad (\text{A.66})$$

tends to a minimum value for processes at constant temperature and chemical potential set by the surrounding medium. As before the  $\Delta$ -changes in equation (A.65) need not be small, nor must  $T$  and  $\mu$  be constant during the process, only at the beginning and at the end of the process is  $\mu = \mu_0$  and  $T = T_0$  required. The minimum work for a process a fixed volume, temperature and chemical potential is

$$\mathcal{R}_{\min} = \Delta\Omega = \Delta(E - TS - \mu N). \quad (\text{A.67})$$

In thermal equilibrium the Landau potential  $\Omega$  is a function of temperature and chemical potential. An infinitesimal change in the state by changes  $dT$  and  $d\mu$  results in a change in  $\Omega$  by  $d\Omega = dE - TdS - SdT - \mu dN - Nd\mu$ . Then using the first law in the form (A.59), we find

$$\boxed{d\Omega = -SdT - Nd\mu, \quad V \text{ constant}} \quad (\text{A.68})$$

This leads to the conclusion that

$$S = -\left(\frac{\partial\Omega}{\partial T}\right)_{V,\mu}, \quad N = -\left(\frac{\partial\Omega}{\partial\mu}\right)_{T,V}. \quad (\text{A.69})$$

It is useful to consider the change in the Gibbs free-energy as a function of pressure and temperature. We find  $dG = dE - TdS - SdT + PdV + VdP$ , and using the first law in the form (A.58), we find another form of the first law:

$$\boxed{dG = -SdT + VdP + \mu dN} \quad (\text{A.70})$$

This leads to the conclusion that

$$S = -\left(\frac{\partial G}{\partial T}\right)_{P,N}, \quad V = \left(\frac{\partial G}{\partial P}\right)_{T,N}, \quad \mu = \left(\frac{\partial G}{\partial N}\right)_{T,P}. \quad (\text{A.71})$$

Since the Gibbs free-energy is extensive, that is, proportional to system size, and therefore has the form  $G = Nf(T, P)$ , we find from equation (A.70) that  $G = \mu N$  and we have

$$\boxed{G = E - TS + PV = \mu N} \quad (\text{A.72})$$

---

<sup>3</sup> $\Omega$  is commonly called the grand potential since it is related to the grand canonical ensemble

Thus the *chemical potential* is the Gibbs free energy per particle. This result for the Gibbs free energy allows us to rewrite the Landau potential as  $\Omega = E - TS - \mu N = E - TS - G = E - TS - E + TS - PV = -PV$  and it follows that

$$\boxed{\Omega(T, \mu) = -PV} \quad (\text{A.73})$$

and we can express the number of particles by

$$N = - \left( \frac{\partial \Omega}{\partial \mu} \right)_{T,V} = V \left( \frac{\partial P}{\partial \mu} \right)_{T,V}. \quad (\text{A.74})$$

## A.10 Thermodynamics of Solutions

Consider a system that has  $N_i$  particles, atoms, or molecules of type  $i$ , then the generalization of the first law in the form of equation (A.70) is simply

$$dG = -SdT + VdP + \sum_i \mu_i dN_i, \quad (\text{A.75})$$

where we have *defined* the chemical potential of species ( $i$ ) as

$$\mu_i = \left( \frac{\partial G}{\partial N_i} \right)_{p,T,\{N_j \neq i\}}, \quad (\text{A.76})$$

that is, as the derivative of the Gibbs free energy at fixed pressure and temperature and all other species kept fixed. All these chemical potentials are *intensive* variables (independent of the ‘size’ of the system) and they can therefore only be functions of intensive variables, such as  $T$ ,  $p$ , and the *mol-fractions*  $X_i = N_i/N$ , where  $N = \sum_i N_i$  is the total number of particles. That is, we may write:

$$\mu_i = \mu_i(p, T, \{X_i\}). \quad (\text{A.77})$$

The total Gibbs free energy may therefore be written

$$G(p, T, \{N_i\}) = \sum_i N_i \mu_i(p, T, \{X_i\}), \quad (\text{A.78})$$

since  $G$  is extensive, and equation (A.78) is the only form consistent with equation (A.76).

### A.10.1 Dilute solutions

For mixtures of ideal gases—where there is no interaction between the particles—it is simple to obtain complete expressions. However, for particles, or molecules, in a solvent there are very strong interactions and we can arrive at a general expression only for *dilute solutions*.

Let us consider a mixture of only two components, a fluid *solvent* containing  $N_1$  molecules, and a *solute* of  $N_2$  molecules (or particles) dissolved in the solvent. We assume that the mol-fraction

$$X = N_2/(N_1 + N_2) \ll 1 \quad (\text{A.79})$$

is very small.

At this point the argument typically runs as follows: The pure solvent has a Gibbs free energy given by

$$G_1^0(p, T, N_1) = N_1\mu_1^0(p, T) . \quad (\text{A.80})$$

Let  $\alpha(p, T, N_1)$  denote the change in the thermodynamic potential by the addition of a single molecule of solute. If we add  $N_2$  molecules of the solute, and  $N_2 \ll N_1$ , then the solute molecules will be far apart and we may ignore their mutual interaction, although each of them interacts strongly with the solvent. We are therefore tempted to write  $G = G^0 + \alpha N_2$ , which unfortunately is not correct since we must take into account the fact that the  $N_2$  particles are identical and there is an additional term in the entropy to account for this. The Gibbs free energy is  $G = E - TS + PV$ , and the entropy may be written  $S = k_B \ln W$  (see equation (A.3)). If all the solvent particles were different (distinguishable) and had the same  $\alpha$ , then we would indeed have  $G = G^0 + \alpha N_2$ , but the particles are identical so the number of distinct configurations,  $W$ , must be reduced by a factor  $1/N_2!$ , which gives a change in entropy  $\Delta S = k_B \ln(1/N_2!)$ , and we conclude that

$$G = N_1\mu_1^0(p, T) + \alpha(p, T, N_1)N_2 + k_B T \ln(N_2!) . \quad (\text{A.81})$$

We may write  $\ln(N_2!) = N_2 \ln(N_2/e)$  so we find

$$\begin{aligned} G &= N_1\mu_1^0(p, T) + N_2[\alpha(p, T, N_1) + k_B T \ln(N_2/e)] \\ &= N_1\mu_1^0(p, T) + N_2 k_B T \ln[(N_2/e)e^{\alpha/k_B T}] . \end{aligned} \quad (\text{A.82})$$

The Gibbs free energy is extensive, and a homogeneous function, so it must have the form

$$G = N_1\mu_1^0(p, T) + N_2 k_B T \ln[(N_2/eN_1)f(p, T)] , \quad (\text{A.83})$$

that is, we have  $e^{\alpha/k_B T} = f(p, T)/N_1$ . Defining a new function

$$\tilde{\mu}_2^0(p, T) = k_B T \ln f(p, T) \quad (\text{A.84})$$

we may write the Gibbs free energy for a dilute solution as

$$G = N_1 \mu_1^0(p, T) + N_2 k_B T \ln[(N_2/eN_1)] + N_2 \tilde{\mu}_2^0(p, T) . \quad (\text{A.85})$$

With  $N = N_1 + N_2$ , and  $X = N_2/N$  this expression may be rewritten as

$$G = N[(1 - X)\mu_1^0(p, T) + X\tilde{\mu}_2^0(p, T)] + \Delta G_{\text{mix}} , \quad (\text{A.86})$$

using the definition

$$\begin{aligned} \Delta G_{\text{mix}} &= Nk_B T[X \ln X - X - X \ln(1 - X)] \\ &\simeq Nk_B T[X \ln X + (1 - X) \ln(1 - X)] \quad X \ll 1 . \end{aligned} \quad (\text{A.87})$$

Here, the last expression is *exact* for a mixture of two ideal gasses, and it is valid for *dilute solutions*.

The generalization to many different solutes is simple and we may write

$$G(p, T, \{Ni\}) = N_1 \mu_1^0(p, T) + N \sum_{i=2}^{\ell} X_i \tilde{\mu}_i^0(p, T) + \Delta G_{\text{mix}} \quad (\text{A.88})$$

$$\Delta G_{\text{mix}} = Nk_B T \sum_i [X_i \ln X_i + (1 - X_i) \ln(1 - X_i)] , \quad X_i \ll 1 . \quad (\text{A.89})$$

Again, this expression is exact for a mixture of perfect gases, but only approximate for dilute solutions. In particular the effective chemical potentials  $\tilde{\mu}_i^0(p, T)$  are not the chemical potentials of the pure substances, except for the solvent.

From the definition of the chemical potential of the pure solvent we find that

$$\begin{aligned} \mu_1(p, T, \{X_i\}) &= \left( \frac{\partial G}{\partial N_1} \right)_{p, T, \{N_j \neq 1\}} = \mu_1^0(p, T) + k_B T \sum_{i=2}^{\ell} \ln(1 - X_i) \\ &\simeq \mu_1^0(p, T) - k_B T \sum_{i=2}^{\ell} X_i \end{aligned} \quad (\text{A.90})$$

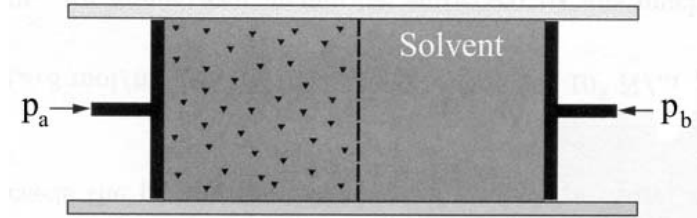


Figure A.5: The solvent may move freely between the compartments (a) and (b). The solute in the left chamber cannot pass through the semipermeable wall to the right chamber. At thermodynamic equilibrium the chemical potential of the solvent must be the same in the two chambers. Equilibrium is possible only if  $p_a > p_b$ .

For the solute of type (i) we find that

$$\begin{aligned}\mu_j(p, T, \{X_i\}) &= \left( \frac{\partial G}{\partial N_j} \right)_{p, T, \{N_{j \neq i}\}} \\ &= \tilde{\mu}_j^0(p, T) + k_B T \ln(X_j) + k_B T \sum_{i=2, i \neq j}^{\ell} \ln(1 - X_j) \quad (\text{A.91}) \\ &\simeq \tilde{\mu}_j^0(p, T) + k_B T \ln(X_j) .\end{aligned}$$

### A.10.2 Osmotic pressure

Consider a vessel consisting of two compartments (labeled (a) and (b)) separated by a semi-permeable wall that allows the solvent to pass from one compartment to the other, whereas the solute molecules (or particles) cannot pass from one compartment to the other. If the pure solvent in (b) has the chemical potential  $\mu_1(p_b, T) = \mu_1^0(p_b, T)$ . Compartment (a) contains the solvent at the mol-fraction  $X$ . From equation (A.90) it follows that the chemical potential of the solvent in (a) is

$$\mu_1(p_a, T, X) = \mu_1^0(p_a, T) - k_B T X . \quad (\text{A.92})$$

For thermal equilibrium the chemical potential of the solvent in the two compartments must be equal:

$$\mu_1(p_b, T) = \mu_1^0(p_b, T) = \mu_1(p_b, T, X) = \mu_1^0(p_a, T) - k_B T X . \quad (\text{A.93})$$

We expand  $\mu_1^0(p_a, T)$  as follows:

$$\mu_1^0(p_a, T) == \mu_1^0(p_b, T) + \left( \frac{\partial \mu_1^0}{\partial P} \right)_T \Big|_{p_b} (p_a - p_b) . \quad (\text{A.94})$$

Now the molecular volume of the pure solvent at the pressure  $p_b$  and temperature  $T$  is

$$v = \left( \frac{\partial \mu_1^0}{\partial p} \right)_T . \quad (\text{A.95})$$

Therefore we obtain from equations (A.93) and (A.94) that the pressure difference is given by

$$\Delta p = (p_a - p_b) = v k_B T X . \quad (\text{A.96})$$

Remember that  $X = N_2/(N_1 + N_2)$ , and that in the limit of very small  $X$  the volume of the solvent in (a) is simply  $V = N_1 v$ . It follows that the *osmotic pressure*  $\Delta p$  is given by<sup>4</sup>

$$\boxed{\Delta p V = N_2 k_B T \quad \text{van't Hoff's equation}} \quad (\text{A.97})$$

That is, the excess pressure (the osmotic pressure) is given by the ideal gas law. It is notable that this equation, valid at for very dilute concentrations is valid not only for molecules such as sugar, proteins, and other small or large molecules, but also for suspensions of small particles, that is, dilute colloids, as pointed out by Einstein.<sup>1</sup>

## A.11 General Forces

The first law has the general form

$$dE = T dS - P dV + \mu dN + \sum_i \Lambda_i d\lambda_i , \quad (\text{A.98})$$

where  $d\lambda_i$  is the change in a parameter (such as  $N$  above) and  $\Lambda_i$  is a function of the state of the system. The term  $\sum_i \Lambda_i \lambda_i$  is added to all the free energies except the entropy:

$$dS = \frac{1}{T} dE + \frac{P}{T} dV - \frac{\mu}{T} dN - \sum_i \frac{\Lambda_i}{T} d\lambda_i , \quad (\text{A.99})$$

---

<sup>4</sup>Jacobus Henricus van't Hoff, born 1852, died 1911. Physical chemist and the first winner of the Nobel Prize for Chemistry (1901) for work on rates of reaction, chemical equilibrium, and osmotic pressure.

For instance, with  $F = E - TS$ , and  $G = E - TS + PV$  we find

$$\begin{aligned} dF &= dE - TdS - SdT \\ &= TdS - PdV + \mu dN + \sum_i \Lambda_i d\lambda_i - TdS - SdT \\ &= -SdT - PdV + \mu dN + \sum_i \Lambda_i d\lambda_i . \end{aligned} \quad (\text{A.100})$$

and

$$\begin{aligned} dG &= dE - TdS - SdT + PdV + VdP \\ &= TdS - PdV + \mu dN + \sum_i \Lambda_i d\lambda_i - TdS - SdT + PdV + VdP \\ &= -SdT - VdP + \mu dN + \sum_i \Lambda_i d\lambda_i . \end{aligned} \quad (\text{A.101})$$

and finally for the Landau potential  $\Omega = E - TS - \mu N$ , we find

$$\begin{aligned} d\Omega &= dE - TdS - SdT - \mu dN - Nd\mu \\ &= TdS - PdV + \mu dN + \sum_i \Lambda_i d\lambda_i - TdS - SdT - \mu dN - Nd\mu \\ &= -SdT - PdV + Nd\mu + \sum_i \Lambda_i d\lambda_i . \end{aligned} \quad (\text{A.102})$$

It follows that

$$\begin{array}{llll} T = \left( \frac{\partial S}{\partial E} \right)_{NV\lambda_i}^{-1} & P = T \left( \frac{\partial S}{\partial V} \right)_{NE\lambda_i} & \mu = -T \left( \frac{\partial S}{\partial N} \right)_{NV\lambda_i} & \Lambda_i = -T \left( \frac{\partial S}{\partial \lambda_i} \right)_{NVE\lambda_{j \neq i}} \\ T = \left( \frac{\partial E}{\partial S} \right)_{VN\lambda_i}^{-1} & P = - \left( \frac{\partial E}{\partial V} \right)_{SN\lambda_i} & \mu = \left( \frac{\partial E}{\partial N} \right)_{SV\lambda_i} & \Lambda_i = \left( \frac{\partial E}{\partial \lambda_i} \right)_{SVN\lambda_{j \neq i}} \\ S = - \left( \frac{\partial F}{\partial T} \right)_{NV\lambda_i} & P = - \left( \frac{\partial F}{\partial V} \right)_{NT\lambda_i} & \mu = \left( \frac{\partial F}{\partial N} \right)_{TV\lambda_i} & \Lambda_i = \left( \frac{\partial F}{\partial \lambda_i} \right)_{NTV\lambda_{j \neq i}} \\ S = - \left( \frac{\partial G}{\partial T} \right)_{NP\lambda_i} & V = - \left( \frac{\partial G}{\partial P} \right)_{NT\lambda_i} & \mu = \left( \frac{\partial G}{\partial N} \right)_{TV\lambda_i} & \Lambda_i = \left( \frac{\partial G}{\partial \lambda_i} \right)_{NTP\lambda_{j \neq i}} \\ S = - \left( \frac{\partial \Omega}{\partial T} \right)_{V\mu\lambda_i} & P = - \left( \frac{\partial \Omega}{\partial V} \right)_{\mu T\lambda_i} & N = \left( \frac{\partial \Omega}{\partial \mu} \right)_{TV\lambda_i} & \Lambda_i = \left( \frac{\partial \Omega}{\partial \lambda_i} \right)_{\mu TV\lambda_{j \neq i}} \end{array}$$

## A.12 The Maxwell's Distribution

Maxwell<sup>5</sup> read a paper at the meeting of the British Association of Aberdeen in September 1859. It was published in the *Philosophical Magazine* in 1860, and it contains the following heuristic argument on the velocity distribution.<sup>6</sup>

" If a great many equal spherical particles were in motion in a perfectly elastic vessel, collisions would take place among the particles, and their velocities would be altered at every collision; so that after a certain time the *vis viva* will be divided among the particles according to some regular law, the average number of particles whose velocity lies between certain limits being ascertainable though the velocity of each particle changes at every collision.

Prop. IV. To find the average number of particles whose velocities lie between given limits, after a great number of collisions among a great number of equal particles.

Let  $N$  be the whole number of particles. Let  $x, y, z$  be the components of the velocity of each particle in three rectangular directions, and let the number of particles for which  $x$  lies between  $x$  and  $x + dx$ , be  $N f(x)dx$ , where  $f(x)$  is a function of  $x$  to be determined.

The number of particles for which  $y$  lies between  $y$  and  $y + dy$  will be  $N f(y)dy$ ; and the number for which  $z$  lies between  $z$  and  $z + dz$  will be  $N f(z)dz$  where  $f$  always stands for the same function.

Now the existence of the velocity  $x$  does not in any way affect that of the velocities  $y$  or  $z$ , since these are all at right angles to each other and independent, so that the number of particles whose velocity lies between  $x$  and  $x + dx$ , and also between  $y$  and  $y + dy$ , and also between  $z$  and  $z + dz$ , is

$$N f(x)f(y)f(z)dxdydz.$$

If we suppose the  $N$  particles to start from the origin at the same instant, then this will be the number in the element of volume ( $dxdydz$ ) after unit of time, and the number referred to unit of volume will be

$$N f(x)f(y)f(z).$$

But the directions of the coordinates are perfectly arbitrary, and therefore this number must depend on the distance from the origin alone, that is

$$f(x)f(y)f(z) = \phi(x^2 + y^2 + z^2).$$

---

<sup>5</sup>Maxwell, James Clerk; born June 13, 1831, Edinburgh, Scotland; died November 5, 1879, Cambridge, Cambridgeshire, England; Scottish physicist best known for his formulation of electromagnetic theory. He is regarded by most modern physicists as the scientist of the 19th century who had the greatest influence on 20th-century physics, and he is ranked with Sir Isaac Newton and Albert Einstein for the fundamental nature of his contributions. In 1931, on the 100th anniversary of Maxwell's birth, Einstein described the change in the conception of reality in physics that resulted from Maxwell's work as "the most profound and the most fruitful that physics has experienced since the time of Newton."

<sup>6</sup>Appendix 10 from Emilio Segrè's book Maxwell's Distribution of Velocities of Molecules in His Own Words

Solving this functional equation, we find

$$f(x) = Ce^{Ax^2}, \quad \phi(r^2) = C^3 e^{Ar^2}.$$

If we make  $A$  positive, the number of particles will increase with the velocity, and we should find the whole number of particles infinite. We therefore make  $A$  negative and equal to  $-\frac{1}{\alpha^2}$ , so that the number between  $x$  and  $x + dx$  is

$$NCe^{-x^2/\alpha^2} dx$$

Integrating from  $x = -\infty$  to  $x = +\infty$ , we find the whole number of particles,

$$NC\sqrt{\pi}\alpha = N, \quad \text{therefore } C = \frac{1}{\alpha\sqrt{\pi}},$$

$f(x)$  is therefore

$$\frac{1}{\alpha\sqrt{\pi}} e^{-x^2/\alpha^2}$$

Whence we may draw the following conclusions:—

1st. The number of particles whose velocity, resolved in a certain direction, lies between  $x$  and  $x + dx$  is

$$N \frac{1}{\alpha\sqrt{\pi}} e^{-x^2/\alpha^2} dx$$

2nd. The number whose actual velocity lies between  $v$  and  $v + dv$  is

$$N \frac{4}{\alpha^3\sqrt{\pi}} v^2 e^{-v^2/\alpha^2} dv$$

3rd. To find the mean value of  $v$ , add the velocities of all the particles together and divide by the number of particles; the result is

$$\text{mean velocity} = \frac{2\alpha}{\sqrt{\pi}}$$

4th. To find the mean value of  $v^2$ , add all the values together and divide by  $N$ ,

$$\text{mean value of } v^2 = \frac{3}{2}\alpha^2.$$

This is greater than the square of the mean velocity, as it ought to be.”

## Appendix B

# Porosity Distributions

In the discussion of porous media one often finds that a concept of *pore size distributions* are introduced. However, except for simple models, such distributions are not well defined. Pore volumes, pore necks, connectivity and other geometric details have to be specified with great care in order to make poresize distributions meaningful.

However, porosity, specific surface, tortuosity are only average measures of pore geometry. We need more detailed information if we are to calculate transport properties such as permeability, formation factor, capillary pressure, dispersivity and so on. In order to give a more complete description one has to balance between excessive detail and oversimplification.

Hilfer<sup>143</sup> has introduced the notion of a *porosity distribution*  $\mu(\phi)$  to characterize a porous medium in a practical way. He has also used this distribution to derive an expression for *Archie's law*<sup>144</sup> for the formation factor. To illustrate the ideas consider the two-dimensional 'porous media' illustrated in figure B.1.

The porosity of a small piece of a homogeneous porous medium will in general be different from the porosity of the sample as a whole. If we measure the porosity of a small sample of volume  $V_c = L \times L \times L$  we will find that the *local porosity* depends on the size of the measurement cell and the position  $\mathbf{R}$  where the cell is located in the sample. We take  $\mathbf{R} = n_1\mathbf{a} + n_2\mathbf{b} + n_3\mathbf{c}$  so that with  $n_i = 0, \pm 1, \pm 2, \dots$  the set of points  $\{\mathbf{R}\}$  define a regular lattice with the basis vectors  $\mathbf{a}$ ,  $\mathbf{b}$ , and  $\mathbf{c}$ . This leads to the

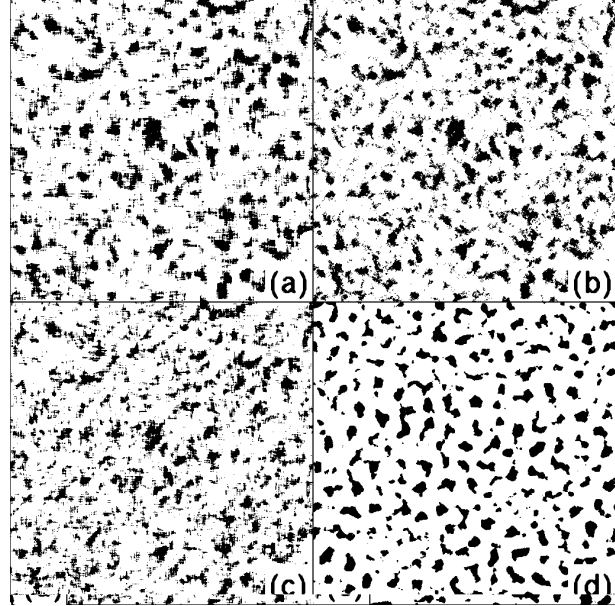


Figure B.1: Simulations of two-dimensional sections of porous media, Black represents the pore space and white the matrix. The bulk porosity is  $\langle \phi \rangle = 0.2$  for each of the four images. The models were generated by starting with a set of random numbers on a  $512 \times 512$  lattice. This random set was *filtered* using different filters that all fit inside a square of dimension  $\xi_F$ . Values inside the filter were averaged and assigned to the site at the center of the filter. The filtered set of numbers was discriminated at a level that gave a porosity of 0.2; (a) square filter; (b) circular filter; (c) L-shaped filter; (d) Fourier space filtering.

following definition of the local porosity:

$$\phi(\mathbf{R}, L) = L^{-d} \int \chi_c(\mathbf{r}; \mathbf{R}, L) \chi(\mathbf{r}) d^d \mathbf{r}. \quad (\text{B.1})$$

Here  $\chi_c$  is the indicator function of the measurement cell, that is,  $\chi_c = 1$  inside the cell and 0 outside the cell. Any shape of the measurement cell is suitable but a cubic cell (or square cell in two dimensions) is most convenient.

The *local porosity distribution* may now be introduced as the probability density  $\mu(\phi; \mathbf{R}, L)$  to find the local porosity  $\phi$  in the range from  $\phi$  to

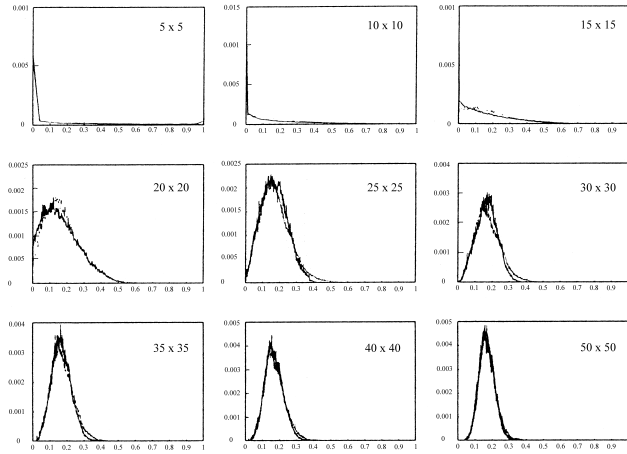


Figure B.2: The local porosity distributions  $\mu(\phi; L)$  as a function of  $\phi$  for increasing values of  $L$  for the image in figure B.1a.

$\phi + d\phi$  in a cell of linear dimension  $L$  at the point  $\mathbf{R}$ .

For a homogeneous porous medium the porosity distribution must be independent of  $\mathbf{R}$  so that  $\mu(\phi; \mathbf{R}, L) = \mu(\phi; L)$ . The function  $\mu(\phi; L)$  will be called the *local porosity distribution* at scale  $L$ . This function gives a characterization of a porous medium at any desired resolution  $L$ . In the limit of very large  $L$  we simply recover the porosity of the complete sample:

$$\langle \phi \rangle = \phi(\mathbf{R}, L \rightarrow \infty) = \int_0^1 \phi \mu(\phi; L) d\phi. \quad (\text{B.2})$$

independent of  $\mathbf{R}$  and  $L$ .

The local porosity distributions  $\mu(\phi; L)$  for the image in figure B.1a are plotted as a function of  $\phi$  for various values of  $L$  in figure B.2. These results show clearly that the local  $\mu(\phi; L)$  depends strongly on  $L$ . There are two competing effects. At small  $L$  the local geometries are simple and the measurement cell will in practice be either in the matrix, giving  $\phi = 0$ , or in the pore space with  $\phi = 1$ . Thus in the limit  $L \rightarrow 1$  one simply recovers the characteristic function  $\chi$  of the porous medium. For large  $L$  the geometry inside the measurement cell is as complicated as the porous medium itself and one finds  $\phi = \langle \phi \rangle$  with negligible fluctuations. The two limiting behaviors are separated by some characteristic length scale  $\xi$  which we call the *correlation length of the porous medium*. Thus we have

the following limits:

$$\begin{aligned}\mu(\phi, L \gg \xi) &= \delta(\phi - \langle \phi \rangle), \\ \mu(\phi, L \ll \xi) &= \langle \phi \rangle \delta(\phi - 1) + (1 - \langle \phi \rangle) \delta(\phi).\end{aligned}\quad (\text{B.3})$$

There are many ways to choose the characteristic length scale  $\xi$  for a porous medium. One important length scale is related by the correlations between local porosities. Let  $\phi_1$  be the local porosity at position  $\mathbf{R}_1$  and  $\phi_2$  the local porosity at  $\mathbf{R}_2$ . The correlations in local porosities are characterized by the two-cell distribution function  $\mu_2(\phi_1, \mathbf{R}_1; \phi_2, \mathbf{R}_2; L)$  that is the probability density for finding porosity  $\phi_1$  in the cell centered at  $\mathbf{R}_1$  and simultaneously the porosity  $\phi_2$  in the cell centered at  $\mathbf{R}_2$ . Again the assumption of homogeneity gives the simplification that we may express  $\mu_2$  in terms of the difference  $\mathbf{R} = \mathbf{R}_2 - \mathbf{R}_1$ , so that  $\mu_2(\phi_1, \mathbf{R}_1; \phi_2, \mathbf{R}_2; L) = \mu_2(\phi_1, \phi_2; \mathbf{R}, L)$ . The porosity *autocorrelation function* at scale  $L$  is defined as

$$\begin{aligned}C(\mathbf{R}, L) &= \frac{\langle (\phi(\mathbf{R}_0) - \langle \phi \rangle)(\phi(\mathbf{R}_0 + \mathbf{R}) - \langle \phi \rangle) \rangle}{\langle (\phi(\mathbf{R}_0) - \langle \phi \rangle)^2 \rangle} \\ &= \frac{\int_0^1 d\phi_1 \int_0^1 d\phi_2 (\phi_1 - \langle \phi \rangle)(\phi_2 - \langle \phi \rangle) \mu_2(\phi_1, \phi_2; \mathbf{R}, L)}{\int_0^1 d\phi (\phi - \langle \phi \rangle)^2 \mu(\phi; R, L)}.\end{aligned}\quad (\text{B.4})$$

For isotropic homogeneous porous media  $C(\mathbf{R}, L)$  depends only on the distance  $R$  between the measurement cells so that we may write  $C(R, L)$  for the correlation function in this case. The correlation function is normalized so that  $C(R \rightarrow 0, L) = 1$  independent of  $L$ . Also, as the separation of the measurement cells increases their porosity becomes *uncorrelated*, and we have  $C(R \rightarrow \infty, L) = 0$ . The correlation function that is most convenient to evaluate is the pixel-pixel correlation function obtained by setting  $L = 1$ , that is, the box size  $L$  equals the pixel size.

In figure B.3 we show the correlation function  $C(R, L = 0)$  calculated for the images shown in figure B.1. Using the correlation function shown in figure B.3 we use equation (B.5) to find the correlation length  $\xi = 20$ .

Hilfer chose<sup>143</sup> to identify the correlation length  $\xi$  separating correlated from uncorrelated measurement cells by the expression

$$\xi^2 = \frac{\int d^3R R^2 C(R, 1)}{\int d^3R C(R, 1)}.\quad (\text{B.5})$$

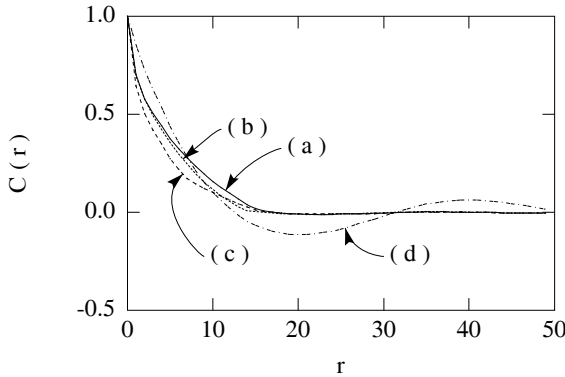


Figure B.3: The pixel-pixel correlation function  $C(r, L = 0)$  as a function of  $r$  for the images in figure B.1.

This definition is simple to evaluate in practice. A more robust definition of the characteristic length<sup>145</sup> related to the *information content* or *information entropy*  $S$  of the distribution

$$S(L) = - \int_0^1 \mu(\phi; L) \ln\{\mu(\phi; L)\} d\phi. \quad (\text{B.6})$$

By choosing the length scale to be  $\xi_S$  defined by  $(dS/dL)|_{L=\xi_S} = 0$  that minimized the information or maximized the entropy consistent with the distribution  $\mu$  being normalized leads to a unique length scale  $\xi_S$  with a distribution  $\mu(\phi, \xi_S)$  that is as ‘wide’ as possible and *unbiased* in the sense that it gives the least precise description of the actual values of the pixel values in the given image being analyzed.

With the length scale  $\xi$  determined we may define *the* local porosity distribution as the distribution

$$\mu(\phi) = \mu(\phi, L = \xi). \quad (\text{B.7})$$

Simultaneously with this convention it will be assumed that the local geometries at scale  $L < \xi$  are ‘simple’. This is called the hypothesis of *local simplicity*, and will be discussed further later on.

The definition of the local porosity distribution as  $\mu(\phi, \xi)$  is optimal in the sense that it contains a maximum amount of information based purely on the concept of porosity. The choices  $L \gg \xi$  and  $L \ll \xi$  yield the  $\delta$ -function distributions given in equation (B.3) that contain little information. We expect that if we consider the porous medium to be composed

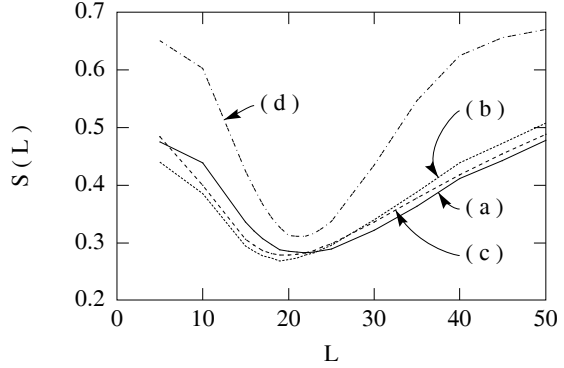


Figure B.4: The information entropy function  $S(L)$  as a function of  $L$  for the images in figure B.1. The image entropy function distinguishes very well the images in figure B.1 that were constructed to differ only in small rather subtle details. This sensitivity to geometrical detail is a very useful aspect of  $S(L)$  and permits the determination of a well defined length scale  $\xi_S$  at which  $S(L)$  is a minimum.

of blocks of linear size  $L = \xi$  then we may to a good first approximation consider these blocks to be statistically independent (uncorrelated) so that we may concentrate on the physical properties within each cell and then combine them use some effective medium or molecular field theory to calculate the global properties of the medium. We shall pursue this discussion further in later chapters.

## Appendix C

# Capillary Rise

We have capillary tubes of three sizes. The volume  $V$  marked on the tube is  $V = \pi a^2 L$ , where  $L$  is the distance of the fill mark from the end of the tube, and  $a$  is the insider radius of the capillary, which may be estimated to be  $a = \sqrt{V/\pi L}$ .

The capillary rise is

$$h = 2\sigma_{l,g} \cos \theta / (\rho_l - \rho_g) ga . \quad (\text{C.1})$$

Here the acceleration of gravity is  $g = 980 \text{ cm/s}^2$ , the density difference between water and air is approximately  $\Delta\rho \simeq 1.0 \text{ g/cm}^3$ . The angle of contact is taken to be  $0^\circ$  for the *receding* meniscus. For a fluid the capillary constant is defined as

$$\alpha^2 = ha = 2\sigma_{l,g}/g\Delta\rho . \quad (\text{C.2})$$

Experimental values for water are found in Table C.1.

### C.1 The Surface Tension of Water

We may measure the surface tension of water, by observing the capillary rise,  $h$ , in capillaries, and using the expression

$$\sigma_{l,g} = h \frac{a\Delta\rho g}{2 \cos \theta} \simeq \frac{1}{2} ha\Delta\rho g \quad (\text{C.3})$$

where we assume that water wets the glass capillaries, that is,  $\theta \simeq 0$ . Dip the tip of a capillary into water and it will rise. However, in practice the

$t$	(°C)	0	20	25
$\sigma$	(dyn/cm)	75.6	72.75	71.97
$\rho$	(g/cm <sup>3</sup> )	0.998647	0.9982041	0.9970449
$\mu$	(poise=g/cm s)		0.010019	0.008904
$\alpha$	(cm)	0.3927	0.3855	0.3837

Table C.1: Capillary constant for water. Acceleration of gravity:  $g = 980.665 \text{ cm/s}^2$

V $\mu\text{l}$	L (cm)	a (cm)	Cat. No.
5	5.5	0.0170	53432-706
20	7.62	0.0289	53432-740
50	7.30	0.0467	53432-783

Table C.2: Dimensions of VWR Scientific glass capillaries

water does not rise to the expected height, due to *contact angle hysteresis*. The point is that although the contact angle is an equilibrium thermodynamic quantity, which in principle only depends on the fluid the vapor (gas) and the solid wall, this equilibrium is in practice not reached. The contact line remains in a non-equilibrium position, in a thermodynamic meta-stable state, due to surface irregularities and impurities that pin the surface locally. Therefore, one obtains better results by dipping the capillary a bit too deep, withdraw it slowly, until a lower meniscus is formed as the capillary leaves the surface of the water. The height of capillary rise,  $h$ , can be approximately measured by a ruler to say 5%. In Table C the results of such measurements are shown, together with the estimated surface tension.

## C.2 Imbibition in Blotting Paper

The Ahlstrom Electrophoresis and Blotting paper (Grade 238, size  $10 \times 15 \text{ cm}$ ) is a paper that will imbibe water spontaneously. With a micro pipette, filled to the mark, touch the paper and an ellipsoidal wet spot will grow until the capillary is empty. Thus the blotting paper (thickness of  $d \simeq 0.035 \text{ cm}$ ) is porous. The pores are smaller than the diameter of the capillaries

	5	20	50
$V$ ( $\mu\text{l}$ )	0.0170	0.0289	0.0467
$a$ (cm)			
$h$ (cm)	9.65 9.72 9.82 9.60	5.25 5.98 5.22 5.20	3.20 3.10 3.15 3.12
$\langle h \rangle$ (cm)	9.70	5.41	3.16
$\sigma$ (dyn/cm)	80.8	76.7	72.5

Table C.3: The capillary rise of water at room temperature in glass capillaries of different diameter, and the estimated surface tension.

	5	20	50
$V$ ( $\mu\text{l}$ )	0.0170	0.0289	0.0467
$a$ (cm)			
$D_a$ (cm)	0.7	1.40	2.10
$D_b$ (cm)	0.63	1.18	1.85
$D_b/D_a$	0.90	0.84	0.88
$A$ ( $\text{cm}^2$ )	0.346	1.30	3.05
$V_{tot}$ ( $\text{cm}^3$ )	0.0118	0.0441	0.1037
$\phi = V/V_{tot}$	0.42	0.45	0.48

Table C.4: Porosity of Grade 238 blotting paper

and therefore the capillary action will draw the water from the capillary to the paper. Table C.2 shows the result of the average dimensions in two experiments for each capillary size. Table C.5 shows results for ordinary blotting paper. The results in the tables show that the paper is anisotropic with the ellipticity of the spot being approximately  $e \simeq 0.9$ . This anisotropy is a result of the paper making process. The results in Tables C.2 and C.5 allows us to estimate the porosity of the paper to be  $\phi \simeq 0.45$  for both types of blotting paper.

	5	20	50
$V$ ( $\mu\text{l}$ )	0.0170	0.0289	0.0467
$a$ (cm)			
$D_a$ (cm)	0.6	1.08	1.60
$D_b$ (cm)	0.52	0.90	1.42
$D_b/D_a$	0.87	0.83	0.89
$A$ ( $\text{cm}^2$ )	0.25	0.76	1.78
$V_{tot}$ ( $\text{cm}^3$ )	0.014	0.044	0.104
$\phi = V/V_{tot}$	0.35	0.45	0.48

Table C.5: Porosity of ordinary blotting paper (DZ/165 # BBL-18);  $d = 0.058$  cm.

### The Porosity of Blotting Paper

## C.3 The Dynamics of Capillary Rise

Fluid rises in a capillary due to surface tension. At what rate does water in the capillary rise?

### C.3.1 A Horizontal Tube

If the capillary tube is horizontal, the meniscus will move with a velocity controlled only by the surface tension  $\sigma$ , the angle of contact  $\theta$ , the fluid viscosity,  $\mu$ , and the capillary radius  $a$ . Use a coordinate system where  $x$  is along the capillary tube, with  $x = 0$  at the entrance of the tube where it is immersed in water.

The pressure in the air is  $p_0$ . The pressure in the fluid, just below the flat interface between the water and the air is also  $p_0$ . Therefore the pressure in the fluid at the entry of the capillary, is

$$p(x = 0) = p_0$$

Let the radius of the capillary be  $a$ , as before. The radius of curvature of the meniscus depends on the angle of contact  $\theta$ , and is given by  $R_c = a/\cos\theta$ . The pressure, inside the fluid, just below the surface of the meniscus is therefore

$$p(x) = p_0 - 2\sigma/R_c$$

Where the Young-Laplace pressure difference is positive if the angle of contact is less than  $\pi/2$ . The pressure drop, in the water inside the capillary,

is  $\Delta p = (p(0) - p(x))$ , is distributed over the length  $x$ , which is the position of the meniscus relative to the inlet. There is therefore a pressure gradient in the fluid given by

$$\frac{dp}{dx} = -\frac{2\sigma}{xR_c} \quad (\text{C.4})$$

For a capillary with a circular cross section, as we discuss here, the meniscus will move with a velocity given by:

$$\frac{dx}{dt} = U = \frac{Q}{\pi a^2} = -\frac{a^2}{8\mu} \left( \frac{dp}{dx} \right)$$

It follows that the position of the meniscus is given by

$$x = a\sqrt{t/\tau} \quad \text{where} \quad \tau = 2\mu R_c/\sigma = \frac{2\mu a}{\sigma \cos \theta} \quad (\text{C.5})$$

The characteristic time,  $\tau$ , depends on surface tension, angle of contact and the capillary radius. A large viscosity and a low surface tension leads to slow imbibition. Note that the characteristic time  $\tau$  is proportional to the radius of curvature of the meniscus. For the situation that the angle of contact is zero, one may find the characteristic pores size by measuring the position of the meniscus as a function of time.

### C.3.2 A Vertical Tube

Taking gravity into account one finds that flow occurs only if there is a gradient in hydraulic potential

$$\Phi = p + \rho g z. \quad (\text{C.6})$$

Thus for  $\Phi = Cte$ , or  $dp/dz = -\rho g$ , we find the well known result from hydrostatics that the pressure increases with depth. The gradient in  $\Phi$  is then

$$\frac{d\Phi}{dz} = \frac{[(p_0 - 2\sigma/R_c) + \rho g z] - p_0}{z} = \rho g - \frac{2\sigma}{zR_c} \quad (\text{C.7})$$

the equilibrium state is reached, as in equation (C.1), for

$$z = h = \frac{2\sigma}{R_c \rho g}.$$

If the meniscus is not at  $z = h$ , then it will move up for  $z < h$  and move down for  $z > h$ . A pressure gradient in the capillary will drive a flow as

given by Darcy's law for the capillary. The average flow velocity is also the rate of advancement of the meniscus, therefore we have

$$\frac{dz}{dt} = U = Q/\pi a^2 = -\frac{a^2}{8\mu} \left( \frac{d\Phi}{dz} \right)$$

Here  $\mu$  is the viscosity of the fluid. Therefore we find that velocity of the meniscus is given by:

$$\frac{dz/h}{dt} = \frac{1}{4\tau} \text{Bo} \left( 1 - \frac{h}{z} \right) = \frac{2}{\tau} \left( \frac{a}{z} - \frac{a}{h} \right) \quad (\text{C.8})$$

Where,  $h$  is the capillary rise equation (C.1), and we have introduced the dimensionless *Bond number*,  $\text{Bo}$ , which measures the relative importance of gravitational to capillary forces:

$$\boxed{\text{Bo} = \frac{g\rho a^2}{\sigma \cos \theta} = 2 \frac{a}{h}} \quad (\text{C.9})$$

The characteristic time is given as in equation (C.5) as before. Equation (C.8) shows that, the meniscus will rise for  $z < h$ , and fall for  $z > h$ , as expected. In the limit  $z \ll h$  we find the same result as in equation (C.5). If we start *near*  $z = h$ , we may solve equation (C.8) explicitly:

$$h - z(t) = (h - z(t_0)) \exp(-(t - t_0)/\tau_h) \quad (\text{C.10})$$

Where the relaxation time to reach height  $z = h$  is

$$\boxed{\tau_h = \frac{8}{\text{Bo}^2} \tau = 2\tau(h/a)^2} \quad (\text{C.11})$$

We find that this relaxation time for a given capillary has the form  $\tau_h \sim \sigma\mu$ , and therefore it increases with viscosity, as expected, but  $\tau_h$  also increases with surface tension, since  $\sigma$  also determines the capillary rise  $h$  that set the relevant length scale.

## C.4 Imbibition in Blotting Paper

Blotting paper is designed to absorb fluids quickly. We use strips of blotting paper that has been laminated between two sheets of plastic in order to prevent evaporation during the wicking process.

When one end of the laminated paper is dipped into water a front is seen to rise in the paper. For the blotting paper used here the capillary

height, and therefore the capillary constant for the paper is not known. However, the capillary height,  $h$ , is well above the length,  $L$ , of the paper, and therefore it does not matter much whether the paper is vertical or horizontal during the imbibition process.

The process of imbibition is due to the water wetting the paper, which can be thought off as a porous medium. Thus there is a capillary pressure

$$\Delta p_c = 2\sigma/a \quad (\text{C.12})$$

where  $a$  is a characteristic pore *radius*, for the paper. The paper has a permeability  $k$ , and the flow velocity is therefore given by *Darcy's law*:

$$U = -\frac{k}{\mu} \frac{dp}{dx}; \quad (\text{C.13})$$

The front velocity is simply  $(dx/dt) = U$ , and the pressure gradient is  $dp/dx = -\Delta p_c/x$ , and we find

$$\frac{dx}{dt} = \frac{k2\sigma}{a\mu} \frac{1}{x} \quad (\text{C.14})$$

We find a solution of this equation has the same form as equation (C.5):

$$x^2 = 2Dt, \quad \text{with} \quad D = \frac{2\sigma k}{a\mu}. \quad (\text{C.15})$$

The constant  $D$  characterizes the imbibition process of a given paper with a given fluid.  $D$  has the dimension as a diffusion constant, that is,  $\text{cm}^2/\text{s}$ . The permeability of the paper is not known, and we write is as  $k = K_0 \frac{a^2}{8}$ , where  $K_0$  is a factor that measures the deviation from what would be expected in a capillary tube. We may determine  $D$  from simple experiments, and for known  $\sigma$  and  $\mu$ , we get an expression for the effective paper pore radius:

$$K_0 a = 4 \frac{D\mu}{\sigma}$$

(C.16)

Figure C.1 shows that equation (C.15) accurately describes the imbibition front.

We found the results shown in table C.6: Thus we find that the typical pore radius  $a$  is a fraction of a micron, unless the numerical constant  $K_0$ , happens to be large. I expect  $K_0 \simeq 10\text{--}100$ , and therefore the pore size to be of the order of a few micron. We need to determine  $k$  independently, if we are to estimate  $a$  more precisely. To do that we would need to measure the flow through the paper as function of pressure gradient, and then

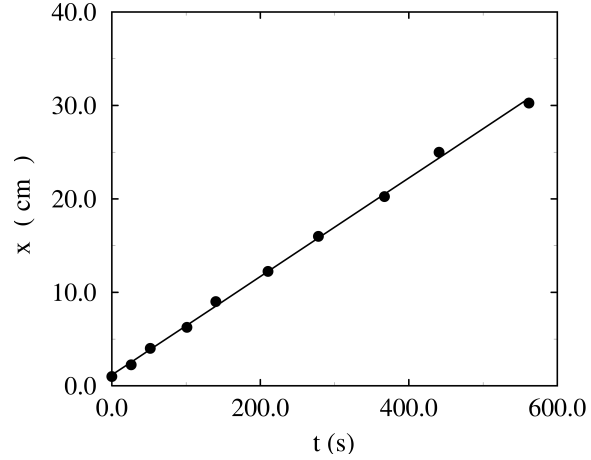


Figure C.1: Imbibition front position as a function of time for the bb18 blotting paper. The slope is  $2D = 0.0526 \pm 0.0007 \text{ cm}^2/\text{s}$ .

Sample	$D (\text{cm}^2/\text{s})$	$K_0a (\mu\text{m})$
238	$0.0491 \pm 0.0002$	0.271
bb-18	$0.0263 \pm 0.0004$	0.145
chalk	$0.0278 \pm 0.0004$	0.143

Table C.6: The effective pore radius  $K_0a$ , for chalk and two types of blotting paper.

find  $k$  from Darcy's law. Such an experiment requires more sophisticated equipment.

The results for chalk and for the type 238 blotting paper are shown in Figures C.3 and C.2

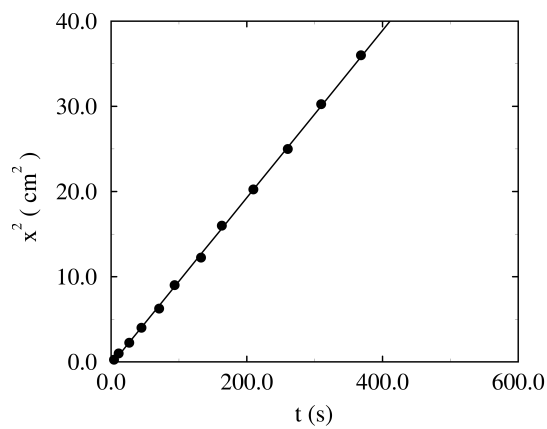


Figure C.2: Imbibition front position as a function of time for the 238 blotting paper. The slope is  $2D = 0.0982 \pm 0.0003 \text{ cm}^2/\text{s}$ .

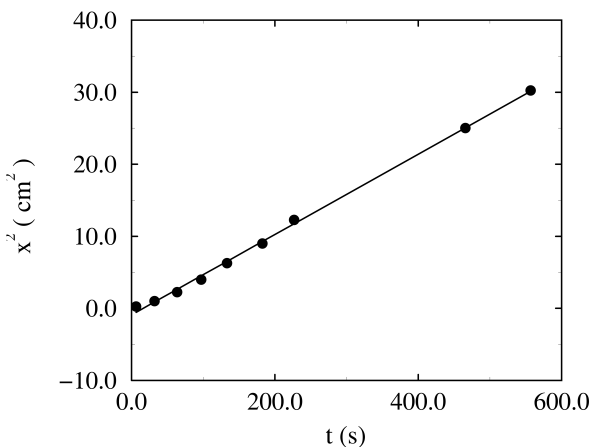


Figure C.3: Imbibition front position as a function of time for chalk. The slope is  $2D = 0.0557 \pm 0.0008 \text{ cm}^2/\text{s}$ .

## Appendix D

# Erosional Flow in Porous Media

When water flows through an unconsolidated sand, the stress due to the flow may cause the sand to fall apart, and a number of spatial and temporal instabilities arise.

A simple case has recently been discussed by Mills, Cerasi and Fautrat (see Ref. [1]).

### D.1 Flow in a Porous Medium

Darcy's equation describes the flow of a fluid in a porous medium.

$$\mathbf{U} = -\frac{k}{\mu}(\nabla p - \rho\mathbf{g}) \quad (\text{D.1})$$

Here the average flow (Darcy) velocity is  $\mathbf{U} = Q/A$ , where  $Q$  is the volume flux (in  $\text{m}^3/\text{s}$ ) through a cross-section of area  $A$ ,  $k$  is the permeability of the porous medium,  $\mu$  the viscosity of the fluid,  $p$  the pressure in the fluid,  $\rho$  the fluid density, and  $\mathbf{g}$  the acceleration of gravity (typically  $(0, 0, -g)$  in a coordinate system with the  $z$ -axis vertical and up).

The permeability  $k$  depends on the packing of the porous medium. The permeability for packs of sand is approximately given by the Carman-Kozeny relation:

$$k = \frac{\phi^3}{K_0 \mathcal{T}^2 S^2} . \quad (\text{D.2})$$

Here  $\phi$  is the porosity,  $\mathcal{T}$  is the tortuosity, and  $S$  is the specific surface of the sand pack. The Kozeny constant,  $K_0$ , is approximately 2. For packings of spheres (of radius  $a$ ) to various porosities the Carman-Kozeny expression for the permeability is

$$k = \frac{a^2}{9K} \frac{\phi^3}{(1 - \phi)^2}, \quad (\text{D.3})$$

is in agreement<sup>92</sup> with experimental results on porous media consisting of packs of spherical particles, with  $K \simeq 5$ . The random close packing limit for spheres<sup>27, 28, 29, 30</sup> is known to be  $c_{\text{RCP}} = 0.6366 \pm 0.0005$  and therefore  $\phi_{\text{RCP}} = 0.3634 \pm 0.0005$ . From equation (D.3) it follows that the permeability for random close packed spheres is approximately

$$k_{\text{RCP}} \simeq \frac{a^2}{380}, \quad \text{with } \phi_{\text{RCP}} = 0.3634. \quad (\text{D.4})$$

If spheres are just poured into a container the density will be somewhat less (see the review [] of granular media by Jaeger & Nagle (1992)). Scott<sup>35</sup> noted different ways of packing  $\frac{1}{8}$ -balls into containers that “there is a range of random packings lying between two well defined limits. The limits are called here ‘dense random packing’ and ‘loose random packing’.” Scott measured the packing density of spheres in cylinders with dimpled walls as a function of filling height  $h$ . The packing density was extrapolated to  $1/h = 0$ . For loose packings the balls fill the vessel essentially by rolling down a slope of random-packed balls. The dense packing are the obtained by gentle shaking and tapping. ‘In both types of packings the balls are always rigid in the sense that uniform pressure over the top will not alter the packing.’

The loosest random packing that is still mechanically stable under a give force  $F$  is called the *random loose packing* (RLP). In sand-piles the force  $F$  is due only to the weight of the particles and thus to the acceleration of gravity  $g$ . Experiments<sup>37</sup> by Onoda and Lininger (1990) show that in the limit  $g \rightarrow 0$  one finds  $c_{\text{RLP}} = 0.555 \pm 0.005$ . A random packing that has a density larger than the RLP density must *expand* when the packing is deformed. In recent computer simulations<sup>38</sup> packing densities of spheres in the range 0.5447 and 0.6053 were found for various algorithms for generating the packings. Thus the lowest density was below the RLP limit. With the Carman-Kozeny expression we therefore have for the random loose packing:

$$k_{\text{RLP}} \simeq \frac{a^2}{157}, \quad \text{with } \phi_{\text{RLP}} = 0.445. \quad (\text{D.5})$$

Figure D.1: Pressures and forces for an unconsolidated sand

## D.2 Dissipation and Forces

We expect the Darcy equation (D.1) and the Carman-Kozeny expression (D.3) to hold for a porous medium consisting of an unconsolidated sand. Consider such a porous medium of cross-section  $A$ , sample length  $L$ . Let the pressure at the inlet surface be  $p_0$  and at the outlet the pressure is  $p_0 - \Delta p$ , when there is a flow (of water, say) with a volume flux  $Q$ , see figure D.1. The *dissipation*,  $\dot{S}$ , in the stationary state is simply the work done per unit time and unit volume:

$$\dot{S} = \frac{Q\Delta p}{AL} = -\mathbf{U} \cdot \nabla p = \frac{\mu}{k} U^2. \quad (\text{D.6})$$

The dissipation has units  $[\dot{S}] = W/m^3$ .

When the fluid is moving through the sample, the solid matrix must be held in place by external (mechanical) forces, that oppose the viscous drag of the fluid at solid matrix surface. This force may be deduced from the mechanical force balance. The force density  $\mathbf{f}$  is simply

$$\mathbf{f} = \frac{p_0 A - (p_0 - \Delta p)}{AL} = -\nabla p. \quad (\text{D.7})$$

For the sake of discussion assume the particles are spherical with radius  $a$ . What is the average force on the particles? Assume that the solid matrix (here the spherical particles) have a filling factor  $c = 1 - \phi$ , where  $\phi$  is the porosity. The volume per particle is therefore  $V = 4\pi a^3/3c$ , and we find the force per sphere from the force density given by

$$\mathbf{F}_s = \mathbf{f} \frac{4\pi a^3}{3c} = \frac{4\pi a^3 \mu}{3ck} \mathbf{U}, \quad (\text{D.8})$$

where we used Darcy's law equation (D.1) for the last expression. The force on a sphere moving with a velocity  $\mathbf{U}$ , through an infinite fluid is given by Stokes law:

$$\mathbf{F}_{\text{stokes}} = 6\pi\mu a \mathbf{U} \quad (\text{D.9})$$

If many spheres move through the fluid, all at the same velocity, we expect the drag on each sphere to be:

$$\mathbf{F}_s = C_D \mathbf{F}_{\text{stokes}} \quad (\text{D.10})$$

where the *drag coefficient*  $C_D$ , is given in terms of the permeability and the filling factor as

$$C_D = \frac{2a^2}{9kc} = \frac{2}{9(1-\phi)} \frac{a^2}{k}. \quad (\text{D.11})$$

Note that this is an exact relation between the drag factor and the permeability for arbitrary (random or periodic) packings of spheres. I expect the relation to hold even for grains of sand of different size and shapes but with  $a^2$  replaced by  $\langle a^2 \rangle$ , and with  $C_D$  being the average drag factor. If we use the Carman-Kozeny expression (D.3) we find a simple expression for the drag coefficient:

$$C_D \simeq \frac{9K(1-\phi)}{\phi^3} \simeq 132, \quad (\text{D.12})$$

where the numerical value is obtained using  $K = 5$  and  $\phi = \phi_{\text{RCP}} = 0.3634$ .

### D.3 Erosion in the Hele-Shaw Cell

For a Hele-Shaw cell consisting of two parallel plates separated by a gap distance  $b$ , the Darcy equation (D.1) holds even if there is no porous material in the gap, that is, the porosity is  $\phi = 1$ . In this case the permeability of the Hele-Shaw cell is

$$k = \frac{b^2}{12}, \quad \text{for } \phi = 1. \quad (\text{D.13})$$

If the gap in the Hele-Shaw cell is filled by an unconsolidated sand, then we still have Darcy's law for the fluid flow, but now with a permeability that depends on the porosity, size distribution and packing of the sand — as long as the sand does not move.

In the other limit,  $\phi \rightarrow 0$ , we have sand particles moving with the fluid as a suspension. In the limit of very small volume fractions  $c$  of the sand

Figure D.2: Flow through a Hele-Shaw channel, where the first half is filled unconsolidated sand, whereas the second half contains a suspension of sand grains. The interface between the two parts may move to the left by erosion of the front. The coordinate system chosen has  $x$  across the channel of width  $W$ ,  $y$  perpendicular to the plates separated by  $b$ , and  $z$  along the flow direction

we expect the flow to behave as if the fluid has an effective viscosity  $\mu_E$ , first calculated by Einstein<sup>63, 64</sup>

$$\mu_E = \mu_0(1 + 2.5c + \dots) . \quad (\text{D.14})$$

### D.3.1 Stationary Erosion

Packings of granular materials in containers have the interesting property that the pressure (stress) does *not* increase with depth. The pressure (stress) in sand packed in a cylindrical container of radius  $R$ , increases with depth, as measured from the top free surface, until a depth approximately equal to  $R$ , and then remains constant independent of depth as depth increases further, the rest of the load is transferred by frictional forces to the container wall, which must be strong enough to support both the radial and the vertical stresses. For flow in a Hele-Shaw cell, we expect the viscous stress on the granular packing to be transferred to the walls, over a distance that equals the cell height  $b$ .

For the sake of discussion assume that the interface between the sand and the flowing suspension moves to the left with a velocity of magnitude

$V$ , that is,  $\mathbf{V} = (0, 0, -V)$ . We have the following equations:

$$U_w^{(1)} = u_w^{(1)}\phi_1 \quad U_p^{(1)} = u_p^{(1)}c_1 = 0 \quad (\text{D.15})$$

$$U_w^{(2)} = u_w^{(2)}\phi_2 \quad U_p^{(2)} = u_p^{(2)}c_2 \quad (\text{D.16})$$

Here  $U_w^{(1)}$  and  $U_w^{(2)}$  are the Darcy velocities of the water on the left (1) and right hand side (2) of the interface respectively. The average actual velocities of the water are  $u_w^{(1)}$  and  $u_w^{(2)}$  for the left and right hand sides respectively. The porosities are  $\phi_1 = (1 - c_1)$  and  $\phi_2 = (1 - c_2)$ .

In a coordinate system that is moving with the front going to the left at a velocity  $V$ , we have the following relations:

$$\hat{u}_w^{(1)} = u_w^{(1)} + V \quad \hat{u}_p^{(1)} = V \quad (\text{D.17})$$

$$\hat{u}_w^{(2)} = u_w^{(2)} + V \quad \hat{u}_p^{(2)} = u_p^{(2)} + V \quad (\text{D.18})$$

Mass (really volume) conservation (of both water and sand) in the moving frame then gives the following relations for the velocities in the moving frame (denoted by a ‘hat’ ^ )

$$\hat{u}_w^{(1)}\phi_1 = \hat{u}_w^{(2)}\phi_2 \Rightarrow (u_w^{(1)} + V)\phi_1 = (u_w^{(2)} + V)\phi_2 \quad (\text{D.19})$$

$$\hat{u}_p^{(1)}c_1 = \hat{u}_p^{(2)}c_2 \Rightarrow Vc_1 = (u_p^{(2)} + V)c_2 \quad (\text{D.20})$$

These equations may be rewritten to give:

$$U_w^{(1)} = U_w^{(2)} + U_p^{(2)} \quad (\text{D.21})$$

$$U_p^{(2)} = c_2u_p^{(2)} = (c_1 - c_2)V \quad (\text{D.22})$$

The particles flowing with water to the right of the front, will move with average velocity that is smaller than the average fluid velocity. However, in the Stokes regime of low Reynolds number flow, the particle velocity is expected to be proportional to the fluid velocity, that is,

$$u_p = \alpha(c, a/b)u_w . \quad (\text{D.23})$$

Here the constant of proportionality  $\alpha(c, a/b)$ , depends on the ratio of the particle radius,  $a$ , to the plate separation  $b$ , and on the filing factor of the suspension. We expect that  $\alpha(c \rightarrow 0, a/b \rightarrow 0) = 1$ , since in this limit the particles are simply tracer particles convected with the flow. As  $c$  is increased towards the packing fraction of the unconsolidated sand, that is,  $c = c_1 \simeq c_{\text{RCP}} = 0.6366 \pm 0.0005$ , we expect the sand velocity to vanish; therefore we must have  $\alpha(c \rightarrow c_1, a/b) \rightarrow 0$ . Using equation (D.23) in

Figure D.3: A local perturbation in the front may grow in time.

equations (D.21) and (D.22) I find the front velocity  $V$  and the velocity of the water on the right hand side:

$$U_w^{(2)} = \frac{1 - c}{1 - c + c\alpha} U_w^{(1)} \quad (\text{D.24})$$

$$V = \frac{c\alpha}{(c_1 - c)(1 - c + c\alpha)} U_w^{(1)} \quad (\text{D.25})$$

Thus the front velocity is given in terms of the suspension particle concentration,  $c = c_2$ , the close-packing concentration  $c_1$ , the Darcy filtration velocity,  $U_w^{(1)}$ , driving the system, and the constitutive relation  $\alpha$ . Of course, we may also consider  $U_w^{(1)}$ ,  $V$  and  $c_1$  to be given; in that case we may determine  $U_w^{(2)}$  and  $c_2$  for the water Darcy velocity of the suspension and the volume fraction of the suspension.

### D.3.2 Stability of the Erosion Front

In a frame of reference moving with the steady state erosion front we just see the flow of particles and water flow past the origin. However, if the front is perturbed, say with a local increase of  $V$  (see figure D.3) this perturbation may grow exponentially in time, since it will see an increase in pressure gradient and therefore release even more particles. This instability is analogous to the Saffman and Taylor<sup>129</sup> viscous fingering instability that arises in a Hele-Shaw cell when a less viscous fluid displaces a more viscous fluid. Following Saffman and Taylor we will introduce velocity potentials that are useful in two-dimensional flow. We first note that the Darcy equation (D.1) holds in the two regions independently. In region (1) we

have:

$$\mathbf{U}_1 = -\frac{k_1}{\mu_1} \nabla p_1 , \quad \nabla \cdot \mathbf{U}_1 = 0 , \quad \Rightarrow \quad \nabla^2 p_1 = 0 . \quad (\text{D.26})$$

Here the permeability of the unconsolidated sand pack is  $k_1$  (which, of course, is less than the Hele-Shaw channel permeability  $k = b^2/12$ ), and  $\mu_1 = \mu$  is the water viscosity. The Darcy water flow,  $\mathbf{U}_1$ , is incompressible as expressed in equation (D.26).

In region (2) the situation is more complicated. The idea is that the flow here is the flow of a suspension. For low concentrations, that is,  $c = c_2 \ll 1$ , we may consider the total flow of water and sand to be given by an equation of the form

$$\mathbf{U}_2 = -\frac{k_2}{\mu_2} \nabla p_2 , \quad \nabla \cdot \mathbf{U}_2 = 0 , \quad \Rightarrow \quad \nabla^2 p_2 = 0 . \quad (\text{D.27})$$

Here  $U_2 = U_w^{(2)} + U_p^{(2)}$  is the total volume flux per unit area. The mobility  $M_2 = k_2/\mu_2$  will be some function of the particle concentration, the channel width,  $b$ , and the particle size  $a$ . For low concentrations we may take  $\mu_2 = \mu_E = \mu(1 + 2.5c)$  and  $k_2 = b^2/12$ .

Following Saffman and Taylor we may introduce the *velocity potential*  $\chi_i$  to give the Darcy velocities in the moving frame (with  $i = 1, 2$ ):

$$\hat{\mathbf{u}}_i = -\nabla \chi_i , \quad (\text{D.28})$$

where the velocity potentials satisfy the Laplace equations

$$\nabla^2 \chi_i = 0 \quad (\text{D.29})$$

are given by

$$\chi_i = \frac{k_i}{\mu_i} \left( p_i + P_i(t) - \frac{\mu_i}{k_i} V z \right) . \quad (\text{D.30})$$

In order to test the stability of the advancing interface we follow standard practice<sup>129</sup> and assume that the straight interface is perturbed by a sinusoidal displacement so that in the frame of reference moving with the average velocity  $V$  the position of the interface is given by the real part of

$$\zeta = \epsilon \exp(\gamma t + iqx) , \quad (\text{D.31})$$

as illustrated in figure D.3. The wavelength of the perturbation is  $\lambda = 2\pi/q$ . The growth rate of the perturbation is  $\gamma$ . For a stable interface the perturbation  $\zeta$  will decay in time and  $\gamma < 0$ . If the growth rate is positive  $\gamma > 0$ , a perturbation of infinitesimal amplitude  $\epsilon$  will grow exponentially.

We shall limit ourselves to a discussion of the onset of instability and assume the perturbation to be *infinitesimal* and neglect terms of order  $\epsilon^2$  and higher.

The velocity of the interface in the moving frame must equal the fluid velocities so that we have the boundary conditions

$$\frac{\partial \zeta}{\partial t} = - \left( \frac{\partial \chi_1}{\partial z} \right)_{z=\zeta} = - \left( \frac{\partial \chi_2}{\partial z} \right)_{z=\zeta}. \quad (\text{D.32})$$

As is easily seen the following solutions of the Laplace equations (D.29)

$$\begin{aligned} \chi_1 &= -\frac{\gamma}{q}\epsilon \exp(+qz + iqx + \gamma t), \\ \chi_2 &= +\frac{\gamma}{q}\epsilon \exp(-qz + iqx + \gamma t), \end{aligned} \quad (\text{D.33})$$

satisfy the boundary conditions given in equation (D.32) to *first order* in  $\epsilon$ . The velocity potential of the perturbation  $\chi_1 \rightarrow 0$  as  $z \rightarrow -\infty$  and  $\chi_2 \rightarrow 0$  as  $z \rightarrow \infty$ , so that the perturbation is localized at the interface.

The simplest assumption is that the pressure in fluid  $p_1$  equals the pressure of the suspension  $p_2$  at the interface:

$$p_1(z = \zeta) = p_2(z = \zeta). \quad (\text{D.34})$$

We may also have a pressure jump  $\Delta p$  at the boundary without changing the results obtained below. We note that for  $q\zeta \ll 1$  to order  $\epsilon$  we have that  $\chi_1 = -\zeta\gamma/q$  and  $\chi_2 = +\zeta\gamma/q$ . Therefore we may express the boundary condition (D.34) in terms of the velocity potentials as follows:

$$-\frac{\mu_1}{k_1} \frac{\gamma}{q} \zeta + \frac{\mu_1}{k_1} V\zeta = \frac{\mu_2}{k_2} \frac{\gamma}{q} \zeta + \frac{\mu_2}{k_2} V\zeta. \quad (\text{D.35})$$

Here, we have set  $P_1 = P_2$  since we have assumed that there is no pressure jump across the interface. Equation (D.35) may be rewritten to give:

$$\gamma = \left( \frac{\frac{\mu_1}{k_1} - \frac{\mu_2}{k_2}}{\frac{\mu_1}{k_1} - \frac{\mu_2}{k_2}} \right) Vq = \left( \frac{M_1^{-1} - M_2^{-1}}{M_1^{-1} + M_2^{-1}} \right) Vq. \quad (\text{D.36})$$

Now since  $V$  is positive (see equation (D.25)), and we expect the mobility  $M_1 = \frac{k_1}{\mu_1}$  to be much less than the mobility of the slurry  $M_2 = \frac{k_2}{\mu_2}$ , we find that the growth rate  $\gamma$  is positive and the front is unstable. The instability grows indefinitely with the wavenumber  $q$ . This last result is unreasonable since we must demand that  $qa < 1$  for a continuum description to hold. In fact, we expect the plate separation to be important, since granular media behave differently on depth small compared with the vessel dimension. We

therefore must introduce a cut-off near  $qb = 1$ . Equation (D.36) may be written:

$$\gamma = Vq \frac{1 - M_1/M_2}{1 + M_1/M_2}. \quad (\text{D.37})$$

Here  $M_1/M_2$  is small, and we assume that  $M_1/M_2 = K(1 + (bq)^2)$  with  $K \ll 1$  then expanding in  $M_1/M_2$  we find

$$\gamma = Vq ((1 - K) - Kb^2 q^2). \quad (\text{D.38})$$

There is then a cut-off wave number  $q_c$ , for which  $\gamma = 0$  that is given by:

$$q_c = b^{-1} \sqrt{\frac{1 - K}{K}}. \quad (\text{D.39})$$

The most rapidly growing instability is found by requiring  $d\gamma/dq = 0$  which gives

$$q_m = \frac{1}{b\sqrt{3}} \sqrt{\frac{1 - K}{K}}. \quad (\text{D.40})$$

In order to progress further we need to understand the dependency of  $M_i$  on the system parameters

## D.4 Sedimentation and Creaming

Particles in a fluid will either sink, that is, *sediment*, or float, that is, ‘*cream*,’ depending on their density relative to the surrounding fluid. Thermal *Brownian motion* may be ignored for large particles, in this case the fluid particle mixture is called a *suspension*. Colloids are particle fluid mixture that have particles small enough for thermal motion of the particles to dominate. Sedimentation, flotation, creaming and colloids are important in many industrial, scientific and practical applications. Colloids represent a large and interesting field of science all by itself. The colloid particles in water are generally charged the charges being screened by ions in the water, and the particle interactions become rather complicated. These interactions are, however, short ranged and may be ignored for very dilute solutions. Hydrodynamic interactions between particles are relevant both for dilute and concentrated suspensions and colloids.

Fluidized beds arise when the settling of particles is opposed by an upward flow of the fluid. Fluidized beds have many interesting properties. If the fluid is a liquid then the particle concentration adjusts so that the effective permeability changes to give a pressure drop that just supports the

particles. If the fluid is a gas, that is, has a significant compressibility, then there are also bubbles and other space-time instabilities of the suspension.

In the following discussion I will mainly concentrate on sedimentation processes. I will discuss the basics of the Stokes settling and of particle interactions. I will also discuss some of the elementary concepts involved in fluidized beds.

When particles in suspension settle in water they form *sediment*. For a spherical particle of radius  $a$  the settling velocity,  $U_s$ , is given by Stokes law

$$U_{\text{Stokes}} = \frac{F}{6\pi\mu a} = \frac{2g\Delta\rho}{9\mu} a^2 \quad (\text{D.41})$$

Thus as the density difference  $\Delta\rho$  between the particle and the fluid vanishes the settling velocity vanishes also.<sup>1</sup> Small particles settle very slowly. As the size of  $a \rightarrow 0$  diffusion becomes more important. Particles in a fluid at rest will approach a vertical concentration distribution given by the barometric height formula:

$$C_0(z) \sim \exp(-gmz/kT). \quad (\text{D.42})$$

Here  $T$  is the absolute temperature,  $k$  is Boltzmann's constant,  $g$  is the acceleration of gravity, and  $m$  is the 'mass' of the particle  $m = 4\pi a^3 \Delta\rho/3$ . Thermal motion leads to particle diffusion with a diffusion constant  $D_0$  given by the Stokes-Einstein relation:

$$D_0 = \frac{kT}{6\pi\mu a}. \quad (\text{D.43})$$

Thermal motion is important if the distribution (D.42) does not change much over the particle size, that is, there is a characteristic particle size  $a_c$ , below which diffusion becomes important. We estimate  $a_c$  by setting  $gma_c = kT$ , which gives

$$a_c = \left( \frac{3kT}{8\pi g \Delta\rho} \right)^{1/4} \simeq 0.6 \mu\text{m}, \quad \text{for } T = 293\text{K}, \Delta\rho = 10^3 \text{kg/m}^3 \quad (\text{D.44})$$

Particles do not settle to a uniform density if they are much smaller than  $a_c$ .

We may introduce the Péclet number, Pe, for a sedimenting suspension by

$$\text{Pe} = \frac{2aU_{\text{Stokes}}}{D_0} = \left( \frac{a}{a_c} \right)^4. \quad (\text{D.45})$$

---

<sup>1</sup>If the particles have a lower density than the surrounding fluid they will rise instead of sink, this process is termed creaming.

Lattice	c	$\phi$	$p_{\text{site}}$	$\phi_c$	$p_{\text{bond}}$	$\phi_c$
SC	0.524	0.476	0.3116	0.837	0.2488	0.870
BCC			0.246		0.1803	
FCC	0.2596	0.7404	0.188		0.119	
RCP	0.6366	0.3634				
RLP	0.555	0.445				

If  $\text{Pe} \leq 1$ , that is for  $a \leq a_c$ , thermal fluctuations and diffusion dominates sedimentation. Such systems are conventionally called *colloids*, whereas larger particles in a fluid are called *suspensions* for  $\text{Pe} > 1$ .

#### D.4.1 Force Percolation

Larger particles will settle until they touch each other. What is the loosest sediment that will stop particles from settling further? When particles start touching they will be supported by particles below them. These supporting forces must *percolate* to the bottom support surface, or for Hele-Shaw cells to the walls of the container. Thus we are led to consider three-dimensional percolation of forces in random packings of spheres. The simple cubic lattice (SC) has the lowest density of the simple periodic packings, with  $c_{\text{SC}} = \pi/6$ . Simulations show that the percolation threshold for *bond percolation* is  $p_{\text{SC}}(\text{bond}) = 0.2488$  whereas the site percolation threshold is  $p_{\text{SC}}(\text{site}) = 0.3116$  therefore we have an upper limit for the force-percolation threshold. We have collected some of the relevant packing fractions and porosities in table I.

## D.5 Brownian Motion

The theory of Brownian motion has played a central role in statistical physics. Brownian motion forms the basis of our understanding of stochastic processes and important contributions come from Pearson, Lord Rayleigh, Einstein,<sup>1,64</sup> Smoluchowski, Wiener and others. A selection of review papers are found in the book edited by Wax.<sup>147</sup> Notably the papers by Chandrasekhar,<sup>148</sup> by Uhlenbeck and Ornstein<sup>149</sup> and by Wang and Uhlenbeck.<sup>150</sup> Chandrasekhar's<sup>148</sup> review also contains a section with historical notes.

## Appendix E

# Fokker-Planck Equation with Detailed Balance

A stochastic process is simply a function of two variables, one is the time, the other is a *stochastic variable*  $X$ , defined by specifying:

- a:** the set  $\{x\}$  of possible values for  $X$ ;
- b:** the probability distribution,  $P_X(x)$ , over this set, or briefly  $P(x)$

The set of values  $\{x\}$  for  $X$  may be discrete, or continuous. If the set of values is continuous, then  $P_X(x)$  is a probability density so that  $P_X(x)dx$  is the probability that one finds the stochastic variable  $X$  to have values in the range  $[x, x + dx]$ .

An arbitrary number of other stochastic variables may be derived from  $X$ . For example, any  $Y$  given by a mapping of  $X$ , is also a stochastic variable. The mapping may also be ‘time’ dependent, that is, the mapping depends on an additional variable  $t$ :

$$Y_X(t) = f(X, t) . \quad (\text{E.1})$$

The quantity  $Y(t)$  is called a *random function*, or, since  $t$  often is time, a *stochastic process*. A stochastic process is a function of two variables, one is the time, the other is a *stochastic variable*  $X$ . Let  $x$  be one of the possible values of  $X$  then

$$y(t) = f(x, t) , \quad (\text{E.2})$$

is a *function* of  $t$ , called a *sample function* or *realization* of the process. In physics one considers the stochastic process to be an *ensemble* of such sample functions.

For many physical systems initial distributions of a stochastic variable  $y$  tend to equilibrium distributions:  $P(y, t) \rightarrow P_0(y)$  as  $t \rightarrow \infty$ . In equilibrium detailed balance constrains the transition rates:

$$W(y|y')P_0(y') = W(y'|y)P_0(y), \quad (\text{E.3})$$

where  $W(y'|y)$  is the probability, per unit time, that the system changes from a state  $|y\rangle$ , characterized by the value  $y$  for the stochastic variable  $Y$ , to a state  $|y'\rangle$ .

Note that for a system in equilibrium the transition rate  $W(y|y')$  and the reverse  $W(y'|y)$ , may be very different. Consider, for instance, a simple system that has only two energy levels  $\epsilon_0 = 0$  and  $\epsilon_1 = \Delta E$ . Then we find that

$$W(\epsilon_1|\epsilon_0) \exp(-\epsilon_0/kT) = W(\epsilon_0|\epsilon_1) \exp(-\epsilon_1/kT). \quad (\text{E.4})$$

Therefore  $W(\epsilon_1|\epsilon_0)/W(\epsilon_0|\epsilon_1) = \exp(-\Delta E/kT) \rightarrow 0$  when  $\Delta E/kT \rightarrow \infty$ , that is,  $T$  tends to zero.

Assume that  $W(y|y')$  is finite only for small jumps, and that it varies slowly with  $y$ . It is convenient to introduce the transition rate  $R_+$  for positive (or forward) jumps:

$$W(y'|y) = R_+(\rho; y), \quad \text{for } y' = y + \rho, \quad \text{and } \rho > 0. \quad (\text{E.5})$$

The forward jump rate is assumed to be sharply peaked so that  $R_+(\rho; y) \simeq 0$  for  $r > \delta$ , and  $R_+(\rho; y + \Delta y) \simeq R_+(\rho; y)$  for  $\Delta y < \delta$ . The change in the probability distribution is then given by the Master equation

$$\begin{aligned} \frac{\partial}{\partial t} P(y, t) &= \int_0^\infty \{W(y|y - \rho)P(y - \rho, t) - W(y - \rho|y)P(y, t)\} d\rho \\ &\quad + \int_0^\infty \{W(y|y + \rho)P(y + \rho, t) - W(y + \rho|y)P(y, t)\} d\rho. \end{aligned} \quad (\text{E.6})$$

Here we note that the detailed balance equation (E.3) may be written

$$\begin{aligned} R_+(r; y - \rho)P_0(y - \rho) &= W(y|y - \rho)P_0(y - \rho) = W(y - \rho|y)P_0(y), \\ W(y|y + \rho)P_0(y + \rho) &= W(y + \rho|y)P_0(y) = R_+(\rho; y)P_0(y). \end{aligned} \quad (\text{E.7})$$

With these expressions equation (E.6) take the form

$$\begin{aligned} \frac{\partial}{\partial t} P(y, t) &= \int_0^\infty d\rho R_+(\rho; y) P_0(y) \left( \frac{P(y + \rho, t)}{P_0(y + \rho)} - \frac{P(y, t)}{P_0(y)} \right) \\ &\quad + \int_0^\infty d\rho R_+(\rho; y - \rho) P_0(y - \rho) \left( \frac{P(y - \rho, t)}{P_0(y - \rho)} - \frac{P(y, t)}{P_0(y)} \right) \end{aligned} \quad (\text{E.8})$$

Now we may expand the terms in the parentheses to give

$$\begin{aligned} \frac{\partial}{\partial t} P(y, t) &= \int_0^\infty d\rho \rho R_+(\rho; y) P_0(y) \left( \frac{\partial}{\partial y} \frac{P(y, t)}{P_0(y)} \right)_y \\ &\quad - \int_0^\infty d\rho \rho R_+(\rho; y - \rho) P_0(y - \rho) \left( \frac{\partial}{\partial y} \frac{P(y, t)}{P_0(y)} \right)_{y-\rho} \end{aligned} \quad (\text{E.9})$$

The two terms in the integral differ only slightly and we expand the last term around  $y$  and obtain

$$\frac{\partial}{\partial t} P(y, t) = \frac{\partial}{\partial y} \left( D(y) P_0(y) \frac{\partial}{\partial y} \frac{P(y, t)}{P_0(y)} \right). \quad (\text{E.10})$$

Here the generalized *diffusion constant*  $D$  is given by:

$$D(y) = \int_0^\infty \rho^2 R_+(\rho; y) d\rho \simeq \frac{1}{2} \int (y' - y)^2 W(y'|y) dy', \quad (\text{E.11})$$

where the second expression uses that we assumed that  $P_0(y)$  varies little over the range where  $R_+$  has a significant value. Equation (E.10) is a consequence of detailed balance.

In the case of *multivariate stochastic processes* we have more than one stochastic variable and if we write  $\mathbf{r} = (y_1, y_2, \dots, y_n)$ , then the Fokker-Planck equation for stationary Markov processes with narrow transition rates takes the convenient form:

$$\frac{\partial}{\partial t} P(\mathbf{r}, t) = \nabla \cdot \left( \mathbf{D}(\mathbf{r}) P_0(\mathbf{r}) \cdot \nabla \frac{P(\mathbf{r}, t)}{P_0(\mathbf{r})} \right) \quad (\text{E.12})$$

where the  $\nabla = (\frac{\partial}{\partial y_1}, \frac{\partial}{\partial y_2}, \dots, \frac{\partial}{\partial y_n})$ . The Fokker-Planck equation in this form makes explicit that there is no time dependence if  $P(\mathbf{r}, t) = P_0(\mathbf{r})$ .

The diffusion tensor  $\mathbf{D}$  is given in terms of an expression similar to equation (E.11)

$$\mathbf{D}(\mathbf{r}) = \frac{1}{2} \int (\mathbf{r}' - \mathbf{r}) \cdot W(\mathbf{r}'|\mathbf{r}) \cdot (\mathbf{r}' - \mathbf{r}) d^n \mathbf{r}', \quad (\text{E.13})$$

$$D_{ij}(\mathbf{r}) = \frac{1}{2} \int (y'_i - y_i) W(\mathbf{r}'|\mathbf{r}) (y'_j - y_j) d^n \mathbf{r}', \quad (\text{E.14})$$

## E.1 The Einstein Relations

In a system of Brownian particles undergoing diffusion, the stochastic variable describing particle is its position  $\mathbf{r}$ . The probability density  $P(\mathbf{r}, t)$  is proportional to the *concentration of particles*,  $c(\mathbf{r}, t)$ . Therefore the Fokker-Planck equation (E.12) becomes an equation for the concentration of the Brownian particles:

$$\boxed{\frac{\partial}{\partial t} c(\mathbf{r}, t) = \nabla \cdot \left( \mathbf{D}(\mathbf{r}) c_0(\mathbf{r}) \cdot \nabla \frac{c(\mathbf{r}, t)}{c_0(\mathbf{r})} \right)} \quad (\text{E.15})$$

We have assumed that the concentration at position  $\mathbf{r}$  is proportional to  $P(\mathbf{r}, t)$ , that the Brownian particle positions are well approximated by a Markov process, and that the jumps are short ranged. However, the Brownian particles need not be at a low concentration, in fact they may interact strongly. The equilibrium concentration has the general form

$$\boxed{c_0(\mathbf{r}) \sim \exp(-\Delta G(\mathbf{r})/kT)} \quad (\text{E.16})$$

for a system at constant temperature  $T$ , pressure  $P$ , and number of particles  $N$ . Here,  $\Delta G(\mathbf{r})$  is the change in Gibbs free energy, from some reference state. For systems at constant volume  $V$ , one uses the Helmholtz free energy change  $\Delta F(\mathbf{r})$  instead of the Gibbs free energy. Other system constraints replaces the appropriate free energy for  $\Delta G$ .

The diffusion tensor  $\mathbf{D}$  has components

$$D_{ij}(\mathbf{r}) = \frac{1}{2} \int (y'_i - y_i) W(\mathbf{r}'|\mathbf{r})(y'_j - y_j) d^n \mathbf{r}', \quad (\text{E.17})$$

If we define the jump rate  $\Gamma$  as

$$\boxed{\Gamma = \int W(\mathbf{r}'|\mathbf{r}) d^n \mathbf{r}'} \quad (\text{E.18})$$

Then we may define the mean square jump distances as

$$\langle (y'_i - y_i)(y'_j - y_j) \rangle_w = \frac{\int (y'_i - y_i) W(\mathbf{r}'|\mathbf{r})(y'_j - y_j) d^n \mathbf{r}'}{\int W(\mathbf{r}'|\mathbf{r}) d^n \mathbf{r}'} , \quad (\text{E.19})$$

and we arrive at the *Einstein relation* for the diffusion constant

$$\boxed{D_{ij} = \frac{1}{2} \Gamma \langle (y'_i - y_i)(y'_j - y_j) \rangle_w \quad \text{1st Einstein relation}} \quad (\text{E.20})$$

That is, the diffusion constant is one half the mean square jump distance times the jump rate.

The Fokker-Planck equation for the concentration may also be written as a continuity equation:

$$\frac{\partial}{\partial t} c(\mathbf{r}, t) + \nabla \cdot \mathbf{J} = 0 \quad (\text{E.21})$$

Where the *probability flux*, or rather Brownian particle flux,  $\mathbf{J}$  is given by

$$\begin{aligned} \mathbf{J}(\mathbf{r}) &= -\mathbf{D}(\mathbf{r})c_0(\mathbf{r}) \cdot \nabla [c(\mathbf{r}, t)/c_0(\mathbf{r})] \\ &= -\mathbf{D}(\mathbf{r}) \cdot \nabla c(\mathbf{r}, t) + c(\mathbf{r}, t)\mathbf{D}(\mathbf{r}) \cdot \nabla \ln c_0(\mathbf{r}) \\ &= -\mathbf{D}(\mathbf{r}) \cdot \nabla c(\mathbf{r}, t) + c(\mathbf{r}, t)\boldsymbol{\mu} \cdot \mathbf{F} \end{aligned} \quad (\text{E.22})$$

Here  $\mathbf{F}$  is the *driving force* that generates a *drift velocity*

$$\mathbf{v} = \boldsymbol{\mu} \cdot \mathbf{F} \quad (\text{E.23})$$

The driving force is

$$\mathbf{F} = \nabla \ln c_0(\mathbf{r}) = kT \nabla (-\Delta G(\mathbf{r})/kT) = -\nabla(\Delta G(\mathbf{r})) \quad (\text{E.24})$$

whereas the *mobility*  $\boldsymbol{\mu}$  is given by the *second Einstein relation*

$$\boldsymbol{\mu} = \frac{1}{kT} \mathbf{D} \quad \text{2nd. Einstein relation} \quad (\text{E.25})$$

The driving force is just the negative gradient of the related potential—as driving forces should be. The second Einstein relation is a relation between the mobility of a particle and the diffusion constant. One of the best known uses of this relation is for a single spherical particle radius  $a$  in a fluid of viscosity  $\mu$  in this case the Stokes equation gives the mobility of the particle to be

$$\boldsymbol{\mu} = (6\pi\mu a)^{-1} \quad (\text{E.26})$$

and therefore, by the second Einstein relation (E.25), we find the diffusion constant of a Brownian particle

$$D = \frac{kT}{6\pi\mu a} \quad \text{Stokes-Einstein relation} \quad (\text{E.27})$$

This expression for the diffusion constant of Brownian particles, in terms of the Stokes expression for the mobility, is valid only for non-interacting particles. For sedimenting particles at a finite density, which allows the Brownian particles to interact, the Stokes expression (E.26) is no longer valid, however, the second Einstein relation between mobility and Diffusion constant still holds.

# References

- [1] Einstein, A. Über die von der molekularkinetischen Theorie der Wärme geforderte Bewegung von in ruhenden Flüssigkeiten suspendierten Teilchen. *Ann. Phys.*, **322**, 549–560, (1905).
- [2] Taylor, G. I. Dispersion of soluble matter in solvent flowing slowly through a tube. *Proc. Roy. Soc. A*, **219**, 186–203, (1953).
- [3] de Ligny, C. L. Coupling between diffusion and convection in radial dispersion of matter by fluid flow through packed beds. *Chem. Eng. Sci.*, **25**, 1177–1181, (1970).
- [4] Dullien, F. A. L. *Porous Media. Fluid Transport and Pore Structure*. (Academic Press, Inc, San Diego, CA 92101, 2 edition, 1992).
- [5] Hiby, J. W. Longitudinal and transverse mixing during single-phase flow through granular beds. In Rottenburg, P. A. & Sheperd, N. T., editor, *Symposium on the Interaction between Fluids and Particles*, pages 312–325, (Inst. Chem. Engineers, London, 1962).
- [6] Oxaal, U., Flekkøy, E. G., and Feder, J. Irreversible dispersion at a stagnation point: Experiments and lattice Boltzmann simulations. *Phys. Rev. Lett.*, **72**, 3514–3517, (1994).
- [7] Sloane, N. J. A. The packing of spheres. *Scientific American*, **250**, 92–101, (1984).
- [8] Stewart, I. How to succeed in stacking. *New Scientist*, **131**, 29–32, (1991).
- [9] Hilbert, D. Matematische probleme. *Archiv Mth. Physik*, **1**, 44–63, (1901).
- [10] Reynolds, O. Experiments showing dilatancy. *Roy. Inst. Proc.*, , 897, (1885). British Assosiation Report, Aberdeen, 1985.

- [11] Kelvin, L. *Baltimore Lectures on Molecular Dynamics and the Wave theory of Light.* (C. J. Clay and Sons, Cambridge University press warehouse, ave Maria lane, London, 1904). Founded on Mr. A. S. Hathaway's stenographic report of twenty lectures delivered in John Hopkins University, Baltimore, in October 1884: followed by twelve appendices on allied subjects.
- [12] Thue, A. Om nogle geometrisk-thaltheoretiske Theoremer. Forhandlinger ved de skandinaviske Naturforskeres 14de møde, (1892).
- [13] Nelson, D. R. Order, frustration and two-dimensional glass. In Yonezawa, F. and Ninomiya, T., editors, *Topological disorder in condensed matter: Proceedings of the fifth Taniguchi International symposium*, pages 164–180, (Springer-Verlag, Berlin, 1983).
- [14] Feder, J. Random sequential adsorption. *J. Theor. Biol.*, **87**, 237–254, (1980).
- [15] Feder, J. and Giaever, I. Adsorption of ferritin. *J. of Colloid and Interface Science*, , 144–154, (78).
- [16] Hinrichsen, E. L., Feder, J., and Jøssang, T. Geometry of random sequential adsorption. *Jour. of Statistical Physics*, **44**(5), 793–827, (1986).
- [17] Hinrichsen, E., Feder, J., and Jøssang, T. Random packing of disks in two dimensions. *Phys. Rev.A*, **41**(8), 4199–4209, (1990).
- [18] Coxeter, H. S. M. *Introduction to geometry.* (John Wiley & Sons, Toronto, 2 edition, 1969).
- [19] Kepler, J. *Gesammelte Werke*, volume 4. (Beck, München, 1941).
- [20] Kepler, J. *The Six-Cornered Snowflake.* (Oxford University Press, London, 1966). Edited by L. L. Whyte. The book contains Kepler's original (1611) text in latin with English translation by Colin Hardie. The book also contains comments by B. J. Mason: '*On the shape of snow crystals*', and by L. L. Whyte: '*Kepler's Unsolved Problem and the FACULTAS FORMATRIX*'.
- [21] Zallen, R. *The Physics of Amorphous Solids.* (John Wiley & Sons, New York, 1983).
- [22] Hsiang, W.-Y. On the sphere packing problem and the proof of Kepler's conjecture. *Int. J. Math.*, **4**(5), 739–831, (1993).

- [23] Hales, T. C. The status of the Kepler conjecture. *Math. Intelligencer*, **16**, 47–58, (1994).
- [24] Hsiang, W.-Y. A rejoinder to T. C. Hales's article "the status of the Kepler conjecture". *Math. Intelligencer*, **17**, 35–42, (1995).
- [25] Hales, T. C. Sphere packings I–V, (1998). His computer based proof is found at Hales web site. Version 7/29/98. His site has many interesting historical notes and pointers to other sites. <http://www.math.lsa.umich.edu/hales/countdown/>.
- [26] Rogers, C. A. The packing of equal spheres. *Proc. Lond. Math. Soc.*, **8**, 609–620, (1958).
- [27] Bernal, J. D. and Mason, J. Co-ordination of randomly packed spheres. *Nature*, **188**, 910–911, (1960). Available from: <file:///C:/DocumentsandSettings/feder/MyDocuments/Reprints/BlueBook/BernalMason1960.pdf>.
- [28] Bernal, J. D. The structure of liquids. *Proc. Roy. Soc. A*, **280**, 299–333, (1964).
- [29] Bernal, J. D. The geometry of the structure of liquids. In Hughel, T. J., editor, *Liquids: Structure Properties, Solid Interactions*, pages 25–50, (Elsevier, Amsterdam, 1965).
- [30] Scott, G. D. and Kilgour, D. M. The density of random close packing of spheres. *J. Phys. D.*, **2**, 863–866, (1969).
- [31] Bernal, J. D. A geometrical approach to the structure of liquids. *Nature*, **183**, 141–147, (1959).
- [32] Coxeter, H. S. M. Close packing and froth. *Illinois J. Math.*, **2**, 746, (1958).
- [33] Finney, J. L. Random packings and the structure of simple liquids. I. The geometry of close packing. *Proc. Roy. Soc. (London) A*, **319**, 479–493, (1970).
- [34] Jaeger, H. M. and Nagel, S. R. Physics of the granular state. *Science*, **255**, 1523–1531, (1992).
- [35] Scott, G. D. Packing of equal spheres. *Nature*, **188**, 908–909, (1960).
- [36] Liu, C.-h., Nagel, S. R., Schechter, D. A., Coppersmith, S. N., Majumdar, S., Narayan, O., and Witten, T. A. Force fluctuations in bead packs. *Science*, **269**, 513–515, (1995).

- [37] Onoda, G. Y. and Liniger, E. G. Random loose packings of uniform spheres and the dilatancy onset. *Phys. Rev. Lett.*, **64**, 2727–2730, (1990).
- [38] Jullien, R., Pavlovitch, A., and Meakin, P. Random packings of spheres built with sequential models. *J. Phys. A: Math. Gen.*, **25**, 4103–4113, (1992).
- [39] Frette, V., Christensen, K., Malthe-Sørensen, A., Feder, J., Jøssang, T., and Meakin, P. Avalanche dynamics in a pile of rice. *Nature*, **379**, 49–5, (1996).
- [40] Wu, X., Måløy, K. J., Hansen, A., Ammi, M., and Bideau, D. Why hour glasses tick. *Phys. Rev. Lett.*, **71**, 1363–1366, (1993).
- [41] Jullien, R., Meakin, P., and Pavlovitch, A. Three-dimensional model for particle-size segregation by shaking. *Phys. Rev. Lett.*, **69**, 640–643, (1992).
- [42] Weissberg, H. L. Effective diffusion coefficient in porous media. *J. Appl. Phys.*, **34**, 2636, (1963).
- [43] Strieder, W. and Aris, R. *Variational Methods Applied to Problems of Diffusion and Reaction*. (Springer-Verlag, Berlin, 1973).
- [44] Berryman, J. G. and Blair, S. C. Use of digital image analysis to estimate fluid permeability of porous materials: Application of two-point correlation functions. *J. Appl. Phys.*, **60**, 1930–1938, (1986).
- [45] Debye, P. and Bueche, A. M. Scattering by an inhomogeneous solid. *J. Appl. Phys.*, **20**, 518, (1949).
- [46] Berryman, J. G. Measurement of spatial correlation functions using image precessing techniques. *J. Appl. Phys.*, **57**, 2374–22384, (1985).
- [47] Debye, P., Anderson, H. R., and Brumberger, H. Scattering by an inhomogeneous solid ii. The correlation and its application. *J. Appl. Phys.*, **28**, 679–683, (1957).
- [48] Newton, I. *Philosophiae Naturales Principia Mathematica*. (Imprimatur S. Pepys. Re. Soc. Praeses, Berkeley and Los Angeles, 1867). See A. Motte's and 1729. Revised and supplied with historical and explanatory appendix by F. Cajori, Edited by R. T. Crawford (1934) and published by University of California Press, Berkeley and Los Angeles (1966).

- [49] Dowson, D. *History of Tribology*. (Longman, London and New York, 1979).
- [50] Reynolds, O. On the theory of lubrication. *Philosophical Transactions*, **177**, 157–234, (1886).
- [51] Batchelor, G. K. *An introduction to fluid dynamics*. (Cambridge University Press, Cambridge, 1967).
- [52] Hagen, G. H. L. Ueber die Bewegung des Wassers in engen cylindrischen Röhren. *Poggendorfs Annalen der Physik und Chemie*, **16**, (1839).
- [53] Poiseuille, J. L. M. Recherches expérimentales sur le mouvement des liquides dans les tubes de très-petits diamètres. *Academie des Sciences, Comptes Rendus*, **xii**, (1840-1). Mem. des Sav. Étrangers, ix. (1846).
- [54] Stokes, G. G. On the theories of the internal friction of fluids in motion, and of the equilibrium and motion of elastic solids. *Trans. Cambr. Phil. Soc.*, **8**, 287–319, (1845).
- [55] Landau, L. D. and Lifshitz, E. M. *Fluid Mechanics*. (Pergamon Press, Oxford, New York, 1987).
- [56] Bird, R. B., Armstrong, R. C., and Hassager, O. *Dynamics of Polymeric Liquids*. (John Wiley & sons, New York, 1987).
- [57] Navier, C. L. M. H. Mémoire sur les lois du mouvements des fluides. *Mémoires de l'Academie Royale des Sciences de l'Institut de France*, **VI**, (1822). Chez Firmin Didot, père et fils, libraires, Paris 1827.
- [58] Poisson, S. D. Mémoire sur les équations générales de l'équilibre et du mouvement des corps solides élastiques et des fluides. *Journal de l'école royale polytechnique*, **XIII**(Vingtieme Cahier), (1829). de l'Imprimerie Royale, Paris 1831.
- [59] Tritton, D. J. *Physical Fluid Dynamics*. (Clarendon Press, Oxford, 2 edition, 1988).
- [60] Kolmogorov, A. N. The local structure of turbulence in incompressible viscous fluid for very large Reynolds' numbers. *Dokl. Akad. Nauk SSSR*, **30**, 301–305, (1941).
- [61] Kolmogorov, A. N. Dissipation of energy in locally isotropic turbulence. *Dokl. Akad. Nauk SSSR*, **32**, 16–18, (1941).

- [62] Kolmogorov, A. N. A refinement of previous hypotheses concerning the local structure of turbulence in a viscous incompressible fluid at high Reynolds number. *J. Fluid Mech.*, **13**, 82–85, (1962).
- [63] Einstein, A. Eine neue Bestimmung der Moleküldimensionen. *Annalen der Physik, 4. folge*, **19**, 289–306, (1906). Correction in [].
- [64] Einstein, A. Berichtigung zu meiner Arbeit: ‘Eine neue Bestimmung der Moleküldimensionen’. *Annalen der Physik, 4. folge*, **34**, 591–592, (1911).
- [65] Vergeles, M., Kebinski, P., Koplik, J., and Banavar, J. R. Stokes drag at the molecular level. *Phys. Rev. Lett.*, **75**, 232–235, (1995).
- [66] Proudman, I. and Pearson, J. R. A. Expansion at small Reynolds numbers for the flow past a sphere and a circular cylinder. *J. Fluid. Mech.*, **2**, 237–262, (1957).
- [67] Taneda, S. Experimental investigation of the wake behind a sphere at low Reynolds numbers. *J. Phys. Soc. Jpn.*, **11**, 1104–1108, (1956).
- [68] Oseen, C. W. *Neuere Methoden und Ergebnisse in der Hydrodynamik*. (Akademische Verlagsgesellschaft m.b.h., Leipzig, 1927).
- [69] Oseen, C. W. Über die Stokes’sche Formel und über eine verwandte Aufgabe in der Hydrodynamik. *Arkiv för matematik, astronomi och fysik*, **6**, 1–20, (1910).
- [70] Oseen, C. W. Über den Gültigkeitsbereich der Stokesschen Widerstandsformel. *Arkiv för matematik, ast. och fysik*, **9**, (1913).
- [71] Mazur, P. and Weisenborn, A. J. The Ossén drag on a sphere and the method of induced forces. *Physica A*, **123**, 209–226, (1984).
- [72] Taylor, T. D. and Arcivos, A. On the deformation and drag of a falling viscous drop at low Reynolds number. *J. Fluid. Mech.*, **18**, 466–476, (1964).
- [73] Darcy, H. *Les Fontaines Publiques de la Ville de Dijon*. (Dalmont, Paris, 1856).
- [74] Nutting, P. G. Physical analysis of oil sands. *Bull. Amer. Ass. Petr. Geol.*, **14**, 1337–1349, (1930).
- [75] Wyckoff, R. D., Botset, M., Muskat, M., and Reed, D. W. The measurement of the permeability of porous media for homogeneous fluids. *Rev. Sci. Instr.*, **4**, 394–405, (1933).

- [76] Carman, P. C. Determination of the specific surface of powders I. *J. Soc. Chem. Ind.*, **57**, 225–234, (1938).
- [77] Aronovici, V. S. and Donnan, W. W. Soil-permeability as a criterion for drainage design. *Trans. Amer. Geophys. Un.*, **27**, 95, (1946).
- [78] Muskat, M. *The flow of homogeneous fluids through porous media*. (Edwards, Ann Arbor, 1 edition, ). 2nd printing, 1946.
- [79] Locke, L. C. and Bliss, J. E. Core analysis for limestone and dolomite. *World Oil*, , 206–207, (1950).
- [80] Stull, R. T. and Johnson, P. V. Some properties of the pore system in bricks and their relation to frost action. *J. Res. Nat. Bur. Stand.*, **25**, 711–730, (1940).
- [81] McLaughlin, J. F. and Goetz, W. H. Permeability, void content, and durability of bituminous concrete. *National Research Council, Highway Res. Bd. Proc.*, **34**, 274–286, (1955).
- [82] Mitton, R. G. The air permeabilities of light leathers and their specific surfaces. *J. Int. Soc. Leather Trades' Chem.*, **29**, 255–263, (1945).
- [83] Brown, R. L. and Bolt, R. H. The measurement of flow resistance of porous acoustic materials. *J. Acous. Soc. Amer.*, **13**, 337–344, (1942).
- [84] Wiggins, E. J., Campbell, W. B., and Maass, O. Determination of the specific surface of fibrous materials. *Canad. J. Res. Section B, Chemical sciences*, **B17**, 318–324, (1939).
- [85] Pallmann, H. and Deuel, H. *Experientia*, **1**, 325, (1945).
- [86] Bear, J. *Dynamics of Fluids in Porous Media*. (Elsevier Publishing Co., Amsterdam, 1972). Republished by Dover Publications Inc, New York (1988). ISBN 0-486-65675-6.
- [87] Bear, J. and Bachmat, Y. *Introduction to Modeling of Transport Phenomena in Porous Media*. (Kluwer, Academic Publishers, Dordrecht, Boston, London, 1990).
- [88] Scheidegger, A. E. *The physics of flow through porous media*. (University of Toronto Press, Toronto, 1974).
- [89] Fleischer, R. L. and Price, P. B. Tracks of charged particles in high polymers. *Science*, **140**, 1221–1222, (1963).

- [90] Fleischer, R. L. Technological applications of ion tracks in insulators. *MRS Bulletin*, **XX**, 35–41, (1995).
- [91] Dupuit, A. J. E. *Traite theoretique et pratique de la conduite et de la distribution des eaux.* (, Paris, 1863).
- [92] Carman, P. C. Fluid flow through granular beds. *Trans. Inst. Chem. Eng. Lond.*, **15**, 150–166, (1937).
- [93] Kozeny, J. über kapillare Leitung des Wassers im Boden (Aufstieg, Verzickerung und Anwendung auf die Bewässerung). *Royal Academy of Science, Vienna, Proc. Class I*, **136**, 271–306, (1927).
- [94] Schriever, W. Law of flow for the passage of agas-free liquid through a spherical-grain sand. *Trans. Amer. Inst. Min. Metall. Engrs., Pet. Div.*, **86**, 329–336, (1930).
- [95] Zick, A. A. and Homsy, G. Stokes flow through periodic arrays of spheres. *J. Fluid. Mech.*, **115**, 13–26, (1982).
- [96] Blake, F. C. The resistance of packing to fluid flow. *Trans. Amer. Inst. Chem. Engrs.*, **14**, 415–421, (1922).
- [97] Stanton, T. E. and Pannell, J. R. Similarity of motion in relation to the surface friction of fluids. *Collected Researches, National Physical Laboratory*, **11**, 295–320, (1914). Reprinted from the Philosophical Transactions of the Royal Society, **A214**.
- [98] Mott, R. A. The laws of motion of particles in fluids and their application to the resistance of beds of solids to the passage of fluid. In Lang, H. R., editor, *Some Aspects of Fluid Flow, being the papers presented at a conference organized by The Institute of Physics at Leamington Spa on 25th–28th October, 1950, and the reports of the conference discussion groups*, pages 242–256, (Edward Arnold, London, 1951).
- [99] Rumpf, H. and Gupte, A. R. Einflüsse der Porosität un Korngrößenverteilung im Widerstandsgesetz der Porenströmung. *Chem. Ing. Tech.*, **43**, 367–375, (1971).
- [100] Forchheimer, P. H. Wasserbewegung durch Boden. *Zeitschrift des vereins Deutscher Ingenieure*, **45**, 1781–1787, (1901).
- [101] Ahmed, N. and Sunada, D. K. Nonlinear flow in porous media. *J. Hydraulics Div. Proc. ASCE*, **95**, 1867–1856, (1969). HY6.

- [102] Maxwell, J. C. *A Treatise on Electricity and Magnetism.* (Oxford University Press (Clarendon), London, second edition, 1881).
- [103] Lorentz, H. A. Eene algemeene stelling omrent de beweging eener vloeistof met wrijving en eenige afgeleide gevollen. *Zittingsverl. Akad. van Wet.*, **5**, 168, (1896). neue bearb.: Abhandl. theoret. phys. **1**, 23 (1907).
- [104] Rayleigh, L. On the influence of obstacles arranged in rectangular order upon the properties of a medium. *Phil. Mag.*, **34**, 481–502, (1892).
- [105] Batchelor, G. K. and O'Brien, R. W. Thermal or electrical conduction through a granular material. *Proc. Roy. Soc. Lond. A*, **355**, 313–333, (1977).
- [106] Rutgers, M. A. *Experiments with hard, soft, and hydrodynamically interacting spheres.* PhD thesis, Department of Physics, Princeton University, (1995).
- [107] Hasimoto, H. On the periodic fundamental solution of the stokes equations and their application to viscous flow past a cubic array of spheres. *J. Fluid Mech.*, **5**, 317–328, (1959).
- [108] Ewald, P. P. Die Berechnung optischer und elektrostatischer Gitterpotentiale. *Ann. Phys.*, **64**, 253–287, (1921).
- [109] Burgers, J. M. On the influence of the concentration of a suspension upon the sedimentation velocity (in particular for a suspension of spherical particles). *Proc. K. Akad. Wet. Amst.*, **44**, 1045–1051, 1177–1184, (1941).
- [110] McPhedran, R. C. and McKenzie, D. R. The conductivity of lattices of spheres. I. the simple cubic lattice. *Proc. R. Soc. Lond. A*, **359**, 46–63, (1978).
- [111] Sangini, A. S. and Acrivos, A. On the effective thermal conductivity and permeability of regular arrays of spheres. In Burridge, R., Childress, S., and Papanicolaou, G., editors, *Macroscopic Properties of Disordered Media*, volume 154 of *Lecture Notes in Physics*, pages 216–225, (Springer Verlag, Heidelberg, 1982).
- [112] Maxwell, J. C. Capillary action. In *Encyclopædia Britannica*. (, 9th edition, 1876). Reprinted in *The Scientific Papers of James Clerk Maxwell*, **2**, 541–591 (Cambridge University Press, 1890), reprinted by Dover publications, New York (1952).

- [113] Hooke, R. Pamphlet, (1661). Hooke's first publication was a pamphlet on capillary action.
- [114] Rowlinson, J. S. and Widom, B. *Molecular Theory of Capillarity*. (Oxford University Press, Oxford, 1982).
- [115] Adamson, A. W. *Physical Chemistry of Surfaces*. (J. Wiley, New York, 4th edition, 1982).
- [116] Israelachvili, J. N. *Intermolecular and Surface Forces*. (Academic Press, London, 2nd, 4th printing edition, 1992).
- [117] de Gennes, P. G. Wetting: statics and dynamics. *Rev. Mod. Phys.*, **57**, 827–863, (1985).
- [118] Young, T. An essay on the cohesion of fluids. *Philos. Trans. R. Soc. London*, **95**, 65–87, (1805). reprinted in *Collected Works*, **1**, 461.
- [119] Laplace. *Traité de Mécanique Céleste; Supplément au dixième livre, Sur l'Action Capillaire; and Supplement à la Théorie de l'Action Capillaire*, volume 10. (Courcier, Paris, 1806, 1807). English translation by N. Bowditch: *Mécanique Céleste* by Marquis de la Place, Vol. 4 p. 685, 806, (Little and Brown, Boston (1839)), reprinted by Chelsea Publ. Co. New York (1966).
- [120] Landau, L. D. and Lifshitz, E. M. *Statistical Mechanics*. (Pergamon Press, Oxford, New York, 1987).
- [121] Schick, M. Introduction to wetting phenomena. In Charvolin, J., Joanny, J. F., and Zinn-Justin, J., editors, *Liquids at Interfaces*, pages 417–497, (Elsevier Science Publishers B.V., Amsterdam, 1990). Les Houches, Session XLVIII, 1988.
- [122] Thomson, W. On the equilibrium of vapour at a curved surface of liquid. *Phil. Mag. (Ser. 4)*, **42**, 448–452, (1871).
- [123] von Helmholtz, R. Untersuchungen über Dämpfe und Nebel, besonders über solche von Lösungen. *Ann. d. Physik u. Chem. (Wied.)*, **27**, 508–543, (1886).
- [124] Fahrenheit, D. G. Experimente und Beobachtungen über das Gefrieren des Wassers im Vacuum. *Phil. Transact. London*, **XXXIII**, 78–84, (1724). The experiments were done 1–3 March 1721. (Translated from Latin in<sup>151</sup>).
- [125] Gibbs, J. W. *The collected works of J. W. Gibbs*, volume I. (Longmans, Green and Co., New York, 1928).

- [126] Feder, J., Russell, K. C., Lothe, J., and Pound, G. M. Nucleation and growth in homogeneous vapors. *Advances in Physics*, **15**, 111, (1966).
- [127] Hele-Shaw, H. S. The flow of water. *Nature*, **58**, 34–36, (1898).
- [128] Engelberts, W. F. and Klinkenberg, L. J. Laboratory experiments on the displacement of oil by water from packs of granular material. *Petr. Congr. Proc. Third World*, , 544–554, (1951).
- [129] Saffman, P. G. and Taylor, G. The penetration of a fluid into a medium or Hele-Shaw cell containing a more viscous liquid. *Proc. Soc. London, Ser. A*, **245**, 312–329, (1958).
- [130] Chuoke, R. L., van Meurs, P., and van der Poel, C. The instability of slow, immiscible, viscous liquid-liquid displacements in permeable media. *Trans. Metall. Soc. of AIME*, **216**, 188–194, (1959).
- [131] Bensimon, D., Kadanoff, L. P., Liang, S., Shraiman, B., and Tang, C. Viscous flows in two dimensions. *Rev. Mod. Phys.*, **58**, 977–999, (1986).
- [132] Feder, J. *Fractals*. (Plenum, New York, 1988).
- [133] Tryggvason, G. and Aref, H. Numerical experiments on Hele-Shaw flow with a sharp interface. *J. Fluid Mech.*, **136**, 1–30, (1983).
- [134] McLean, J. W. and Saffman, P. G. The effect of surface tension on the shape of fingers in a Hele-Shaw cell. *J. Fluid Mech.*, **102**, 455–469, (1981).
- [135] Pitts, E. Penetration of a fluid into a Hele-Shaw cell: the Saffman-Taylor experiment. *J. Fluid Mech.*, **97**, 53–64, (1980).
- [136] Maher, J. V. Development of viscous fingering patterns. *Phys. Rev. Lett.*, **54**, 1498–1501, (1985).
- [137] Buckley, S. E. and Leverett, M. C. Mechanism of fluid displacement in sands. *Trans. Am. Inst. Min. Eng.*, **146**, 107–116, (1942).
- [138] Honarpour, M., Koederitz, L., and Harvey, A. H. *Relative Permeability of Petroleum Reservoirs*. (CRC Press, Inc., Boca Raton, Florida, 1986).
- [139] Corey, A. T. The interrelation between gas and oil relative permeabilities. *Prod. Mon.*, **19**, 38, (1954).

- [140] Kalaydjian, F. Origin and quantification of coupling between relative permeabilities for two-phase flows in porous media. *Transport in porous media*, **5**, 215–229, (1990).
- [141] Gunstensen, A. K. and Rothman, D. H. Lattice-Boltzmann modeling of two-phase flow through porous media. *J. Geophys. Res.*, **98**, 6431–41, (1993).
- [142] van Genabeek, O. and Rothman, D. H. Macroscopic manifestations of microscopic flows through porous media: phenomenology from simulation. *Ann. Rev. Earth and Planetary Sci.*, , (1996).
- [143] Hilfer, R. Geometric and dielectric characterization of porous media. *Phys. Rev. B*, **44**, 60–75, (1991).
- [144] Archie, G. E. The electrical resistivity log as an aid in determining some reservoir characteristics. *A.I.M.E.*, **146**, 54–62, (1942).
- [145] Boger, F., Feder, J., Jøssang, T., and Hilfer, R. Microstructural sensitivity of local porosity distributions. *Physica A*, **187**, 55, (1992).
- [146] Mills, P., Cerasi, P., and Fautrat, S. Erosion instability in a non-consolidated porous medium. *Europhys. Lett.*, **29**, 215–220, (1995).
- [147] Wax, N., editor. *Selected Papers on Noise and Stochastic Processes*. (Dover Publications Inc., New York, 1954). ISBN: 0-486-60262-1; Library of Congress: 54-4062.
- [148] Chandrasekhar, S. Stochastic problems in physics and astronomy. *Rev. Mod. Phys.*, **15**, 1–89, (1943). Reprinted in Wax: *Selected Papers on Noise and Stochastic Processes*. Reference [], pp. 3–91.
- [149] Uhlenbeck, G. E. and Ornstein, L. S. On the theory of the Brownian motion. *Phys. Rev.*, **36**, 823–841, (1930). Reprinted in Wax: *Selected Papers on Noise and Stochastic Processes*. Reference [], pp. 93–111.
- [150] Wang, M. C. and Uhlenbeck, G. E. On the theory of the Brownian motion II. *Rev. Mod. Phys.*, **17**, 323–342, (1945). Reprinted in Wax: *Selected Papers on Noise and Stochastic Processes*. Reference [], pp. 113–132.
- [151] von Oettingen, A. J., editor. *Abhandlungen über Thermometrie von Fahrenheit, Réaumur, Celsius*. Ostwald's Klassiker der exakten Wissenschaften, Nr. 57. (Verlag von Wilhelm Engelmann, Leipzig, 1894).

# Author Index

- Acrivos, A. 104 [94]  
Adamson, A. W. 108 [97]  
Ahmed, N. 83 [85]  
Ammi, M. 25 [28]  
Anderson, H. R. 29 [35]  
Arcivos, A. 65 [60]  
Aref, H. 130, 134, 135 [114]  
Aris, R. 27, 28, 30 [31]  
Armstrong, R. C. 47, 65 [44]  
Aronovici, V. S. 68 [65]  
Bachmat, Y. 69 [75]  
Banavar, J. R. 64 [53]  
Batchelor, G. K. 40, 42 [39]; 92  
[88]  
Bear, J. 69 [74,75]  
Bensimon, D. 127 [112]  
Bernal, J. D. 23 [18]; 22 [16–18,  
20]  
Berryman, J. G. 29 [33]; 29, 30  
[34]  
Bideau, D. 25 [28]  
Bird, R. B. 47, 65 [44]  
Blair, S. C. 29, 30 [34]  
Blake, F. C. 77 [81]  
Bliss, J. E. 68 [67]  
Boger, F. 34 [37]  
Bolt, R. H. 68 [71]  
Botset, M. 67 [63]  
Brown, R. L. 68 [71]  
Brumberger, H. 29 [35]  
Buckley, S. E. 145–148 [118]  
Bueche, A. M. 28 [32]  
Burgers, J. M. 102 [92]  
Carman, P. 75, 77 [77]  
Carman, P. C. 68 [64]  
Chuoke, R. L. 127–131 [111]  
Coppersmith, S. N. 24 [25]  
Corey, A. T. 145 [120]  
Coxeter, H. S. M. 23 [21]; 17, 18  
[12]  
Darcy, H. 66 [61]  
Debye, P. 28 [32]; 29 [35]  
Deuel, H. 68 [73]  
de Gennes, P. G. 108 [99]  
de Ligny, C. L. 5 [3]  
Donnan, W. W. 68 [65]  
Dullien, F. A. L. 5, 81 [4]  
Einstein, A. 4, 8 [1]; 64 [51]; 64,  
171 [52]  
Engelberts, W. F. 126 [109]  
Ewald, P. P. 102 [91]  
Fahrenheit, D. G. 118 [105]  
Feder, J. 118 [107]; 34 [37]  
Feder, J. 127 [113]; 6 [6]  
Finney, J. L. 23 [22]  
Flekkøy, E. G. 6 [6]  
Forchheimer, P. H. 81 [84]  
Gibbs, J. W. 118 [106]  
Goetz, W. H. 68 [69]  
Gunstensen, A. K. 154 [122]  
Gupte, A. R. 81 [83]  
Hagen, G. H. L. 43, 44 [40]  
Hansen, A. 25 [28]  
Harvey, A. H. 145 [119]  
Hasimoto, H. 102, 103, 105 [90]  
Hassager, O. 47, 65 [44]  
Hele-Shaw, H. S. 125 [108]  
Hiby, J. W. 6 [5]  
Hilfer, R. 31, 34 [36]; 34 [37]  
Homsy, G. 77, 104, 105 [80]  
Honarpour, M. 145 [119]  
Israelachivili, J. N. 108 [98]

- Jaeger, H. M. 23, 25 [23]  
 Johnson, P. V. 68 [68]  
 Jullien, R. 24 [27]; 25 [29]  
 Jøssang, T. 34 [37]  
 Kadanoff, L. P. 127 [112]  
 Kalaydjian, F. 154 [121]  
 Kebinski, P. 64 [53]  
 Kelvin, L. 10 [10]  
 Kilgour, D. M. 22 [19]  
 Klinkenberg, L. J. 126 [109]  
 Koederitz, L. 145 [119]  
 Kolmogorov, A. N. 61 [48]; 61  
 [49]; 61 [50]  
 Koplik, J. 64 [53]  
 Kozeny, J. 76 [78]  
 Landau, L. D. 112, 117, 154, 157  
 [102]; 45 [43]  
 Laplace. 110 [101]  
 Leverett, M. C. 145, 146, 147, 148  
 [118]  
 Liang, S. 127 [112]  
 Lifshitz, E. M. 112, 117, 154, 157  
 [102]; 45 [43]  
 Liniger, E. G. 24 [26]  
 Liu, C. 24 [25]  
 Locke, L. C. 68 [67]  
 Lorentz, H. A. 88 [87]  
 Lothe, J. 118 [107]  
 Maher, J. V. 139 [117]  
 Majumdar, S., Narayan, O. 24 [25]  
 Mason, J. 22 [16]  
 Maxwell, J. C. 84 [86]; 107, 110  
 [95]  
 Mazur, P. 65 [59]  
 McKenzie, D. R. 104 [93]  
 McLaughlin, J. F. 68 [69]  
 McLean, J. W. 133 [115]  
 McPhedran, R. C. 104 [93]  
 Meakin, P. 24 [27]; 25 [29]  
 Mitton, R. G. 68 [70]  
 Muskat, M. 67 [63]; 68 [66]  
 Måløy, K. J. 25 [28]  
 Nagel, S. R. 24 [25]; 23, 25 [23]  
 Navier, C. L. M. H. 55 [45]  
 Nelson, D. R. 20 [13]  
 Nutting, P. G. 67 [62]  
 O'Brien, R. W. 92 [88]  
 Onoda, G. Y. 24 [26]  
 Oseen, C. W. 64, 65 [56-58]  
 Oxaal, U. 6 [6]  
 Pallmann, H. 68 [73]  
 Pannell. 77 [82]  
 Pavlovitch, A. 24 [27]; 25 [29]  
 Pearson, J. R. A. 64 [54]  
 Pitts, E. 133 [116]  
 Poiseuille, J. L. M. 43, 44 [41]  
 Poisson, S. D. 55 [46]  
 Pound, G. M. 118 [107]  
 Proudman, I. 64 [54]  
 Rayleigh, L. 104, 94 [89]  
 Reed, D. W. 67 [63]  
 Reynolds, O. 10 [9]; 40 [38]  
 Rogers, C. A. 21 [15]  
 Rothman, D. H. 154 [122]; 154  
 [123]  
 Rowlinson, J. S. 107, 108, 122 [96]  
 Rumpf, H. 81 [83]  
 Russell, K. C. 118 [107]  
 Saffman, P. G. 127, 128, 131 [110] ;  
 133 [115]  
 Sangini, A. S. 104 [94]  
 Schechter, D. A. 24 [25]  
 Scheidegger, A. E. 70 [76]  
 Schick, M. 112 [103]  
 Schriever. 77 [79]  
 Scott, G. D. 22 [19]  
 Scott, G. D. 23 [24]  
 Shraiman, B. 127 [112]  
 Sloane, N. J. A. 21, 22, 9 [7]  
 Stanton. 77 [82]  
 Stewart, I. 21, 9 [8]  
 Stokes, G. G. 43 [42]  
 Strieder, W. 27, 28, 30 [31]  
 Stull, R. T. 68 [68]  
 Sunada, D. K. 83 [85]  
 Taneda, S. 64 [55]  
 Tang, C. 127 [112]  
 Taylor, G. I. 4 [2]; 127-131 [110]  
 Taylor, T. D. 65 [60]  
 Thue, A. 11 [11]

- Tritton, D. J. 58 [47]  
Tryggvason, G. 130, 134, 135 [114]  
van Genabeek, O. 154 [123]  
van Meurs, P. 127, 128, 131 [111]  
van der Poel, C. 127, 128, 131  
[111]  
Vergeles, M. 64 [53]  
von Helmholtz, R. 116, 118 [104]  
Weisenborn, A. J. 65 [59]  
Weissberg, H. L. 27, 28 [30]  
Widom, B. 107, 108, 122 [96]  
Wiggins, E. J. 68 [72]  
Witten, T. A. 24 [25]  
Wu, X. 25 [28]  
Wyckoff, R. D. 67 [63]  
Young, T. 110, 121 [100]  
Zallen, R. 21 [14]  
Zick, A. A. 104, 105, 77 [80]

# Subject Index

- absolute scale of temperature, 182  
    temperature, 175  
acceleration on fluid elements, 56  
additive quantities, 176  
adhesion, 116  
adiabatic compression, 181  
    expansion, 181  
adsorption, 116  
air displaces oil, 143  
    displacing glycerol, 144  
algorithmic models, 157  
angle of contact, 134  
Archie's law, 197  
attractive interaction, 116  
Atwood ratio, 143  
autocorrelation function, 200  
auto-correlation function, 225  
    time, 225  
average flow velocity, 51  
    pore velocity, 81  
    quantities, 76  
    viscosity, 148  
binary mixture, 149  
boiling, 126  
Boltzmann constant, 171  
bond percolation, 223  
boundary condition, 41, 92, 166  
    conditions, 77  
    conditions at infinity, 64  
break through, 157  
Brownian motion, 221, 227  
    particle, 236  
bubble, 116, 126  
Buckley-Leverett equation, 162  
bulk viscosity, 61  
capilla, 115  
capillary, 163  
    action, 115  
    force, 139  
    length  $\lambda$ , 137  
model for porous media, 79  
number, 72, 144  
pressure, 142, 158, 161, 164,  
    165  
pressure curve, 10  
rise, 115  
tube, 115  
wave, 120  
Carman relation, 84  
Carman-Kozeny constant  $K$ , 84  
    equation, 84  
    expression, 84, 106, 212  
    relation, 212  
cavitation, 126  
Chapman-Kolmogorov equation,  
    227, 228  
characteristic function  $\chi$ , 35  
chemical potential, 122, 189  
    potential  $\mu$ , 186  
    reaction, 179  
chromatography, 1  
closed system, 172, 175, 176  
close-packed structure, 12  
coexistence, 122  
colloidal chemistry, 1  
colloids, 223  
complete wetting, 133  
concentration of particles, 236  
conditional probability, 226  
conducting sphere, 97

- conductivity, 77, 98  
conservation of angular momentum, 53  
consistency relations, 226  
constraint, 172  
contact angle, 116, 139  
contact-angle, 158  
continuity equation, 53, 54, 76, 92, 161  
equation for flow in porous media, 76  
convection, 57  
convective dispersion, 4, 5  
correlation length of the porous medium, 199  
cream, 221  
creaming, 221, 222  
creeping flow, 8, 68, 90  
critical nucleus, 129  
point, 137  
unmixing temperature  $T_c$ , 149  
wave length, 149  
wavelength, 143  
cross-term permeability  $k_{ij}$ , 167  
current density, 92  
currents, 168  
cylindrical container, 216  
dam foundations, 73  
Darcy, 73  
equation, 167  
equations, 2  
darcy (unit), 74  
Darcy velocity, 76, 103, 167  
Darcy's equation, 105, 156, 212  
equation, differential form, 76  
experiment, 73  
law, 73, 74, 77, 80  
defending phase, 157  
definition of a stochastic process, 224  
degrees of freedom, 171  
demonstration experiment, 6  
dense random packing, 213  
density of points, 29  
detailed balance, 230  
detergency, 116  
detergent, 120  
die, 172  
dielectric constant, 98  
differential equation, 156  
diffusion, 3, 77  
constant, 98  
constant  $D$ , 236  
tensor, 237  
dilute solutions, 190, 191  
dimensionless combination, 64  
distance, 143  
time, 143  
dipole field, 94  
potential, 94  
disclinations, 21  
discrete probability law, 31  
disorder, 171  
dispersion, 4, 10  
dissipation, 58, 214  
drag coefficient, 111, 215  
coefficient  $C_D$ , 105  
drainage, 156  
drift term, 132  
velocity, 238  
driving force, 238  
drop, 116, 121, 133  
dyadic product, 55  
dynamical equation, 77  
effective length  $L_e$ , 82  
medium, 92  
porous medium, 157  
resistance, 98  
resistivity, 98, 101  
viscosity, 215  
Einstein relation, 3, 237  
Einstein-Stokes relation, 9  
elastic constant, 98  
elasticity theory, 77  
electric current, 77  
field, 92  
potential  $V$ , 92  
resistivity, 84  
electrical conduction, 101  
potential, 77

- electrolyte, 84  
 electrostatics, 77  
 emulsions, 116  
 energy, 171, 175, 186  
     dissipation, 55  
     eigenstates, 173  
 ensemble, 224  
 entropy, 171, 172, 175  
 equation of continuity, 138  
 equilibrium angle of contact  $\theta_0$ ,  
     134  
     contact angle, 133  
     distribution, 230  
 Euler description, 53  
     equation, 56  
 Euler-Poincare theorem, 18  
 Euler's equation, 55, 68  
     theorem, 25  
 evaporation frequency, 130  
 extensive, 173  
 external bath, 122  
 face centered cubic (FCC), 23  
 face-centered cubic lattice, 22  
 filling factor, 97, 111  
     factor  $c$ , 105  
 filtration velocity, 76, 81, 157  
 first law of thermodynamics, 53,  
     122, 177, 179, 186  
 first-order phase transition, 126  
 flotation, 116, 221  
 flow of water, 138  
     through porous media, 73  
     to wells, 73  
 fluctuations, 127  
 fluid density, 212  
 fluidized beds, 105  
 Fluidized beds, 221  
 flux, , 0  
 foam, 116  
 Fokker-Planck equation, 233, 234,  
     236  
 force, 135  
 forces of adhesion, 115  
 Forchheimer equation, 90  
 formation factor, 10  
 fractal fronts, 157  
     viscous fingering, 140, 157  
 fractional flows, 161  
 free surface boundary condition, 64  
 friction, 216  
     factor, 87  
 frictional force, 86  
 frustration, 15  
 fully developed turbulence, 69  
 fundamental solution, 110  
 Galerkin method, 112  
 Gauss divergence theorem, 55  
 Gauss's divergence theorem, 54  
 generalized Darcy equation, 160  
     Darcy equations, 163  
     force, 168  
 Gibbs distribution, 174  
     free energy  $G$ , 186  
     surface free-energy, 123  
 glass, 115, 134  
 glycerol, 6  
 granular material, 101  
     materials, 28  
 gravity, 55  
     effects, 142  
 Green's function, 109  
 ground water, 156  
 growth rate  $\gamma$ , 143  
 Hagen-Poiseuille, 49  
     law, 50  
 Hamiltonian, 173  
 heat, 177, 179  
     bath, 178  
     transport, 183  
 Hele-Shaw cell, 138, 140, 145, 148,  
     216  
     channel, 143  
 Helmholtz expression, 125  
     free energy  $F$ , 184  
     surface free-energy, 123  
 hexagonal close packing, 11  
     close-packed (HCP), 23  
 homogeneous porous medium, 199  
 hydraulic radius, 86  
 Hydrodynamic interactions, 221

- hydrodynamics, 53  
 hydrostatic pressure, 137  
 hyper-spheres, 29  
 hysteresis, 158  
 ideal fluid, 55  
 incompressible fluid, 61, 62  
     fluids, 138  
 inertia parameter, 90  
 inertial range, 69  
 information content, 201  
     entropy, 172  
     entropy  $S$ , 201  
 inhomogeneous medium, 92  
 instability, 163, 212  
 intensive, 189  
 interface tension, 158  
 interfacial tension, 139  
 invasion percolation, 156  
 irreversible process, 179  
 isobutyric acid, 149  
 isothermal compressibility, 126  
 jammed state, 16  
 jump moments, 234  
     moments  $a_\nu(y)$ , 231  
 Kelvin relation, 125  
 Kepler problem, 11  
 kinematic viscosity  $\nu$ , 40, 64  
 Kozeny constant, 84, 212  
 Lagrange description, 53  
     parameter, 172  
 Laminar Channel Flow, 38  
 Landau potential, 121  
     potential  $\Omega$ , 187  
 Laplace equation, 77, 139, 141  
 Laplace's equation, 92, 94, 98  
 lattice Fourier sum, 106  
     Kronecker  $\delta$ -function, 107  
 lattice-periodic  $\delta$ -function, 107  
 law of similarity, 68  
 linear differential equation, 94  
     response function, 109  
 linearized equation, 231  
 local porosity, 197  
     porosity distribution, 198, 199  
     simplicity, 201  
 longitudinal dispersion coefficient  
      $D_{\parallel}$ , 4  
 low Reynolds number, 138  
 macroscopic variables, 172  
 Madelung energy, 110  
 Markov process, 227  
 mass balance equation, 160  
     flux, 54  
 Master equation, 229  
 maximum packing density, 11  
     work, 121, 181, 184  
 Maxwell's law of mixtures, 98, 111  
 mechanical equilibrium, 177  
 medium, 178, 179  
 meniscus, 146, 158  
 mercury, 134  
 meta-stable, 158  
 minimum work, 121, 183  
 mobility, 238  
      $\mu$ , 132  
 molecular diffusion, 7  
     diffusion coefficient, 3  
     volume, 125, 186  
 mol-fractions, 189  
 momentum flux, 55  
 multiphase flow, 116  
 Multiphase flow, 156  
 multivariate stochastic processes,  
     236  
 municipal water supply, 73  
 Navier-Stokes equation, 64, 67, 72  
     equations, 62, 102  
 Newtonian fluid, 60  
 Newton's assumption, 39, 60  
     equation, 53, 57  
     law, 55  
 Nigrosin, 6  
 no slip boundary condition, 46  
 non-Newtonian fluid, 40  
 non-slip boundary condition, 102,  
     111  
 non-wetting fluid, 156  
 normalized, 171  
 no-slip boundary condition, 63  
 nucleation, 120, 126

- equation, 132  
 rate, 132  
 theory, 116  
 Nuclepore filter, 79  
 number density, 122  
 observed fingering pattern, 153  
 Ohm's law, 77, 92  
 oil production, 156  
 one-dimensional displacement process, 160  
 Onsager relations, 168  
 Oseen equation, 72  
 osmotic pressure, 193  
 packed column, 3  
 packing of spheres, 10  
 packings of spheres, 212  
 parabolic velocity profile, 41  
 partial wetting, 133  
 particle flux, 237  
     Reynolds number, 87  
 partition function  $Z$ , 175  
 Peclet number, 5, 8  
 percolate, 223  
 percolation, 1  
     threshold, 157, 159  
 periodic arrays, 102  
     function, 106  
     point force, 110  
 peristaltic pump, 6  
 permeability, 10, 73, 80, 84, 98,  
     212, 221  
      $k$ , 2, 74  
 permeability–porosity correlation, 81  
 Perspex, 6  
 perturbation, 141  
 phase-transition, 1  
 piezometric head, 74  
 piston flow velocity, 162  
 plug flow, 3  
 Poisson distribution, 31  
     point process, 31  
 polar coordinates, 70, 93  
 pore neck, 197  
     size distribution, 197  
 porosity, 12, 36, 81, 105, 212  
     distribution, 197  
     function, 88  
      $\phi$ , 10  
 position-space renormalization method, 92  
 pressure, 55, 103, 177, 182, 212  
     gradient, 40, 73, 76, 103, 166  
     gradient  $G$ , 41  
 primary migration, 29  
 principal radii of curvature, 158  
 probability, 171  
     density, 198, 225  
     distribution, 172, 224  
     distribution of distances, 31  
     flux, 238  
 quantum state, 171  
 radii of curvature, 139  
 random close packed spheres, 213  
     close-packing (RCP), 24  
     function, 224  
     loose packing (RLP), 27, 213  
     packing of penetrable spheres, 37  
     sequential adsorption (rsa), 16  
 rate of strain tensor, 59  
 Rayleigh-Benard instability, 154  
 realization, 224  
 reciprocal lattice, 106  
 relative permeability, 10, 157, 159  
     permeability matrix, 167  
 rescaling of Euler's equation, 68  
 residual oil saturation, 160  
 resistance coefficient  $\psi$ , 86  
 resistivity, 92  
 reversible flow, 9  
     process, 179, 183  
     work, 121  
 Reynolds number, 8, 65, 68, 86,  
     102  
 sample function, 224  
 sand, 73  
     pack, 212  
 saturation, 157, 158, 164

- S*, 164  
second Einstein relation, 238  
law of thermodynamics, 172,  
182, 183  
secondary migration, 29  
sediment, 221, 222  
seepage velocity, 76  
Self-Organized Critical behavior,  
29  
shear stress, 166  
simple cubic lattice, 21  
size distribution, 215  
soap, 116  
solid surface, 133  
solute, 190  
solvent, 190  
source rocks, 29  
specific discharge, 76  
    resistance, 92  
    surface, 10, 37, 212  
    surface area, 82  
    surface, *S*, 37  
spheres embedded in a matrix, 98  
stability of finger solutions, 146  
stagnation effect, 5  
    point, 4, 6  
stationary flow, 41, 77  
    Markov process, 228, 234, 236  
    state, 157, 214  
    stochastic process, 225  
statistical mechanics, 171  
Statistical Physics, 120  
statistical weight, 171  
steady state, 92, 157  
stochastic process, 224  
    variable, 224, 236  
Stokes drag on a sphere, 105  
    equation, 68, 110  
    equations, 102, 163  
    flow, 112  
    law, 71, 214  
Streamline, 102  
streamlines, 138  
stress, 39, 212  
    tensor, 59, 104  
structure, 36  
sub-ensemble, 226, 229  
substantive derivative, 57, 58  
sub-system, 175  
super-saturated, 126  
    vapor, 121  
super-saturation, 127  
surface energy, 123  
    entropy, 123  
    excess density, 123  
    free-energy, 123, 163  
    normal, 96  
    tension, 116, 120, 123  
surface-tension coefficient, 148  
surroundings, 121  
suspension, 215, 216, 221  
suspensions, 223  
system, 121  
Taylor instability, 154  
temperature, 182  
theory of lubrication, 42  
thermal contact, 175  
    equilibrium, 172, 176, 177,  
        188  
    resistivity, 98  
thermodynamic potential, 122  
thermodynamics, 120, 171  
time reversed, 6  
topological constraint, 17  
tortuosity, 84, 212  
transition probability, 227  
    probability per unit time, 228  
    rate, 130, 228  
transport coefficients, 168  
transverse dispersion coefficient  
     $D_{\perp}$ , 5  
turbulent, 90  
    flow, 65, 138  
two-cell distribution function, 200  
two-dimensional flow equations,  
    148  
two-phase flow, 156, 163  
    fluid flow, 164  
typical pore size, 82  
unconsolidated sand, 212, 214, 215

- unit vectors, 56
- unstable interface, 139, 142
- vapor pressure, 126
  - pressure of a drop, 125
- velocity field, 56
  - potential, 141
- viscosity, 6, 39, 40, 164
  - coefficient, 149
  - ratio  $A$ , 148
- viscous fingering, 140
  - fingers, 144
  - force, 61
- void-void correlation function, 36
- volume flow rate  $Q$ , 50
  - flow velocity, 81
  - flux, 76
  - fraction, 215
- Voronoi polyhedra, 17
- vortex-in-cell method, 148
- water, 115, 133
- wetting, 116, 120
  - fluid, 156
- work, 177, 178, 183
- Young-Laplace's equation, 119

# Notation

## Lower Case Latin

$A$	area cross section [ $\text{m}^2$ ] 73, 76, 81–86, 121–124, 128, 136, 161, 164, 212.
$A$	constant for uniform field potential [ $\text{V}/\text{m}$ ], 96.
$A$	viscosity ratio (Atwood ratio) 143.
$B$	constant in dipole potential [ $\text{V m}^2$ ], 94, 96, 97.
$C(\mathbf{R}, L)$	porosity autocorrelation function at scale $L$ 200.
$C_D$	drag coefficient $= F_s/F_{\text{Stokes}}$ , 105, 106, 111.
$C_D$	drag coefficient 215.
$C_{\parallel}$	empirical coefficient 5.
$C_{\perp}$	empirical coefficient 5.
$\text{Ca}$	capillary number $= U\mu/\sigma$ 144.
$D$	effective density diffusion coefficient [ $\text{m}^2/\text{s}$ ] 78.
$D_{\parallel}$	dispersion coefficient parallel to flow [ $\text{m}^2/\text{s}$ ] 4.
$D_{\perp}$	dispersion coefficient transverse to flow 5.
$D_m$	molecular diffusion coefficient [ $\text{m}^2/\text{s}$ ], 3, 8, 9.
$D_p$	surface average sphere diameter [m] 88.
$\frac{D}{Dt}$	substantive derivative $= \frac{\partial}{\partial t} + \mathbf{u} \cdot \nabla$ [1/s], 57, 58.
$E$	energy [J] 122 172–179, 183, 184, 186, 188.
$E$	number of polyhedron edges 25.
$E_0$	electric field (uniform) [ $\text{V}/\text{m}$ ] 93–96, 97, 98.
$E_1$	electric field inside sphere (uniform) [ $\text{V}/\text{m}$ ] 96.
$(E_r, E_{\theta}, E_{\phi})$	electric field vector in polar coordinates [ $\text{V}/\text{m}$ ] 93.

---

$\mathbf{E}$	electric field vector [V/m] 92–95, 96, 97.
$F$	Helmholtz free energy $F(TV) = E - TS$ [J], , 123, 184.
$F$	formation factor = (resistivity of fluid filled rock)/(resistivity of fluid) 10.
$F$	frictional force due to fluid flow per pore surface area [N/m <sup>2</sup> ], 86.
$F$	number of polyhedron faces 25.
$F(\ell)$	force per unit area between two fluids separated by $\ell$ [N/m <sup>2</sup> ], 117, 118.
$F_{\parallel}$	force parallel to surface [N/m <sup>2</sup> ] 48.
$F_{\perp}$	force perpendicular to surface [N/m <sup>2</sup> ] 48.
$F_p$	force on volume element due to pressure gradient [N] 104.
$\mathbf{F}$	force [N] 177.
$\mathbf{F}$	force density from (external) fields [N/m <sup>3</sup> ], 57, 102, 108.
$\mathbf{F}_s$	force acting on a sphere [N] 104, 105, 111, 215.
$\mathbf{F}_q$	force density Fourier amplitude [N/m <sup>3</sup> ], 108, 109.
$\mathbf{F}_{\text{stokes}}$	Stokes force on a sphere = $6\pi\mu a\mathbf{U}$ [N], 105, 111, 215.
$G$	Gibbs free energy $G(TP) = E - TS + PV$ [J] 121, 123, 186, 188.
$G$	pressure gradient $G = -\partial p/\partial x$ [Pa/m], 41, 50, 104.
$G(r)$	radial distribution function = $n(r)dr/4\pi r^2$ [1/m <sup>2</sup> ] 25.
$G(\mathbf{r})$	void-void correlation function 36.
$G_i$	pressure gradient $G_i = -\partial p_i/\partial x$ [Pa/m] 166.
$\mathbf{G}_q$	pressure gradient Fourier amplitude [Pa/m], 108, 109.
$H$	Hamilton operator [J] 173.
$H$	Laplace work per unit area required to separate a fluid into two halves [N/m] 118.
$J_i$	generalized (Onsager) current 168.
$K$	Kozeny constant = $K_0\mathcal{T}^2$ , 84, 113, 212.
$K$	constant introduce by Laplace [N/m <sup>2</sup> ] 118.
$K$	empirical coefficient in Darcy's equation (6.3) 74.
$K_0$	Kozeny constant, 82, 212.

---

$L$	length of line sample [m] 47, 51, 73, 80–83, 87, 104, 197, 199.
$L_e$	effective capillary length [m], 83.
$L_{ij}$	Onsager transport coefficient 168.
$M$	integer 107.
$N$	number of molecules or particles 122 123, 128, 186, 188.
$N$	number of points 29.
$N$	number of unit cells, 107, 109.
$P$	pressure [N/m <sup>2</sup> ] 123–128 136, 137, 177–179, 183, 186.
$P_0$	probability for having no points in a volume $v$ 29.
$P_c$	capillary pressure [N/m <sup>2</sup> ] [Pa] 142.
$P_i$	probability for having $i$ points in a volume $v$ 31.
$\text{Pe}$	Peclet number 5, 8.
$\text{Pe}^*$	critical Peclet number 8.
$\text{Pr}$	probability 128.
$Q$	heat [J], 178, 179.
$Q$	volume flow rate [m <sup>3</sup> /s] 50 73, 76, 80, 83, 161, 212.
$Q$	volume flow rate per unit channel width [m <sup>3</sup> /s m], 41, 47.
$Q_i$	volume flow rate of fluid ( $i$ ) [m <sup>3</sup> /s] 167.
$\mathbf{Q}$	vector in the reciprocal lattice [1/m] 107.
$R$	radius [m] 124–128, 164–166, 167, 216.
$R$	resistance [ $\Omega$ ] 99.
$R^*$	critical radius [m] 128.
$R_1 R_2$	principal radii of curvature [m], , 139, 158.
$R_m$	molecular radius [m] 9.
$\text{Re}$	Reynolds number = $\rho U d / \mu$ , 9, 65, 86.
$\text{Re}_p$	particle Reynolds number = $\rho U D_p / \mu$ 88.
$\mathbf{R}$	position of measurement volume $V_c$ 197.
$\mathbf{R}$	vector distance [m], 58.
$\mathcal{R}_{\min}$	minimum work [J] 121 128, 183, 184, 188.
$\mathbf{R}_n$	lattice vector = $n_1 \mathbf{a} + n_2 \mathbf{b} + n_3 \mathbf{c}$ [m], 102, 107.
$\mathcal{R}$	work done on system by the surroundings [J], 177, 178, 183.

---

$S$	entropy [J/K] 122 171–179, 183, 184, 186, 188.
$S$	information entropy 201.
$S$	saturation = (fluid volume/pore volume) 157–163, 164, 167.
$S$	specific surface = (pore space area)/(sample volume) [1/m] 10 36, 37, 82, 84, 86, 213.
$S$	surface [ $\text{m}^2$ ] 53, 55, 105, 113.
$S_1, S_2$	utility sums [ $\text{m}^{-1}$ ], [m] 110.
$S_i$	saturation fluid $i$ = (fluid volume/pore volume), 161, 164.
$S_{oc}$	critical saturation of water at the oil percolation threshold = (fluid volume/pore volume), 159.
$S_{or}$	residual oil saturation = $(1 - S_{oc})$ , 159.
$S_{wc}$	critical saturation of water at the water percolation threshold = (fluid volume/pore volume), 157, 159.
$\mathcal{S}$	super-saturation = $P_g/P_0$ 127.
$T$	temperature [K] 9 56, 122–128, 136, 174–179, 183, 184, 186, 188.
$\mathcal{T}$	tortuosity = $L_e/L$ , 84, 212.
$U$	Darcy velocity, filtration velocity [ $(\text{m}^3/\text{s})/\text{m}^2$ ] = [m/s] 76–83, 161, 212.
$U$	average flow velocity [m/s] 3.
$U$	velocity of bottom plate [m/s] 46.
$U(S)$	Buckley-Leverett front velocity = $U_0(\text{d}f/\text{d}S)$ [m/s] 162.
$U_0$	‘piston’ flow velocity = $Q/\phi A$ [m/s] 162.
$U_c$	critical velocity [m/s] 143.
$U_i$	Darcy velocity, filtration velocity of fluid ( $i$ ) [ $(\text{m}^3/\text{s})/\text{m}^2$ ] = [m/s] 167.
$\mathbf{U}$	Darcy velocity filtration velocity [ $(\text{m}^3/\text{s})/\text{m}^2$ ] = [m/s] 103, 105, 113, 138, 156, 157, 158, 212.
$\mathbf{U}$	velocity of Stokes particle [m/s] 215.
$V$	electrical potential [V] 77, 92, 94, 96.
$V$	number of polyhedron vertices 25.
$V$	unit cell volume = $\mathbf{a} \cdot (\mathbf{b} \times \mathbf{c})$ [ $\text{m}^3$ ] 103–107, 109, 113.

---

$V$	volume [ $\text{m}^3$ ] 29 53, 55, 86, 122–124, 128, 136, 172–179, 183, 184, 186.
$V^*$	reciprocal lattice unit cell volume = $(2\pi)^3/V$ [ $\text{m}^{-3}$ ] 106.
$V_1$	electrical potential inside sphere [V] 96.
$V_c$	measurement cell volume [ $\text{m}^3$ ] 197.
$W$	number of states 172.
$X_i$	generalized (Onsager) force 168.

### Upper Case Latin

$A$	area cross section [ $\text{m}^2$ ] 73, 76, 81–86, 121–124, 128, 136, 161, 164, 212.
$A$	constant for uniform field potential [V/m], 96.
$A$	viscosity ratio (Atwood ratio) 143.
$B$	constant in dipole potential [V $\text{m}^2$ ], 94, 96, 97.
$C(\mathbf{R}, L)$	porosity autocorrelation function at scale $L$ 200.
$C_D$	drag coefficient = $F_s/F_{\text{Stokes}}$ , 105, 106, 111.
$C_D$	drag coefficient 215.
$C_{\parallel}$	empirical coefficient 5.
$C_{\perp}$	empirical coefficient 5.
$\text{Ca}$	capillary number = $U\mu/\sigma$ 144.
$D$	effective density diffusion coefficient [ $\text{m}^2/\text{s}$ ] 78.
$D_{\parallel}$	dispersion coefficient parallel to flow [ $\text{m}^2/\text{s}$ ] 4.
$D_{\perp}$	dispersion coefficient transverse to flow 5.
$D_m$	molecular diffusion coefficient [ $\text{m}^2/\text{s}$ ], 3, 8, 9.
$D_p$	surface average sphere diameter [m] 88.
$\frac{D}{Dt}$	substantive derivative = $\frac{\partial}{\partial t} + \mathbf{u} \cdot \nabla$ [1/s], 57, 58.
$E$	energy [J] 122 172–179, 183, 184, 186, 188.
$E$	number of polyhedron edges 25.
$E_0$	electric field (uniform) [V/m] 93–96, 97, 98.
$E_1$	electric field inside sphere (uniform) [V/m] 96.
$(E_r, E_{\theta}, E_{\varphi})$	electric field vector in polar coordinates [V/m] 93.
$\mathbf{E}$	electric field vector [V/m] 92–95, 96, 97.
$F$	Helmholtz free energy $F(TV) = E - TS$ [J], , 123, 184.

---

$F$	formation factor = (resistivity of fluid filled rock)/(resistivity of fluid) 10.
$F$	frictional force due to fluid flow per pore surface area [N/m <sup>2</sup> ], 86.
$F$	number of polyhedron faces 25.
$F(\ell)$	force per unit area between two fluids separated by $\ell$ [N/m <sup>2</sup> ], 117, 118.
$F_{\parallel}$	force parallel to surface [N/m <sup>2</sup> ] 48.
$F_{\perp}$	force perpendicular to surface [N/m <sup>2</sup> ] 48.
$F_p$	force on volume element due to pressure gradient [N] 104.
$\mathbf{F}$	force [N] 177.
$\mathbf{F}$	force density from (external) fields [N/m <sup>3</sup> ], 57, 102, 108.
$\mathbf{F}_s$	force acting on a sphere [N] 104, 105, 111, 215.
$\mathbf{F}_q$	force density Fourier amplitude [N/m <sup>3</sup> ], 108, 109.
$\mathbf{F}_{\text{stokes}}$	Stokes force on a sphere = $6\pi\mu a\mathbf{U}$ [N], 105, 111, 215.
$G$	Gibbs free energy $G(TP) = E - TS + PV$ [J] 121, 123, 186, 188.
$G$	pressure gradient $G = -\partial p/\partial x$ [Pa/m], 41, 50, 104.
$G(r)$	radial distribution function = $n(r)dr/4\pi r^2$ [1/m <sup>2</sup> ] 25.
$G(\mathbf{r})$	void-void correlation function 36.
$G_i$	pressure gradient $G_i = -\partial p_i/\partial x$ [Pa/m] 166.
$\mathbf{G}_q$	pressure gradient Fourier amplitude [Pa/m], 108, 109.
$H$	Hamilton operator [J] 173.
$H$	Laplace work per unit area required to separate a fluid into two halves [N/m] 118.
$J_i$	generalized (Onsager) current 168.
$K$	Kozeny constant = $K_0\mathcal{T}^2$ , 84, 113, 212.
$K$	constant introduce by Laplace [N/m <sup>2</sup> ] 118.
$K$	empirical coefficient in Darcy's equation (6.3) 74.
$K_0$	Kozeny constant, 82, 212.
$L$	length of line sample [m] 47, 51, 73, 80–83, 87, 104, 197, 199.
$L_e$	effective capillary length [m], 83.

---

$L_{ij}$	Onsager transport coefficient 168.
$M$	integer 107.
$N$	number of molecules or particles 122 123, 128, 186, 188.
$N$	number of points 29.
$N$	number of unit cells, 107, 109.
$P$	pressure [ $\text{N}/\text{m}^2$ ] 123–128 136, 137, 177–179, 183, 186.
$P_0$	probability for having no points in a volume $v$ 29.
$P_c$	capillary pressure [ $\text{N}/\text{m}^2$ ] [ $\text{Pa}$ ] 142.
$P_i$	probability for having $i$ points in a volume $v$ 31.
$\text{Pe}$	Peclet number 5, 8.
$\text{Pe}^*$	critical Peclet number 8.
$Pr$	probability 128.
$Q$	heat [J], 178, 179.
$Q$	volume flow rate [ $\text{m}^3/\text{s}$ ] 50 73, 76, 80, 83, 161, 212.
$Q$	volume flow rate per unit channel width [ $\text{m}^3/\text{s m}$ ], 41, 47.
$Q_i$	volume flow rate of fluid ( $i$ ) [ $\text{m}^3/\text{s}$ ] 167.
$\mathbf{Q}$	vector in the reciprocal lattice [1/m] 107.
$R$	radius [m] 124–128, 164–166, 167, 216.
$R$	resistance [ $\Omega$ ] 99.
$R^*$	critical radius [m] 128.
$R_1 R_2$	principal radii of curvature [m], , 139, 158.
$R_m$	molecular radius [m] 9.
$\text{Re}$	Reynolds number = $\rho U d / \mu$ , 9, 65, 86.
$\text{Re}_p$	particle Reynolds number = $\rho U D_p / \mu$ 88.
$\mathbf{R}$	position of measurement volume $V_c$ 197.
$\mathbf{R}$	vector distance [m], 58.
$\mathcal{R}_{\min}$	minimum work [J] 121 128, 183, 184, 188.
$\mathbf{R}_n$	lattice vector = $n_1 \mathbf{a} + n_2 \mathbf{b} + n_3 \mathbf{c}$ [m], 102, 107.
$\mathcal{R}$	work done on system by the surroundings [J], 177, 178, 183.
$S$	entropy [J/K] 122 171–179, 183, 184, 186, 188.
$S$	information entropy 201.

---

$S$	saturation = (fluid volume/pore volume) 157–163, 164, 167.
$S$	specific surface = (pore space area)/(sample volume) [1/m] 10 36, 37, 82, 84, 86, 213.
$S$	surface [ $\text{m}^2$ ] 53, 55, 105, 113.
$S_1, S_2$	utility sums [ $\text{m}^{-1}$ ], [m] 110.
$S_i$	saturation fluid $i$ = (fluid volume/pore volume), 161, 164.
$S_{oc}$	critical saturation of water at the oil percolation threshold = (fluid volume/pore volume), 159.
$S_{or}$	residual oil saturation = $(1 - S_{oc})$ , 159.
$S_{wc}$	critical saturation of water at the water percolation threshold = (fluid volume/pore volume), 157, 159.
$\mathcal{S}$	super-saturation = $P_g/P_0$ 127.
$T$	temperature [K] 9 56, 122–128, 136, 174–179, 183, 184, 186, 188.
$\mathcal{T}$	tortuosity = $L_e/L$ , 84, 212.
$U$	Darcy velocity, filtration velocity [ $(\text{m}^3/\text{s})/\text{m}^2$ ] = [m/s] 76–83, 161, 212.
$U$	average flow velocity [m/s] 3.
$U$	velocity of bottom plate [m/s] 46.
$U(S)$	Buckley-Leverett front velocity = $U_0(\text{d}f/\text{d}S)$ [m/s] 162.
$U_0$	‘piston’ flow velocity = $Q/\phi A$ [m/s] 162.
$U_c$	critical velocity [m/s] 143.
$U_i$	Darcy velocity, filtration velocity of fluid ( $i$ ) [ $(\text{m}^3/\text{s})/\text{m}^2$ ] = [m/s] 167.
$U$	Darcy velocity filtration velocity [ $(\text{m}^3/\text{s})/\text{m}^2$ ] = [m/s] 103, 105, 113, 138, 156, 157, 158, 212.
$U$	velocity of Stokes particle [m/s] 215.
$V$	electrical potential [V] 77, 92, 94, 96.
$V$	number of polyhedron vertices 25.
$V$	unit cell volume = $\mathbf{a} \cdot (\mathbf{b} \times \mathbf{c})$ [ $\text{m}^3$ ] 103–107, 109, 113.
$V$	volume [ $\text{m}^3$ ] 29 53, 55, 86, 122–124, 128, 136, 172–179, 183, 184, 186.
$V^*$	reciprocal lattice unit cell volume = $(2\pi)^3/V$ [ $\text{m}^{-3}$ ] 106.

---

$V_1$	electrical potential inside sphere [V]	96.
$V_c$	measurement cell volume [ $\text{m}^3$ ]	197.
$W$	number of states	172.
$X_i$	generalized (Onsager) force	168.

**Lower Case Greek**

$\Delta(\mathbf{r})$	lattice-periodic $\delta$ -function = $\sum_{\mathbf{n}} \delta(\mathbf{r} + \mathbf{R}_n)$ [ $\text{m}^{-3}$ ]	108.
$\Delta \dots$	change in $\dots$ , 183, 186, 188.	
$\Delta_q$	Fourier amplitude of $\Delta(\mathbf{r})$ , $=1/V$ [ $\text{m}^{-3}$ ]	108.
$\Delta p$	pressure difference [Pa]	80–86, 104, 119.
$\Delta x$	change in position [m], 3, 104.	
$\Omega$	Landau potential $\Omega(T\mu) = E - TS - \mu N = -PV$ [J]	
	121–124, 128, 136, 188.	
$\Phi$	cohesive energy density [ $\text{J}/\text{m}^3$ ]	120.
$\Lambda$	viscosity tensor [ $\text{Ns}/\text{m}^2$ ]	60.

**Upper Case Greek**

$\Delta(\mathbf{r})$	lattice-periodic $\delta$ -function = $\sum_{\mathbf{n}} \delta(\mathbf{r} + \mathbf{R}_n)$ [ $\text{m}^{-3}$ ]	108.
$\Delta \dots$	change in $\dots$ , 183, 186, 188.	
$\Delta_q$	Fourier amplitude of $\Delta(\mathbf{r})$ , $=1/V$ [ $\text{m}^{-3}$ ]	108.
$\Delta p$	pressure difference [Pa]	80–86, 104, 119.
$\Delta x$	change in position [m], 3, 104.	
$\Omega$	Landau potential $\Omega(T\mu) = E - TS - \mu N = -PV$ [J]	
	121–124, 128, 136, 188.	
$\Phi$	cohesive energy density [ $\text{J}/\text{m}^3$ ]	120.
$\Lambda$	viscosity tensor [ $\text{Ns}/\text{m}^2$ ]	60.

**Small Caps**

BCC	body-centered cubic lattice	111.
FCC	face-centered cubic lattice	21, 23, 111.
HCP	hexagonal close-packed lattice	23.
RCP	random close packing	25, 27, 213.
RCP	random close-packing	24.
RLP	random loose packing	25, 27, 213.
SC	simple cubic lattice	21, 111.

**Subscripts**

<sub>1 2</sub>	invading fluid (1) and defending fluid (2) in Hele-Shaw cell 139–142, 143, 219.
<sub>ℓ</sub>	liquid 122–128, 136, 137.
<sub>i</sub>	$i = o, w$ for oil and water respectively,, 161.
<sub>0</sub>	at equilibrium, 125, 127.
<sub>c</sub>	capillary, for pressure,, 142, 158.
<sub>c</sub>	critical, for saturation 157.
<sub>g</sub>	gas 122–128, 136, 137.
<sub>max</sub>	maximum 183.
<sub>min</sub>	minimum 183.
<sub>o</sub>	oil 156–161, 163, 164.
<sub>s</sub>	solid 136.
<sub>s</sub>	surface 123.
<sub>0</sub>	surrounding, heat-bath 122, 123, 136, 183, 186, 188.
<sub>w</sub>	water 156–161, 163, 164.